ELUCIDATING THE ROLE OF FOXO3A SIGNALING IN RESCUING INTESTINAL INFLAMMATION IN IL-10-DEFICIENT MURINE HOSTS

STEPHANIE HAJJAR

Thesis Submitted to the University of Ottawa

In partial fulfillment of the requirements for the PhD in Microbiology and Immunology

Department of Biochemistry, Microbiology, and Immunology

Faculty of Medicine

University of Ottawa

ABSTRACT

The transcription factor FoxO3a plays an essential role in metabolism, cell proliferation, cell differentiation, cell death and stress resistance. Originally identified as a tumor suppressor, FoxO3a was later shown to regulate inflammation by modulating the innate and adaptive immune responses. Recently, genome-wide association studies have identified mutations in the FoxO3a gene that promote the progression of an aggressive course of Crohn's disease, a form of inflammatory bowel disease in humans. Indeed, mutations in susceptibility genes, such as IL-10, correlate with IBD; however, they may not necessarily impact disease progression implying the existence of compensatory genes. Herein, we unravel the role of FoxO3a in preventing the progression of a spontaneous CrD-like phenotype in an IL-10-deficient mouse model of colitis. Our findings indicate that reduced FoxO3a activity enhances the inflammatory response and leads to a compensatory increase in the expression of IL-10. Deficiency in IL-10 production, in the context of poor FoxO3a signaling, removes all the regulatory brakes and unleashes a pathological inflammatory response in the gut. We show that deficiency in both FoxO3a and IL-10 leads to an abundant presence of death-resistant immune cells in the colon lamina propria, while being constantly replenished by enhanced myelopoiesis in the bone marrow. The myeloid cells exhibit an intrinsic hyperactivation of mTORC1 and other inflammatory signaling pathways resulting in flaming levels of inflammatory mediators. The created pro-inflammatory milieu cannot be attenuated by dysfunctional regulatory T cells despite their abundance in the gut. We also demonstrate that through transcriptional repression of glutaminase (GLS/GLS2), FoxO3a signaling prevents excessive glutaminolysis in activated T cells and downregulates an overt Th17-like immune response. Finally, we show that FoxO3a restricts the abundance of colitogenic microbiota, such that antibiotic administration improves the survival of the *FoxO3a*$^{-/-}$ *Il10*$^{-/-}$ mice. In summary, we report that FoxO3a acts as a key checkpoint that restrains the aberrant metabolic activity in myeloid cells and T cells and prevents the accumulation of colitogenic microbiota that contribute altogether to the development of an aggressive form of gut inflammation in *Il10*$^{-/-}$ hosts. The potent effect of FoxO3a in controlling the severity of gut inflammation, through an intricately antagonistic cooperation with IL -10, brings about a great interest in IBD research and may lead to new therapeutic avenues.

PREFACE

This thesis contains original research that was published in *Cell Death & Differentiation*.

Hajjar, Stephanie., Nathan, Nathan., Joseph, Julie., Mottawea, Walid., Ariana, Ardeshir., Pyatibrat, Sergey., Harper, Mary-Ellen., Alain, Tommy., Blais, Alexander., Russell., Rayan. & Sad., Subash. FoxO3a tempers excessive glutaminolysis in activated T cells to prevent fatal gut inflammation in the murine *Il-10*$^{-/-}$ model of colitis. *Cell Death Differ* **29,** 585–599 (2021). https://doi.org/10.1038/s41418-021-00876-y

Specific contributions are listed below:

- S.H designed and performed nearly all experiments, analyzed data and wrote the manuscript. N.N assisted with LP immune cell isolation and FACS analysis. J.J contributed to the conceptualization of the study and initiated the survival curve in Figure 1. W.M performed the analysis and generated the graphs for V4-16S rRNA sequencing (Figures, 44, 45, 46). A.A. assisted with *in vivo* experiments and generated Figure 30-d. S.P performed the blinded examinations of the stained tissue sections (Histopathology & IHC). M.E.H. provided all the reagents used for the Seahorse assay, and the assay was performed using the Seahorse Bioscience XF96 Extracellular Flux Analyzer from Dr. Harper's laboratory. T.A., A.B., and R.R. contributed to the methodology and manuscript editing. S.S. conceptualized the study, designed experiments, cooperated with writing the manuscript and data analysis.

- The experimental protocols [BMI1638 and BMI3486 (Replacing BMI1639)] used were approved by the University of Ottawa Animal Care Committee.
- Histology/Imaging/Staining services were provided by the Louise Pelletier HCF (RRID: SCR_021737) at the University of Ottawa.
- Flow cytometry experiments were conducted at the Flow Cytometry & Virometry Core facility at the University of Ottawa.
- The V4-16S rRNA sequencing was completed by Microbiome Insights, University of British Columbia, Vancouver, BC, Canada.
- The work was funded by a grant from the Canadian Institutes of Health Research (#420007 to Dr. Subash Sad). Stephanie Hajjar was supported by Alexander Graham Bell-Canada Graduate Scholarship from NSERC.

ACKNOWLEDGEMENTS

My deepest gratitude and appreciation go to my advisor Dr. Subash Sad. I have always felt supported through your words and actions in both science and in life. You have shaped my abilities to think critically over years of mentorship. Thank you for the thoughtful anecdotes, valuable advice, direction, and great discussions we had about life in general. Thank you for giving me a shot and bringing out the best in me.

I thank my thesis advisory committee members Dr. Tommy Alain, Dr. Jim Sun, and Dr. Marceline Cote for challenging my knowledge as my thesis developed. Thank you each for your input, support and encouraging words over the years.

I thank all the former and current members of Sad lab with whom I crossed paths during my time in the lab. Each one of you has been an indispensable source of inspiration, collaboration, and support, which was invaluable in my training and scientific work. Working with all of you has been an extremely rewarding experience. Thank you all from the bottom of my heart and I hope our friendship continues for many years to come.

Special thanks to all members of ACVS for teaching me essential mouse skills and for their help and patience with monitoring our sick mice. I thank all the members at Louise Pelletier HCF for assisting me with sample processing and staining. I would also like thank Dr. Vera Tang for her training and assistance with flow cytometry.

Thank you to the University of Ottawa, Ontario Graduate Scholarship Program and NSERC for funding me throughout the years.

Finally, I thank my family for being my rock of strength, wise counsel, and sympathetic ear. Thank you for your unwavering love and sacrifices that allowed me to reach for and realize my dreams. I owe all that is good in my life to you.

TABLE OF CONTENTS

LIST OF ABBREVIATIONS

APC Antigen presenting cell

ATP Adenosine Triphosphate

BFA Brefeldin A

BMDM Bone Marrow-Derived Macrophage

CD Cluster of Differentiation

CrD Crohn's disease

cDNA Complementary DNA

CLP Common Lymphoid Progenitor

CMP Common Myeloid Progenitor

DAMP Damage associated molecular pattern

DC Dendritic cell

DSS Dextran sulfate sodium

ELISA Enzyme-Linked Immunosorbent Assay

ER Endoplasmic Reticulum

ERK Extracellular Signal-Regulated Kinase

FBS Fetal Bovine Serum

FoxO Forkhead Box O

GALT Gastrointestinal associated-lymphoid tissue

GI Gastrointestinal

GLUT1 Glucose Transporter 1

GMP Granulocyte-Monocyte Progenitor

HSC Hematopoietic Stem Cell

IBD Inflammatory Bowel Disease

IEC Intestinal epithelial cells

IEL Intraepithelial lymphocytes

IFN Interferon

IL Interleukin

iNOS Inducible Nitric Oxide Synthase

LP Lamina Propria

LPS Lipopolysaccharide

LT-HSC Long-Term Hematopoietic Stem Cell

M cells Microfold cells

MAPK Mitogen-Activated Protein Kinase

M-CSF Macrophage Colony-Stimulating Factor

MEP Megakaryocyte-Erythrocyte Progenitor

MFI Median Fluorescence Intensity

MHC Major Histocompatibility Complex

MLN Mesenteric Lymph nodes

MOI Multiplicity of Infection

mRNA Messenger RNA

MTT 3-(4,5-dimethylthiazol-2-yl)-2,5-diphenyltetrazolium bromide

NADH Nicotinamide Adenine Dinucleotide

NFκB Nuclear Factor Kappa-light-chain-enhancer of activated B cells

NK cells Natural Killer cells

NLR Nod-Like Receptor

NLRP3 NOD-LRR-Pyrin domain-containing protein 3

NO Nitric Oxide

O.D. Optical Density

OCR Oxygen Consumption Rate

PAMP Pathogen-Associated Molecular Pattern

PBS Phosphate-Buffered Saline

PCR Polymerase Chain Reaction

PI3K Phosphatidylinositol 3-kinase

PKB Protein Kinase B

PMN Polymorphonuclear

PP Peyer's patches

PRR Pattern recognition receptors

RBC Red Blood Cell

RLU Relative Light Units

ROS Reactive oxygen species

RPMI Roswell Park Memorial Institute Medium

rRNA Ribosomal RNA

qRT-PCR quantitative Real-Time PCR

SCFA Short chain fatty acids

SEM Standard Error of the Mean

SOD1/2 Superoxide Dismutase 1/2

STAT3 Signal transducer and activator of transcription 3

ST2 Suppression of Tumorigenicity 2 protein.

ST-HSC Short-Term Hematopoietic Stem Cell

TCR T cell Receptor

TGF-β Transforming growth factor β

Th T helper

TLR Toll-Like Receptor

TMB Tetramethylbenzidine

TMRE Tetramethylrhodamine Ethyl Ester

TNF-α Tumor Necrosis Factor α

Treg Regulatory T cells

UC Ulcerative colitis

WT Wild Type

LIST OF FIGURES AND TABLES

INTRODUCTION

1. The Immune System

The immune system is a multicomponent interactive network of organs, cells and molecules that serve to protect the host from foreign or dangerous invaders, such as pathogens or cancer cells, in the aim of achieving homeostasis. Human pathogens can be broadly classified into four major categories: viruses, bacteria, fungi, and parasites. To match the diversity of potential invaders, the mammalian immune system has continually evolved its search-and-destroy missions by establishing a range of recognition and destruction mechanisms. Moreover, by interleaving with other body systems, including the endocrine, nervous, and metabolic systems, the immune system plays a key role in regulating homeostasis.

The immune system can be divided into two main axes, termed innate and adaptive immunity. While innate immunity is the first to respond to breaches of physical barriers (i.e., skin, and mucous membranes), both axes may collaborate to effectively resolve infections during an immune response (Parkin and Cohen, 2001). An effective defense relies heavily on the nature of the offense and the microenvironment in which the engagement occurs. For example, under physiological conditions, the central nervous system microenvironment tightly regulates immune cell migration across the blood brain barrier. In the context of infections or autoimmune diseases, there is considerable non-specific recruitment of pro-inflammatory leukocytes into the CNS (Ludowyk et al., 1992; Hickey, 2001). In contrast, the GI tract microenvironment is exposed to an enormous microbial environment and must therefore come with inherent directional cues by which commensal microbiota are tolerated by immune cells to aid in digesting foreign compounds (Kindt et al., 2012).

However, failures of the system do occur, such that inappropriate or dysfunctional immune responses can result in damage to the host. This can lead to a range of disorders that fall into one of three broad categories: hypersensitivity, autoimmune diseases, and immune deficiency (Kindt et al., 2012). Many mediators secreted during an inflammatory response are cytotoxic and cause

severe tissue damage and organ failure, known as immunopathology. Additionally, uncontrolled immune response mechanisms can cause dysbiosis by enabling the out-growth of pathogenic microbes over beneficial ones. Hence, "immune regulatory" mechanisms must be parallelly initiated to temper the excessive activation of the effector inflammatory mechanisms by inducing death of inflammatory cells, degrading inflammatory mediators, blocking signaling pathways and repressing gene transcription. In fact, a fine equilibrium of pro- and anti-inflammatory responses must be maintained to avoid a breakdown in this balance that can potentially lead to a disease.

1.1.The Innate Immune System

Key elements of innate immunity comprise the physical and chemical barriers. Physical barriers constitute the epithelial layers of the skin, mucosal tissues (GI, respiratory and urogenital) and glandular tissues (salivary, lacrimal, and mammary glands). Chemical barriers include the enzymes present in sweat, saliva, mucus, and tears. When pathogens breach these barriers, the innate immune response is the first to respond typically within minutes of invasion (Delves and Roitt, 2000; Medzhitov and Janeway, 2000). This is triggered by cell surface or intracellular receptors that recognize conserved molecular components of the pathogen. Pathogen recognition occurs as a variety of receptors, such as Toll-like receptors (TLRs), Nod-like receptors (NLRs) and AIM2-like receptors (ALRs) that belong to the family of pattern-recognition receptors (PRRs), detect pathogen-associated molecular patterns (PAMPs), which are broad structural motifs conserved within each microbial species. For instance, *Salmonella* expresses several PAMPs, such as lipopolysaccharide (LPS), flagellin and lipoproteins that are recognized by TLR4, TLR5, and TLRs 1/2/6 respectively (Gilchrist et al., 2015). Damage-associated molecular patterns (DAMPs), released by cell or tissue damage, can also be recognized by cell-surface or intracellular PRRs. The PRR-PAMP/DAMP interaction activates downstream signaling in innate immune cells that promote pathogen clearance and subsequent activation of the acquired immune response (Medzhitov, 2008; Medzhitov and Janeway, 1997). The innate immune system can eliminate the pathogen through humoral responses, such as the complement system, or the production of antimicrobial peptides. Innate immune cells include neutrophils, eosinophils, basophils, mast cells, natural killer cells, monocytes, macrophages, and dendritic cells. Each cell type has a specialized function. The proportion of each cell subset varies but remains stable during homeostasis. During infection, cancer, or exposure to allergens, the numbers of various innate immune cell subsets are modulated, and this is highly dependent on the chronicity and nature of the stimulus. Soluble factors include complement proteins, which function in a cascade of reactions that result in the attraction of phagocytes and enhancement of the adaptive immune response (Parkin and Cohen, 2001). Cytokines,

reactive oxygen species (ROS) and antimicrobial peptides are also soluble mediators of the innate immune system.

1.1.1. Neutrophils

Neutrophils are among the first innate immune cells to migrate to the site of infection and contribute to reducing the microbial burden by phagocytosis (Parkin and Cohen, 2001). Neutrophils are PMNs that constitute the human body's most abundantly circulating immune cells. They make up 50-70% of all blood leukocytes in humans and 10-30% of those in mice. Neutrophils are generated in the bone marrow by descending from the myeloid-specific granulocyte macrophage progenitors (GMP) that finally develops into the lineage committed neutrophil promyelocyte. A pool of neutrophils is retained in the bone marrow through the chemokine receptor CXCR4 (De Filippo and Rankin, 2018). Granulocyte colony stimulating factor (G-CSF) stimulation downregulates CXCR4 expression on neutrophils reducing their retention in the bone marrow. CXCR2 is the major receptor allowing for neutrophil exit from the bone marrow by recognition of constitutive CXCL1 and CXCL2 expression on the endothelium. Previous studies had agreed that at steady state, aged circulating neutrophils return to the bone marrow to be cleared by the bone marrow macrophages (De Filippo and Rankin, 2018). Recently, the liver and spleen have been identified as other possible major sites of neutrophil clearance. After differentiation in the bone marrow, neutrophils are released into the blood and subsequently migrate into the tissues. The lifetime of neutrophils has been shown to be between 9-18 hours in humans and about 1.5 hours in mice but can also be increased in the presence of inflammatory stimuli (Summers et al., 2010). As they constantly circulate in the bloodstream, they are the first responders during acute inflammation, such that they are recruited to the site of infection in response to inflammatory molecules generated by activated innate cells.

One of the most distinctive features of neutrophils is their segmented nucleus and cytoplasmic granularity, which ties in closely to their anti-microbial activity. Neutrophil granules contain an armada of anti-microbial peptides and enzymes (Papayannopoulos, 2018). Additionally, neutrophils are capable of phagocytosis, releasing reactive oxygen species and producing neutrophil extracellular traps (NETs) in response to bacteria (Papayannopoulos, 2018). These are non-specific mechanisms that will be employed against most pathogens. An essential aspect of their ability to respond to infections is their recruitment and migration into tissues. Neutrophils

can be characterized by their expression for glycosylphosphatidylinositol (GPI)–anchored protein Ly6G in mice or the structurally related Ly6/uPAR family member CD177 in humans (Wang et al., 2012). These markers directly correlate with the cell's level of differentiation and maturation and mainly help with neutrophil recruitment and migration. Although early in the inflammatory response, neutrophil recruitment is also tightly controlled to avoid excess damage to host tissue. Multiple roles for neutrophils have been demonstrated in several inflammatory diseases, such as cancer, lupus, HIV, and colitis. For example, a significant neutrophil infiltration has been observed to persist at the site of intestinal inflammation, thus contributing to the development of a chronic and detrimental environment through ROS production and over-expression of inflammatory cytokines (Liu et.al, 2016). Neutrophils play a role in both the inflammatory and resolution phases of an inflammatory response. Recent studies have also demonstrated that neutrophils can be categorized into phenotypically distinct subpopulations based on density, function, and expression of markers related to their differential effects on cancer initiation, development, and progression (Sagiv et al., 2015;Sagiv et al., 2016).

1.1.2. Dendritic cells

Dendritic cells (DCs) are considered as the professional antigen-presenting cells (APCs) due to their constitutive expression of MHC II and co-stimulatory molecules along with their ability to capture, process and present exogenous antigens to T cells (Banchereau and Steinman, 1998). DCs constitute a unique class of innate immune cells that phagocytose and control pathogens and present antigenic peptides to T cells, thus initiating the activation of the innate and adaptive immune responses. In addition to performing phagocytosis DCs also secrete cytokines and anti-microbial peptides. DCs are derived from the myeloid and lymphoid lineages of hematopoietic cells in the bone marrow and reside in the lymphoid or non-lymphoid tissues sampling the environment for foreign invaders and non-self-molecules. Immature DCs reside in several tissues (skin, pharynx, esophagus, or genitals) and mucous membranes (respiratory and GI tract), where they outstretch their extensions through the tight junctions of tissue epithelial cells to enhance their ability to capture antigens.

1.1.2.1. Antigen processing and presentation to T cells

Upon capturing the foreign antigen, DCs are activated and go through a process of maturation: they lose their phagocytic activity but gain the ability to present antigens to T cells by increasing their surface expression of MHC II and co-stimulatory molecules along with the induction of inflammatory cytokine and chemokine expression (Cella et al., 1997; Guermonprez et al., 2002). Mature DCs can migrate to nearby secondary lymphoid tissues from the circulation and from non-lymphoid tissues to present antigens to and activate naïve T cells (Guermonprez et al., 2002; Banchereau and Steinman, 1998). This interaction promotes the differentiation of naïve antigen-specific T cells into effector and memory T cells. While DCs were discovered for their ability to serve as potent APCs, they also have non-redundant roles in innate immune responses. For instance, their early recognition of pathogens and rapid cytokine production activate innate immune cells, such as innate lymphoid cells (ILCs) and natural killer (NK) cells, to limit pathogen spread until adaptive immunity can be initiated (Mashayekhi et al., 2011; Satpathy et al., 2013).

1.1.2.2.Dendritic cell subsets

Different subtypes of DCs have been described based on the surface expression of specific markers, activity of transcription factors, tissue distribution, and functions. The subsets are broadly classified into classical (cDC) and non-classical. cDCs express the integrin CD11c and MHC II, and each subset can be distinguished by additional markers (Steinman et al., 1979; Metlay et al., 1990). cDC1s in the spleen and lymph nodes express CD8α, CD24, CD103 and XCR1 and are also referred to as lymphoid DCs. cDC2s, often referred to as myeloid DCs, constitute a functionally and phenotypically heterogeneous population that mainly expresses CD11b, CD4 and Sirpα (Mildner and Jung, 2014;Brown et al., 2019; Rivera et al., 2021). $CD8\alpha^+$ DCs recognize intracellular pathogens and initiate type 1 immune responses that require the early activation of ILC1s and NK cells as well as eventual Th1 polarization (Mashayekhi et al., 2011). $CD8\alpha^+$ DCs also promote cross presentation of antigens to activate $CD8^+$ T cells (Den Haan et al., 2000). $CD11b^+$ DCs are superior in the induction of $CD4^+$ T cell-mediated immune responses (Den Haan et al., 2000). Some cDC2s govern type 2 immune responses against parasites, such that they activate ILC2s and Th2 cells (Tussiwand et al., 2015). Other cDC2s sense extracellular bacteria and initiate type 3 immune responses by activating ILC3s and Th17 cells (Lewis et al., 2011; Satpathy et al., 2013). Intestinal $CD11b^+$ cDC2s comprise both $CD103^+$ and $CD103^-$ fractions (Satpathy et al., 2013). Non-classical DCs include plasmacytoid DCs (pDCs), monocyte-derived DCs (moDCs) and Langerhans cells (LCs) (Mildner and Jung, 2014). pDCs secrete high amounts of type 1 interferons during a viral infection (Shortman and Liu, 2002). pDCs also express CD11c and MHC II and can be segregated by their additional expression of B220, Siglec-H, and Bst2 (Blasius et al., 2006; Zhang et al., 2006). moDCs can differentiate from circulating monocytes that infiltrate the site of infection or inflammation (Shi and Pamer, 2011). LCs are a unique population of DCs that reside in the skin epidermal layers and sample their microenvironment for antigens. Upon encountering the antigen, they migrate to skin draining lymph nodes and activate naïve T cells (Mildner and Jung, 2014).

1.1.3. Monocytes and Macrophages

Monocytes and macrophages are mononuclear phagocytes of the innate immune system. They play major roles in pathogenesis through sensing and clearing microbes or foreign molecules.

1.1.3.1.Monocytes

Monocytes comprise a heterogeneous group of cells that make up about 5-10% of white blood cells (Owen et al., 2013). They are short-lived, so they are continuously generated in the bone marrow through hematopoiesis by descending from granulocyte-monocyte progenitors (GMPs). Blood monocytes can be characterized into subsets based on their expression of CD14 in humans and of the member of the Ly-6 superfamily of GPI-anchored cell surface proteins Ly6C in mice (Ziegler-Heitbrock, 2015). Human $CD14^{hi}$ or murine $Ly6C^{hi}$ monocytes account for ~90% of the blood monocyte population and are classical "M1" inflammatory monocytes (Shi and Pamer, 2011). They are pro-inflammatory with enhanced phagocytic capacities and are the most transmigrating monocytes due to their expression for CCR2 and VLA-4 (α4β1 integrin) (Shi and Pamer, 2011). During an infection or tissue injury, inflammatory monocytes infiltrate into the inflamed tissue and differentiate into macrophages or dendritic cells based on the cues obtained from the tissue microenvironment. Monocytes can also cross the vascular endothelium during steady state and replace tissue resident macrophages. Notably, intestinal macrophages are constantly being replenished by circulating $Ly6C^{hi}$ monocytes (Bogunovic, 2009).

$CD14^{low}$ or $Ly6C^{low}$ monocytes constitute 5-10% of the total blood monocytes and are labeled as non-classical "M2" macrophages due to their predominant anti-inflammatory nature and tissue-repair functions. These monocytes also express high levels of CX3CR1 that allows them to "patrol" the vascular endothelium and resolve inflammation (Thomas, 2015). $Ly6C^{low}$ monocytes may not be a distinct subset but rather a mature form of $Ly6C^{high}$ monocytes (Sunderkotter, 2004).

1.1.3.2.Macrophages

Macrophages can be defined by their surface expression for CD68 in humans or the glycoprotein F4/80 in mice. Macrophages can either differentiate in the tissues from circulating monocytes or can be long-lived and self-renewing tissue-resident cells seeded during embryonic development (Varol et. al, 2015). The initial seeding of macrophages is derived from two waves: generation in the yolk sac at murine embryonic day 8 (E8) and generation in the fetal liver at murine E11.5 from aorta-gonad mesonephros- derived hematopoietic stem cells. Exceptionally, microglia, brain – resident macrophages, are exclusively derived from the yolk sac (Alliot et. al., 1999; Ginhoux et al., 2010). The relative contribution of each wave is dependent on the seeding tissue and activation of specific transcription factors. Following seeding, the tissue microenvironment completes the maturation of embryonic-derived macrophages and promotes their acquisition of tissue-specific functions.

Like monocytes, macrophages can play various roles. Long-term resident macrophages can function in tissue repair and regeneration. Inflammatory macrophages participate in the innate immune response as both APCs that activate T cells and as effective phagocytes that clear out the invading pathogens. They also increase their secretion of inflammatory and cytotoxic mediators upon activation by pathogens or PAMPs.

1.2. The Adaptive Immune System

The acquired or adaptive immune response involves a complex and interconnected network of cells and mediators that come together to incorporate signals received from the innate immune cells into their tailored response. Being much more attuned to subtle molecular differences, adaptive immune cells can recognize, eliminate, and remember the invading pathogens with very high specificity (Bonilla and Oettgen, 2010). Unlike the innate immune system, the adaptive arm evolves in real time and is slower to develop, since it relies on "categorizing" the antigens undertaken by innate processes (Bonilla and Oettgen, 2010).

Adaptive responses are driven by specialized B cells and T cells that develop from progenitor cells within the bone marrow, in which B cells remain for the duration of their development, while T cells migrate to the thymus at an early stage. They bear unique antigen-specific receptors from a diverse repertoire generated through random Variable (V) Diversity (D) and Joining (J) receptor gene rearrangements. Defined by the T cell receptor (TCR), αβ and γδ T cell lineages result from the rearrangement of four TCR loci. The highly variable heterodimer of α and β chains, in complex with the invariant CD3 chains on the surface, constitute the TCR on most T cells. In contrast, variable γ and δ chains are expressed with CD3 on a smaller subset of T cells that recognize different types of antigens (Vantourout & Hayday, 2013). γδ T cells are at their highest abundance in the gut mucosa, within a population of lymphocytes known as intraepithelial lymphocytes (Vantourout & Hayday, 2013).

B cells can recognize antigens through their B cell receptor (BCR), and with the help of differentiated helper T cells, B cells can undergo potent activation and clonal expansion. Activated B cells eventually mature into plasma cells that secrete antibodies (Pieper, Grimbacher, and Eibel 2013). Cytokines secreted by helper T cells promote isotype switching of B cells resulting in the secretion of different types of antibodies. Antibodies in turn bind to pathogens and their products to neutralize them, hence promoting their phagocytosis by APCs. Some of the activated B cells differentiate to memory cells and survive for a long time.

Innate-like lymphocytes, such as NK-like T cells (NKT) and γδ T cells, have been discovered to share overlapping innate- and adaptive- like characteristics (Godfrey et al., 2004; Holtmeier & Kabelitz, 2005). Moreover, innate lymphoid cells (ILCs) constitute a newly identified family of mononuclear hematopoietic cells with integrated innate and adaptive immune responses. They

have innate properties by virtue of their ability to rapidly secrete cytokines, most notably IL-17 and IL-22, but unlike innate-like and adaptive lymphocytes, they do not express rearranged antigen specific receptors (Spits & Cupedo 2012).

1.2.1. T cell Activation

The activation and sustainment of activated T cells requires three signals: Signal 1 is known as the canonical activation signal and occurs by binding of the TCR to a specific peptide presented by the MHC molecules; signal 2 is known as the co-stimulatory signal and occurs through the interaction between B7-1/B7-2 ligands located on the APC and the CD28 receptor on the T cell; and signal 3 is provided by cytokines secreted by APCs facilitating the expansion of the T cell response and polarizing activated T cells towards various phenotypes. Signal 3 can be provided by many cells, including fibroblasts and innate cells like APCs (Lanzavecchia & Sallusto, 2001; Delves et al., 2004, Medzhitov and Janeway, 2000).

Signals 1 and 2 work cooperatively to enhance the function and survival of T lymphocytes (Egerton et al., 1996; Yokosuka and Saito, 2010). CD28 co-stimulation lowers the threshold for T cell activation and promotes metabolic changes enhancing T cell survival (Frauwirth et al. 2002; Klein Geltink et al. 2017). T cells activated without Signal 2 become anergic or apoptotic (Jenkins, 1994).

Once activated, T cells proliferate and differentiate into various effector subsets categorized based on cluster of differentiation (CD) markers. $CD8^+$ T cells differentiate into cytotoxic T cells that kill infected cells presenting their specific peptide on MHC I molecules. $CD8^+$ T cells also express various cytokines such as IFN-γ or TNF-α upon recognition of infected target cells. In contrast, $CD4^+$ T cells or helper T cells (Th) recognize antigenic peptides presented by MHC II molecules and express a diverse array of inflammatory and anti-inflammatory cytokines.

1.2.2. T cell Differentiation

Specific antigenic stimulation (i.e. intracellular vs. extracellular viral, bacterial, fungal or helminth), in synergy with cytokines present in the milieu, initiates a series of developmental pathways in naïve $CD4^+$ T cells that subsequently differentiate into specific Th subsets, each with unique properties and effector functions . Particularly, Th subtypes are classified into Th1, Th2, Th17, Th22, T follicular helper (Tfh), Th9 and regulatory T cells based on their expression for unique transcription factors that become lineage-specific markers (Chaudry, 2011, Schmitt and Ueno, 2015). Each subtype will produce its own set of cytokines and chemokines that serve to activate other innate and adaptive cells. Through employing distinct cytokine profiles, Th cells engage and amplify the appropriate inflammatory reaction in response to cellular mediators of the innate immune system (Littman & Rudensky, 2010).

1.2.2.1.The classic Th1/Th2 paradigm

Traditionally, effector $CD4^+$ T cells belonged to either the Th1 or Th2 lineage depending on their pattern of cytokine production and effector activities (Bottomly, 1988). Cells from the Th1 subset promote cell-mediated immunity to eradicate intracellular pathogens (Mosmann et al. 1986; Bottomly, 1988; Mosmann and Coffman, 1989). IL-12 is required for the differentiation of Th1 cells through signal transducer and activator of transcription- 1 (STAT1), the transcription factor T-bet and STAT4. In contrast, Th2-cell differentiation is prompted by IL-4, which signals through STAT6 and GATA-3 to induce mature Th2 effector cells that secrete IL-4, IL-5, and IL-13. Mediators of the Th2 response are associated with enhanced mast cell, eosinophil and IgE production, which are crucial in the control of parasitic infections. Both Th1 and Th2 lineages have been implicated in the immunopathogenesis of inflammatory disease in the setting of unrestrained and dysregulated activation, with Th1 cells associated with chronic autoimmune disorders and Th2 cells linked to allergy (Romagnani, 1996). In keeping with this functional dichotomy, Crohn's disease, multiple sclerosis, psoriasis, and rheumatoid arthritis have been regarded as prototypical Th1 diseases, whereas ulcerative colitis and allergic asthma are representative of Th2 diseases (De Carli et al. 1994; Singh et al. 1999; Kidd, 2003).

1.2.2.2.Th17 cells

The discovery of a third Th lineage, Th17, has called into question the classic Th1/Th2 paradigm as Th17 signature cytokines, namely the IL-17 family members, have been demonstrated to play a role in the pathogenesis of both autoimmune and allergic disorders (Harrington et al., 2005; Langrish et al., 2005; Korn et al., 2007; Chen and O'Shea, 2008). Th17 cells are generally found to be pro-inflammatory through the production of IL-17A and IL-17F. Th17 cells have been demonstrated to participate in the immune defense against extracellular bacteria and fungi by recruiting neutrophils and macrophages to infected tissues and also promote IL-17-mediated autoimmune inflammation (Harrington et al., 2005; Park et al., 2005).

Th17 cells differentiate from naive $CD4^+$ cells following antigenic stimulation in the presence of IL-6 and TGF-β (Bettelli et al., 2006). IL-23 signaling to constitutively expressed IL-23 receptors on the surface of activated $CD4^+$ cells is required for both the development and maintenance of the differentiated Th17 phenotype (Aggarwal et al., 2003; McGeachy & Cua, 2008). STAT3 activation downstream of cytokine receptors mediates Th17 commitment via activation of the retinoid orphan receptor, RORγt, the major transcriptional regulator of Th17 differentiation (McGeachy & Cua, 2008). Mature Th17 cells in turn produce several effector cytokines including TNF-α, IL-21, IL-22, and most notably, members of the IL-17 cytokine family, IL-17A, B, C, D, E, and F (Korn et al., 2007).

1.2.2.3.Regulatory T cells

Regulatory T cells or Tregs can arise during maturation in the thymus from autoreactive cells and are termed natural Tregs. They can also be induced in the periphery where immune responses are initiated in an antigen-dependent manner and are termed 'induced Tregs'. Tregs are characterized by their expression for CD4, CD25 and the X-chromosome-encoded transcription factor FoxP3. FoxP3 is a DNA-binding fork-head winged helix transcription factor that acts as a master regulator in promoting Treg cell development. The gene's complete or partial deletion leads to disruption in Treg cell development leading to severe multi-organ autoimmunity as seen in *Foxp3*$^{-/-}$ or scurfy mice (Brunkow et al., 2001). FoxP3 creates the Treg transcriptional program by repressing inflammatory genes encoding IFN-γ, IL-2 and IL-17 while activating genes that encode the Treg-

specific surface markers, such as IL-2Rα (CD25), CD73, CTLA-4, TGF-β, GITR, and CD39. The series of activation and repression collectively enables Treg cell development and suppressive function (Piccirillo, 2020). Tregs express higher levels of the high affinity form IL-2 receptor, consisting of the β chain (CD122), γ chain and α chain (CD25). This enables Tregs to preferentially uptake IL-2 over other IL-2R- expressing T cells. Binding of IL-2 to its receptor on Tregs has been shown to enhance the expression of FoxP3 *via* a STAT-5 dependent pathway and promote cell survival (Laurence et al., 2007).

$CD4^+$ Tregs represent a rare and specialized subset of $CD4^+$ T cells residing throughout primary and secondary lymphoid organs, as well as in non-lymphoid tissues. They play a critical role in preventing destructive self-reactive inflammatory reactions through limiting normal T cell responses to a pathogen. A successful immune defense strategy requires intricate negative regulation to restrict host tissue damage caused by prolonged inflammation. The negative regulation afforded by immune effector functions is complemented by Treg suppression of inflammatory responses. In fact, ablation of Tregs in adult healthy mice leads to augmented generation of Th1, Th2, and Th17 cells and death within two weeks from highly aggressive inflammatory lesions in a variety of organs (Kim et al., 2007). In Tregs, activated STAT3 and FoxP3 co-operatively regulate a subset of genes, which likely endows Tregs with the ability to suppress Th17 cell-mediated inflammation (Chaudhry et al., 2009). Compared to IL-6, IL-10 and its receptor play a more important role in promoting potent STAT3 phosphorylation in Tregs, and mice harboring IL-10R-deficient Tregs develop severe immune-mediated colitis (Chaudhry et al., 2011).

1.2.3. Treg plasticity

Tregs can undergo plasticity by modulating their transcriptional program as they adapt to the dynamics of the inflammatory response in the local inflammatory milieu. The network of local inflammatory and non-inflammatory signals can impact the fate of Tregs, particularly by driving them to either lose their FoxP3-associated transcriptional program or develop a complementary one. This occurs through epigenetic changes in their Treg-specific demethylated region (TSDR) (Huehn et al., 2009). By de-stabilizing their expression for FoxP3, Tregs become non-suppressive and convert into inflammatory cytokine-producing (IL-2, IFN-γ, IL-17) ex-Tregs, which enhance their homing and cytokine-sensing machinery in response to polarizing conditions (Yurchenko, et al., 2012). This allows them to migrate to sites of effector T cell-mediated inflammation and contribute to the onset and maintenance of inflammation and pathology. By modulating their transcriptional programs, Tregs can co-express the lineage-defining transcription factor of the target effector T cell: T-bet (Th1), GATA3 (Th2) and RORγT (Th17). Furthermore, besides the transcriptional regulation of genes, Tregs can integrate tissue-specific environmental cues, deriving from metabolism, nutrition, inflammatory cytokines and alarmins, and hence, differentially regulate their translotome.

Research studies have shown that the relative amounts of IL-6 and TGF-β can deviate the fate of a naïve T cell towards either Th17 or peripherally induced Tregs (Zhou et al., 2008; Bettelli et al., 2006; Ivanov et al., 2006). TGF-β exerts pleiotropic effects on the reciprocal regulation of Th17/Treg cell differentiation. On one hand, TGF-β signaling through TGF-β receptor can lead to the formation of SMAD 2-3-4 complex that binds to the CNS1 region in the FoxP3 locus, thus stabilizing FoxP3 expression. On the other hand, TGF-β superfamily members can synergize with inflammatory cytokines like IL-6 or IL-21 and promote the development of Th17 cells. More to the point, the combination of TGF-β and IL-21 induces the expression of IL-17 in naïve T cells and suppresses that of FoxP3. This suggests that similarly to IL-6, IL-21 can regulate the reciprocal developmental pathway of generation of Tregs and Th17 cells (Korn et al., 2007).
High salt conditions have been shown to activate serum/glucocorticoid-regulated kinase 1 (SGK1) in conventional T cells through $p38^{MAPK}$ signaling. This leads to the deactivation of FoxO1 and subsequent expression of IL-23 receptor that is involved in the maturation and survival of Th17

cells (Wu et al., 2013). In fact, in non-lymphoid tissues, such as the gut and the kidney, high salt diet favors the differentiation of FoxP3$^+$ Tregs towards the specialized RORgT$^+$ Th17 cells, thus promoting a Th17-driven inflammation (Wu et al., 2013).

Originally described to promote Th2 immunity, IL 33/ST2 signaling has later been shown to play an important role in maintaining the stability and suppressive function of FoxP3$^+$ Tregs *in vivo* (Coyle et al., 1999; Schiering, et. al., 2014). IL-33 is an IL-1 family member, which mediates its biological effects by interacting with the heterodimeric receptor complex formed by IL-1RL1 (or ST2) and its co-receptor, IL-1R accessory protein (IL-1RAP). IL-33 is constitutively expressed as a nuclear factor, particularly by cells in the mucosal tissues (Liu et al., 2013). Upon injury, it can be released as an alarmin that activates lymphocytes and myeloid cells. ST2 expression induces a more activated and migratory phenotype in FoxP3$^+$ Tregs favoring their immunosuppressive functions during intestinal tumorigenesis (Pastille et al., 2019).

During the early phase of *C. neoformans* fungal infection, IL-33 is released in the lung mucosa to facilitate its implantation. This occurs while expanding the population of highly suppressive GATA3$^+$ Tregs. As the disease progresses, effector immune responses are initiated in the lungs characterized by increased secretion of the pro-inflammatory IL-1β and the differentiation and expansion of Th17-like RORγT$^+$ Tregs. This favors a pro-inflammatory environment that effectively eliminates fungi (Alvarez et al., 2019). Hence, IL-1 and IL-33 exert opposing functions in modulating the functional adaptation of Tregs in infections, ultimately determining the dynamics of adaptive immunity to pathogens and the ensuing course of infection.

1.3. Hematopoiesis

A stem cell niche is a specialized anatomic microenvironment that supports the ability of stem cells to self-renew and differentiate. The region is populated by a supportive network of stromal cells that express soluble and membrane-bound mediators that control cell survival, proliferation, differentiation, and trafficking. Generation of hematopoietic stem cells (HSCs) takes up residence in the microenvironments of the bone marrow, a primary lymphoid organ that remains responsible for maintaining the HSC pool from mid to late gestation all throughout the life of an adult vertebrate. More than 10^9 hematopoietic cells are produced each day in the homeostatic bone marrow to maintain blood cell counts in the human body (Petvises and O'Neill, 2012). In addition, the bone marrow is responsible for the replenishment of blood cells by supporting the development and maturation of all erythroid and myeloid cells and B lymphocytes in humans and mice. Unlike B- cells, T cells complete their maturation in the thymus. There are extra-medullary sites of minor hematopoiesis such as the spleen or the liver that become essential in supporting the immune response during an infection (Zhu & Emerson, 2002). It is important to recognize that the bone marrow constitutes a site to which fully mature myeloid and lymphoid cells can return and take up long-term residence.

In mice, embryonic hematopoiesis begins after gastrulation at E6 (McGrath, 2005; Galloway & Zon, 2003). Primitive hematopoiesis, consisting mainly of large nucleated red blood cells, is initiated in the yolk sac across E7–E7.5. This marks the start of a second wave of blood cell production on day E8.5. Since the yolk sac cannot support their differentiation, the definitive hematopoietic progenitors move on to differentiate sequentially in aorta-gonad-mesonephros region, placenta, fetal liver, spleen and finally bone marrow at E17.5 persisting through postnatal life (Mikkola and Orkin, 2006). The progenitors migrate to the fetal spleen at E13-E14 and undergo proliferation and differentiation to give rise to mature blood cells. Unlike the fetal liver, the fetal spleen consists of special microenvironments that appear to restrict or favor the development of blood cell lineages and generally does not have significant hematopoietic activity at a normal physiological state (Godin, et al., 1999). Under stress, the spleen can contribute to extramedullary hematopoiesis (Bronte & Pittet, 2013).

HSCs are both self-renewing and multipotential since they can give rise to all differentiated blood cells of lymphoid and myeloid lineages. HSCs are categorized into long term (LT-HSCs) and short

term (ST-HSCs) (Rosenbauer & Tenen, 2007). The former cells are multipotent and capable of self-renewal. They give rise to ST-HSCs, which have a significantly reduced self-renewal capacity but can further differentiate into both common myeloid and common lymphoid progenitors, CMP and CLP respectively (**Figure I**). An individual HSC may possess primed gene characteristics of multiple lineages and depending on the environmental stimuli to which the HSC is exposed, primed chromatin regions will be targeted by transcription factors driving the cell down several possible developmental pathways.

HSCs have no lineage markers and are described as Lin^-. They express the cell surface receptor tyrosine kinase c-Kit (CD117), whose interaction with the stem cell factor (SCF) cytokine is critical for the development of multipotential progenitor cells (MPPs). Membrane-bound SCF retains the HSC and its daughter progenitor cell in the appropriate environmental niche in the bone marrow. HSCs also express the stem cell associated antigen (Sca-1). The HSC-containing $Lin^-Sca\text{-}1^+c\text{-}Kit^+$ (LSK) cell population is capable of self-renewal and differentiation. The HSCs differentiate towards MPPs, which differentiate further to various progenitor types.

Common myeloid progenitors (CMPs; $CD34^+$ $CD16/32^-$) give rise to granulocyte-monocyte progenitors (GMPs) and megakaryocyte-erythrocyte progenitors (MEPs). GMPs ($CD34^+$ and $CD16/32^+$) differentiate to granulocytes, monocytes, and dendritic cells. MEPs ($CD34^-CD16/32^-$) give rise to erythrocytes and megakaryocytes. Common lymphoid precursors (CLPs; $IL\text{-}7R^+$) give rise to all lymphoid cells, particularly B cells, T cells, NK cells and DCs. The $Flt3^+$ subset of CMPs and CLPs gives rise to dendritic cells (Karsunky et al., 2003). More recently additional progenitor subsets, including macrophage and dendritic cell precursor (MDP) and common monocyte progenitors (cMoPs), were introduced as progenies of the GMP population. (Alvarez-Errico et al., 2015; Ginhoux & Jung, 2014). Overall, distinct checkpoints, specific transcription factors and discrete epigenetic changes are required for differentiation from one progenitor state to the next (Alvarez-Errico et al., 2015). Nevertheless, the concept of distinct progenitor states defined by cell-surface markers has been challenged by a newer model of hematopoiesis due to its limitation in faithfully reflecting the internal state of progenitor cells (Paul et al., 2015). The current model implies that an early commitment with a protracted phase of differentiation would lead to a gradual change over time from an HSC into a fully committed lineage cell (Schultze, & Beyer 2016). Based on transcriptional sorting of myeloid progenitors, the researchers proposed that multiple

transcription factors combinatorially drive the differentiation within the myeloid compartments and towards multiple functional cell types (Paul et al., 2015). Furthermore, later studies have implicated the role of myelopoiesis (i.e., generation of myeloid cells) as integral to the process of "trained immunity", which results in a sustained favorable response of myeloid cells to a secondary challenge despite their short lifespan in circulation (Mitroulis et al., 2018; Khan et al., 2020).

In the adult, HSCs migrate from the bone marrow into the bloodstream at steady state to maintain homeostasis. Their egress from the BM to extramedullary tissues is dependent on several mechanisms: CXCL12 or stroma-derived factor-1 (SDF-1) and its receptor CXCR4; Very late antigen-4 (VLA-4: integrin-α4β1) that binds to vascular cell adhesion molecule-1 (VCAM-1) expressed on BM stromal or endothelial cells; and the expression of sphingosine-1-phosphate receptors ($S1P_1$) (Lapid et al., 2012). HSCs are further retained within tissue sites and amplify in response to the activation of their surface- expressed Toll-like receptors, and this is mediated by the reduction in the expression of $S1P_1$ (Lapid et al., 2012).

While some studies challenge the existence of quiescence by suggesting that HSCs constitute a homogenous infrequently dividing pool of cells that regularly but asynchronously enter the cell cycle, other studies report the existence of a highly dormant HSC population harboring the vast majority of stem cell activity (Cheshier etal., 1999; Kiehl et al., 2007; Wilson et al., 2008). To elaborate, HSCs divide infrequently with the turnover of the HSC pool occurring ever few weeks. In mice, dormant HSCs divide every 145 days or five times per lifetime. The HSC pool is maintained by protecting the HSCs from premature exhaustion under stressful conditions, in which cells can undergo reversible self-renewal. In response to bone marrow injury or G-CSF stimulation, quiescent cells can enter the cell cycle then reversibly switch back to dormancy (Wilson et al., 2008). In adulthood, the HSC system requires maintenance for the most part. Although the HSC compartment is needed for producing billions of cells to replace short-lived cell types, it requires significantly less cellular proliferation compared to the rate needed to sustain the expansion and growth phases of embryonic and postnatal development (Wilson et al., 2008).

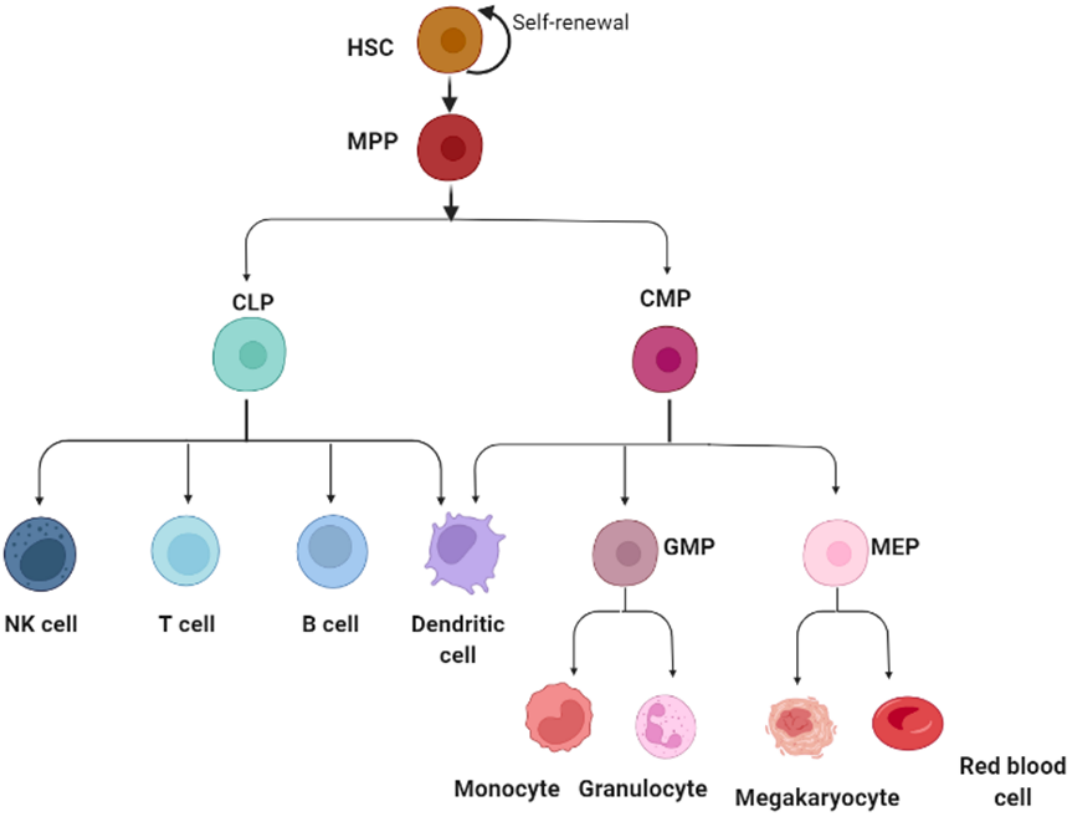

Figure I. Schematic representation of a simplified model of the hematopoietic tree.

Hematopoietic stem cells (HSCs) in the bone marrow give rise to all immune cells. Stem cells are capable of self-renewal and differentiation. HSCs give rise to multipotent progenitors (MPPs), which in turn differentiate into common lymphoid progenitors (CLPs) and myeloid progenitors (CMPs). CMPs give rise to granulocyte-monocyte progenitors (GMPs) and megakaryocyte-erythrocyte progenitors (MEPs). GMPs give rise to granulocytes (neutrophils, eosinophils, basophils, mast cells) and to monocytes, while MEPs give rise to erythrocytes/red blood cells (RBCs) and to megakaryocytes. CLPs give rise to T cells, B cells, and NK-cells. Dendritic cells can be derived from both myeloid and lymphoid progenitors. *The diagram was created in Biorender.*

1.4. Cytokines and Chemokines

Cytokines and chemokines are low molecular weight proteins released from a broad range of cells, including immune (innate and adaptive) and non-immune cells (e.g., epithelial cells, endothelial cells, adipocytes, and fibroblasts). They relay soluble regulatory signals that modulate inflammatory responses towards a pro- or anti-inflammatory phenotype. Cytokines may act locally on the cells that secrete them (autocrine), on neighboring cells (paracrine), or on distant cells (endocrine) (Zhang & An, 2007). They can be pleiotropic, such that one cytokine has different effects on different cells, or redundant, such that different cytokines exert the same effect. They can also act in synergy or antagonize each other, and their signaling can have a cascade effect, whereby cytokines stimulate the production of other cytokines (Zhang & An, 2007).

Cytokines released by activated immune cells particularly heighten the inflammatory state in the body and facilitate pathogen-control (Parkin and Cohen, 2001). Increased secretion of pro-inflammatory cytokines (e.g., TNF, IL-6, IL-1) causes an influx of other immune cells, mainly neutrophils, lymphocytes, and monocytes from the circulation into the site of infection or injury. However, exacerbated production of these cytokines may be deleterious and even lead to death of the host organism (Cavaillon, 2001; Dinarello, 2000). Hence, their secretion must be transient and controlled for by a series of immunoregulatory molecules, such as IL-10, IL-4, IL-13 and TGF-β, which exert an anti-inflammatory effect (Dinarello, 2000; Zhang and An, 2007).

1.4.1. Pro-inflammatory Cytokines

1.4.1.1.Tumor Necrosis Factor-α (TNF-α)

TNF-α was first discovered as a molecule that induces necrosis in tumors (Carswell, 1975). It is a powerful pro-inflammatory cytokine and one of the most abundant early mediators in inflamed tissues. Its ability to exert its effects on many organs allows it to induce septic shock (Duque and Descoteaux, 2014). The TNF superfamily regulates several critical normal physiological functions including cell proliferation, survival, differentiation, and apoptosis. By interacting with its receptors TNFR1 and TNFR2, TNF-α can activate various signaling pathways, including NF-κB, extracellular signal-regulated kinase (ERK), p38 mitogen-activated protein kinase ($p38^{MAPK}$) and c-Jun N terminal kinase (JNK) (Aggarwal et al., 2012). Moreover, TNF induces vasodilation,

disrupts vascular permeability, and regulates chemokine release enabling infiltration of lymphocytes, neutrophils, and monocytes. TNF-α can regulate the production of pro-inflammatory cytokines thus orchestrating the cytokine cascade in various inflammatory conditions. As such, aberrant TNF-α production or signaling has been associated with the pathogenesis of inflammatory diseases, such as Crohn's disease, atherosclerosis, and arthritis (Parameswaran and Patial, 2010).

1.4.1.2.Interleukin-6 (IL-6)

IL-6 is a pleiotropic cytokine with both pro-inflammatory and anti-inflammatory functions that affect inflammation, immune responses, metabolism, and neural processes. Produced by stimulated immune cells and fibroblasts, IL-6 is one of the most extensively documented cytokines due to its ubiquitous nature and chronic elevation within various inflammatory disease states (Andus, et al., 1998; Akira, et al., 1993). IL-6 can interact with membrane-bound IL-6 receptor (IL-6R), in a process known as classic signaling, and it can also interact with soluble IL-6R to form a complex that binds to glycoprotein GP-130, in a process known as trans-signaling. These interactions lead to IL-6-signal transduction, which includes the activation of JAK/STAT, ERK, and PI3K signal transduction pathways (Scheller, 2011). IL-6 signaling leads to the recruitment of monocytes to sites of inflammation, the development of Th17 cells, the inhibition of T cell apoptosis, and the regeneration of the intestinal epithelium (Scheller, 2011). It also contributes to the host defense mechanism/acute phase response to trauma (i.e., burns or infections), hematopoiesis and the synthesis and release of acute phase proteins and antibodies (Andus, et al., 1988; Tanaka, Narazaki and Kishimoto, 2014).

1.4.1.3.Interferon- γ (IFN-γ)

Interferons are known to induce an anti-viral state by blocking viral replication and curbing the spread of infections. Mammals possess three classes of IFNs: type I (IFN-α/β), type II (IFN-γ) and type III (IFN-λs) (McNab et al., 2015).

IFN-γ was classified in the IFN family due to its ability to 'interfere' with viral replication (Wheelock et al., 1965). Yet, unlike other interferons, IFN-γ is more notable for its broader ability to modulate the immune system. Secreted by activated Th cells and NK cells, IFN- γ can help drive a Th1 response and can initiate a positive feedback mechanism by further enhancing the secretion

of IL-12 by DCs and macrophages. Further studies showed that IFN- γ can help facilitate bacterial control and clearance (Gilchrist et al., 2015; Kawai and Akira, 2006).

The full biologic function of IFN-γ is mediated by the interaction with the dimerized receptor complex: IFN-γR1 and IFN-γR2. Signaling through the receptor complex recruits the tyrosine kinases JAK1 and JAK2 that activate STAT1 through phosphorylation on tyrosine residue 701. Phosphorylated STAT1 homodimerizes, and the complex translocates to the nucleus to activate the transcription of IFN-γ-associated genes required for protective immunity (Begitt et al., 2014; Boehm et al., 1997; Platanias, 2005; Shtrichman and Samuel, 2001). IFN-γ is extremely pleiotropic, as it influences the expression of over 200 genes (Boehm et al., 1997). Furthermore, IFN-γ undergoes a self-regulatory process critical to the homeostasis of the immune system. As the inflammation intensifies, IFN-γ production increases. When inflammation reaches its culmination, IFN-γ activates regulatory mechanisms that deliver negative feedback driving its reduction. Thereby, its uncontrolled expression has been linked to inflammatory and autoimmune diseases (Sarvetnick et al., 1990; Hirsch et al., 1985; Neurath, 2014; Verma et al., 2013; Ito et al., 2006).

1.4.1.4.Interleukin-12 (IL-12)

The IL-12 family includes the following heterodimeric cytokines: IL-12, IL-23, IL-27 and IL-35. IL-12 is comprised of the p35 and p40 subunits that bind together to form the bioactive form of IL-12 (P70) (Duque and Descoteaux, 2014). It is a pro-inflammatory cytokine that is primarily released by antigen presenting cells in response to cancer or infections. IL-12 promotes cell-mediated immunity via stimulation of Th1 cells. It synergizes with TNF and other proinflammatory cytokines in stimulating IFN-γ production, as well as the cytotoxicity of NK and $CD8^+$ T cells.

1.4.1.5.Interleukin-1 (IL-1)

Both IL-1α and IL-1β are pro-inflammatory cytokines and perform redundant functions through interacting with the IL-1 receptor (IL-1R). They are members of the interleukin family of cytokines acting as important pro-inflammatory mediators involved in various cellular functions, such as inflammasome signaling, cell death, proliferation, and survival (Schroder and Tschopp, 2010; Duque and Descoteaux, 2014). IL-1β, secreted out of pyroptotic cells, is an endogenous

pyrogen that induces fever apart from stimulating leukocyte migration and chemokine production (Delaleu and Bickel, 2004).

1.4.1.6.Interleukin-17 (IL-17)

IL-17A is the founding member of the IL-17 family that also includes IL-17B through to IL-17F. IL-17A/IL17F homo- and heterodimers bind to the heterodimeric receptor IL-17R. IL-17R can be found on the surface of neutrophils, keratinocytes, and other non-lymphoid cells. IL-17, also known as IL-17A, can be produced by various immune cells, most notably Th17 cells, γδ T cells, NK cells, $CD8^+$ T cells and NKT cells (McGeachy, Cua and Gaffen, 2019). IL-17A and most of the other members of the IL-17 family of cytokines share the property of linking the activation of T cells to neutrophil mobilization and activation. Exceptionally, IL-17E promotes the anti-inflammatory Th2 responses and suppresses Th17 responses (McGeachy, Cua and Gaffen, 2019). As such, IL-17A plays a role in mediating a protective innate immunity to infectious pathogens or in driving the pathogenesis of inflammatory diseases, such as psoriasis and rheumatoid arthritis. Analogous to signaling through IL-1R, signaling through most IL-17 receptors results in the activation of different pathways: 1. NF-kB pathway to induce cytokine expression; 2. MAP-Kinase pathway that imposes an inhibitory phosphorylation on Tristetraproline (TTP) enhancing the stability of cytokine mRNA; 3. C/EBP transcription factor to promote the expression of the pro-inflammatory cytokine IL-6 (McGeachy, Cua and Gaffen, 2019).

A critical role for IL-17R signaling in mediating protection against bacterial and fungal infections, particularly by *Candida albicans* and *Klebsiella pneumoniae*, has been described in various studies in mice (Gu and Li, 2013). In humans, mutations in IL-17 signaling genes (*Act1*, *Il17RA*, *Il17RC*) are associated with chronic mucocutaneous candidiasis (Puel et al., 2011; Boisson et al., 2013). Moreover, there is tissue-specific IL-17-dependent gene induction (Chang and Dong, 2011). In fact, IL-17 has been shown to be crucial in the pathogenesis of autoimmune diseases including Experimental Autoimmune Encephalomyelitis (EAE), arthritis, psoriasis, and IBD (Steinman, 2010). Thus, IL-17 has been targeted for therapeutic approaches that include the use of anti-IL-17 and anti-IL-17 receptor antibodies to treat several autoimmune syndromes. In particular, the administration of IL-17-neutralizing antibodies were shown to attenuate the intestinal inflammation in a T cell transfer model of colitis, implicating the critical role that IL-17-secreting T cells play in the induction of colitis (Yen et al., 2006).

1.4.1.7.Interleukin-10 (IL-10)

IL-10 is the founding member of the so-called IL-10 family (including IL-10, IL-19, IL-20, IL-22, IL-24 and IL-26). It is a cytokine with anti-inflammatory properties and is broadly expressed by many immune cells. These include cells of the adaptive immune system (Th1, Th2, Th17, Tregs, $CD8^+$ T cells and B cells) and cells of the innate immune system (dendritic cells, macrophages, mast cells, natural killer cells, eosinophils, and neutrophils) (Saraiva and O'Garra, 2010). All these cell types secrete IL-10 in response to different stimuli, thus providing the immune system with an exquisitely regulated mechanism to control the effects of pro-inflammatory cytokines in a tissue-specific and temporal manner. Murine and human *Il-10* genes carry sequence identity and similar location of recognized transcription factors. Both species contain a TATA box and a CCAAT box (CCAGT in mice) in the promoter region of the *Il-10* gene (Iyer and Cheng, 2012; Saraiva and O'Garra, 2010).

IL-10 assembles as a homodimer with each monomer consisting of 6 alpha helices (Moore, et al., 1993). Its immunosuppressive activity is mediated by the heterodimeric IL-10 receptor consisting of two molecules of IL-10R α-chain (IL-10R1) and two molecules of the IL-10R β-chain (IL-10R2) (Zdanov, et al., 1995). IL-10R1 specifically binds IL-10 promoting a conformational change that enables the oligomerization with IL-10R2 (Yoon et al., 2006).

Several transcription family members including specificity protein (Sp), signal transducers and activators of transcription (STAT), interferon regulatory factors (IRF), activator protein (AP), cAMP response element binding protein (CREB), CCATT enhancer/binding protein (C/EBP), c-musculoaponeurotic fibrosarcoma factor (c-MAF), and nuclear factor κ-B (NF-κB) have been proposed as critical factors that regulate IL-10 activation (Iyer and Cheng, 2012).

One of the several mechanistic pathways through which IL-10 operates is the JAK-STAT3 pathway (Mosser and Zhang, 2008). Receptor ligation activates Jak1 and Tyk2 kinases, resulting in the recruitment of the transcription factor STAT3. Phosphorylated STAT3 dimer is translocated into the nucleus within seconds to activate the transcription of specific immunomodulatory genes involved in immunosuppression. Ultimately, this results in the inhibition of the release of pro-inflammatory mediators, reduction in antigen presentation and phagocytic capacities while enhancing the inhibitory, tolerance and scavenger functions of cells. In fact, IL-10 can help reduce the expression of MHC molecules on APCs, mainly macrophages and dendritic cells, and

accordingly dampen T- cell priming (de Waal, et al., 1991; Mittal and Roche, 2015). Tregs exert their functions in part through the production of anti-inflammatory cytokines, including IL-10 and TGF-β (Moore, et al., 2001). IL-10 is induced at later phases of the immune response to help resolve inflammation and prevent tissue damage caused by excessive immune activation.

Deficiency in IL-10 production by Tregs has been shown to result in the development of spontaneous gut inflammatory disease, highlighting the importance of IL-10 in maintaining gut homeostasis (Engelhardt and Grimbacher, 2014; Glocker et al., 2009).

Although abrogation of IL-10 signaling imposes detrimental long-term consequences, it can also be beneficial in accelerating the clearance of intracellular bacteria, as well as certain viruses, parasites, and fungi, thereby improving survival post-infection (Cyktor & Turner, 2011; Sabat et al., 2010; Greenberger et al., 1995; Dai et al., 1997). However, heightened Th1 responses, in the prolonged absence of IL-10 signaling, can also result in severe pathology and lethal inflammatory responses in particular infections (Igietseme et al., 2000). For instance, IL-10-deficient mice exhibit increased mortality rate upon infection with the intestinal helminth *Trichuris muris* due to increased intestinal inflammation related to loss of Paneth cells and mucus production (Schopf et al., 2002).

1.4.2. Chemokines

Chemokines, or chemotactic cytokines, are a superfamily of approximately low molecular weight (8-15KDa) soluble cytokines that differ from other cytokines by binding to several G-protein-coupled serpentine receptors to mediate various intracellular signaling pathways. As a chemoattractant, the chemokine primarily induces the recruitment of immune cells (chemotaxis) to inflammatory sites and secondary lymphoid organs (Moser and Loetscher 2001). For a cell to respond to a chemokine, it must express a complementary chemokine receptor.

In addition to serving as immune regulators, chemokines play important roles in development, inflammation, immune diseases, cancer, angiogenesis, hematopoiesis, and atherosclerosis (Luster 1998; Romagnani et al. 2004; Vandercappellen et al. 2008; Singh et al. 2011). Chemokines were initially named according to their function or based on the cell type that produced them. Some examples include monocyte chemoattractant protein 1 (MCP-1), stromal derived factor 1 (SDF-1) and mucosae-associated epithelial chemokine (MEC) (Proudfoot, 2002). This was later followed by adopting a systematic nomenclature. According to the number and position of conserved cysteines in the amino-terminal domains, chemokines can be divided into four subgroups: C, CC, CXC and CX3C. These are followed by the letter L (denoting 'ligand') and a number according to when the gene was first isolated (Murphy et al., 2000; Zlotnik and Yoshie, 2000).

Excessive recruitment of leukocytes is a well-orchestrated process at steady state but can also be the hallmark of inflammation occurring in both acute and chronic inflammatory disorders. On one hand, CC chemokines typically mediate chronic inflammation to recruit eosinophils and T cells in asthma, and monocytes/macrophages and T cells in autoimmune diseases, such as multiple sclerosis. On the other hand, CXC chemokines are mainly responsible for acute inflammation to recruit neutrophils in syndromes/diseases such as acute respiratory distress syndrome (Proudfoot, 2002). Exceptionally, CXCR3 plays a specific role in Th1 priming during chronic inflammation (Bromley et al., 2008; Groom et al., 2012; Proudfoot, 2002).

Different T cells express distinct chemokine receptors that define their functions. For instance, CCL1 (I-309), CCL11 (Eotaxin), CCL17 (Tarc), CCL22 (MDC; macrophage-derived chemokine), CCL24 (MPIF-2; myeloid progenitor inhibitory factor 2) and CCL26 (Eotaxin-3) selectively recruit Th2 lymphocytes, which express CCR4, CCR8 and CCR3 (Mathew et al., 2001; Ono et al., 2003). In contrast, Th1 cells preferentially express CCR5, CXCR3 and CXCR6 and migrate in response to CCL3 (MIP-1α; macrophage inflammatory protein 1α), CCL4 (MIP-1β), CCL5 (RANTES) or the ELR negative CXC chemokines (Luther and Cyster, 2001). CCL2 (MCP-1) attracts CCR2- expressing monocytes to migrate from the blood to injured and inflamed tissues, where they transform into tissue macrophages. CXCL1 (GROα), CXCL2 (SDF-1), CXCL3 (GROγ), CXCL5 (ENA-78; epithelial cell–derived neutrophil attractant) are members of the CXCL class of chemokines with neutrophil chemotactic and angiogenic biologic properties. CXCL9 (MIG; monokine induced by gamma) and CXCL10 (IP-10; IFN-γ–inducible 10 kDa protein) are produced by mature DCs in the draining lymph nodes. They promote stable contacts between migrating $CD4^+$ T cells and DCs, necessary for optimal Th1 differentiation (Groom et al., 2012). In response to IFN-γ, macrophages and stromal cells release CXCL9, directing other immune cells toward the sites of infection (Sung et al., 2012).

1.5. Inflammatory Signaling & Cell Death Pathways

1.5.1. NF-κB signaling pathway

NF-kB (nuclear factor kappa-light-chain-enhancer of activated B cells) is a protein complex that serves as an inducible transcription factor influencing the expression of numerous genes involved in multiple physiological and pathological responses. Its activity is tightly regulated at multiple levels through a diverse array of post-translational modifications (Oeckinghaus and Ghosh, 2009). NF-kB is a central mediator of immune and inflammatory responses allowing the host to respond and adapt effectively to environmental changes. Its activation is induced by infections, cytokines, physical stress (i.e., UV- or γ-irradiation), physiological stresses (i.e., ischemia and hyperosmotic shock) or oxidative stresses. In mammals, the NF-kB/Rel family comprises five members: p100/52 (NF-κB2), p65 (RelA), RelB, p105/p50 (NF-κB1) and c-Rel (Oeckinghaus and Ghosh, 2009). These proteins associate with each other to form distinct transcriptionally active homo- and heterodimeric complexes, with p50/65 heterodimer being the most abundant and found in all cell types (Oeckinghaus and Ghosh, 2009). Inactive NF-kB dimers are usually retained in the cytoplasm via interactions with regulatory proteins called inhibitors of κB (IκB), of which the most important may be IκBα, IκBβ, and IκBε. Different IκB molecules have distinct and overlapping specificities. Upon stimulation, these inhibitors are phosphorylated by the IKK (IκB kinase) complex which leads to their degradation and consequent relocation of NF-κB to the nucleus. In the nucleus, activated NF-κB can induce the transcription of target genes that encode pro-inflammatory mediators, growth factors and immunoregulatory proteins (Oeckinghaus and Ghosh, 2009). It may also act in concert with other transcription factors to regulate the expression of genes that are involved in various key cellular processes, including cell survival, proliferation, and immunity. Hence, aberrant activation of NF-κB has been associated with various inflammatory conditions, such rheumatoid arthritis, colitis, cancer, and multiple sclerosis (Courtois & Gilmore, 2006).

1.5.2. p38 ^{MAPK} signaling pathway

Mitogen activated protein kinases (MAPKs) are serine-threonine protein kinases that modulate numerous processes, including innate immune responses, apoptosis, metabolism, and proliferation (Keshet and Seger, 2010). Four distinct subgroups within the MAP kinase family have been described: (1) ERKs, (2) c-jun N-terminal or stress-activated protein kinases (JNK/SAPK), (3) ERK/big MAP kinase 1 (BMK1), and (4) the p38 group of protein kinases.

The p38 ^{MAPK} pathway is known to be activated in response to stress, inflammatory stimuli, or DNA damage (Kotlyarov et al., 1999). P38 family members include p38α (p38), p38β, p38γ (ERK6, SAPK3) and p38δ (SAPK4), with a 60% similarity among the isoforms. They are characterized by a Thr-Gly-Tyr (TGY) dual phosphorylation motif in the activation segment (Zarubin and Han, 2005). p38β are ubiquitously expressed, while p38γ and p38δ are differentially expressed depending on tissue type. Like all MAPKs, p38 kinases are activated by dual kinases termed the MAP kinase kinases (MKKs). The upstream cascade for the p38^{MAPK} pathway includes MKK3, MKK6, MLK2, MLK3, MEKKs, ASKs, TAK1, TAO1 and TAO2 (Keshet and Seger, 2010). Furthermore, downstream of p38 are the kinases MK2/3, PRAK, MSK1 and MSK2, as well as various transcription factors (Morrison, 2012).

MAPK-activated protein kinase 2 (MK2) is a stress-activated kinase that plays a role in many cellular processes including cytokine production, cellular migration, cell cycle, DNA damage response and transcriptional regulation. MK2 promotes the regulation of cytokines at a post-transcriptional level and can be targeted for specific anti-inflammatory therapy (Kotlyarov et al., 1999). For instance, it is known to phosphorylate TTP at Ser-52 and Ser-178 which impairs the ability of TTP to bind to the ARE elements in TNF-α mRNA resulting in increased stability of TNF-α mRNA (Hitti et al., 2006).

MK2 activation is involved in the inflammatory response by regulating the production of cytokines such as TNF-α and IL-6. Hence, MK2 is implicated in the pathogenesis of acute and chronic diseases, such as IBD, arthritis, pancreatitis, skin inflammation and asthma (Feng and Li, 2011; Fiore et al., 2016; Singh et al., 2017). Taken together, these studies implicate a high potential role of MK2 as a regulator of immune responses.

1.5.3. Reactive oxygen species (ROS)

Reactive oxygen species (ROS) comprise highly reactive small molecules/compounds derived from oxygen (O_2). ROS include oxygen ions (such as hypochlorite ion, OCl^-), free radicals (such as hydroxyl radical, ·OH) and molecules such as hydrogen peroxide (H_2O_2) (Thannickal et al., 2000).

ROS can be generated from oxygen by a process called the respiratory burst, which is induced upon external stimulation, such as ionizing radiation/ultraviolet light, and as natural byproducts of cellular respiration (Redza-Dutordoir and Averill-Bates, 2016). While free radical production was considered as an "electron slippage" in the past, it is now deemed to have beneficial effects at low or physiological concentrations. On one hand, ROS can act as signaling agents and participate in phagocytosis as potent microbicidal agents. On the other hand, they can damage DNA and trigger apoptosis (Redza-Dutordoir and Averill-Bates, 2016). Due to the dual nature of ROS, cells need to exquisitely balance their generation and removal to ensure signaling is properly achieved without causing significant damage to the cell.

To ensure maximum efficiency and protection from the harmful effects of ROS, cells activate their enzymatic and non-enzymatic antioxidant defense mechanisms that can work collaboratively. Antioxidant enzymes include glutathione peroxidase, thioredoxin, superoxide dismutase, and catalase. Ascorbic acid (vitamin C), α-tocopherol (vitamin E), glutathione (GSH), carotenoids, flavonoids and others are non-enzymatic antioxidants (Cadenas, 1997; Valko et al., 2007; Mailloux et al., 2013a).

In case of a dysfunctional antioxidant system or when the cellular production of ROS overwhelms the cell's antioxidant capacity, damage to cellular macromolecules such as lipids, proteins, and DNA may ensue. Such a state of "oxidative stress" is thought to contribute to the pathogenesis of several human diseases (Cross et al., 1987; Alzoghaibi, 2013; Van Eeden & Sin, 2013).

In innate immune cells, ROS production occurs both at the plasma membrane, by NADPH oxidase, and within the cytosol by the mitochondria. Some forms of these small ROS are also able to diffuse across membranes and into neighboring cells, where they can propagate the effects of inflammation (Thannickal et al., 2000; Fernandez-Checa and Kaplowitz, 2005).

1.5.4. Cell Death

Cell death is an indispensable mechanism for the development and the maintenance of all forms of complex life. The maintenance of an appropriate balance between cell death, cell proliferation, and cell differentiation is necessary for adult tissue homeostasis throughout life (Fuchs and Steller, 2011). From the outset, cell death, induced by cellular damage or by pathogens directly, is thought to play a central role in the initiation of an inflammatory response. In some cases, immune cells must also become resistant to normal cell death pathways to function within infected and cytotoxic microenvironments. Many forms of programmed cell death (PCD) have been characterized and are distinguished by their impact on the host. These forms include necroptosis, autophagy, pyroptosis, parthanatos, NETosis, mitochondrial permeability transition (MPT)-driven necrosis, and ferroptosis (Galluzzi et al., 2018; Y. Yang, Jiang, Zhang, & Fan, 2015). Currently, biochemical events along with morphological manifestations are used to identify and classify different types of PCD. In general, PCD is categorized into two major subtypes: caspase-dependent and caspase-independent. Caspase-dependent cell death includes apoptosis and pyroptosis.

1.5.4.1. Apoptosis

Apoptosis is a non-immunogenic and anti-inflammatory form of PCD that promotes the immune response. It is associated with various biochemical and physical changes in the cytoplasm, nucleus and plasma membrane and is driven by the activation of caspases and inhibition of Bcl-2 proteins (Lawen, 2003). These factors can be activated by an intrinsic or an extrinsic cell death mechanism (Elmore, 2007; Heckmann et al., 2019; Taylor et al., 2008). Apoptosis can be induced intrinsically by non-receptor-mediated internal stimuli, including oxidative stress, hypoxia, toxins or viral infections (Elmore, 2007). This leads to the opening of the mitochondrial permeability transition pore in the inner mitochondrial membrane and the subsequent release of several pro-apoptotic proteins into the intermembrane space to form the apoptosome complex. In turn, the complex recruits procaspase-9 and induces its allosteric activation to caspase-9, which then cleaves other downstream caspases (caspase-3, -6 and -7) resulting in their activation (Parrish et al., 2013). Apoptosis can also be induced extrinsically by binding of ligands, such as TNF-α, Fas ligand (FasL) and TNF-related apoptosis inducing ligand (TRAIL), to their respective cognate receptors: TNFR1, FasR, TRAILR1 and TRAIL-R2 (Fulda & Debatin, 2006). The ligand/receptor interaction

induces a conformational change in the receptor's death domain resulting in the recruitment of several adaptor molecules and the subsequent activation of pro-caspase 8 or 10 (Elmore, 2007). Together, these changes result in formation of a complex called the death inducing signaling complex (DISC), which recruits and activates caspase 8 (Elmore, 2007; Lawen, 2003). The catalytically active caspase-8 then activates the "executioner" caspases, 3 and 7, promoting apoptosis (Heckmann, Tummers, & Green, 2019). The extrinsic apoptotic pathway can be regulated by cellular FLICE inhibitory protein (cFLIP), an endogenous inhibitor of apoptosis, and by X-linked inhibitor of apoptosis protein (XIAP), an E3 ubiquitin ligase and member of the IAP family (Heckmann, Tummers, & Green, 2019; Eckelman, Salvesen, & Scott, 2006).

There is an additional pathway that involves T cell mediated cytotoxicity and perforin-granzyme-dependent pathway that can induce apoptosis via either granzyme B or granzyme A. The granzyme A-mediated pathway activates a parallel, caspase-independent cell death via single stranded DNA damage (Martinvalet et al., 2005). The intrinsic, extrinsic and granzyme B-mediated cell death pathways converge at the step that involves the cleavage-mediated activation of the executioner Caspase 3 (Elmore, 2007).

Apoptosis is characterized by cell shrinkage, plasma membrane blebbing, nuclear condensation and nuclear fragmentation (Heckmann, Tummers, & Green, 2019; Kerr, Wyllie, & Currie, 1972). Apoptotic bodies are formed and express 'eat me' signals that are recognized and cleared by the tissue resident phagocytes (i.e., macrophages, dendritic cells, and neutrophils). The integrity of the plasma membrane is maintained preventing the leakage of intracellular content into the microenvironment thereby limiting inflammation (Elmore, 2007). If apoptotic cells are not cleared efficiently by phagocytes, apoptosis can proceed to secondary necrosis (Wyllie at al., 1980).

1.5.4.2. Necrosis

Necrosis involves a sudden loss of membrane integrity that causes the release of cytoplasmic contents, also known as DAMPs, to the external milieu leading to a massive immune response (Martin & Henry, 2013). The direct damage of cell membranes and the interference with the energy supply of the cells are two main mechanisms that distinguish necrosis from apoptosis (Elmore, 2007). Necrosis can be induced in response to uncontrolled exogenous stress conditions, trauma, depletion of ATP or physical damage (Elmore, 2007; Fink and Cookson, 2005; Yang et al., 2015).

Morphologically, necrosis comprises oncosis (cell swelling), dilated organelles, DNA fragmentation and plasma membrane rupture. While necrosis is used to indicate nonapoptotic accidental cell death, it more importantly refers to the morphological stigmata seen after a cell has already died without reflecting how death actually occurred. Both necroptosis and pyroptosis share many of the morphological changes that occur during necrosis, including membrane rupturing and release of DAMPs.

1.5.4.3. Necroptosis

As a highly regulated form of necrosis, necroptotic death induces a robust inflammatory response referred to as "necroinflammation" in the absence of caspase activation or when apoptosis is inhibited (Heckmann, Tummers, & Green, 2019). While caspase 8 is an initiator for extrinsic apoptosis, its inactivation is required to induce necroptosis. It is hypothesized that necroptosis has evolved as an alternative cell death mechanism to control infections with highly virulent and evasive pathogens. Necroptosis is executed by the necrosome, which constitutes the receptor-interacting protein kinase 1 (RIPK1) and RIPK3. It is usually activated by ligand binding on death receptors, such as TNFR1, TNFR2, and Fas (Pasparakis and Vandenabeele, 2015).

1.5.4.4. Pyroptosis

Pyroptosis is an inflammatory form of PCD that is activated following infection or stimulation by sterile triggers, such as aggregated proteins, urate crystals, and cholesterol crystals. Pyroptosis can be defined as caspase-1-, caspase-11-, or caspase-8- mediated cell death that is associated with excessive inflammation and driven by the activation of inflammasomes during an innate immune response (Bergsbaken et al., 2009; Jorgensen and Miao, 2015; Sarhan et al., 2018; Chen et al., 2019; Orning et al., 2018). Upon their activation, inflammatory caspases-1 and 11 cleave pro-IL-1 cytokines such as pro- IL-1β and pro- IL-18, resulting in the activation and secretion of mature IL-1 β and IL-18 (Linkermann and Green, 2014). In contrast to other cytokines that possess a secretory signal for export out of the cell, IL-1 cytokine family lacks a secretory signal and therefore requires processing by the inflammasomes. Among the cytosolic PRRs, certain subsets of NLRs and ALRs are known to form multiprotein complexes, called canonical and non-canonical inflammasomes, which activate pro-inflammatory caspases-1 and 11 respectively (Kayagaki et al.,

2011, Martinon et al., 2002). Among the members of the NLR family, the NLRP3 inflammasome is activated through Priming Signal 1 and Activation Signal 2 in sterile inflammation or microbial infection. NLRP3 has a pyrin domain (PYD) that interacts with the "adaptor protein apoptosis associated speck like protein containing a CARD" (ASC) through its PYD domain. The presence of CARD domain in ASC facilitates the interaction with caspase-1 leading to inflammasome assembly and activation. Pro-caspase-1 is activated via autoproteolytic cleavage within this complex. Active caspase-1 then cleaves the precursors of IL-1β and IL-18, whose production is induced by TLR signaling, into mature cytokines (Lamkanfi &Dixit, 2014). Along with this, active caspase-1 also cleaves gasdermin D (GSDMD), which acts as an effector molecule that compromises the integrity of cell membrane leading to pyroptosis (He et al., 2015). Caspase-11-driven pyroptosis is called the non-canonical inflammasome pathway, which is typically activated in response to cytosolic LPS (Hagar et al., 2013; Kayagaki et al., 2013). It was shown that caspase-11 can directly bind to LPS via its CARD domain without requiring any intermediate intracellular receptor (Shi et al., 2014). Furthermore, three independent studies have shown that apoptotic caspase-8 can cleave GSDMD leading to pyroptosis-like cell death and IL-1β release in murine macrophages (Orning et al., 2018; Chen et al., 2019; Sarhan et al., 2018).

2. Immunometabolism

Inflammation and metabolism are inextricably linked. Modulation of cellular metabolism has been shown to play an important role in inflammatory responses (O'Neil et al., 2016). Alterations in the metabolic pathways, also known as metabolic reprogramming, are coupled to immune cell effector functions, most notably in the production of distinct sets of cytokines. Immune cells activate diverse metabolic pathways to generate adequate levels of energy stores to support their growth, proliferation, and unique functions, as they respond to diverse immunological challenges. In turn, the metabolic status of immune cells can influence their phenotype, polarization to a pro- or anti-inflammatory state, and the resulting efficacy of the immune response (Pearce, 2013). For example, patients with IBD have high numbers of activated immune cells that secrete pro-inflammatory cytokines in both the circulation and the inflamed mucosa. High levels of cytokines can divert a healthy functioning resident cell to a disease promoter by altering its metabolic configuration thus perpetuating chronic inflammation (Zaiatz Bittencourt et al., 2021). Most of the normal tissue is well vascularized and enriched with nutrients and oxygen, but during an immune response, the local microenvironment can become significantly less accommodating due to the competitive prodigious appetite for nutrients (Taylor & Colgan, 2007). Moreover, the inflammatory site can become hypoxic due to the pronounced influx of neutrophils and monocytes (Taylor & Colgan, 2007).

2.1. Metabolism Overview

Occurring in the cytoplasm of the cell, glycolysis is the enzymatically catalyzed process of converting glucose into pyruvate along with generating reduced nicotinamide adenine dinucleotide (NAD+; Reduced, NADH) and adenosine triphosphate (ATP). Pyruvate molecules can either be further metabolized in the tricarboxylic acid (TCA) cycle in the mitochondria or can be alternatively reduced into lactate to replenish the pool of available NAD^+ in oxygen-restricted environments (**Figure II**). Accordingly, glycolysis can occur aerobically or anaerobically depending on the availability of oxygen in the environment.

Mitochondrial oxidative phosphorylation (OXPHOS) generates more than 80% of ATP under normal conditions in most cell types by restoring the reducing agents (formed through aerobic glycolysis and the TCA cycle) back to their oxidized states. This allows for aerobic glycolysis and the TCA cycle to continue. The reducing agents, NADH or $FADH_2$, are shuttled through the different complexes (complex I, II, III and IV) of the electron transport chain (ETC), reaching the final acceptor molecular oxygen and producing enough energy to pump protons out of the matrix. The proton motive force is then used by complex V "ATP synthase" to phosphorylate ADP to ATP as protons return to the matrix (Nicholls and Ferguson, 2002) (**Figure II**). It is estimated that the bulk majority of ROS is produced by the mitochondrial ETC. Specifically, variable amounts of superoxide and peroxynitrite are formed mainly at complexes I and III and can then be metabolized to form other types of ROS and reactive nitrogen species (RNS) (Nicholls and Ferguson, 2002).

One of the factors that can decrease the efficiency of OXPHOS in ATP production is a process known as proton leak, whereby energy substrates are oxidized without the coincident synthesis of ATP as the protons return to the matrix bypassing complex V (Jastroch et al., 2010; Mailloux et al., 2013a).

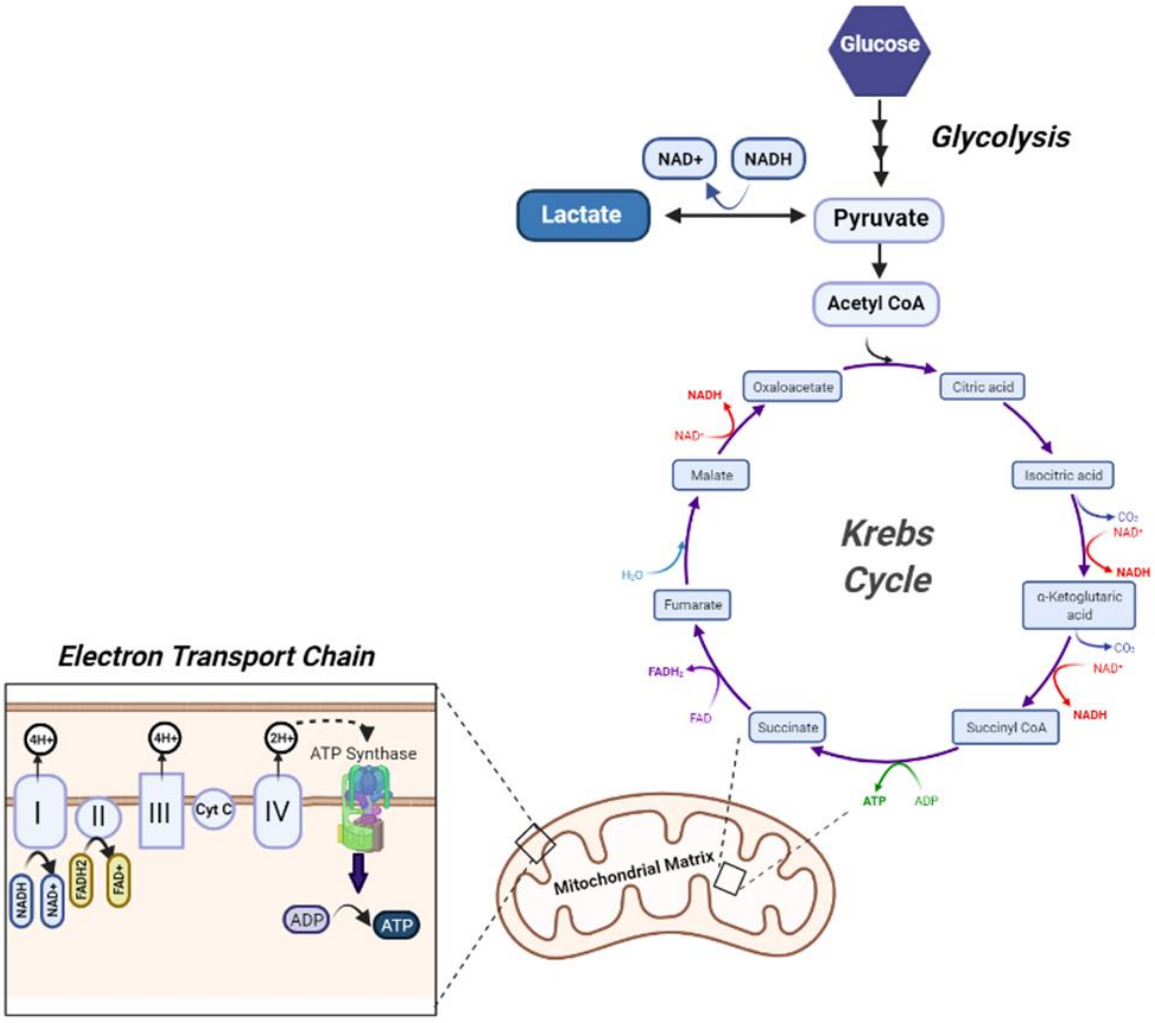
Glucose
Glycolysis
NAD+
NADH
Lactate
Pyruvate
Acetyl CoA
Oxaloacetate
Citric acid
NADH
NAD+
Malate
Isocitric acid
Krebs Cycle
CO2
NAD+
NADH
H2O
Fumarate
α-Ketoglutaric acid
CO2
NAD+
FADH2
FAD
NADH
Succinate
Succinyl CoA
ATP
ADP
Electron Transport Chain
4H+
4H+
2H+
ATP Synthase
I
II
III
Cyt C
IV
NADH
NAD+
FADH2
FAD+
ADP
ATP
Mitochondrial Matrix

Figure II. Schematic representation of the metabolic pathways: glycolysis, Krebs cycle and the electron transport chain.

In the cytosol, glycolysis occurs whereby glucose is oxidized into pyruvate. Pyruvate can then either be converted into lactate, and secreted, or can enter the Krebs cycle (also known as the Tricarboxylic Acid cycle or the Citric acid cycle), in which it will generate NADH and $FADH_2$ for the electron transport chain (ETC), leading to ATP production. To maintain glycolytic flux, cells often reduce pyruvate to lactate to recycle NADH and maintain NAD^+ levels. Glycolytic metabolism is a relatively inefficient pathway netting only two molecules of ATP per unit of glucose. Krebs cycle occurs in the matrix of the mitochondrion, where glucose-derived pyruvate is converted into acetyl coenzyme A (acetyl-CoA) that joins the Krebs cycle by aldol condensation with oxaloacetate to form citrate. NADH and $FADH_2$, major products of the Krebs cycle, can transfer electrons to the ETC. Electrons are shuttled through complexes I, III and IV, and the free energy associated with electron transport drives the pumping of protons out of the mitochondrial matrix into the intermembrane space. This creates an electrochemical gradient, also referred to as the proton motive force, whose potential energy is then used by ATP synthase to phosphorylate ADP to ATP as the protons return to the matrix. The process by which ATP generation is coupled to the movement of electrons through the ETC and the associated oxygen consumption is referred to as Oxidative Phosphorylation. *This diagram was created in Biorender.*

2.2. mTOR signaling

Mitochondrial function and the metabolic flux can be regulated by the mechanistic (or 'mammalian') target of rapamycin (mTOR). mTOR is a serine/threonine protein kinase, activated by the PI3K/AKT pathway, and acts as a sensor for nutrient availability to regulate cellular growth (Brown et al., 1995; Brunn et al., 1997; Burnett et al., 1998). It was named after a natural product isolated in the 1970's from a species of bacteria from the island of Rapa Nui (Vezina et al., 1975). Besides its mild anti-bacterial activity, it was later found to additionally have an inhibitory effect on immune responses in rats (Martel et al., 1977).

Signaling by mTOR is mediated by two distinct core complexes: Raptor-containing TOR complex 1 (TORC1) and Rictor-containing TORC2, which differ in their regulation, function, and sensitivity to rapamycin (Hara et al., 2002; Kim et al., 2002; (Sarbassov et al., 2004). Growth factors regulate both complexes, while several environmental signals, such as levels of oxygen, amino acids, and energy levels additionally regulate mTORC1. mTORC2 regulates cell survival and cytoskeletal reorganization. Activated Akt phosphorylates and inactivates TSC1/2, a GTPase-activating protein for Rheb GTPases, resulting in the activation of mTORC1, and this activation can occur on the surface of lysosomes (Sancak et al., 2010; Bar-Peled et al., 2012). The earliest identified downstream effectors of mTORC1 are the eukaryotic translation initiation factor 4E binding proteins (4E-BP1 and 4E-BP2) and the 70-kDa ribosomal protein S6 kinase (p70S6Kinase) (Brunn et al., 1997; Brunett et al., 1998). S6K1 and 4E-BP1 are the most studied substrates of mTORC1.

In conditions that favor growth, activated mTORC1 phosphorylates 4E-BP1 and P70S6K thereby promoting protein synthesis (Blommaart et al., 1995; Inoki et al., 2012). The highly phosphorylated 4E-BP1 can release the eukaryotic translation initiation factor 4E (eIF4E). This dissociation can recruit the eukaryotic translation initiation factor 4 G (eIF4G) to the 5′ end of most mRNA resulting in increased cap-dependent translation initiation through assembly of the eIF4F complex. P70S6K is a mitogen-activated Ser/Thr protein kinase that promotes cell growth and G1 cell cycle progression. In fact, mTORC1 can regulate protein expression at the transcriptional level or through direct post-translation phosphorylation (Brunn et al., 1997; Burnett et al., 1998; BenSahra et al., 2013).

In addition to protein synthesis, mTORC1 also promotes lipid biogenesis and suppresses autophagy by regulating several other downstream effectors (Porstmann et al., 2008; Ben-Sahra et al., 2013; Ganley et al., 2009; Hosokawa et al., 2009; Jung et al., 2009; Yecies et al., 2011; Ben-Sahra et al., 2016).

Akt-dependent survival function also relies on suppressing the gene expression of cyclin-dependent kinase inhibitors (CDKIs) (e.g., $p27^{Kip1}$ and $p21^{Cip1}$), and pro-apoptotic molecules (e.g., Bcl2-family proteins and Fas ligand) (Zhang et al., 2011). This can be mediated by FoxO family of transcription factors. The rapamycin -FKBP12 complex inhibits mTORC1 following treatment with rapamycin, while effects of rapamycin on mTORC2 are only observed following longer term treatment (Yang et al., 2003; Sarbassov et al., 2006; Gaubitz et al., 2015).

Another critical regulator of metabolism is AMPK that senses the relative concentration of ATP to its low energy enzymatic products AMP and ADP. Hence, when cellular energy stores are low, AMPK is activated and phosphorylates components of cellular energetic pathways, including glycolysis, mitochondrial metabolism, and lipid metabolism (Herzig & Shaw, 2018). A double negative feedback loop exists between AMPK and mTORC1, such that AMPK has both direct and indirect positive effects on autophagy induction (Holczer et al., 2019). It also activates the TSC complex thus inhibiting mTORC1 (Inoki et al., 2003; Gwinn et al., 2008).

2.3. Regulation of Myeloid Cell Metabolism

Although the metabolic response to inflammation varies between cell types, the initial pro-inflammatory phase is typically associated with an increase in the glycolytic rate (O'Neill et al., 2016). Inhibition of glycolysis with the non-metabolizable glucose homolog 2-deoxyglucose (2-DG) prevents pro-inflammatory activation of monocytes and macrophages and suppresses NF-κB signaling in fibroblasts indicating that glycolysis is essential for inflammation in many cell types (Hamilton et al., 1986; Kawauchi et al., 2008b; Lee et al., 2019; Liu et al., 2016; Michl et al., 1976; Tannahill et al., 2013). This is probably due to the need for rapid, as opposed to efficient, ATP production during the initial pro-inflammatory phase.

The metabolism of myeloid cells differs depending on their environment and stimuli, and this impacts their function. The stimulation of TLR4 with LPS induces a quick switch of monocytes and macrophages from OXPHOS to glycolysis; however, the stimulation of other Toll-like receptors, e.g., TLR- 2, by Pam3CysSK4 increases OXPHOS and mitochondrial activity (Loftus & Finlay, 2016). As a matter of fact, mature myeloid cells, such as activated M1 macrophages, DCs and neutrophils, are highly glycolytic with little or no flux through OXPHOS.

In myeloid cells, the TCA enzymes are repurposed to generate molecules with pro-inflammatory functions (Loftus & Finlay, 2016). For instance, DC activation is contingent upon the metabolic switch from fatty acid oxidation and OXPHOS to glycolysis, which is essential in regulating DC-induced T cell responses partly because it impacts DC lifespan and hence the duration over which DCs can activate T cells (Loftus & Finlay, 2016). Initially, within minutes of DC activation, glycolysis is enhanced to support the de novo lipid biosynthesis facilitating the expansion of the endoplasmic reticulum and the Golgi apparatus and increasing the biosynthetic capacity essential for mature DC function. Over the course of 18 h, activated DCs sustain elevated glycolysis and inactivate OXPHOS (Loftus & Finlay, 2016). Metabolic reprogramming to aerobic glycolysis allows cells to adapt and survive as they encounter metabolically restrictive conditions, such as hypoxia. Certainly, in activated DCs, preserving OXPHOS results in an increased cellular lifespan.

In dendritic cells, c-Myc promotes the transcription and expression of glycolytic genes, whereas in macrophages and T cells, HIF-1α promotes an increase in aerobic glycolysis (Rodríguez-Prados et al., 2010; Shi et al., 2011; Wang et al., 2011; Tannahill et al., 2013; Liu et al., 2016; Wang et al., 2017; Shi et al., 2019). In macrophages, switching cellular metabolism from glycolysis to OXPHOS promotes a shift from short-lived M1 macrophages to longer-lived M2 macrophages, which function mainly in the resolution phase, tissue repair and inflammation. Through oxidizing both glucose and fatty acids in the mitochondria, M2 macrophages can sustain OXPHOS (Loftus & Finlay, 2016).

2.4. Regulation of T cell Metabolism

Naive T cells are metabolically quiescent as they mainly perform immune surveillance in the peripheral tissues and lymphoid organs, until they encounter APCs expressing specific MHC-peptide complexes. During migration and homeostatic proliferation, naïve T cells rely heavily on mitochondrial OXPHOS to satisfy their energetic needs (Michalek & Rathmell, 2010). Additionally, naïve T cells engage in other catabolic pathways, like fatty acid b-oxidation and glutaminolysis, to feed the TCA cycle, generating reducing equivalents for ATP (Patsoukis et al., 2016).

Upon activation, effector T cells switch to aerobic glycolysis, a process of converting glucose-derived pyruvate to lactate even in the presence of oxygen. Since effector T cells need to rapidly proliferate to carry out the effector functions, they switch to aerobic glycolysis as the higher rate of glucose uptake and metabolism may compensate for the less efficient ATP production (Pfeiffer et al., 2001). Glycolysis also forms pyruvate and the reducing agents, NADH and $FADH_2$, which can further feed the mitochondrial TCA cycle and thus support OXPHOS. As a matter of fact, T cells divert 85% of the products of glycolysis into lactate rather than into the TCA cycle, but importantly, the presence of oxygen allows regeneration of NAD+ from NADH using the ETC allowing continued glycolysis (Fox et al., 2005).

Increased glycolysis in T cells is supported by enhanced glucose import through the localization of glucose transporter 1(GLUT1) to the plasma membrane (Frauwirth et al., 2002). Regulation of GLUT1 is driven by PI3K/Akt, whose activation is mediated through mTOR signaling (Makinoshima et al., 2015).

Both OXPHOS and glycolysis are critical for sustaining optimal functioning of effector T cells. Indeed, inhibition of OXPHOS using Oligomycin, an inhibitor of mitochondrial ATP synthase, reduces proliferation and blocks the expression of T cell activation markers (Chang et al., 2013).

Along with increasing glucose metabolism, activated T cells enhance their uptake and metabolism for nutrients, and this includes large changes in amino acid metabolism, to meet the significant energetic and biosynthetic demands. This helps in enhancing protein synthesis, redox control, ATP production, nucleotide synthesis and supplying intermediates for the TCA cycle (Michalek and

Rathmell, 2010). Several metabolic pathways are upregulated in activated T cells, including the TCA cycle, OXPHOS, glutaminolysis, and lipid biosynthesis (Pollizzi and Powell, 2014).

mTORC1 activity is required for cell cycle entry and coordination of early metabolic changes that occur upon T cell activation. In fact, it is essential for the initial induction of glycolysis in T cells and is also required to maintain aerobic glycolysis in effector T cells subsets. In stimulated T cells, activation of PI3K/Akt/mTORC1 signaling pathway induces Myc and metabolic flux through glycolysis and mitochondrial oxidative phosphorylation (Sena et al., 2013; Ho et al., 2015). Amino acid regulation of mTOR activity is not restricted to effector T cells. Tregs also rely on amino acid-induced mTORC1 activation. Like inflammatory effector T cells, effector Tregs display greater mTORC1 activity than their central counterparts (Zeng et al., 2013). Also, mTORC1 activation seems to modulate the differentiation into Th17 cells via an S6K1/2-dependent fashion as S6K2 was shown to bind and carry RORγ to the nucleus (Kurebayashi et al., 2012).

2.5. Glutamine Metabolism in T cells

While glucose is a major substrate fueling ATP production in proliferating T cells, alternative carbon sources—such as glutamine, acetate, amino acids, and fatty acids—play an important role in maintaining T cell survival under conditions of nutrient limitation (Pearce et al. 2009; Sinclair et al. 2013; Balmer et al. 2016; Bachem et al. 2019; Qiu et al. 2019).

Glutamine metabolism has emerged in actively proliferating T cells. Glutamine is a non-essential amino acid, abundantly present in the serum, that has proven to be a key metabolite contributing to the anaplerotic flux of carbon into the TCA cycle through glutaminolysis. Activated T cells upregulate amino acid transporters and enzymes that metabolize glutamine (Wang et al., 2011; Sinclair et al., 2013; Nakaya et al., 2014).

The first step of glutaminolysis is the conversion of glutamine to glutamate via the enzyme glutaminase (GLS) which is followed by the conversion of glutamate to a-ketoglutarate (a-KG) and subsequent entry of a-KG to the TCA cycle, resulting in a net gain of carbon contributions to the cycle (Wang et al., 2010). Glutamate is a metabolic nexus that plays direct roles in protein synthesis and generation of glutathione to ROS production and can be exchanged to promote cystine uptake (Siska et al., 2016). Glutamine can also serve as an amine group donor for nucleotide synthesis. Lymphocytes consume glutamine at rates comparable to, or even higher than, glucose consumption (Ardawi & Newsholme, 1983; Brand et al., 1984; Ardawi, 1988). Moreover, T cell proliferation and cytokine production in culture require high levels of glutamine (Szondy & Newsholme, 1989; Horig et al., 1993; Yaqoob & Calder, 1997). Indeed, several “non-essential” amino acids were required for T- cell proliferation, and the removal of glutamine consistently resulted in the strongest inhibition in comparison to other amino acids. Particularly, glutamine was unique in being absolutely required to induce the production of both IL-2 and IFN-γ by activated T cells (Carr et al., 2010). Glutamate, asparagine, and proline were also unable to substitute for glutamine in supporting cytokine production (Carr et al., 2010).

The induction of glutamine transporter gene expression is consistent with the increased glutamine uptake in activated T cells. Although cells can import glutamine via multiple systems, the major glutamine transporters are classified as importers, including members of the sodium-dependent neutral amino acid transporter (SNAT) family and ASCT2/Slc1a5, and as exporters (LAT1/CD98

heterocomplex). However, glutamine supplementation is sufficient to partially restore signaling in amino acid-depleted media, and supplementing T cells with high levels of glutamine can overcome the impact of Slc1a5 deficiency on mTORC1 activity (Nakaya et al., 2014; Sinclair et al., 2013).

In addition to effector T cell activation, glutamine metabolism is implicated in the establishment of specific $CD4^+$ T cell subsets. Glutamine metabolism has been shown to differentially regulate the development of T cells into Th17 or Th1 subsets (Johnson et al., 2018). T cell activation and differentiation showed increased dependence on glutamate and α-KG relative to naive T cells. This was most pronounced in Th17 cells, which also had the highest relative ratio of glutamate to glutamine (Johnson et al., 2018).

Modulation of mTOR pathway activity by amino acids is critical for T cell activation, such that their deprivation results in potent inhibition of mTORC1 in activated T cells (Saxton & Sabatini, 2017). T cells fail to properly engage mTORC1 signaling when they lack Slc1a5 or are cultured in glutamine-free media (Nakaya et al., 2014; Sinclair et al., 2013). Glutamine has also been shown to indirectly regulate mTORC1 through glutaminase GLS1 and glutaminolysis in a Th cell program-specific manner. Overall, glutamine metabolism plays a key role in facilitating T cell proliferation, activation, and cytokine production.

3. FoxO3a

3.1. Forkhead box protein family

The first member of the Fork-head box (Fox) family of transcription factors was found to play a critical role in the embryonic development of the fly Drosophila melanogaster. Mutations in that gene resulted in the development of flies with ectopic head structures that resembled a fork hence the name "Fork-head" (Weigel et al., 1988). Another well-studied homolog is Daf-16 in the worm Caenorhabditis elegans. The Fox genes originated in unicellular eukaryotes and are present exclusively in animals and fungi but not in plants (Baldauf, 1999).

The Fox family of proteins is evolutionarily conserved, and it is characterized by the DNA-binding fork-head (FH) domain (Weigel and Jackle, 1990). While the FH domain is conserved, such that it recognizes a similar consensus DNA motif, the other flanking regions lack similarity. Fox genes exhibit distinct spatio-temporal expression patterns; thus, they are involved in redundant as well as distinct functions (Hannenhalli and Kaestner, 2009).

The crystal structure of FH domain exhibits a "winged-helix" motif, with three α helices that are interspersed with two disordered loops that look like the wings of a butterfly (Clark et al., 1993). More than 100 Fork-head transcription factors have been identified and can be divided into 19 subclasses based on phylogenetic analysis (Tuteja and Kaestner 2007a, b). Fox is used as the root symbol, followed by a letter (from A to S) that indicates the subclass, and each protein is represented by a number. This thesis will focus on one Forkhead box class O member, FoxO3a.

3.2. FoxO subclass

Fox genes belonging to subclass O were identified in many species: *C. elegans, D. rerio, D. melanogaster, G. gallus*, mice and humans (Arden, 2006). In humans, FoxO transcription factors were discovered at chromosomal translocations in rhabdomyosarcomas and acute myeloid leukemias (Eijkelenboom and Burgering, 2013). FoxO1 was identified as part of a fusion protein resulting from chromosomal translocations in alveolar rhabdomyosarcoma (Galili et al., 1993). This protein was named fork head in rhabdomyosarcoma (FKHR). Formerly known as AFX1, FoxO4 gene was found to be fused to mixed lineage leukemia (MLL) in acute leukemia patients

(Corral et al., 1993). A third closely related protein, AF6q21 or FoxO2, was also found as part of an MLL fusion in acute leukemia (Hillion et al., 1997). FoxO3 (FKHRL1) was first identified through cDNA library screening and is also a fusion partner of MLL (Anderson et al., 1998). This research also uncovered a pseudogene for both FKHR and FKHRL1, now designated as FoxO1b and FoxO3b respectively. The existence of this pseudogene has led to FoxO3 being widely and more commonly referred to as FoxO3a, although FoxO3 is the official gene symbol. FoxO5 is the fish ortholog of FoxO3 (Rudd et al., 2003; Berry et al., 2008; Peng et al., 2010). Zebrafish also express homologues of FoxO1 and FoxO3a. Finally, FoxO6 is mainly expressed in the CNS in mammals and is involved in memory consolidation. (Jacobs, et al., 2003, Kim et al., 2011 b).

In mammals, the FoxO family contains four members: FoxO1, FoxO3, FoxO4 and FoxO6. They recognize the same consensus sequence, 5'-TTGTTTAC-3', via their DNA binding domain (Furuyama et al., 2000). While being ubiquitous, the FoxO proteins are differentially expressed depending on the tissue type and developmental stage (Furuyama et al., 2000, Maiese et al., 2008). Although they may act redundantly, they do have unique and specific functions. Overall, they have been found to regulate a broad range of cellular activities: cell survival, antioxidant defense, cell division and energy utilization.

Many FoxO transcription factor functions have been studied using mouse knockout models that differ phenotypically from each other: *FoxO1*$^{-/-}$ mice are embryonically lethal due to incomplete and disordered vascular development; *FoxO3a*$^{-/-}$ mice are viable but exhibit defects in female fertility due to early exhaustion of the oocyte pool, *FoxO4*$^{-/-}$ mice are viable with impaired neointima formation; and *FoxO6*$^{-/-}$ mice are viable but exhibit impaired memory consolidation and abnormal hippocampal neuron morphology. (Castrillon et al., 2003; Paik et al., 2007; Tothova et al., 2007; Salih et al., 2012).

3.3. FoxO3a structure and function

The *FoxO3a* gene is located on chromosome 6q21 in humans and on chromosome 10qB2 in mice. The gene contains five domains: a highly conserved fork head winged helix-turn-helix DNA binding domain (FKH), two nuclear localization sequence (NLS), a nuclear export sequence (NES) and a C-terminal transactivation domain (TAD). The protein is 71 kDa in size, and its structure is conserved across different species (Anderson et al., 1998).

As a central transcription factor, FoxO3a modulates the transcription of a wide range of target genes involved in metabolism, apoptosis, autophagy, proliferation, survival, and DNA damage, thus influencing multiple physiological and pathological processes. In general, FoxO3a is known to suppress cell cycle progression and promote cell death. Thus, FoxO3a is considered as a bona fide tumor suppressor (Dansen and Burgering, 2008). For instance, FoxO3a binds to the promoter of apoptosis-inducing genes, such as *Bim*, *FasL* and *TNF-related apoptosis-inducing ligand (TRAIL)*, and to the promoter of cell cycle inhibitors, such as *p27* (*Kip1*) and *p21* (*Cip1/Waf1*) (Greer and Brunet, 2005; Wilson et al., 2010; Hauck et al., 2007; Chandramohan et al., 2004). FoxO3a was shown to promote the transcription of antioxidant enzymes such as catalase, SOD1 and SOD2 in mouse erythroid precursors (Marinkovic et al., 2007). This highlights the important role of FoxO3a in controlling the cellular redox balance and promoting cell survival in unfavorable redox environments. The reduction of ROS levels and mitochondrial function by FoxO3a has been partly attributed to its antagonism with the transcription factor c-MYC, an important driver of bioenergetic processes. In fact, FoxO3a is a negative regulator of c-MYC, which promotes cell-cycle progression, glutaminolysis and mitochondrial biogenesis (Peck et al., 2013).

Upon DNA damage, FoxO3a induces cell cycle arrest at the G2-M phase and mediates DNA repair in a GADD45-dependent manner (Tran et al., 2002). In response to hypoxia, FoxO3a stimulates the transcription of CITED2, a transcriptional co-repressor of HIF-1, with which it competes for CBP/p300 binding and consequently limits the induction of apoptosis by HIF-1(Bakker et al., 2007). Thus, through fine-tuning the activity of HIF- 1, FOXO3a promotes the survival of both normal and cancer cells. Therefore, FoxO3a represents a cell fate switch that performs either a pro-survival or a pro-apoptotic function in a context-dependent manner.

Accordingly, the deregulation in its expression and/or activity can lead to various diseases, such as leukemia, prostate cancer, breast cancer and neurodegeneration (Chen et al., 2010; Wong et al., 2013). FoxO3a regulates the homeostasis of hematopoietic cells, consistent with the finding that chromosomal translocation of *FoxO3a* gene is associated with leukemias (Anderson et al., 1998). In fact, deletion of somatic FoxO1, 3a, or 4 in mice resulted in a cancer-prone phenotype, such as thymic lymphomas and hemangiomas (Paik et al., 2007).

A very interesting aspect is the association of FoxO3a with longevity. Daf-16 is the first identified FoxO protein in *C. elegans* that regulated the dauer larva formation (Kenyon et al., 1993). Overexpression or increased activation of dFOXO in the adult peri cerebral fat body prolongs the lifespan of *D. melanogaster* by ~15-52% (Giannakou et al., 2004; Hwangbo et al., 2004). In addition, further investigations have established that various *FoxO3a* SNPs, located in the intronic regions, have a significant association with human longevity, especially in samples of Hawaiian, German, Chinese and Jewish centenarians, or nonagenarians (Willcox et al., 2008; Flachsbart et al., 2009; Li et al., 2009; Pawlikowska et al., 2009). Furthermore, GWAS has identified the contribution of FoxO3a among other genetic loci (*XACT, MHC, and IGFBP 1-3*) in dictating the severity of Crohn's disease prognosis in IBD patients (Lee et al., 2017). Mutations in these genes dictate "disease progression" rather than susceptibility (Mondal et al., 2017). Overall, effects of these SNPs on splicing or mRNA/protein levels have not been explored, so the molecular mechanisms of ageing and FOXO3a-related longevity are still largely elusive.

3.4. Regulation of FoxO3a expression

The expression of FoxO3a is regulated at many levels including transcriptional initiation and mRNA stability. E2F-1 was the first identified transcription factor that activates the transcription of *FoxO1* and *FoxO3a* (Nowak et al., 2007). Both form a complex and act in a feed-forward regulatory loop to reinforce gene induction of multiple apoptotic genes (Shats et al., 2013). STAT3 also binds to *FoxO3a* promoter enhancing its transcription. This contributes to lymphocyte quiescence by preventing T lymphocyte proliferation (Oh et al., 2011). It has been reported that p53 directly transactivates *FoxO3a* gene by binding to its second intron, and these two transcription factors exist in a complex interplay during apoptosis and aging (Renault et al., 2011). Intriguingly, FoxO3a itself stimulates the transcription of *FoxO* genes, thus forming a positive

feedback loop. Cytoplasmic sequestration of FoxO3a can be induced via the activation of PI3K by platelet-derived growth factors and fibroblast growth factors, thus disrupting FoxO-dependent transcription of *FoxO* genes and promoting cell proliferation (Essaghir et al., 2009).

At the mRNA level, some microRNAs (miRNAs) have been shown to modulate the expression of FoxO3a. miRNAs are a class of endogenous non-coding RNAs that post-transcriptionally suppress mRNA of the protein-coding genes and generally repress gene expression (Lagos-Quintana et al., 2001; Lau et al., 2001; Bartel, 2009). miR-155 and miR-96, frequently expressed in breast cancer, down-regulate FoxO3a through interacting with its 3'-UTR and induce cancer cell survival and chemoresistance (Kong et al., 2010; Lin et al., 2010). miRNA-23a has also been shown to inhibit the translational activity of *FoxO3a* 3'-UTR, reducing the protein level and consequently inducing cardiac hypertrophy (Wang et al., 2011). These miRNAs enrich our understanding of the regulation of FoxO3a at the post-transcriptional level and can serve as therapeutic targets for various diseases.

3.5. Post-translational Modifications of FoxO3a

FoxO3a is subject to various post-translational modifications (PTMs) that control its stability, subcellular localization, DNA-binding efficiency, and transactivation function. PTMs, such as phosphorylation, acetylation, ubiquitination, methylation, and poly ADP-ribosylation (Sakamaki et al., 2009), can exert an additive effect or may compete forming a FoxO code that is essential in regulating its function (Calnan and Brunet, 2008).

The most well-known and extensively studied pathway to regulate FoxO activity is the insulin/PI3K signaling pathway. In the presence of insulin or growth factors, the PI3K pathway is activated and causes inactivation of FoxO3a through protein kinase Akt. Akt phosphorylates FoxO3a at three conserved sites T^{32}, S^{253}, and S^{315}, two of which form binding sites for 14-3-3 protein. This decreases DNA-binding of FoxO3a and facilitates its nuclear exclusion. While retained in the cytoplasm, FoxO3a can be ubiquitinated and targeted for proteasomal degradation. (Brunet et al., 1999;Arden, 2006). Other kinases like protein kinase B (PKB), ERK, Casein kinase 1 (CK1) and serum and glucocorticoid-regulated kinase (SGK) also contribute to FoxO3a phosphorylation and translocation into the cytoplasm (Brunet et al., 2001; Rena et al., 2002; Yang et al., 2008; Luo et al., 2016). FoxO3a phosphorylation, associated with its inactivation, was found

to have a negative effect on the survival of acute myeloid leukemia patients (Kornblau et al., 2010).

In contrast, in presence of oxidative/genotoxic stress, phosphorylation of FoxO3a by mammalian sterile 20-like kinase 1 (MST1) or JNK can result in its nuclear entry by disrupting the binding of 14-3-3 (Green & Brunet, 2005; Lehtinen et al., 2006). AMPK phosphorylation of FoxO3a enhances its transcriptional activity without altering its subcellular localization and DNA-binding ultimately promoting cellular stress resistance (Greer et al.,2007).

Besides phosphorylation, which acts like a general ON/OFF switch, other PTMs can alter the affinity of FoxO3a to DNA or other co-reguators resulting in differential transcription of genetic programs. The effects of acetylation are gene- and cell-type specific and can lead to either enhancing or reducing FoxO-dependent transcription (Brunet et al., 2004; Motta et al., 2004; Van der Horst et al., 2004). For example, unlike SIRT1, deacetylation by SIRT2 increases FoxO3a DNA-binding activity to enhance the antioxidant response to stress (Wang et al., 2007). Moreover, the lysine SET9 methyltransferase has also been shown to modulate the transcriptional activity and protein stability of FoxO3a by methylating its DNA-binding domain (Eijkelenboom and Burgering, 2013).

Together, FoxO3 PTMs form a ‘code’ for fine-tuning the activity of this transcription factor in cells. Balancing the nuclear import and export is critical to maintain FoxO3a function, as loss of this balance can lead to the development and progression of various diseases.

4. Gut Immunity and Chronic Inflammatory Diseases

4.1.The Intestinal Epithelium

The gastrointestinal tract includes the mouth, esophagus, stomach, small intestine, large intestine, and rectum. The mammalian GI tract presents a unique challenge to the immune system. On one hand, it must tolerate the presence of the commensal microbiome and enable the absorption of essential nutrients (small intestine) and water (colon). On the other hand, it must keep exerting its protective function by restricting the invasion of harmful substances or pathogens. In fact, low numbers of commensal microbes can translocate to allow normal bacterial sampling and successful clearance by the innate and adaptive immune cells (Slack et al. 2009). To this end, the GI tract is lined by a single layer of intestinal epithelial cells (IECs) that constitute a physical anatomical barrier separating the luminal content (bathed in nutrients, microbes, IgA and mucus) from the immune cells residing in the lamina propria (LP) and localized between the IECs (Laukoetter et al, 2008; Abreu, 2010). In fact, the intestinal epithelium acts as a coordinating hub for the cross talk between immune cells and the microbiota, and this emphasizes the central role for all these cell types in promoting host enteric defense (**Figure III**.)

IECs are structurally and functionally polarized, such that their apical surface faces the intestinal lumen, and their basolateral surface faces the underlying basement membrane and the LP (Abreu, 2010). Due to the high cell turnover, the epithelium in the small and large intestines must maintain a homeostatic balance in cellular proliferation and differentiation, and this is based on the proliferative activity of the stem cells in intestinal crypts. Stem cells are located at the crypt base feeding daughter cells into the Transit-Amplifying (TA) compartment. After undergoing around 4-5 rounds of rapid cell division, TA cells finally move out of the crypt and terminally differentiate into multiple functionally distinct cell types: absorptive enterocytes, mucin-producing goblet cells, tuft cells (chemical sensors for luminal content), microfold (M) cells (portals in small intestine for transporting luminal antigens), hormone-producing enteroendocrine cells and Paneth cells that produce antimicrobials and growth factors (Marshman et al., 2002; Bevins, Salzman 2011; Clevers, 2013; van der Flier, Clevers 2009).

The epithelium of the small and large intestines varies notably in architecture and cellular composition. The small intestine is subdivided into three regions from proximal (at the stomach)

to distal: the duodenum, jejunum, and ileum. The cecum, which is the first part of the large intestine, blends seamlessly with the colon. The colon is sub-classified as transverse, ascending, descending and sigmoid finally attaching to the rectum.

While the small intestinal epithelium exists in a 2-dimensional structure (villus/crypt axis), the intestinal villi are absent in colons beyond the ileocecal valve (Abreu, 2010). The large intestine is composed of the mucosa, submucosa, muscular layer, and serosa beginning from the lumen outwards. In fact, the mucosa of the large intestines is lined by a simple columnar epithelium with a thin brush border containing absorptive enterocytes and numerous goblet cells. At the base of the crypts, undifferentiated cells and endocrine cells are present; however, Paneth cells are not usually present (Abreu, 2010).

Goblet cells produce and secrete glycosylated mucins forming the mucosal layer that lies on top of the epithelium. Mucus comprises the first line of defense against the microbes in the lumen (Johansson, Ambort et al. 2011). Unlike the small intestine, which has a loose single layer of mucus to allow absorption of nutrients, the colon has a dual mucus layer restricting the adhesion of microbiota to the epithelium (Johansson, Larsson et al. 2011; Sonnenburg, Xu et al. 2005). It has been observed that the mucus layer of the colon follows an increasing gradient across its length. The thickness of the inner mucus layer in the distal colon has been estimated to approximate 50 μm in mice and 100 μm in rats (Atuma et al., 2001; Malmberg et al., 2006). The inner layer is separated from the thicker outer mucus layer, in which commensal microbes live and thrive (Johansson et al., 2008).

The intestine possesses the capacity to recover from the acute loss of its active stem cell pool. This can be related to the presence of quiescent “reserve” stem cells and/or to the plasticity of TA progenitors to fall back into the stem cell niche and regain stemness (Li & Clevers, 2010; Cheng & Leblond, 1974b; Potten, 1977).

4.2.The Intestinal Immune System

Along with the lymph nodes and the spleen, the gut provides secondary lymphoid microenvironments, where immune cells encounter antigens and initiate immune responses. In fact, the gut mucosa is exposed to massive amounts of diverse foreign antigens, as the GI tract represents the largest surface area of the human body that comes in direct contact with the external environment (Abreu, 2010).

Mucosal membranes are considered vulnerable since they are the major site of entry for most pathogens. These membranes are protected by a group of organized lymphoid tissues collectively known as mucosa-associated lymphoid tissue (MALT). The one associated with the intestinal epithelium is referred to as the gut-associated lymphoid tissue (GALT). The GALT comprises loose structures of lymphoid cells in the LP of intestinal villi and well-organized structures, such as Peyer's patches (PP) within the intestinal lining. Intraepithelial lymphocytes (IELs) are interspersed in the outer mucosal epithelial layer. Underneath the epithelial layer is the lamina propria that contains large numbers of immune cells (B & T cells, stromal cells, macrophages, and dendritic cells) (Abreu, 2010) (**Figure III**).

Antigens may enter the GI tract via several routes. These include the specialized M-cells that transport antigens across the epithelium. Local DCs can directly present the antigens to T cells within PP, thus priming them and activating B cell Ig class switching from IgM to IgA (Mason et al. 2008, MacPherson et al. 2004). Antigen loaded-DCs can also traffic to other areas of the GALT including the mesenteric lymph nodes (MLN) for antigen presentation to T cells (Mason et al. 2008). Activated T cells differentiate in the PP and MLNs and traffic via the thoracic duct into the LP, which carries the major effector functions in the GALT and is populated with primed T- and B cells, IELs, DCs, macrophages and neutrophils. Additionally, DCs present in the LP can also extend out into the lumen for direct antigen sampling. Alternatively, antigens can access the MLNs by crossing the epithelium of the villus or they can be taken up by LP macrophages and DCs that express MHC class I/II molecules enabling them to prime local innate and adaptive immune cells (MacPherson et al. 2004, Mason et al. 2008). Moreover, the highly phagocytic intestinal macrophages have also been shown to participate in antigen sampling and T cell priming. Interestingly, in non-inflamed mucosa, resident macrophages are inflammation anergic and exhibit an anti-inflammatory phenotype through increased secretion of IL-10 and reduced expression of

TNF (Bain et al. 2013). They phagocytose and kill microbes without inducing an inflammatory response. Nevertheless, they retain avid scavenger and host defense function (Smith et al., 2011).

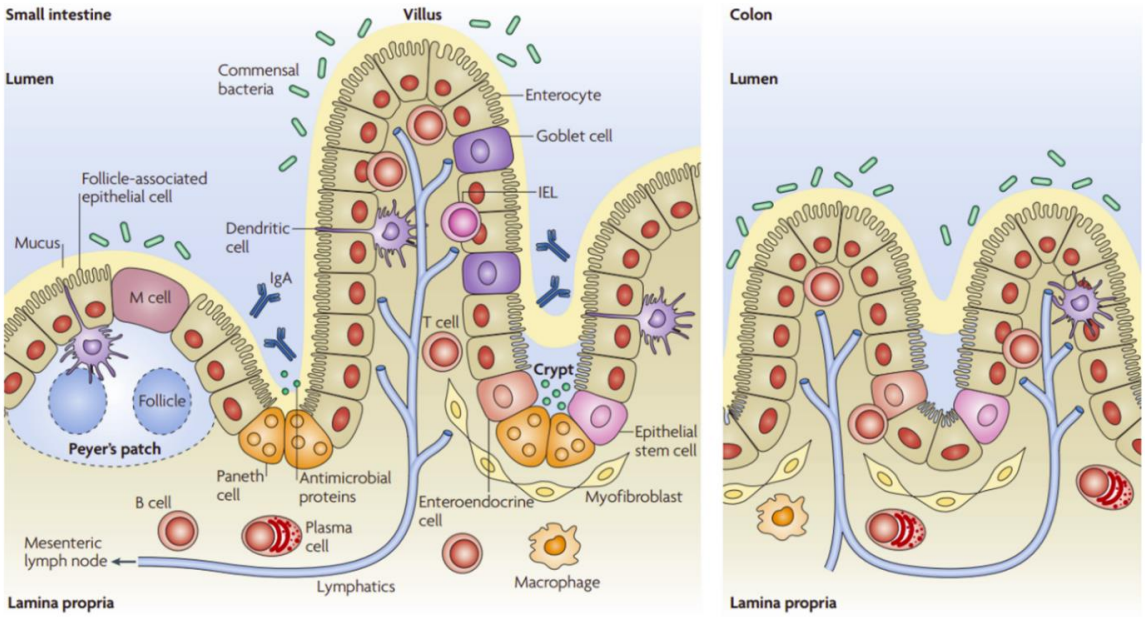

Figure III. Anatomy of the intestinal immune system.

This schematic represents anatomical differences between the small intestine (left) and the large intestine/colon (right). Crypts house intestinal stem cells that can proliferate to generate daughter progenitors with proliferative potential. These progenitors can give rise to more differentiated cells including villous or colonic absorptive enterocytes, goblet cells, enteroendocrine cells, and Paneth cells (present at the base of the small intestinal crypts). All these cells constitute a single layer of intestinal epithelial cells (IECs), which provides a physical barrier that separates the intestinal microbial lumen from the underlying lamina propria. IECs facing the lumen are exposed to trillions of commensal bacteria, nutrients, mucus, and IgA. The LP comprises non-immune (i.e., stromal cells) and immune cells, including B cells (especially IgA-producing plasma cells), T cells, macrophages, and dendritic cells. DCs and intraepithelial lymphocytes (IELs) can be localized between the IECs. In the small intestines, microfold (M) cells and follicle-associated epithelium overlie Peyer's patches and sample the intestinal lumen. **This image is re-printed from (Abreu, 2010) and is Copyright © Springer Nature. under License #5263740838262.**

4.3.IBD

Breakdown of the fine balance between host protection and tolerance of its intestinal microbiota can lead to intestinal inflammation. In some cases, an inflammatory stimulus persists which can promote the development of a chronic inflammatory disease. Chronic inflammation may have infectious or noninfectious origins. Inflammatory bowel diseases (IBD) are idiopathic diseases characterized by chronic mucosal inflammation of the GI tract. The complexity of IBD indicates that there are numerous underlying molecular events that sustain chronic and recurring inflammation (Laukoetter et al, 2008).

4.3.1. Types of IBD

IBD encompasses a heterogeneous group of disorders that have two major phenotypic forms: Crohn's disease (CD) and ulcerative colitis (UC). A prevailing hypothesis is that they arise because of the confluence of aberrant host immune responses, imbalance in gut microbiome (dysbiosis), dysfunctional epithelial barrier and environmental factors (Li et al., 2015).

UC is a relapsing non-transmural continuous chronic inflammation that is restricted to the large intestines (Baumgart & Sandborn, 2007). CrD is a chronic granulomatous disease that is segmental in nature and can affect any part of the GI tract from the mouth to the anus (Baumgart & Sandborn, 2007). CrD most often includes skip lesions that may extend through the thickness of the bowel wall. Unlike UC, CrD is commonly associated with complications such as abscesses, fistulas, and strictures. Both forms are characterized by alternating phases of clinical relapse and remission. The classification of indeterminate colitis is reserved for cases, which do not clearly fall into the CrD or UC definitions.

Common symptoms exhibited by IBD patients include diarrhea, rectal bleeding, abdominal pain, and mucus discharge (Baumgart & Sandborn 2007). In certain cases, inflammation can also extend to organs beyond the digestive system, including the eyes, joints, skin, and liver (Mintz et al. 2004; Orchard et al. 1998; Lebwohl & Lebwohl, 1998; Raj &Lichtenstein 1999). In addition to the direct burden associated with disease, IBD patients also carry an increased risk for colon cancer, another indication for colectomy in patients with longstanding and refractory IBD (Eaden et al. 2001; Rutter et al. 2006).

4.3.2. Prevalence

The prevalence of IBD is increasing globally with the incidence rate spiking in the Western world in the latter half of the 20th century (Kaplan, 2015; Ng, 2018). Due to the low mortality rate, the incidence has outpaced death leading to the addition of newly diagnosed patients to the pool of prevalent patients. Canada harbors one of the highest incidence rates of IBD worldwide with more than 10,000 new diagnoses made every year. Based on a nation-wide analysis using historical population-based data from 7 provinces, the prevalence rate of IBD was 510 per 100,000 in 2008, and it increased up to 725 per 100,000 in 2018. The average annual percentage change of IBD prevalence in Canada was estimated at 2.86%. Thus, by 2030, it is forecasted that more than 400,000 people will be living with IBD: 202,216 with CrD and 178,909 with UC (Coward, 2019). While it can appear at any age, the age of onset of IBD is primarily during adolescence and young adulthood with a smaller peak of onset in individuals at the age of 50 to 80 years old (Feagan et al. 2003).

4.3.3. Etiology

Despite remarkable advances in our understanding of clinical manifestation and epidemiology, the challenge remains in identifying the pathogenesis of IBD. Although the exact etiology of IBD remains largely unknown, research has highlighted the multifactorial nature of IBD that encompasses the contribution of genetic predisposition, environmental factors and the gut microbiome as functionally integrated in its pathogenesis.

4.3.3.1.Environmental Factors

Numerous environmental factors are considered risk factors for IBD, and they include smoking, diet, social stress, drugs, exposure to gastrointestinal infections and geography (Hansen et al. 2011, Jakobsen et al. 2013, Turner et al. 2009, Sutherland et al. 1990, Porter et al. 2008). Malnourishment and smoking have been shown to worsen the clinical course of CrD by promoting fistulas and accelerating the need for surgery after surgically induced remission (Buchman et al. 2003; Feagan et al. 2003; Baumgart et al. 2007; Cosnes 2004). Moreover, IBD is more common after gastrointestinal infections caused by contaminated food or water (Feagan et al. 2003; Garcia Rodriguez et al. 2006). Vitamin D has been shown to impact IBD incidence, which is suggested to increase in areas less exposed to UV light, such as northern latitudes (Ananthakrishnan, Khalili

et al. 2012). In addition, low levels of Vitamin D in both CrD and UC patients were associated with increased risk for surgery and hospitalizations (Ananthakrishnan, Cagan et al. 2013).

4.3.3.2. Microbial Factors

Numerous studies over the years have evaluated the microbial composition associated with IBD, as gastrointestinal bacteria have frequently been suspected as the cause of IBD relapses. In fact, inflammation drives dysbiosis, and alterations in the levels of oxygen and nutrients in the gut can also impact the relative abundance of certain microorganisms. Compared to healthy controls, IBD patients exhibit a reduction in resident aerobic and anaerobic microbiota along with an increase in potentially pathogenic microorganisms (Manichanh et al., 2006). Specifically, it has been reported that patients suffering from IBD exhibit a significant reduction in the bacterial species *Lactobacilli* and *Bifidobacteria* as well as an expansion in certain detrimental bacteria, such as *Proteobacteria and Enterobacteriaceae* (Braun et al., 2009). *Nod2*-deficient mice have exhibited a significant increase in *Bacteroides, Firmicutes, and Bacillus* bacterial loads in the terminal ileum and their ability to clear the pathogenic *Helicobacter hepaticus* was impaired (Petnicki-Ocwieja, 2009*).* In surgical specimens from CrD and UC patients with a NOD2 risk allele, the microbial composition had reduced *Clostridium Group XIVa and IV* and increased *Actinobacteria* and *Proteobacteria* compared with controls (Frank et al., 2011; Lee et al., 2012). However, there is limited information on causality and mechanism of disease.

Challenging the prevailing model of decreased diversity in IBD patients, other studies reported that microbial diversity was unchanged between controls and the CrD/UC patients; however, the microbial profile was distinct between first-onset pediatric patients and adults (Mottawea et al., 2016). Besides the microbial alterations, the biological significance of metabolic byproducts of microbial fermentation was also highlighted in the impact on gut health. In particular, the study showed a significant downregulation of mitochondrial proteins that was associated with a depletion of butyrate producers, mainly *Blautia, Lachnospiraceae, Roseburia, Eubacterium rectale, Ruminococcus, Clostridium* and *Faecalibacterium* (Mottawea et al., 2016). This leads to a bloom of pathobionts, many of which are known to be potent H_2S producers. Since butyrate is the main energy source of anti-inflammatory short chain fatty acids for colonocytes, its reduced production will in turn impair mitochondrial functions, likely resulting in ROS production,

increased epithelial permeability and translocation of commensal microbes across the epithelial barrier (Mottawea et al., 2016).

It is commonly recognized that intestinal dysbiosis, or the imbalance in the structural and/or functional properties of the gut microbiota that can disrupt host-microbe homeostasis, is critical to the pathogenesis of IBD, yet the field remains descriptive. Does intestinal dysbiosis cause IBD or is it a mere consequence? Is IBD caused by the emergence of pathobionts and/or disappearance of symbionts? Or is it merely due to an aberrant host immune response to commensal microbiota? As a matter of fact, the discovery of susceptibility genes has shed light on fundamental relationships between host genetics with gut microbes. In particular, genetic mutations have been found to disrupt the innate and adaptive immune functions (i.e., impairment of autophagy, defective Paneth cell function) that affect the assemblage of the gut microbiome.

4.3.3.3. Genetic Factors

Over the past decades, there have been huge advances in our understanding of genetic contributions to IBD (Gaya, 2006). In fact, there are gene mutations that predispose one to be susceptible to the disease in the presence of an environmental trigger. Genome-wide association studies (GWAS) have highlighted the complexity of IBD by identifying new associations bringing the number close to 163 single nucleotide polymorphisms (SNPs) as IBD-associated loci, of which 110 are associated with both diseases, 30 CrD specific and 23 UC specific (Jostins et al., 2012). These genes are involved in bacterial recognition, epithelial barrier integrity and immune activation (Jostins, et al., 2012). Since a number of these susceptibility alleles are shared between ulcerative colitis and Crohn's disease, this suggests the existence of shared pathways in IBD pathogenesis despite differences in clinical phenotype (Budarf et al. 2009; Zhernakova, van Diemen, 2009).

The first ever described polymorphisms associated with increased risk for CrD were found in the susceptibility gene nucleotide oligomerization domain 2 (NOD2) (Hugot et al. 2001). NOD2 gene encodes for an intracellular PRR that senses bacterial peptidoglycans and can be activated by a small peptidoglycan component known as muramyl dipeptide resulting in the activation of NF-κB and MAPK signaling pathways (Girardin et al. 2003, Inohara et al. 2003, Kobayashi et al. 2005). However, individuals homozygous for the NOD2 mutations exhibit limited disease penetrance

suggesting the need for environmental triggers. This is corroborated by the fact that NOD2 KO mice do not develop intestinal inflammation (Kobayashi et al. 2005; Pauleau & Murray 2003).

Later, genetic analyses revealed the critical role of autophagy in immune responses in IBD by identifying IBD-associated polymorphisms in autophagy-related genes, such as ATG16L1 and Immunity Related GTPase M (IRGM) (Rioux, 2007, McCarol, 2008). Epithelial cells and dendritic cells with ATG16L1 and NOD2 variants showed defects in antibacterial autophagy (Travassos, 2010). CrD patients with the ATG16L1 SNP have abnormal Paneth cell morphology, as do mice with low ATG16L1 protein levels (Cadwell, Liu et al. 2008).

Components of the adaptive immune system have also been implicated in susceptibility to IBD. Associations with CrD susceptibility have been reported for several genetic loci of the IL-23:IL-17A axis (Duerr et al. 2006; Barrett et al. 2008). Increased CrD risk has been associated to SNPs in the *Il-23R* gene, which encodes a subunit of the receptor for the pro-inflammatory cytokine IL-23 pertinent to the generation of Th17 cells (Duerr et al. 2006). The expression of IL-23 and Th17-relevant cytokines are increased in the colonic mucosa of both CrD and UC patients (Annunziato, Cosmi et al. 2007; Fujino et al. 2003a; Saruta et al. 2007) highlighting the significance of this pathway in the pathogenesis of IBD. Moreover, it has been demonstrated that inflammatory Th1 and Th17 responses can both facilitate colitis development and progression (Brand, 2009).

Other susceptibility genes that regulate immune function encode CARD9, IL1R2, REL, SMAD3, IL12B, JAK2, STAT3 and PRDM1, MyD88, TLR4, NLRP6, NLRP12 and CYLD (Karrasch, 2008; Brand, 2009; Anderson, 2011; Elinav et al., 2011; Chen et al., 2017). Modulation of various susceptibility genes does not lead to spontaneous IBD in mice, unless the gut barrier is compromised by treatment with chemicals such as DSS.

Furthermore, mutations in the *Il10/Il10Rα* gene have been shown to be the cause of severe infantile IBD by family association studies and gene sequencing. *Il10*$^{-/-}$ mice were reported to develop colitis that was dependent on the genetic background of the mouse (Kuhn et al., 1993; Glocker et al., 2009; Buchler et al. 2012). *Il10* is one of the few genes whose inactivation causes spontaneous CrD-like phenotype, but this occurs only in the 129 Sv strain of mice and at much slower kinetics. Mice with Treg-specific ablation of IL-10 develop spontaneous colitis (Rubtsov et al., 2008), and IL-10 produced by Tregs or immune effector cells, would elicit STAT3 activation-dependent IL-10 production and suppressive functions, including suppression of Th17-mediated inflammation

(Chaudhry et al., 2011). Additionally, researchers have shown that Th17 cell-associated cytokines, IL-17 and IL-22, are expressed by $CD4^{+}FoxP3^{-}$ T cells in the presence of IL-10R-deficient Treg cells (Chaudhry et al., 2011).

Due to the expanding number of susceptibility gene loci associated with IBD, genetic influences are deemed critical components of the disease pathogenesis. However, these susceptibility genes do not seem to influence disease outcome (Liu et al. 2015; Uhlig & Muise, 2017). Attempts to correlate and associate the susceptibility loci to disease outcome in IBD have resulted in limited success, and this has led to the hypothesis that the genes that correlate to susceptibility may not be the same that lead to disease outcome in CrD. This may explain why some people have a milder disease course compared to others despite having inherited the same susceptibility genes. Indeed, GWAS has identified the contribution of four different genetic loci (*XACT, MHC, FoxO3 and IGFBP 1-3*) that associate with CrD prognosis. Mutations in these genes dictate "disease progression" rather than susceptibility (Mondal & Kugathasan, 2017). For example, a noncoding polymorphism in *FoxO3a* (rs12212067: T > G) was identified in CrD patients, where the minor "G" allele is associated with a milder course of CrD and rheumatoid arthritis and with an increased risk of severe malaria. The minor allele carriage was shown to dampen the inflammatory responses in monocytes via a FoxO3-driven pathway, through reducing the production of pro-inflammatory cytokines and enhancing that of anti-inflammatory IL-10 (Lee et al., 2013). The researchers also demonstrated that reducing transcriptional FoxO3a activity in mice has predisposed them to a more severe course of colitis upon dextran sodium sulfate (DSS) administration (Lee et al., 2013). To further illustrate, another study showed that in human IBD tissue samples, the relative expression of FoxO3 transcript was significantly reduced compared with normal matched control tissue. Researchers also examined the impact of reducing FoxO3a expression in the AOM/DSS model of inflammation-mediated colon cancer. They found that reducing FoxO3a expression in the colon of mice specifically led to enhanced infiltration of immune cells and activation of inflammatory pathways overlapping with those associated with mouse and human colonic inflammation and cancer (Penrose et al., 2019).

4.4. Management of IBD

Treatment of IBD depends on numerous factors such as the location and extent of inflammation, severity of symptoms, and presence of other GI disorders. Overall, IBD treatment concept can be

represented as a pyramid, and as the disease severity increases, the pyramid is moved up for stronger treatments. While there is no cure, administering the appropriate medical treatment can keep the disease in remission. During the last decade, new and effective drugs have been developed to treat IBD. Primarily, they are considered as the first option for treatment prior to considering surgery and are ranked by strength in a bottom-up approach as follows: amino salicylates (e.g., mesalamine), antibiotics (e.g., Metronidazole and Ciprofloxacin), corticosteroids, immunomodulators (e.g., azathioprine, methotrexate, cyclosporine) and biological therapy (e.g., anti-TNF, anti-integrin). These have been used to prevent relapses or to induce remission in deterioration of disease activity (Srinivasan et al. 2003). Surgical intervention (i.e., removal of whole or parts of the large intestine) is finally considered when there is a substantial risk of cancer development or when pharmacological intervention fails. Surgical resection becomes challenging as an elective treatment option since CrD can affect any portion of the GI tract unlike UC.

Since many of these drug and biological adjuvant regiments impose significant side effects, it would be advantageous to identify predictive biomarkers associated with the progressive stages of the disease. Yet, this has been difficult in part because of great variability in the contribution of underlying mechanisms in the disease incidence, onset, progression, and remission over time (DeVoss, & Diehl, 2014).

4.5. Mouse Models for Colitis

Mouse models of IBD have rapidly advanced our understanding of mechanisms contributing to chronic GI diseases. The complexity of IBD is not demonstrated through one single model, but each model provides valuable insights into various aspects of IBD.

In general, these models can be grouped as—(a) Inducible (b) Adoptive T cell transfer models (c) Genetic models (d) Antigen-specific and bacterial models.

In inducible models, colitis can be induced immunologically, physically, or chemically. The first ever described animal model of experimental colitis was caused by an immune complex in rabbits (Kirsner 1961). Intestinal inflammation can be physically induced by irradiating MHC II-deficient mice (Marguerat et al. 1999). Chemical induction is based on repeated administration of chemical triggers of acute or chronic intestinal inflammation that resembles human colitis. Administration of hapten molecules, such as trinitrobenzene sulfonic acid (TNBS) and dinitrobenzene sulfonic

acid (DNBS) in mice, causes a transmural inflammation with diarrhea, weight loss and thickening of the bowel wall, and this occurs through promoting a Th1 cell-mediated inflammatory response (Elson et al. 1995; Wirtz & Neurath, 2000; Wirtz et al. 2007). Feeding mice with dextran sulphate sodium (DSS) in their drinking water is thought to exert cytotoxic effects on the intestinal epithelium, effectively compromising the mucosal barrier function and exposing the LP luminal content to the underlying gut immune compartments (Okayasu et al. 1990; Elson et al. 1995; Wirtz & Neurath; 2000). This leads to the activation of an inflammatory response that involves the recruitment and activation of macrophages and T cells, resulting in the elaboration of Th1 and Th2 cytokines (Dieleman et al. 1998). Acute DSS colitis in mice manifests as mucosal ulceration, shortening of the colon and weight loss and induces a response that is primarily dominated by activated macrophages (Elson et al. 1995; Mahler et al. 1998). To induce chronic colitis, where disease lasts for several months, DSS is administered for several cycles resulting in the engagement of the adaptive immune response (Wirtz & Neurath, 2000; Wirtz et al., 2007).

T cell transfer model of chronic colitis occurs by transferring $CD4^+$ $CD45RB^{high}$ T cells (naïve T-cells) into syngeneic immunodeficient (lymphopenic) SCID or *Rag1*$^{-/-}$ recipient mice. This led to a wasting disease and a primarily colonic inflammation that develops 5 to 10 weeks after treatment. Inflammation in these models seems to be driven by Th1 responses, since it can be prevented by *in vivo* blockade of IFN-γ, TNF-α and IL-12 but not IL-4 (Powrie et al., 1994; Leach et al., 1996). Transferring mature $CD4^+CD45RB^{low}$ T cells, containing Tregs, does not cause colitis due to increased IL-10 production (Powrie et al., 1993; Morrissey et al., 1993; Groux et al., 1997).

Antigen-specific models constitute a small category that includes the OVA TCR transgenic (TG) mouse model as well as *Helicobacter hepaticus*-induced models of experimental colitis (Iqbal et al., 2002). In the OVA TCR TG model, *Rag2*$^{-/-}$ mice are colonized with OVA-expressing *E. coli* that receive either polarized Th1 or Th2 cells. *Helicobacter hepaticus* induces IL-7-dependent intestinal inflammation in *Rag2*$^{-/-}$ mice and colitis in mice that are deficient in the p50 chain of NF-κB and heterozygous for the p65 chain (von Freeden-Jeffry et al. 1998; Erdman et al. 2001).

The genetic model is the biggest and most growing category of IBD animal models including both TG and knock-out (KO) animal models. Mice that have deficiencies in specific genes, encoding IL-10, IL-2/IL-2R, NOD2, STAT3, MUC2, are rendered more susceptible to developing colitis that can be exacerbated in the presence of a trigger, such as DSS (Kiesler et al., 2015; Hoffmann

et al. 2002). In fact, animals rarely develop spontaneous colitis. SAMP1/Yit mice, C3H/HeJ mice, mice with Tbet deficiency in the innate immune compartment and TRUC mice (*Tbx21*$^{-/-}$ x *Rag2*$^{-/-}$) have been shown to develop spontaneous intestinal inflammation under very specific housing conditions (Matsumoto et al. 1998; Sundberg et al. 1994; Garrett et al. 2007). Genetic modification of experimental animals can help determine disease causation, identify potential therapeutic targets, and pilot measures contributing to alleviation of pain and distress in model systems.

The various models of intestinal inflammation demonstrate the extensive and sometimes complex mechanisms operative in the genesis of intestinal inflammation and pathogenesis of IBD.

MATERIALS AND METHODS

1. Mice

Mice were housed at the University of Ottawa Animal Facility. They were maintained in accordance with Canadian Council on Animal Care (CCAC) guidelines. *Il10*$^{-/-}$ and wildtype (WT) C57BL/6 J mice were obtained from the Jackson Laboratory (Bar Harbor, Maine, USA). *FoxO3a*$^{-/-}$ mice were previously generated using a gene-trap targeting strategy that deactivated the FoxO3a allele, and they were further maintained by mating *FoxO3a*$^{-/-}$ males and *FoxO3a*$^{+/-}$ females (Lin et al., 2004; Tzelepis et al., 2013). FoxO3a and IL-10 double deficient mice (*FoxO3a*$^{-/-}$*Il10*$^{-/-}$) were generated from mice heterozygous for *FoxO3a* and *Il-10* (*FoxO3a*$^{+/-}$ *Il10*$^{+/-}$ breeding pairs) or from mice deficient in IL-10 and heterozygous for FoxO3a (*FoxO3a*$^{+/-}$ *Il10*$^{-/-}$ breeding pairs). Genomic polymerase chain reaction (PCR) on mouse ear samples was used for genotype determination. Protocols and procedures were approved by the University of Ottawa Animal Care Committee and Ethics Board.

2. Monitoring signs of illness

The development of spontaneous intestinal inflammation was monitored in males and females, and both sexes were equally distributed in the various groups of mice. Age-matched and sex-matched background mice were used for baseline comparison. Mice (minimum n = 15 per group) were monitored for signs of disease and euthanized when reaching humane endpoint, which is characterized by the following criteria: significant weight loss (>20%), rectal bleeding, diarrhea, lethargy, hunched posture, and piloerection.

3. Histopathology and immunohistochemistry

Various organs were harvested and fixed in neutral buffered 10% formalin, embedded in paraffin, and processed for routine and special histopathological examination. Vertical sections (5 μm thick) were stained with haematoxylin and eosin, Alcian Blue pH = 2.5, and Masson's trichrome. Images were acquired on a Zeiss Axio Mirax Midi scanner. Paraformaldehyde-fixed, paraffin-embedded colon sections were de-paraffinized in xylene and rehydrated through a 100-70% ethanol gradient. Heat-induced epitope retrieval was done at 110 °C for 12 min with citrate buffer pH 6.0 and 3%

hydrogen peroxidase was used to block endogenous peroxidases. Sections were blocked with Background Sniper blocking reagent (BioCare Medical, CA, USA) and then incubated with the Cleaved Caspase-3 antibody (Cell Signaling, #9661) at 1:500 dilution for 1 h at room temperature. The MACH4™ + DAB detection system was used for chromogenic staining according to the manufacturer's instructions (BioCare Medical, CA, USA).

Anti-Ki67 (Cell Signaling, #12202) IHC staining was performed on formalin-fixed paraffin embedded tissue sections using the Leica Bond™ system. For the rabbit antibodies, a modification of protocol F that eliminates the post-primary step when using rabbit antibodies on mouse tissue was used. Sections stained using sodium citrate buffer (pH=6.0, epitope retrieval solution 1) for 20 minutes. The sections were then incubated using 1:200 dilution for 30 minutes at room temperature and detected using an HRP conjugated compact polymer system. Slides were then stained using DAB as the chromogen, counterstained with Hematoxylin, mounted and cover slipped. Blinded samples were sent for evaluation of pathology at the Ottawa Hospital.

4. Isolation of lamina propria leukocytes

Mice were sacrificed by CO_2 inhalation followed by cervical dislocation. Colons were excised a few millimeters below the cecum and a few millimeters above the rectum to prevent the introduction of excessive toxins and waste into the culture. Colon segments were placed in ice cold 1x PBS in a petri dish and cut open length wise. The intestines were moved through clean buffer several times using forceps to rinse thoroughly. Using forceps, the colon was held by one end over a 50 mL Falcon tube, containing a pre-digestion solution, and was cut into 0.5 cm pieces starting from the bottom end. The fragments were transferred to the 50 mL Falcon tube and incubated in a pre-digestion 1x HBSS solution containing 5 mM EDTA and 1 mM DTT at 37 °C for 20 min. at 250 rpm. After 20 min., the supernatant was discarded. The pre-digestion step was repeated twice for a total of 3 incubations. After discarding the supernatants, the remaining colon fragments were further minced and incubated in a digestion solution containing 0.5 mg/ml collagenase D (Roche) and 0.5 mg/mL DNase I (Roche) at 37 °C for 20 min. at 250 rpm. The supernatant was poured off through a 70 μM filter into a new 50 mL Falcon tube containing 5 mL of complete media. A total of 3 rounds of digestion were performed. The remaining tissue was disaggregated using an 18 G needle and syringe and added to the collected digestion supernatants. Complete media was added

to top off collected supernatant, and cells were washed with 1xPBS and re-suspended in 40% (v/v) isotonic Percoll (GE Life Sciences) in complete media. 40% Percoll cell suspension was layered onto an 80% Percoll layer, and cells were centrifuged at 1000 x g for 20 mins with no brake. Lamina propria immune cells were obtained from the interphase between the two Percoll layers, and cells were washed and re-suspended in complete media prior to antibody staining. LP immune cells were extracted following a modified version of a previously described protocol (Weigmann, 2007).

5. Flow cytometry staining

Flow cytometry was used for immunophenotyping in various organ samples. Upon processing uninfected colons, spleens and/or bone marrow, up to 6×10^6 cells were transferred to 5 mL FACS tubes (Fisher, catalog # 14-961-10) and washed with 1x PBS twice. To assess cell viability, Zombie Yellow™ (BioLegend, San Diego, CA) was added to each sample at 1:100 dilution in 1x PBS and incubated for 20 minutes at room temperature. Cells were washed with 1-2 mL of FACS buffer (1-2% BSA in 1x PBS) and then incubated with Fc block (anti-CD16/32; BD, catalog #553142) for 10 min at 4 °C to prevent non-specific binding. Next, fluorochrome-tagged antibodies against various cell surface receptors (**Table 1**) were added in PBS-BSA followed by incubation for 30 mins. at 4 °C protected from light. Gating strategy employed: dendritic cells (MHC II^+CD11c^+), neutrophils ($CD11b^+$ $Gr\text{-}1^{hi}$ $Ly6C^{-/int}$), monocytes ($CD11b^+$ $Gr\text{-}1^{-/int}$ $Ly6C^{hi}$), macrophages ($CD11b^+$ $Gr\text{-}1^{-/lo}$ $Ly6C^{lo/int}$ $F4/80^+$), T cells ($CD11b^-$ $CD3^+$), B cells ($CD11b^-$ $B220^+$) and NK-cells ($DX5^+$). After washing, samples were fixed with 1% paraformaldehyde before acquisition on flow cytometer BD LSR Fortessa. Data were analyzed using Kaluza software (Beckman Coulter, version 1.2) or FlowJo V10 (FlowJo).

For intracellular nuclear staining, cells were first stained for surface markers as previously described. Then, they were fixed and permeabilized using FoxP3 Transcriptions Factor Fix/Perm Buffer Set (Biolegend #421403) followed by staining with anti-FoxP3-PE or -APC.

To assess the viability of HSCs and progenitor subsets, cells were initially stained with Zombie Yellow™ (1:100 in 1x PBS) and incubated for 20 minutes at room temperature. Following Zombie staining, cells were stained for various surface markers following the previously described

protocol. Cells were then washed twice with 1x PBS and treated with Annexin V (APC/Fire™ 750; Biolegend #640952; 3μL per 6 million bone marrow cells) in Annexin Binding Buffer (Biolegend #422201) for 20 mins. Finally, cells were washed once with 2 mL of Annexin Binding Buffer and were processed right away. Cells must remain in Annexin Binding buffer during acquisition, as it facilitates the binding of Annexin V to phosphatidylserine. The Zombie Yellow + Annexin V staining combination allows for the separation of dead vs. apoptotic cells.

Table 1: List of fluorochrome -tagged antibodies used against different surface and intracellular markers.

Marker	Clone	Fluorochrome	Company and Catalogue number
CD8α	53-6.7	APC-eFluor780	eBioscience #47-0081-82
	53-6.7	eF450	eBioscience # 48-0081-82
	53-6.7	Pe-eF610	eBioscience # 61-0081-82
CD11c	N418	eF450	eBioscience #48-0114-80
	N418	FITC	Biolegend #117305
CD62L	MEL-14	PerCp Cy5.5	eBioscience #25-0621-82
MHC II	M5/114	BV510	BD Pharmigen #742893
TCRβ	H57-597	Pe	eBioscience # 12-5961-82
Sirpα (CD172a)	P84	APC	eBioscience # 17-1721-80
B220	RA3-6B2	PerCP Cy5.5	Biolegend #103235
CD3ε	145-2C11	Pe	Biolegend #100307
	GK1.5	eF450	eBioscience #48-0032-82
CD4	RM4-5	APC	eBioscience # 17-0042-82
	GK1.5	FITC	Biolegend #100405
CD11b	M1/70	APC	eBioscience #17-0112-82
	M1/70	eF450	eBioscience # 48-0112-82
	ICRF44	PeCy7	eBioscience # 25-0118-42
CD49b	DX5	APC	eBioscience # 17-5971-81
Ly6C	HK1.4	Pe	eBioscience #12-5932-82
c-kit	2B8	PE-Cy7	eBioscience #25-1171-81
Sca-1	D7	PerCp-Cy5.5	eBioscience #45-5981-80
Lin*	17A2, RA3-6B2, M1/70, TER-119, RB6-8C5	FITC	eBioscience #22-7770-72
ST2	RMST2-2	PerCP-eFluor 710	eBioscience #46-9335-80
CD34	RAM34	eF450	eBioscience #48-0341-80
CD127(IL7R)	A7R34	APC	eBioscience #17-1271-82
CD16/32	93	Pe	eBioscience #12-0161-81
PD-1	J43	Pe	BD Pharmigen #561788
CD25	PC61	Pe-Cy7	Biolegend #102015
	PC61	BV421	Biolegend #102033
FoxP3	FJK-16s	APC	eBioscience #17-5773-80
	MF-14	Pe	Biolegend #126403
F4/80	BM8	APC ef780	eBioscience 47-4801-80
TNF	MP6-XT22	Pe-Cy7	eBioscience #25-7321-80

Marker	Clone	Fluorochrome	Company and Catalogue number
Ly6G/Ly6C (Gr-1)	RB68C5	FITC	eBioscience #11-5931-82
CD45.2	104	eF450	eBioscience #48-0454-82
IL1R1	35F5	BV421	BD Biosciences #564387

*Lin cocktail contains antibodies against the following markers: CD11b, Ly6G, CD3, B220, Ter119.

6. *In vivo* survival experiments

For the neutrophil/monocyte depletion experiment, InvivoPLUS grade Anti-Ly6C (Clone 1A8) and anti-Ly6C/G (clone: RB6-8C5) were obtained from BioXCell and injected i.p. (200 micrograms/mouse given twice per week from day 30 till 100). For $CD4^+$/$CD8^+$ T cell depletion, InvivoPLUS grade anti-CD4 (Clone GK1.5) and anti-CD8α (clone: 2.43) were obtained from BioXCell and injected i.p. (200 micrograms/mouse given twice per week from day 30 till 100). For suppression of mTORC1 activation, Rapamycin was obtained from LC laboratories and injected i.p. at a dose of 5 mg/kg every 3 days from day 28 till day 130.

7. Measurement of inflammatory genes by qPCR

The 30 mg sections of colon and/or spleen were harvested from mice and immediately frozen in RNAlater stabilization reagent (Qiagen, Hilden, Germany) then homogenized for RNA extraction. Total tissue RNA was extracted using the RNeasy Mini Kit (Qiagen) according to manufacturer's instructions. The 5 µg high-quality total RNA was then reverse transcribed using the First Strand Synthesis Kit (Qiagen) and loaded onto an inflammatory cytokine and chemokine RT2 profiler array (Qiagen). Real-time PCR was done using RT² SYBR Green qPCR Mastermix (Qiagen) and the reactions were run on a Biorad CFX 384 Real time PCR System. All data was normalized to an average of five housekeeping genes (*Gusb, Hprt, Hsp90ab1, Gapdh,* and *Actb*). For measurement of the expression of specific transcripts by qRT-PCR, data was normalized to *Actb* and the reactions were run on a Biorad CFX 96 Real time PCR System. Wherever possible, exon–exon spanning primers were used to avoid amplification of genomic DNA. The primer sequences were generated using the NCBI primer tool. Primers used are mentioned in **Table 2**.

Table 2. Primers used for qRT-PCR

Gene	Forward primer sequence (5'-3')	Reverse primer sequence (5'-3')
β-actin	GATCAAGATCATTGCTCCTCCTG	AGGGTGTAAAACGCAGCTCA
Cytochrome c oxidase 1	GCCCCAGATATAGCATTCCC	GTTCATCCTGTTCCTGCTCC
iNOS	GCCACCAACAATGGCAACAT	TCGATGCACAACTGGGTGAA
LIGHT	CTGCATCAACGTCTTGGAGA	GATACGTCAAGCCCCTCAAG
NLRP3	ATGCTGCTTCGACATCTCCT	AACCAATGCGAGATCCTG AC
PYDC3	CAGCTTCATCAGAGGAAAGCAA	TGGAAACCTCTGGGGAGTCA
TGF-β1	TGACGTCACTGGAGTTGTACGG	GGTTCATGTCATGGATGGTGC
XIAP	TTTTGTTTTGGGCCGGAACG	ATCGCCTTCACCTAAAGCAT
SNAT5 (slc38a5)	CCAGTGTTGTAGGCATCCGT	GTGCCAATAACAAGGGGGA
SNAT 1 (slc38a1)	TTACCAACCATCGCCTTC	ATGAGAATGTCGCCTGTG
SNAT 2 (Slc38a2)	GGTATCTGAACGGTGACTATCTG	TCTGCGGTGCTATTGAATGC
CD98 (slc3a2)	CAAAGTGCCAAGAAAAAGAGC	CTGAGCAGGGAGGAACCAC
LAT 1 (Slc7a5)	CTGGATCGAGCTGCTCATC	GTTCACAGCTGTGAGGAGC
GLUT1	CCAGCAGCAAGAAGGTGAC	ATGTTTGATTGTAGAACTCCTC
GLS	ACAGGAGCTGGGGAAGGG	ACCCTGTTTTATTTTATTGTCGCC
GLS2	CTTAGGCACTGACTACGTGCACAAG	CCGAGACATCTCCACTATATGCAGC
GLUL	CTCCATCCTGTTGCCATGTTTCGAG	GAGAGGGATCACTGGAAGTCTAGTC
ASCT2 (slc1a5)	TGCTTTCGGGACCTCTTCTA	TGATGTGTTTGGCCACACCA
BCL3	CCTTTGATGCCCATTTACTCTA	AGCGGCTATGTTATTCTGGAC
USP7	CCCGAGGACATGGAGATG	CATTGATGACAGGGTTCTGAGTA
FoxO1	AAGAGCGTGCCCTACTTCAA	CTCCCTCTGGATTGAGCATC
GPR83	TGACAGCTATCGCAGTGGAC	AGGTAGCCATGACCCAGATG
NRP1	GGAGCTACTGGGCTGTGAAG	CCTCCTGTGAGCTGGAAGTC
PRG4	AATGGTAAGCCAGTGGATGG	AGGGAATACCCCAAACTTCG
IGFR1	CAAGCTGTGTGTCTCCGAAA	TGATTCGGTTCTTCCAGGTC
PLAGL1	AAAATGTGGCAAGTCCTTCG	TGAATCTTCTGTGGCGAGTG

TET2	AACCTGGCTACTGTCATTGCTCCA	ATGTTCTGCTGGTCTCTGTGGGAA
IL-23p19	GCCCCGTATCCAGTGTGA	GCTGCCACTGCTGACTAG
CTLA4	CATGGTGTCGCCAGCTTTC	AGTCACCCGGACCTCATCA
Helios	ACACCTCAGGACCCATTCTG	CCATGCTGACATTCTGGAG
IL-33	CTACTGCATGAGACTCCGTTC TG	AGAATCCCGTGGATAGGC AGAG
ST2 (Ilrl1)	CGTGTCCAACAATTGACCTG	CAAGTAGGACCTGTGTGCCC
FoxP3	GCGAAAGTGGCAGAGAGGTA	TCCAAGTCTCGTCTGAAGGC

8. ROS imaging

WT, FoxO3a$^{+/-}$*, Il-10*$^{-/-}$ *and FoxO3a*$^{+/-}$*Il10*$^{-/-}$ mice were injected via the intraperitoneal route with L-012 (Wako, Osaka, Japan) dissolved in 1X PBS at a concentration of 20 μg/g of body weight in a 100μL volume. Bioluminescence signal was measured at 5 min post-injection of L-012 using an IVIS Spectrum imaging system (Perkin Elmer, MA, USA).

9. *In vivo* NAC treatment

For NAC treatment, *FoxO3a*$^{-/-}$*Il10*$^{-/-}$ mice were randomized to *ad lib* drinking water supplemented with 40 mM N-acetyl cysteine (Sigma-Aldrich, MO, USA) or regular drinking water starting at 4 weeks old and continuing throughout the entire duration of the study.

10. Measurement of cytokines at the protein level

The following cytokines were measured in the supernatants by enzyme-linked immunosorbent assays (ELISA) according to the manufacturer's instructions: IL-1β (Mouse R&D Duo Set #DY401), IL-1α (Mouse R&D Duo Set #DY400), TNF-α (BD #555268), IL-10 (BD #555252), IL-6 (BD 555240), IL-12p70 (BD #555256), IL-17A (Biolegend #432501), and IFN-γ (Biolegend #430801).

The steps were as follows: extra-high binding 96-well plates were coated with 50 µl/well of diluted capture antibody and incubated overnight at 4°C (RT for IL-1β and IL-1α), after which they were washed 3 times with PBS-T wash buffer consisting of 1X PBS and Tween 20 in H_2O. Wells were then blocked with 150µL of assay diluent (1%BSA in PBS for IL-1β and IL-1α, and 10% FBS in 1x PBS for the remaining cytokines) for one hour at room temperature. Plates were washed 3 times and up to 50µL of culture supernatants, along with the standards, were added to the respective wells for a two-hour incubation at RT. The wells were then washed five times with wash buffer, and 50µL of detection antibody conjugated with streptavidin-HRP (horseradish peroxidase) was added to all the wells and incubated for 1 hour in the dark. Finally, the plates were washed again 7 times with wash buffer and 50µL of tetramethylbenzidine (TMB) (Invitrogen #2023) was added and incubated in the dark for up to 30 minutes. The reaction was stopped by adding 25µL of stop solution (2N sulphuric acid diluted in H_2O). The absorbance of the plate was measured at 450-570 nm on FilterMaxTM F5 plate reader. The data was analyzed using SoftMax Pro software and Graphpad Prism 8.

For intracellular cytokine staining, cells were stimulated with LPS (100 ng/ml) and treated with Brefeldin A (1:1000, Biolegend #420601). After staining for surface markers, cells were fixed and permeabilized using the BD Cytofix/Cytoperm buffer system followed by staining with anti-TNF-PE-Cy7.

11. Generation of bone marrow-derived macrophages and in vitro stimulation with LPS

The bones (tibia, femur, and hip bone) were extracted from the mouse hind limbs. By using a 26-gauge needle (BD Biosciences #309625), bone marrow cells were then flushed out of the bones through a 100 µm strainer (Fisher Scientific #22363549) into an empty 50mL falcon tube on ice. Bone marrow cells were centrifuged, after which the cells were re-suspended in RPMI-1640 (Thermo Fisher Scientific #31800089) supplemented with 8% fetal bovine serum (FBS) (Gibco #12483020) and 55 µM β-mercaptoethanol (Thermo Fisher Scientific #21985-023). The media is referred to as R8. 100 mm plastic petri dishes were evenly coated with M-CSF (R&D Systems #416-ML-010) at 5 ng/ml using an L-stick (Sigma-Aldrich #SPR-L-S10). Approximately, 10-15 million cells were added in a final volume of 10 mL to each petri dish. Cells were incubated at 37°C for 6 days to allow macrophage differentiation to occur. After 6 days, bone-marrow derived macrophages (BMDMs) were washed with warm 1x PBS then scraped off the petri dishes into 10 mL of 1x PBS in a 50 mL Falcon tube. Following centrifugation at 500 G for 5 mins, the cells were re-suspended in R8. 100,000 cells were seeded per well of a 96 well flat bottom plate and incubated at 37°C overnight to ensure proper adherence. The next day, BMDMs were stimulated with LPS (1ng/mL), and supernatants were collected at various time intervals.

12. *In vitro* spleen cell culture

Spleens were homogenized using frosted-end glass slides (Fisher Scientific #12- 550-343). Red blood cells were lysed using RBC lysis buffer (Sigma-Aldrich #R7757) according to the manufacturer's instructions. Spleen cells were washed and re-suspended in R8 media. 10^7 cells were seeded per well in a 24-well plate. To ensure that the cells are properly adhered to the wells and to avoid stimulating them when stressed, the cells were incubated at 37 °C for 2 h. Next, cells were either treated with LPS (100 ng/ml) or infected with *Salmonella typhimurium*. Lower multiplicity of infection (10 MOI) was used for measurement of cytokines and immunoblotting. For the infection protocol, cells were centrifuged at 2500 rpm for 7 min to enhance bacterial uptake. Following incubation of 30 min at 37 °C, the media with the bacteria was aspirated out, and media containing 50 µg/ml Gentamicin (Thermo Fisher Scientific #15750-060) was added for 2 h to eliminate extracellular bacteria. Finally, the media was replaced with media containing a lower concentration of gentamicin (10 µg/mL). The infection was then allowed to proceed for desired timepoints.

13. Purification of splenic CD11c$^+$ cells and in vitro stimulations

CD11c$^+$ cells were purified from the spleens of WT, *FoxO3a*$^{-/-}$, *Il10*$^{-/-}$ and *FoxO3a*$^{-/-}$ *Il10*$^{-/-}$ mice using EasySep™ Mouse CD11c Positive Selection Kit II with Spleen Dissociation Medium (STEMCELL, # 18781) according to the manufacturer's protocol. 100,000 cells were seeded per well in a 96-well plate and incubated at 37 °C for 1-2 hours. Cells were then either treated with LPS (1 ng/mL) or infected with *Salmonella typhimurium* (10 M.O.I) for 6 hours. Supernatants were collected for measurement of cytokines.

14. Purification of CD4$^+$ T cells

CD4$^+$ and CD4$^+$CD25$^+$ T cells were purified from the spleens of WT, *FoxO3a*$^{-/-}$, *Il10*$^{-/-}$ and *FoxO3a*$^{-/-}$ *Il10*$^{-/-}$ mice using EasySep™ Mouse CD4$^+$CD25$^+$ Regulatory T-Cell Isolation Kit II (STEMCELL, # 18783) according to the manufacturer's protocol. 100,000 cells were seeded in a 96-well plate and were stimulated with plate-bound 1 μg/ml anti-CD3ε (Biolegend #100340) and 1 μg/ml anti-CD28 (Biolegend # 102115). CD4$^+$CD25$^+$ T cells were additionally stimulated with the addition of recombinant IL-2 and TGF-β (both at a concentration of 2.5 ng/mL). RNA and protein extracts were collected at different timepoints (24, 48 and 72H). Cells were either seeded in regular R8 or glutamine/glucose free RPMI (Biological Industries # 01-101-1A) supplemented with 8% dialyzed FBS (Thermofisher #A3382001), 55 μM β-ME, and either glutamine or glucose or both and further treated with the following inhibitors: 6-Diazo-5-oxo-L-norleucine or DON (Sigma # D2141) and L-Glutamic acid γ-monohydroxamate or GAH (Sigma # G2253).

For the co-culture experiments, cell death and proliferation of CD4$^+$T cells were evaluated using flow cytometry. 1x10^7 splenocytes per ml were labelled with 0.125μM Carboxyflurescein succinimidyl ester (CFSE) obtained from Sigma (St Louis, MO) in 1x PBS at 37°C for 10 min. Excess CFSE was quenched by adding an equal volume of R8 and placed on ice for 5 minutes followed by two washes with 1x PBS. T- cells were isolated from CFSE-labelled splenocytes as previously described and seeded for various experiments with and without co-cultured CD11c$^+$ cells. CFSE dilution is measured by flow cytometry to assess cellular proliferation. To assess cell viability, T cells were stained with Zombie Yellow dye following the protocol described under "Flow Cytometry staining" section.

15. Glutamine and glucose measurements

Glutamine, glutamate, and glucose levels were measured using the Glutamine/Glutamate-Glo™ Assay and Glucose-Glo™ Assay kits from Promega (J8021 and J6021 respectively) following the instructions of the manufacturer.

16. Purification of CD11b^{+} cells and *in vitro* stimulation

CD11b^{+} cells were purified from the spleens of WT, *FoxO3a*$^{-/-}$, *Il10*$^{-/-}$, *and FoxO3a*$^{-/-}$*Il10*$^{-/-}$ mice using EasySep™ Mouse CD11b Positive Selection Kit II (STEMCELL #18970) as per the manufacturer's instructions. 400,000 cells were seeded per well in a 24 well plate followed by treatment with LPS (100 ng/ml) in R8. Lysates were collected at various time intervals for Western blotting.

17. Western blotting

Cells were lysed in 1% SDS lysis buffer containing 1% β-ME and boiled immediately after for 5 min. Lysates were resolved by sodium dodecyl sulfate-polyacrylamide gel electrophoresis at 134 V for 75 min and then transferred to methanol-activated PVDF membrane (Biorad #1620177). The transfer was run at 100 V for one hour on ice. After transferring, the membranes were blocked in 5% bovine serum albumin in Tris Buffered Saline Solution (TBS-0.5 M Tris, 1.5 NaCl pH 7.6) with 0.5% Tween-20 for 1 h at room temperature on a rocker. The membranes were probed with primary antibodies, diluted in the same blocking buffer, overnight on a rocker at 4 °C. After incubation, the membranes were washed 3 times (10 min each) with TBS + 0.5% Tween-20 followed by incubation with a conjugated secondary antibody, diluted in the same blocking buffer, for 1 h at room temperature on a rocker. Finally, the membranes were washed 3 times and visualized using either Super Signal West Pico Plus (Thermo Scientific #34578) or the Super Signal Femto Plus (Thermo Scientific #34096). Antibodies used were as follows: p-p65 (Cell Signaling #3033), p65 (Cell Signaling #8242), p-Stat3 (Ser727) (Cell Signaling #9134), p-Stat3 (Tyr705) (Cell Signaling #9131 S), Stat3 (Cell Signaling #4904), p-4E-BP1 (Cell Signaling #2855), 4E-BP1 (Cell Signaling #9644), p-P70S6K (Cell Signaling # 9234), P70S6K (Cell Signaling # 2708), FoxO3a (Cell Signaling # 12829), p-MK2 (Cell Signaling #30075), MK2 (Cell

Signaling # 3042), p-ERK (Cell Signaling #4370), ERK (Cell Signaling #4695), and β-actin (Santa Cruz Biotechnology #sc-81178).

18. Bicinchoninic acid assay (BCA)

Protein concentration in whole cell lysates (in RIPA buffer) was measured using the BCA kit (Fisher # 23225) following the manufacturer's instructions.

19. Glycolysis cell-based assay

L-lactate levels were measured in supernatants using the Glycolysis Cell-Based Assay kit from Cayman Chemical (Michigan, USA), according to manufacturer's instructions.

20. MTT assay

Mitochondrial function was measured by adding MTT (3-[4,5-dimethylthiazol-2-yl]−2,5-diphenyltetrazolium bromide) to cells. The MTT reagent was diluted with R8 media at a final concentration of 0.5 mg/ml. Supernatants were aspirated, and100 μL of MTT solution was added per well. Cells were incubated at 37 °C. After 2 h, 5 mM HCl isopropyl alcohol (100 μL/well) were added to solubilize MTT crystals and absorbance was measured at a wavelength of 570 nm with a reference wavelength of 650 nm on a Molecular Devices FilterMax plate reader.

21. Mitochondrial bioenergetics assay

Wells of a 96-well Seahorse tissue culture plate (Seahorse Bioscience # 101085-004) were coated with cell adhesive Cell-Tak (Corning #354240), following the manufacturer's instructions, to promote adherence of cells. BMDMs were seeded into the wells at a density of 1.5×10^5 cells/well and incubated overnight at 37 °C. Next day, cells were treated with LPS (100 ng/ml) for 24 h. Splenocytes were seeded into the wells at a density of 8×10^5 cells/well and were incubated for 2 h at 37 °C followed by treatment with LPS (100 ng/mL) for ~5 h. The R8 medium was then removed, and cells were washed twice with warm Seahorse assay medium XF RPMI Medium pH 7.4 (Agilent Seahorse #103576-100). The medium was supplemented differently based on the assay performed: for glycolysis, XF media was supplemented with 2 mM glutamine; and for Mito stress test, XF media contained 1 mM sodium pyruvate, 2 mM glutamine and 10 mM glucose.

Cells were then allowed to equilibrate at 37 °C for 1 h without CO_2. Next, oxygen consumption rates (OCR, in pmol/min) or extracellular acidification rate (ECAR, in mph/min) were recorded on a Seahorse Bioscience XF96 Extracellular Flux Analyzer. Basal OCR and ECAR were recorded, as well as their fluctuations in response to sequential addition of various inhibitors in the following order: For Mito-stress test: Oligomycin (2 μM), FCCP (1 μM), and Rotenone/Antimycin A (1 μM); for glycolysis stress test: Glucose (10 mM), Oligomycin (2 μM) and 2-deoxyglucose or 2-DG (30 mM).

22. Cell-type-specific quantification of protein synthesis *in vivo*

100 μL of OP-Puro (R&D) in 1X PBS were injected intraperitoneally into a 10–12-weeks-old mice at a dose of 49.5 mg per kg of body weight. PBS injection was used as negative control. Bone marrow cells and splenocytes were harvested after 1 h. San Jose & Signer (2019) showed that the maximum OP-Puro signal in hematopoietic cells was detected 1 h after OP-Puro administration. 1×10^6 bone marrow cells were distributed per FACS tube and were stained with antibodies against cell surface markers, fixed and permeabilized using Fix/Perm Buffer set (Invitrogen). OP-Puro was detected by performing an azide-alkyne cycloaddition with the Click-iT Cell Reaction Buffer Kit (Life Technologies) and analyzed by flow cytometry. Antibody cocktails were prepared for different panels: Panel A (Gr-1, Ly6C, CD11b, CD11c, F4/80), Panel B (CD3, CD4, CD8α, B220) and Panel C (Sca-1, c-kit, Lin, CD34, CD16/32).

23. *In vivo* antibiotic treatment

FoxO3a$^{-/-}$*Il10*$^{-/-}$ mice ($n = 5$; age 5–8 weeks of age) received a 2 month-course of antibiotic treatment consisting of Ciprofloxacin (0.225 mg/mL) and Metronidazole (0.45 mg/mL) in their drinking water. Then, they were maintained on antibiotic-free water for the remainder of the study. As a control group, 5 mice received antibiotic-free drinking water. The numbers of spontaneous deaths were recorded over the course of time.

24. DNA extraction, V4-16S rRNA library construction and sequencing

Metagenomic DNA was extracted using MoBio PowerMag Soil DNA Isolation kit (Qiagen) as per its standard protocol and a KingFisher robot. The V4-16S rRNA sequencing was completed by Microbiome Insights, University of British Columbia, Vancouver, BC, Canada.

25. Microbiota sequencing data analysis

The V4 region of 16 S rRNA gene was amplified using dual-barcoded primers (515 F 5′-GTGCCAGCMGCCGCGGTAA-3′, and 806 R 5′-GGACTACHVGGGTWTCTAAT-3′) and the amplicon library for sequencing was constructed as described before (Kozich et al. 2013). The amplicon libraries were pooled and paired-end sequenced with Illumina MiSeq platform using 300 bp MiSeq Reagent Kit v3. To control for contaminants, a template-free control and extraction kit reagents control were co-sequenced with the specimens. The demultiplexed raw reads are available at NCBI Sequence Read Archive under PRJNA623633.

Sequences were quality filtered and clustered into operational taxonomic units (OTUs) based on 97%-similarity using mothur software package (v. 1.39.5) (Schloss et al., 2009). and the taxonomy was assigned to the generated OTUs using Greengenes (v. 13_8) as the reference database. Contaminant OTUs were identified and removed if their mean abundance in negative and extraction reagents controls is ≥25% of their mean abundance in the samples. Singleton and doubleton OTUs and OTUs that occur in less than 10% of the samples were removed. The remaining OTUs were rarefied into equal number of reads per sample (20,000) using QIIME 1.9.0 (Caporaso et al., 2010). Alpha diversity was estimated with Chao1 estimate and Shannon index. Beta diversity among samples were calculated using Bray-Curtis distance and visualized using Principal Coordinate Analysis (PCoA). The contribution of different mice groups to the variability of gut microbiota community was assessed from the Bray-Curtis distance matrix using adonis (Oksanen et al., 2016) using 999 permutations. To identify differential taxa among mice groups, linear discriminant effect size analysis was conducted on the relative abundance of different taxa levels using LEfSe (Segata et al., 2011). The taxa with log10 LDA score ≥2 and $P < 0.05$ were considered significant. When required Kruskal-Wallis test was applied for statistical analysis, and *P* values were corrected using Two-stage Benjamini, Krieger, and Yekutieli false discovery rate (FDR) procedure.

26. Serum determination of FITC-Dextran

13-15 weeks old ***FoxO3a*$^{-/-}$*Il-10*$^{-/-}$** were fasted for a total of 8 hours. At the beginning of the experiment, food was withdrawn from mice for 4 hours. Subsequently, one group of mice (n=3) received FITC-D (44mg/100g of body weight diluted in PBS;70 KDa; Sigma Aldrich Co., St. Louis, MO, USA; #46945) via oral gavage, and another group of mice (n=3) received PBS only. 4 hours post-gavage, mice were euthanized, and their blood was collected. The blood was centrifuged (1,000 × *g* for 15 min) to separate the serum from the red blood cells. Serial dilutions of FITC-D in PBS were used to calculate a standard curve. FITC-D levels of diluted sera were measured at excitation wavelength of 485 nm and emission wavelength of 528 nm on a Molecular Devices FilterMax plate reader.

27. Statistics

Error bars show standard error of the mean. Wherever mentioned in the text, one way-ANOVA and Mantel-Cox tests was used to determine the significance of the results. Statistical analyses were performed using GraphPad Prism software.

RATIONALE

Previous studies in our lab showed that *FoxO3a*$^{-/-}$ mice succumb rapidly to a challenge with the highly virulent, chronic enteropathogenic *Salmonella typhimurium* and express increased levels of the anti-inflammatory cytokine IL-10 (Joseph et al., 2016). Thus, we considered the possibility that increased IL-10 expression in *FoxO3a*$^{-/-}$ mice may abrogate the pro-inflammatory response required to contain the infection, and this can result in their early fatality. We therefore evaluated the role of IL-10 in the context of FoxO3a signaling and generated mice with a double-deficiency of both genes. We inter-crossbred *FoxO3a*$^{+/-}$ *Il10*$^{+/-}$ mice of C57BL/6J background to generate FoxO3a-IL-10 double-deficient mice. Naïve *FoxO3a*$^{-/-}$ *Il10*$^{-/-}$ mice exhibited an IBD-associated phenotype, and by day 120 all mice had reached the humane endpoint. Heterozygosity of FoxO3a was sufficient to induce complete disease penetrance, while minority of *Il10*$^{-/-}$ and no *FoxO3a*$^{-/-}$ mice developed this phenotype. Given the drastic impact of FoxO3a loss on the survival of *Il10*$^{-/-}$ hosts, I here investigate the potential inflammatory mechanisms through which FoxO3a promotes intestinal homeostasis and survival of *Il10*$^{-/-}$ mice.

HYPOTHESIS

This thesis tests the hypothesis that FoxO3a is an important regulator of intestinal inflammation in an IL-10-deficient host by restricting the over-activation of the immune system.

OBJECTIVES

The thesis is framed around four complementary aims:

Aim 1: Characterize the inflammatory phenotype of *FoxO3a* $^{-/-}$ *Il10* $^{-/-}$ mice

Aim 2: Reveal the cellular compartments through which FoxO3a prevents the development of intestinal inflammation in *Il10* $^{-/-}$ mice.

Aim 3: Decipher the mechanistic pathways through which FoxO3a and IL-10 regulate the inflammatory response.

Aim 4: Identify the gut microbiome signature that is created by the deficiency in FoxO3a and IL-10.

RESULTS

Aim 1: Characterize the inflammatory phenotype of FoxO3a$^{-/-}$ Il10$^{-/-}$ mice

1. **Loss of FoxO3a accelerates the development of a spontaneous and aggressive course of intestinal disease in *Il10* $^{-/-}$ mice**

We crossbred *FoxO3a*$^{+/-}$ *Il10*$^{+/-}$ mice on a C57BL/6J background to generate *FoxO3a*$^{-/-}$*Il10*$^{-/-}$ mice. Unexpectedly, the *FoxO3a*$^{-/-}$*Il10*$^{-/-}$ mice started losing weight spontaneously as of day 36 after birth, and within 3 months, they reached a humane endpoint that was characterized by more than 20% drop in body weight and signs of severe illness (i.e., diarrhea, rectal bleeding, hunching, poor movement, and piloerection) (**Fig. 1 a, b**). This phenotype was also observed in IL-10-deficient mice that were heterozygous for FoxO3a (*FoxO3a*$^{+/-}$) albeit at a slightly delayed kinetics, while a minority of *Il10*$^{-/-}$ and no *FoxO3a*$^{-/-}$ mice developed this phenotype (**Fig. 1a**). This implies that a 50% reduction in FoxO3a levels is enough to trigger the disease in susceptible hosts. To verify whether embryonic mortality was occurring due to the double-deficiency of *FoxO3a* and *Il10*, we analyzed the frequency distribution of the different genotypes resulting from the *FoxO3a*$^{+/-}$ *Il10*$^{+/-}$ inter-cross, and consequently, we observed a typical Mendelian distribution of frequencies with ~6.5% of the off-springs being *FoxO3a*$^{-/-}$*Il10*$^{-/-}$ (**Fig. 1c**).

Further examination revealed that while the weights of various organs were comparable, the weights of the colons in *FoxO3a*$^{-/-}$*Il10*$^{-/-}$ mice were significantly increased (**Fig. 2 a**). Their colons macroscopically appeared heavier and inflamed in comparison to the colons of the other three groups (**Fig. 2b**).

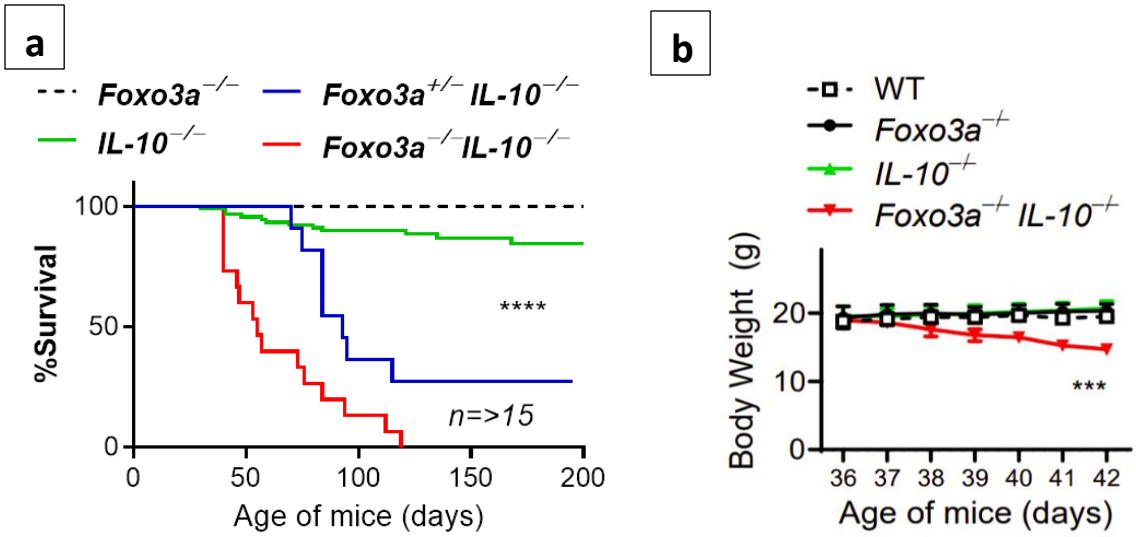

c

Frequency distribution of Foxo3a$^{+/-}$IL-10$^{+/-}$ inter-cross			
Genotype	**% Expected Frequency**	**% Observed Frequency**	**# of mice**
Foxo3a$^{+/+}$IL10$^{+/+}$	6.25	8.06	20
Foxo3a$^{+/+}$IL10$^{+/-}$	12.5	9.27	23
Foxo3a$^{+/+}$IL10$^{-/-}$	6.25	5.24	13
Foxo3a$^{+/-}$IL10$^{+/+}$	12.5	14.51	36
Foxo3a$^{+/-}$IL10$^{+/-}$	25	29.03	72
Foxo3a$^{+/-}$IL10$^{-/-}$	12.5	14.51	36
Foxo3a$^{-/-}$IL10$^{+/+}$	6.25	5.24	13
Foxo3a$^{-/-}$IL10$^{+/-}$	12.5	7.66	19
Foxo3a$^{-/-}$IL10$^{-/-}$	6.25	6.45	16
Total	100	99.97	248

Figure 1. Loss of FoxO3a in IL-10-deficient hosts potentiates illness to the point of fatality within 3 months of birth.

(a) Survival of mice monitored over a period of 200 days. (b) Changes in body weight (grams) of mice prior to reaching humane endpoint (n=7). (c) Frequencies of mice (n=248) born following *FoxO3a*$^{+/-}$ *Il10*$^{+/-}$ inter-cross. Graphs depict mean ± SEM. Statistics were done using One-way ANOVA (*$P < 0.05$, ***$P < 0.001$, and ****$P < 0.0001$) for panel (b). The Mantel-Cox test was used for survival analysis in panel (a).

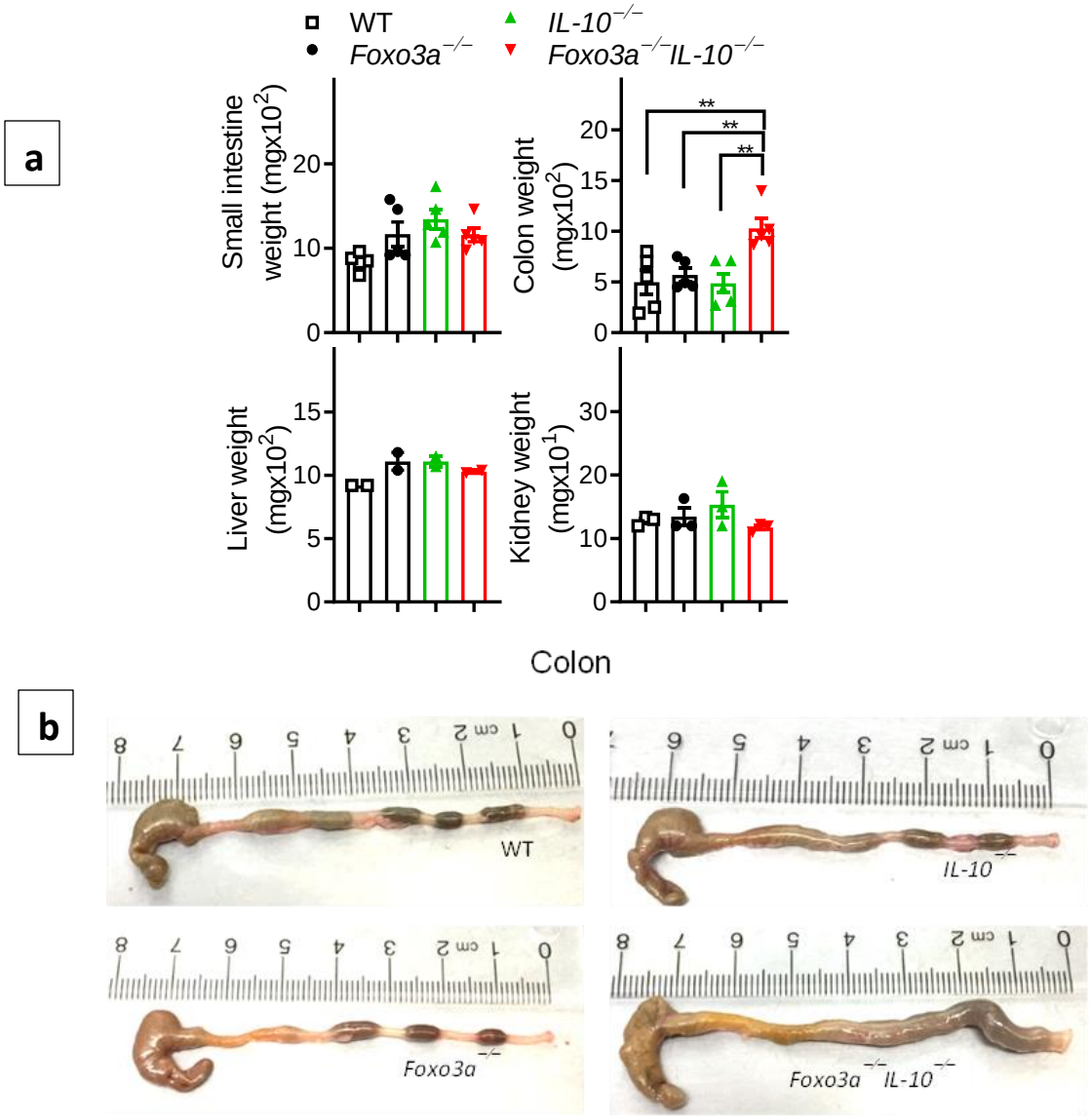

Figure 2. *FoxO3a*$^{-/-}$ *Il10*$^{-/-}$ mice exhibit signs of colitis.

(a) Weights (mg) of different organs in the four groups of 6 weeks old mice (n=2-5). (b) Representative images of the colons of the four groups of 6 weeks old mice. Data are based on a minimum of n=3 mice per group. Graphs depict mean ± SEM. Statistics were done using One-way ANOVA (*$P < 0.05$, ***$P < 0.001$, and ****$P < 0.0001$).

Since the *FoxO3a*$^{-/-}$*Il10*$^{-/-}$ mice displayed signs of rectal bleeding and increased colon weight, intestinal "swiss roll" cross-sections belonging to the four groups were examined in a blinded manner. Hematoxylin & Eosin (H&E) stain is a routine stain that provides a comprehensive picture of the microanatomy of organs, such that Hematoxylin (purple/blue) stains the nuclear components, and eosin (pink) stains the cytoplasmic contents and red blood cells. The analysis revealed histological severity of intestinal inflammation, such that the tissue architecture of the colon and the small intestine was found to be significantly disrupted in *FoxO3a*$^{-/-}$ *Il10*$^{-/-}$ mice (**Fig. 3a, b**). The lesions occurred in a discontinuous or "patchy" pattern throughout the length of the small intestine and the colon to a greater extent, such that the inflamed areas were highly infiltrated with polymorphonuclear and mononuclear cells, and the lamina propria was expanded into the mucosa and submucosa (**Fig. 3a, b**). Moreover, multifocal erosions, marked reduction in the villous/crypt ratio as well as crypt dropout and reactive epithelial regeneration were observed (**Fig. 3 a, b**). Alcian blue staining (pH 2.5) of the colons and the small intestines demonstrated a reduction in the amount of acidic mucin produced by the goblet cells (**Fig. 4 a, b**). Furthermore, to elucidate the gross composition of the extracellular matrix, colonic sections were stained with Mason Trichrome, which stains the nuclei in black, collagen rich regions in blue, and cytoplasm/ muscle fibers in red. We identified increased deposition of collagen into the colon submucosa of the *FoxO3a*$^{-/-}$*Il10*$^{-/-}$ mice in comparison to the other three groups (**Fig. 5).** Additionally, active caspase 3 staining (brown), indicative of apoptosis, was detected in colonic crypts of *FoxO3a*$^{-/-}$ *Il10*$^{-/-}$ mice, while the colons of the WT and the other two single knockout mice showed minor, scattered apoptotic cells in the mucosal epithelium (**Fig. 6a, b**).

a

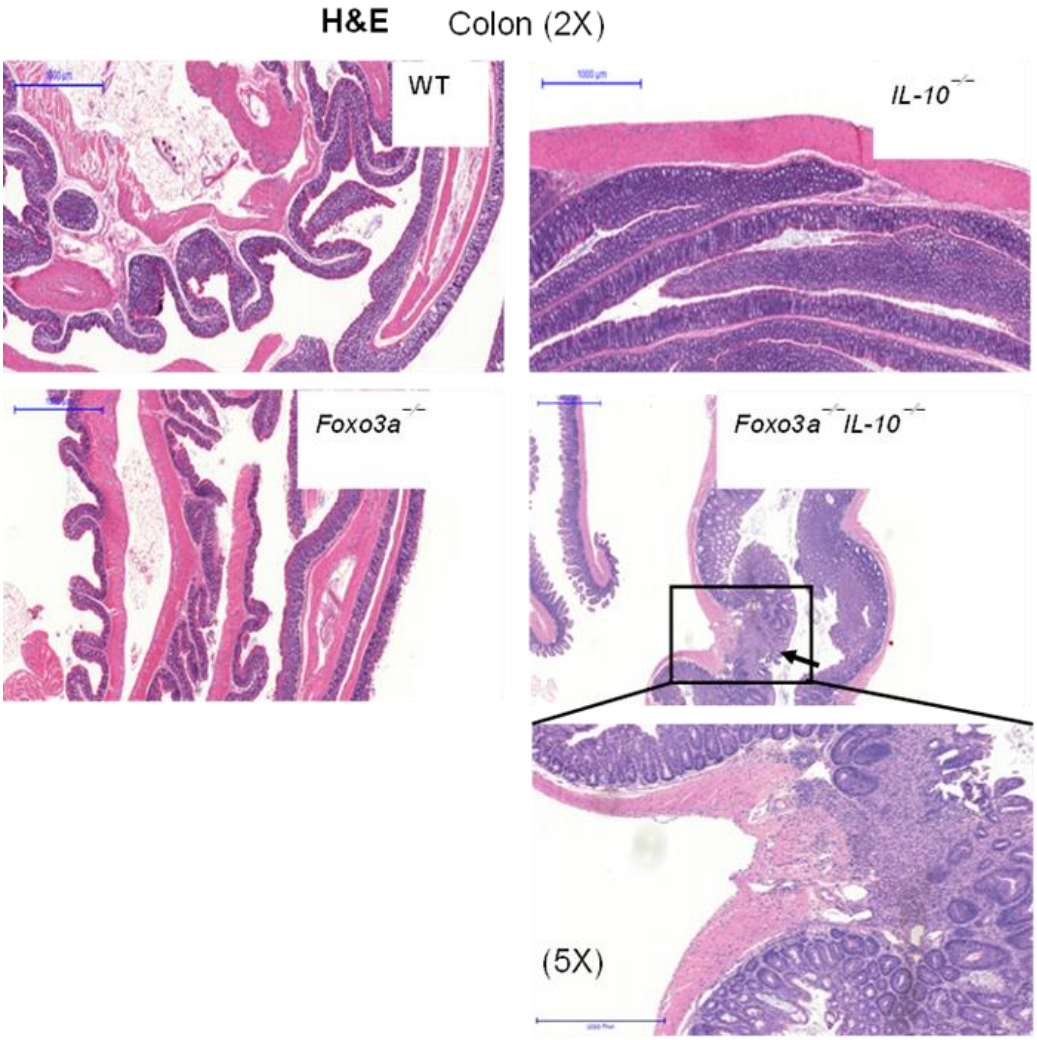

b

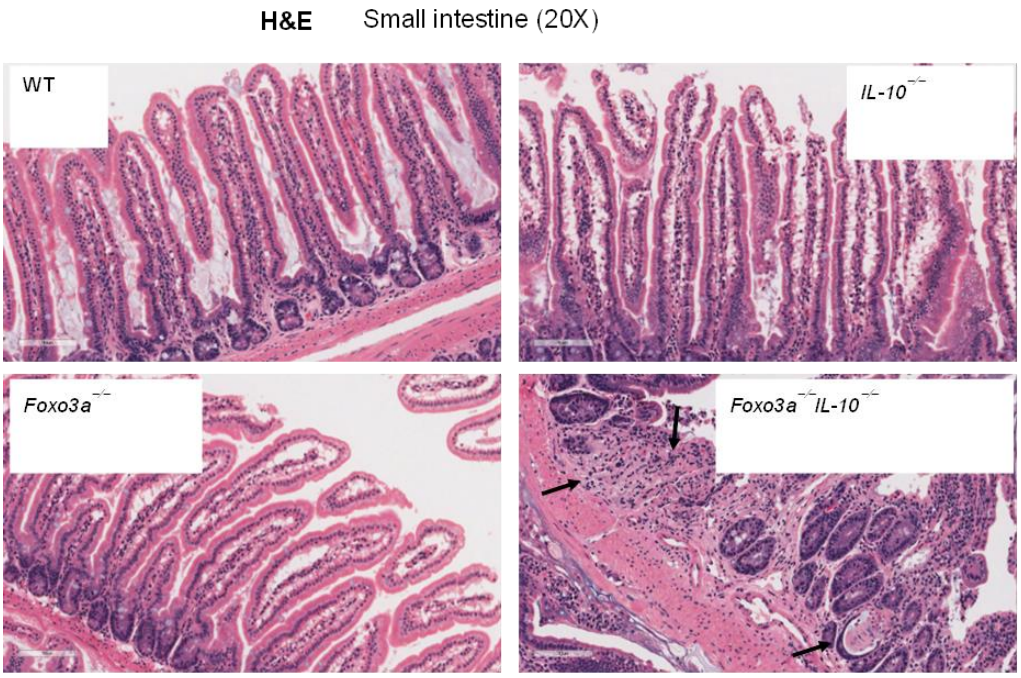

Figure 3. *FoxO3a*$^{-/-}$ *Il10*$^{-/-}$ mice exhibit a patchy pattern of inflammation in the intestines.

(**a)** Representative images (H&E) of the colons of the four groups of 6 weeks old mice. **(b)** Representative images (H&E) of the small intestines of the four groups of 6 weeks old mice. Arrows indicate areas of damage. A minimum of three independent histopathology analyses were conducted.

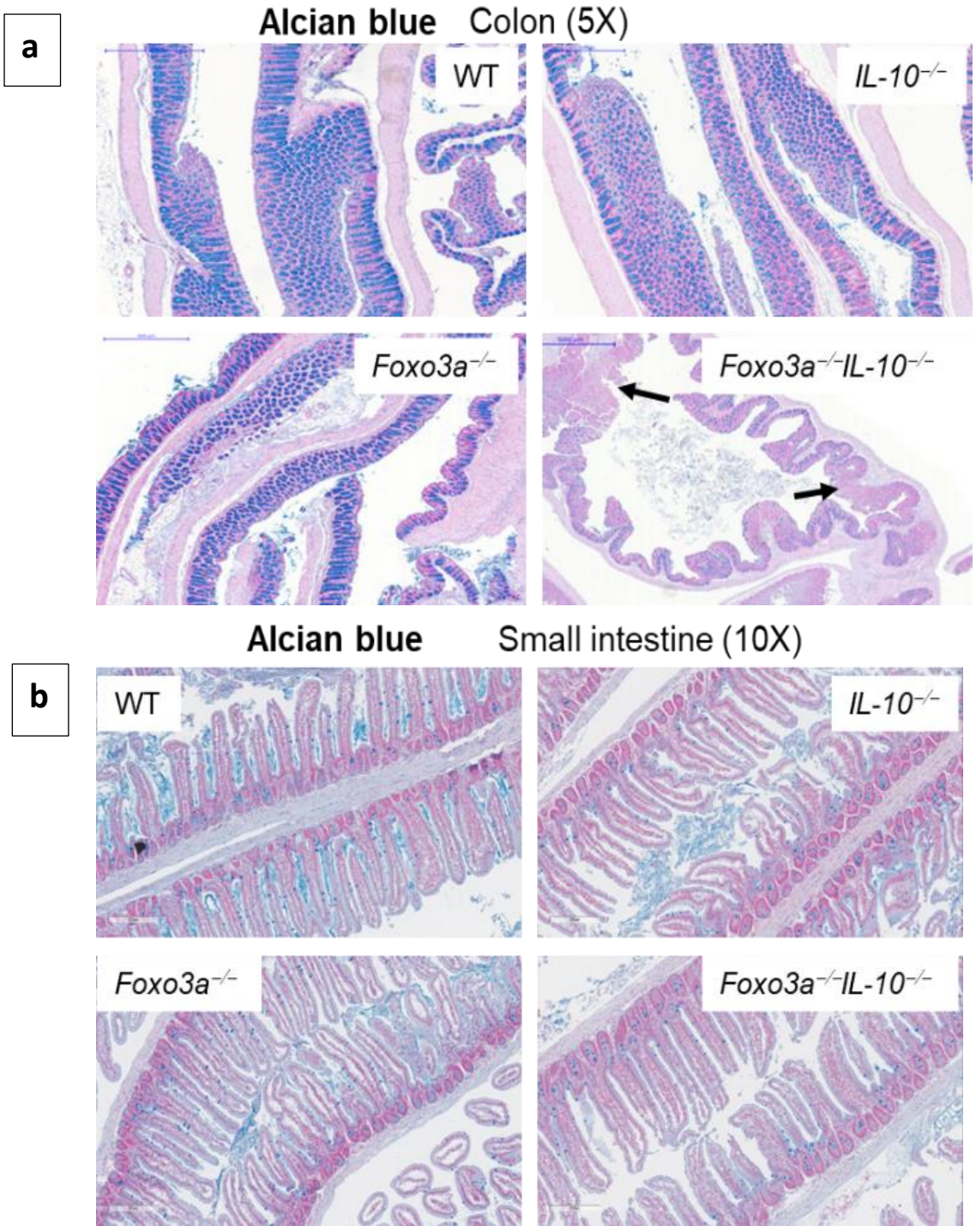

Figure 4. *FoxO3a*$^{-/-}$ *Il10*$^{-/-}$ mice exhibit reduced production of mucin in the intestines.

Representative images of Alcian blue staining of the colons (a) and small intestines (b) of the four groups of 6 weeks old mice. Arrows indicate areas of damage. A minimum of three independent histopathology analyses were conducted.

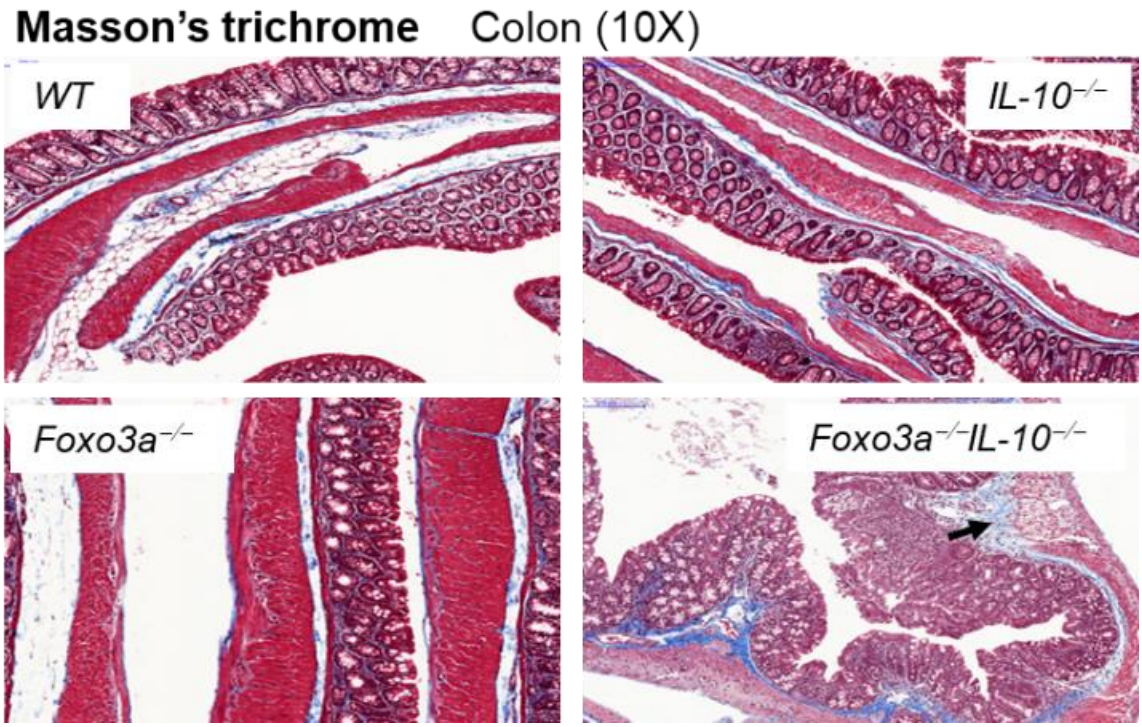

Figure 5. *FoxO3a*$^{-/-}$ *Il10*$^{-/-}$ mice exhibit increased fibrosis in the colons.

Representative images for Masson Trichrome staining of the colons of the four groups of 6 weeks old mice. Arrows indicate areas of mild fibrosis. A minimum of three independent histopathology analyses were conducted.

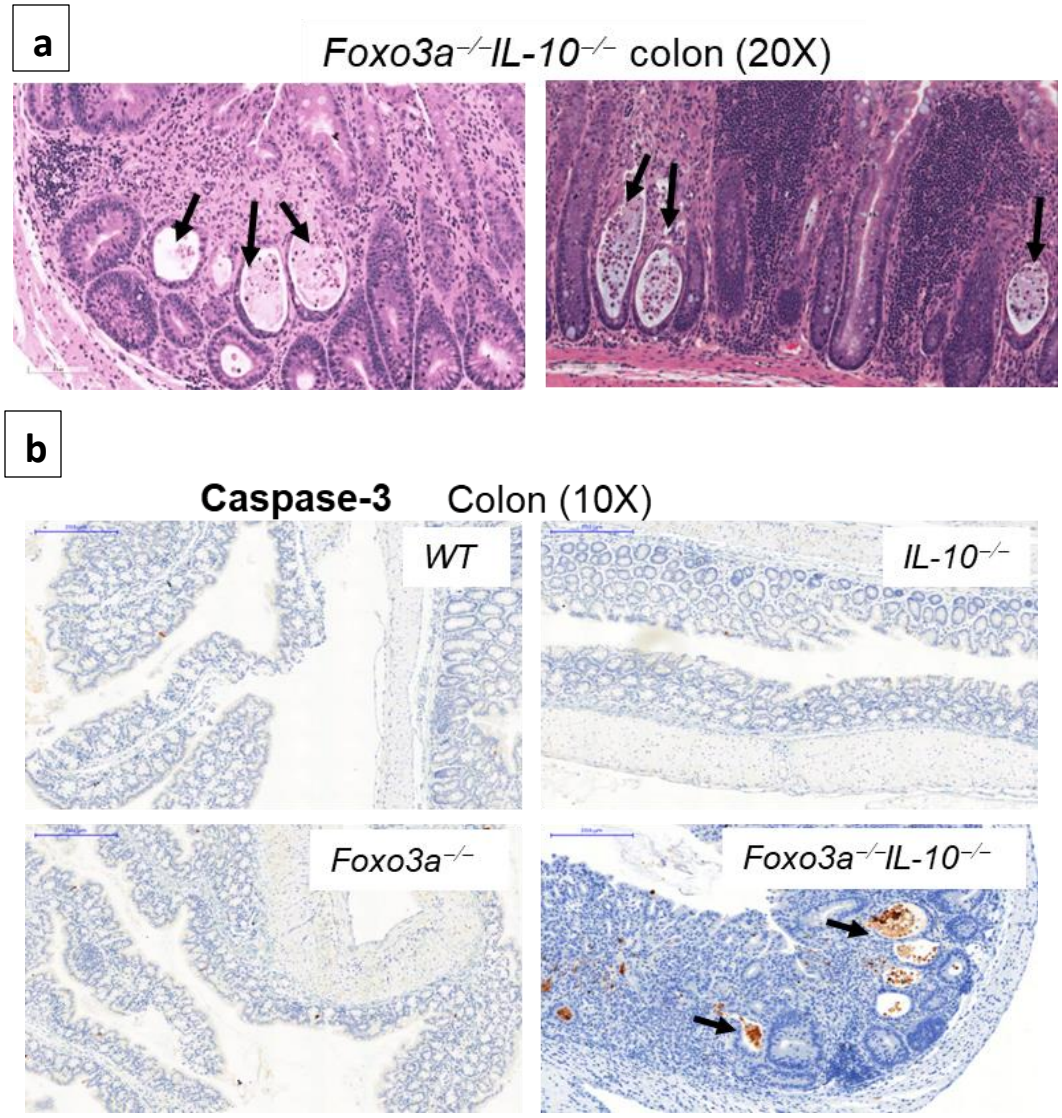

Figure 6. Colons of *FoxO3a*$^{-/-}$ *Il10*$^{-/-}$ mice develop apoptotic crypt abscesses.

(a) Representative images (H&E) of the colons of *FoxO3a*$^{-/-}$ *Il10*$^{-/-}$ mice. Arrows indicate crypt abscesses. (b) Representative images of the colons stained with anti-Caspase 3 antibody by IHC in the four groups of mice. Arrows indicate apoptotic crypts. A minimum of three independent histopathology analyses were conducted.

Damage to the intestinal wall can be healed through the ability of intestinal epithelial cells to initiate repair via cellular proliferation. In fact, a superficial erosion can be resealed by restitution or migration of the epithelial cells, while their cellular proliferation contributes to the resealing of larger areas of damage (Laukoetter et al, 2008). Since cell death was detected along with enhanced regenerative epithelium, we wanted to evaluate the proliferative capacity of the epithelial cells in the colons. Ki67 is a nuclear antigen specifically expressed in G1, S, G2 and M phases of continuously proliferating cells but is absent in Go cells (Holt et al, 1997). In WT and *Il10* $^{-/-}$ mice, Ki67 staining was primarily localized to the base of the crypt (**Fig. 7**). In *FoxO3a*$^{-/-}$ mice, the localization of Ki67 was not only confined to the base of the crypt but also appeared in enterocytes moving away from the base. This was highly augmented in the colons of *FoxO3a*$^{-/-}$*Il10*$^{-/-}$ mice (**Fig. 7**).

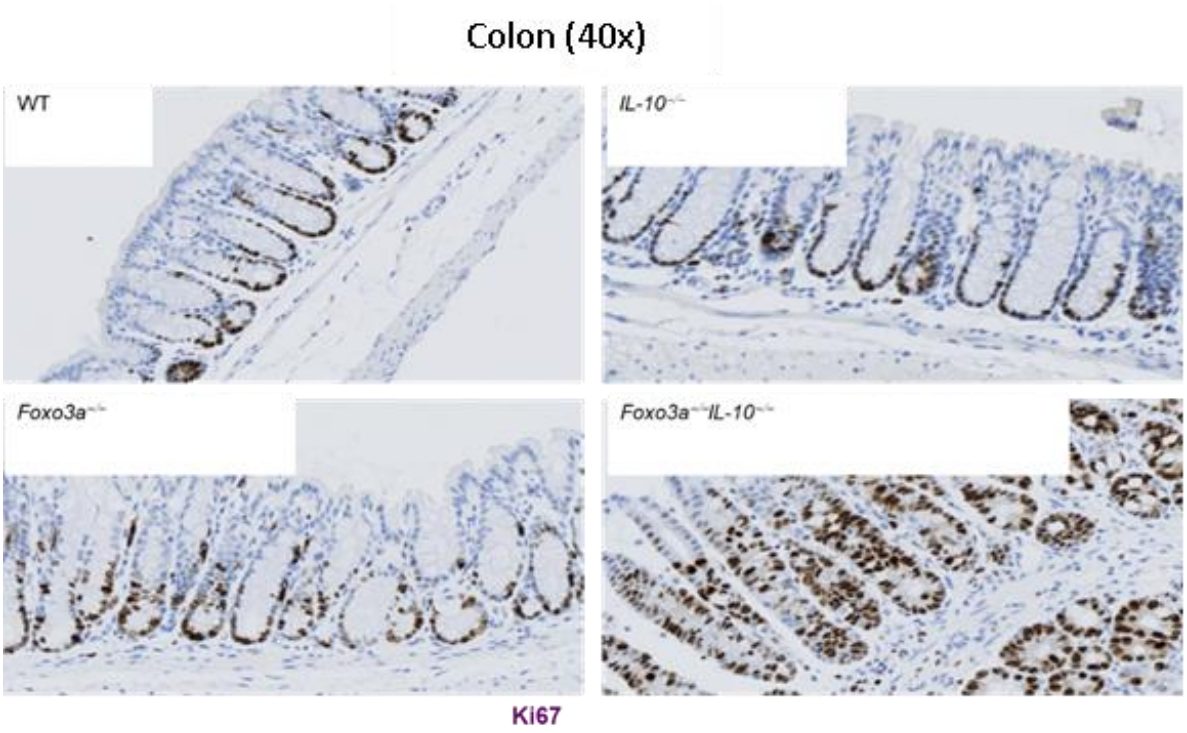

Figure 7. Increased proliferative capacity of the crypts in the colons of *FoxO3a*$^{-/-}$ *Il10*$^{-/-}$ mice.

Representative images of the colons stained with anti-Ki67 antibody by IHC in the four groups of 6 weeks old mice. A minimum of three independent histopathology analyses were conducted.

Finally, because we observed signs of extensive intestinal inflammation, we suspected that the accumulation of inflammatory immune cells in the colons triggers extra-medullary hematopoiesis in peripheral organs like the spleen. In fact, the spleens of *FoxO3a*$^{-/-}$ mice appeared slightly larger than their WT and *Il10*$^{-/-}$ counterparts at 8 weeks old. Histopathological analysis of H&E-stained spleen sections revealed the expansion of the white pulp (containing immune cells), increased cellularity and abundance of megakaryocytes in *FoxO3a*$^{-/-}$*Il10*$^{-/-}$ mice indicating the presence of extramedullary hematopoiesis (**Fig. 8 a, b**).

As confirmed by histopathology and immunohistochemistry analysis, we present a new physiological mouse model, deficient in FoxO3a and IL-10, that recapitulates the hallmarks of Crohn's disease in humans with 100% penetrance. The gut centric phenotype develops spontaneously and is revealed by discontinuous and transmural inflammation. In the next aim, we explore the impact of FoxO3a and IL-10 deficiency on the numbers and proportions of various immune cell types and reveal the cellular compartments contributing to the disease progression.

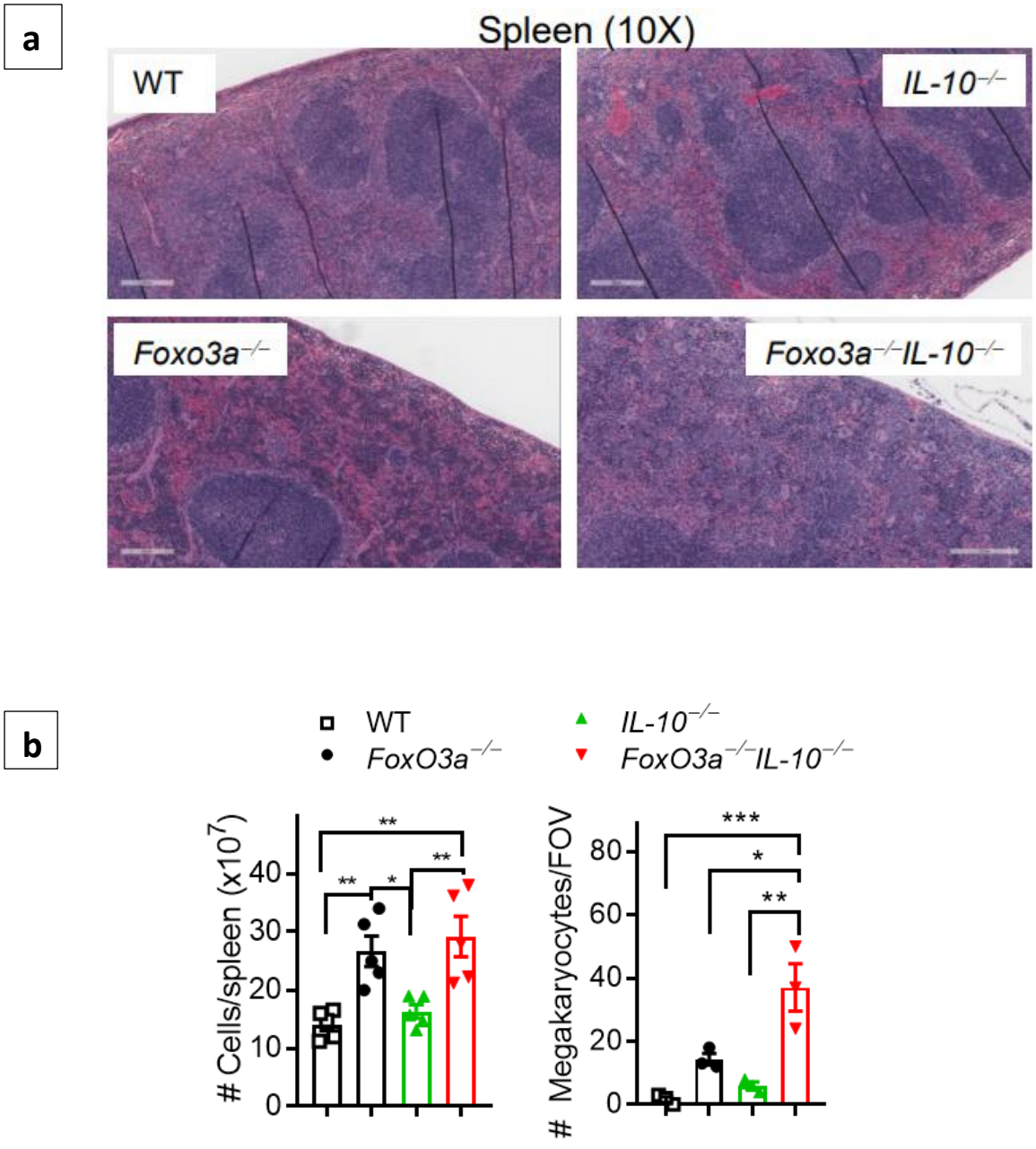

Figure 8. *FoxO3a*$^{-/-}$ *Il10*$^{-/-}$ mice undergo extramedullary hematopoiesis in the spleen.

(a) Representative images of the spleens (H&E) of the four groups of 6-8 weeks old mice. (b) Total spleen cell count and number of megakaryocytes (per field of view) measured in the spleens of the four groups of mice (n=3-5). A minimum of three independent histopathology analyses were conducted. All graphs depict mean ± SEM. Statistics were done using One-way ANOVA (*$P < 0.05$, ***$P < 0.001$, and ****$P < 0.0001$).

Aim 2: Reveal the cellular compartments through which FoxO3a prevents the development of intestinal inflammation in Il10$^{-/-}$ mice.

2. FoxO3a controls the numbers of innate and adaptive immune cells in IL-10-deficient hosts.

Given the increased infiltration of immune cells in the colons of *FoxO3a$^{-/-}$ Il10$^{-/-}$* mice as observed by histopathology, we evaluated the proportions of various immune cell populations in the colonic lamina propria by Flow Cytometry. Generally, CD11b^{+} myeloid cells were found to be highly abundant in *FoxO3a$^{-/-}$Il10$^{-/-}$* mice **(Fig. 9 a, d)**. The proportions and absolute numbers of infiltrating innate immune cells, including DCs (CD11c^{+}), monocytes (CD11b^{+}; Ly6C^{hi} and Ly6C^{int}) and neutrophils (CD11b^{+}; Gr-1^{hi}), were increased in *FoxO3a$^{-/-}$Il10$^{-/-}$* mice in comparison to the other groups (**Fig. 9 a-d**). Staining of cells with Zombie Yellow, which stains dead/dying cells, revealed that there was improved survival of the above-mentioned cell subsets in the LP of *FoxO3a$^{-/-}$Il10$^{-/-}$* mice, and this partly explains their increased cell numbers (**Fig. 10 a-c**).

Given the migratory nature of DCs and their enhanced recruitment to the gut during inflammation, we evaluated the proportions of classified DC subsets in the colon LP of the four groups of mice. While the percentages and absolute numbers of cDC1 (expressing CD8α) and pDC (expressing B220) subsets were comparable in the LP across the four groups of mice, the numbers of the myeloid cDC2 subset (CD11b^{+} SIRP$_{\alpha}^{+}$) were elevated in *FoxO3a$^{-/-}$ Il-10$^{-/-}$* mice in comparison to the other three groups (**Fig. 11 a-e**).

Studies in mice and humans have highlighted the critical role that T cells plays in the induction of IBD. We observed increased percentages and numbers of CD4^{+} T cells in the colonic LP of *FoxO3a$^{-/-}$Il10$^{-/-}$* mice in comparison to the other groups (**Fig. 12 a, b, d**). While the percentages of CD8^{+} T cells were similar across the groups, their total number was highest in the LP of *FoxO3a$^{-/-}$Il10$^{-/-}$* mice (**Fig. 12 b, d**). The proportion of Tregs (CD4^{+}FoxP3^{+}) was slightly reduced (**Fig. 12 c**); however, their absolute number was significantly increased in *FoxO3a$^{-/-}$Il10$^{-/-}$* mice (**Fig. 12 d**). No differences were observed in the expression of the pan-B cell marker B220 in the CD3^{-} population **(Fig. 12 d**).

Due to the expansion in the number of immune cells in the inflamed colon and the augmentation of the splenic white pulp, we considered the possibility that there may also be an increase in the numbers of immune cells in the spleen. While the numbers of lymphoid cells were comparable among the spleens of the four groups of mice (**Fig. 13 c, d, e**), we found higher numbers of macrophages, neutrophils and monocytes in *FoxO3a* $^{-/-}$ and *FoxO3a*$^{-/-}$ *Il10*$^{-/-}$ spleens (**Fig. 13 a, b, e**). Even though the proportions of $CD4^+$ and $CD8^+$T cells were not modulated in the spleens of *FoxO3a*$^{-/-}$*Il10*$^{-/-}$ mice, the cells expressed reduced levels of L-selectin (CD62L), which is indicative of enhanced activation or memory phenotype (**Fig. 14 a, b, c**).

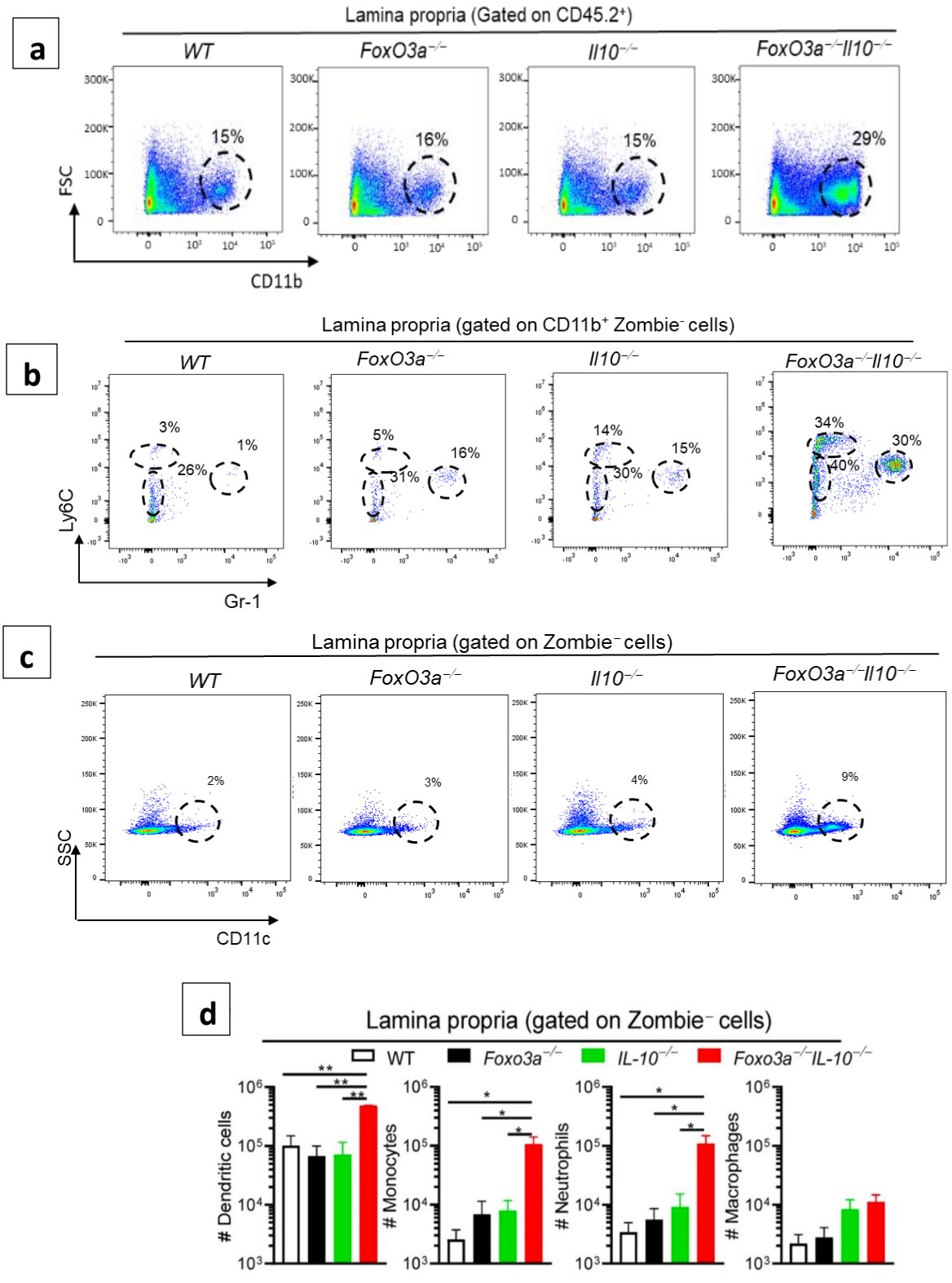
a
Lamina propria (Gated on CD45.2+)
WT
FoxO3a−/−
Il10−/−
FoxO3a−/−Il10−/−
15%
16%
15%
29%
FSC
CD11b
b
Lamina propria (gated on CD11b+ Zombie- cells)
WT
FoxO3a−/−
Il10−/−
FoxO3a−/−Il10−/−
3%
1%
26%
5%
16%
31%
14%
15%
30%
34%
30%
40%
Ly6C
Gr-1
c
Lamina propria (gated on Zombie- cells)
WT
FoxO3a−/−
Il10−/−
FoxO3a−/−Il10−/−
2%
3%
4%
9%
SSC
CD11c
d
Lamina propria (gated on Zombie- cells)
WT
Foxo3a−/−
IL-10−/−
Foxo3a−/−IL-10−/−
Dendritic cells
Monocytes
Neutrophils
Macrophages

Figure 9. Increased expansion of innate immune cells in the colon LP of *FoxO3a*$^{-/-}$ *Il10*$^{-/-}$ mice.

(a-c) Representative FACS plots showing the gating strategy for innate immune cell subsets in the colon LP of the four groups of mice. (d)Total numbers of *viable* innate immune cell subsets in the colon LP of the four groups of mice. Data are based on a minimum of three mice per group (6-12 weeks old). The experimental repeats were performed independently. All graphs depict mean ± SEM. Statistics were done using One-way ANOVA (*$P < 0.05$, ***$P < 0.001$, and ****$P < 0.0001$).

a

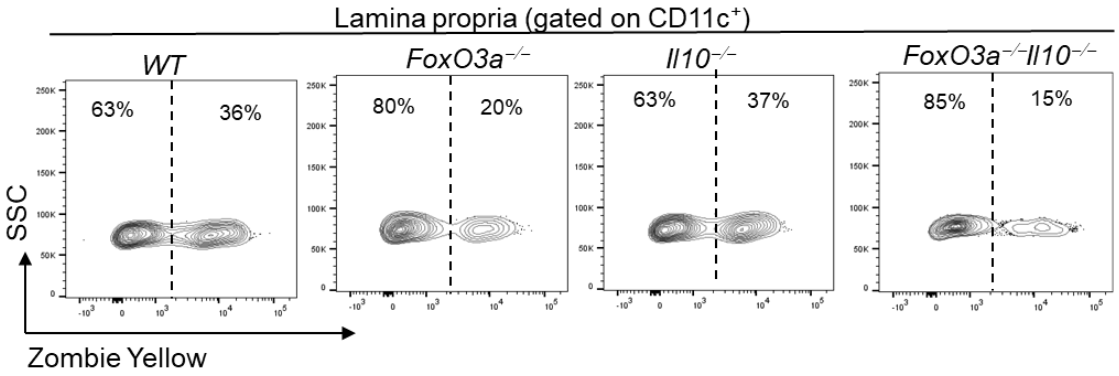
Lamina propria (gated on CD11c+)
WT
FoxO3a−/−
Il10−/−
FoxO3a−/−Il10−/−
63%
36%
80%
20%
63%
37%
85%
15%
SSC
Zombie Yellow

b

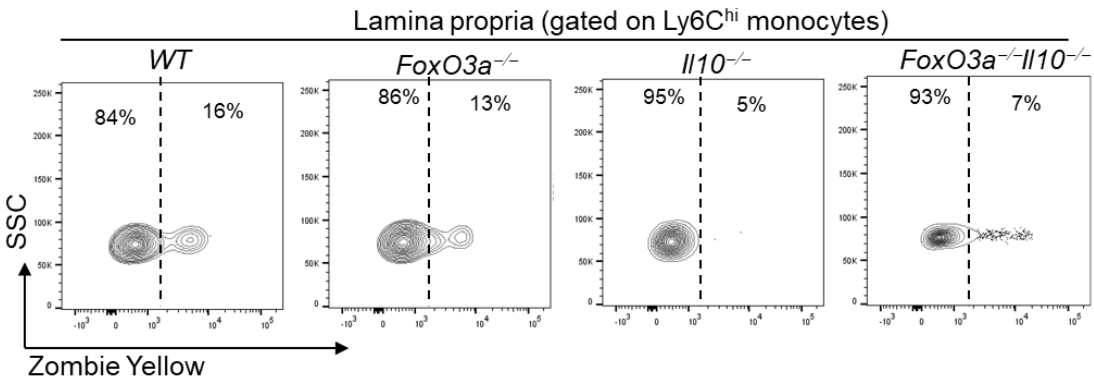
Lamina propria (gated on Ly6Chi monocytes)
WT
FoxO3a−/−
Il10−/−
FoxO3a−/−Il10−/−
84%
16%
86%
13%
95%
5%
93%
7%
SSC
Zombie Yellow

c

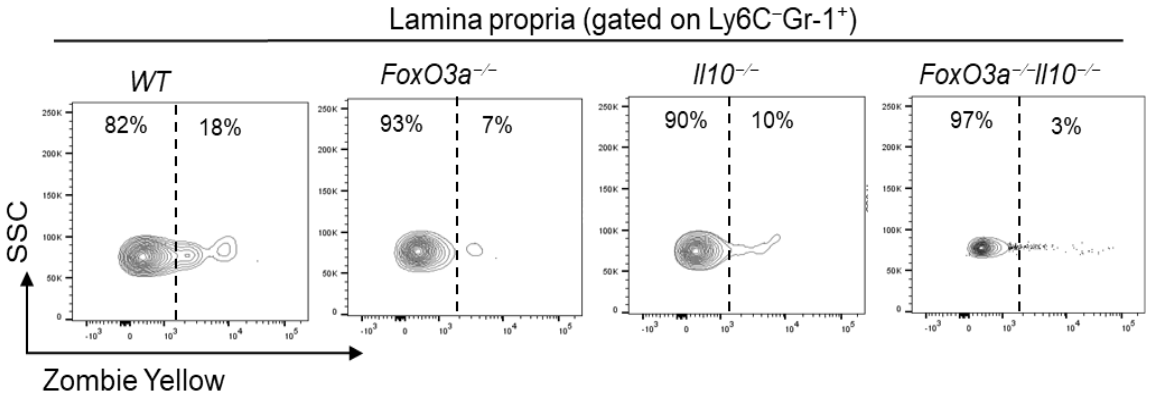
Lamina propria (gated on Ly6C−Gr-1+)
WT
FoxO3a−/−
Il10−/−
FoxO3a−/−Il10−/−
82%
18%
93%
7%
90%
10%
97%
3%
SSC
Zombie Yellow

Figure 10. Increased viability of innate immune cells in the colon LP of *FoxO3a*$^{-/-}$ *Il10*$^{-/-}$ mice.

Representative FACS plots showing the viability (by Zombie Yellow staining) of CD11c^{+} cells (a), monocytes (b) and neutrophils (c) in the colonic lamina propria of the four groups of mice. Data are based on a minimum of three mice per group (6-12 weeks old). The experimental repeats were performed independently.

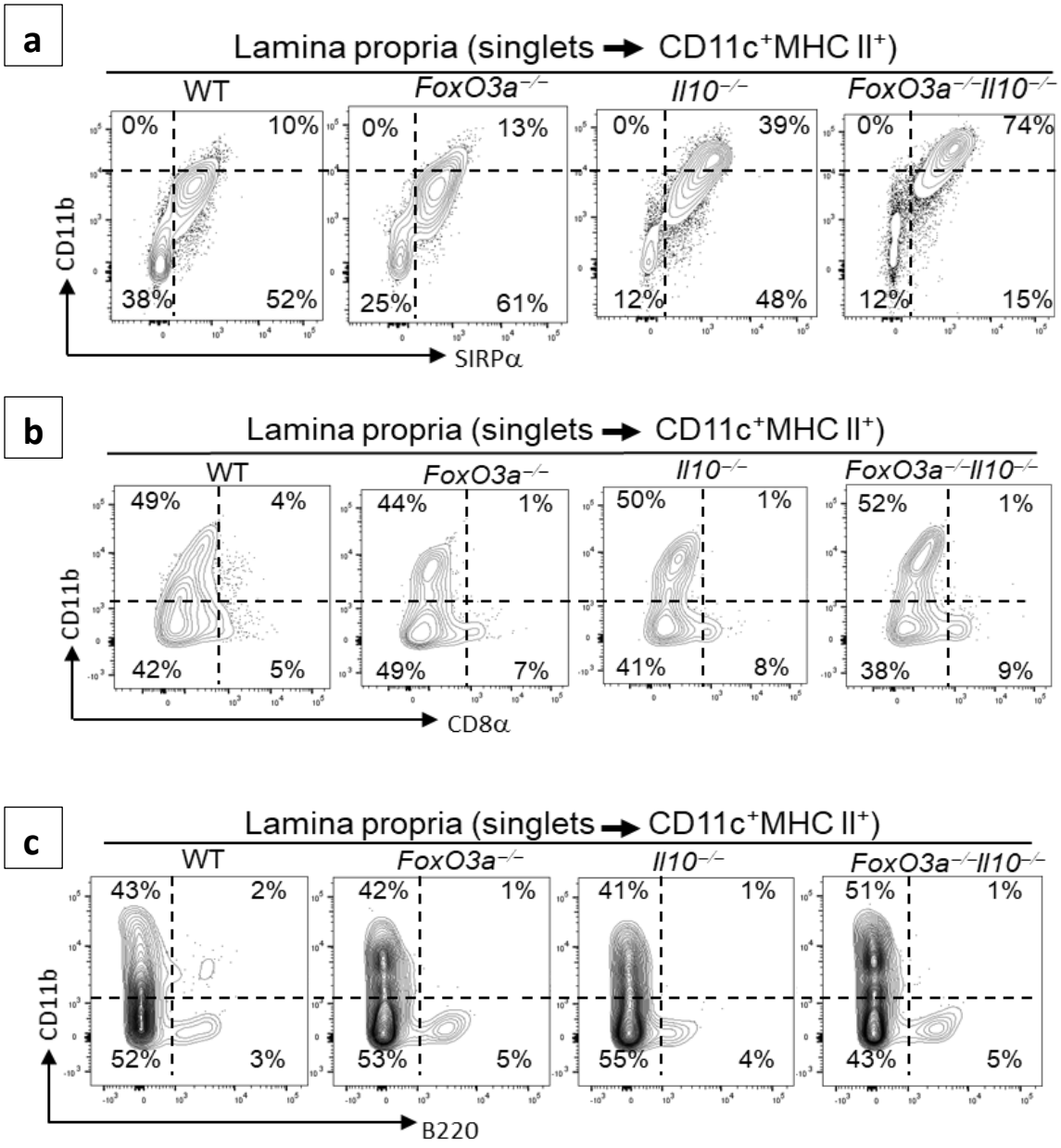
a
Lamina propria (singlets → CD11c+MHC II+)
WT
FoxO3a−/−
Il10−/−
FoxO3a−/−Il10−/−
0%
10%
38%
52%
0%
13%
25%
61%
0%
39%
12%
48%
0%
74%
12%
15%
CD11b
SIRPα
b
Lamina propria (singlets → CD11c+MHC II+)
WT
FoxO3a−/−
Il10−/−
FoxO3a−/−Il10−/−
49%
4%
42%
5%
44%
1%
49%
7%
50%
1%
41%
8%
52%
1%
38%
9%
CD11b
CD8α
c
Lamina propria (singlets → CD11c+MHC II+)
WT
FoxO3a−/−
Il10−/−
FoxO3a−/−Il10−/−
43%
2%
52%
3%
42%
1%
53%
5%
41%
1%
55%
4%
51%
1%
43%
5%
CD11b
B220

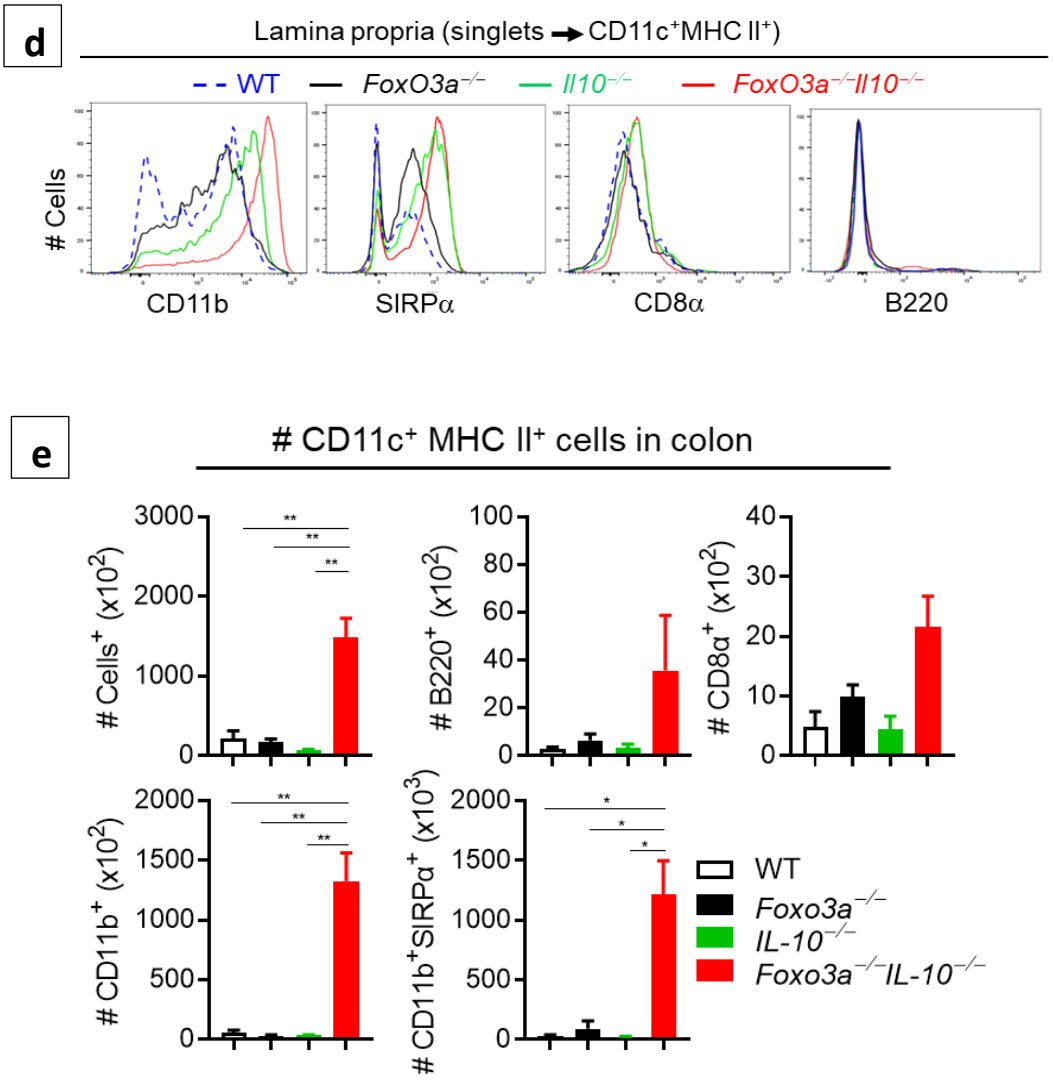

Figure 11. Increased expansion of the myeloid DCs in the colon LP of *FoxO3a*$^{-/-}$ *Il10*$^{-/-}$ mice.

(a-c) Representative FACS plots showing the gating strategy for DC subsets in the colon LP of the four groups of mice. (d) Representative histograms showing the expressions of markers pertaining to distinct DC subsets in the colonic LP of the four groups of mice. (e) Total numbers of DC subsets in the colon LP of the four groups of mice. Data are based on a minimum of three mice per group (8-12 weeks old). The experimental repeats were performed independently. All graphs depict mean ± SEM. Statistics were done using One-way ANOVA (*$P < 0.05$, ***$P < 0.001$, and ****$P < 0.0001$).

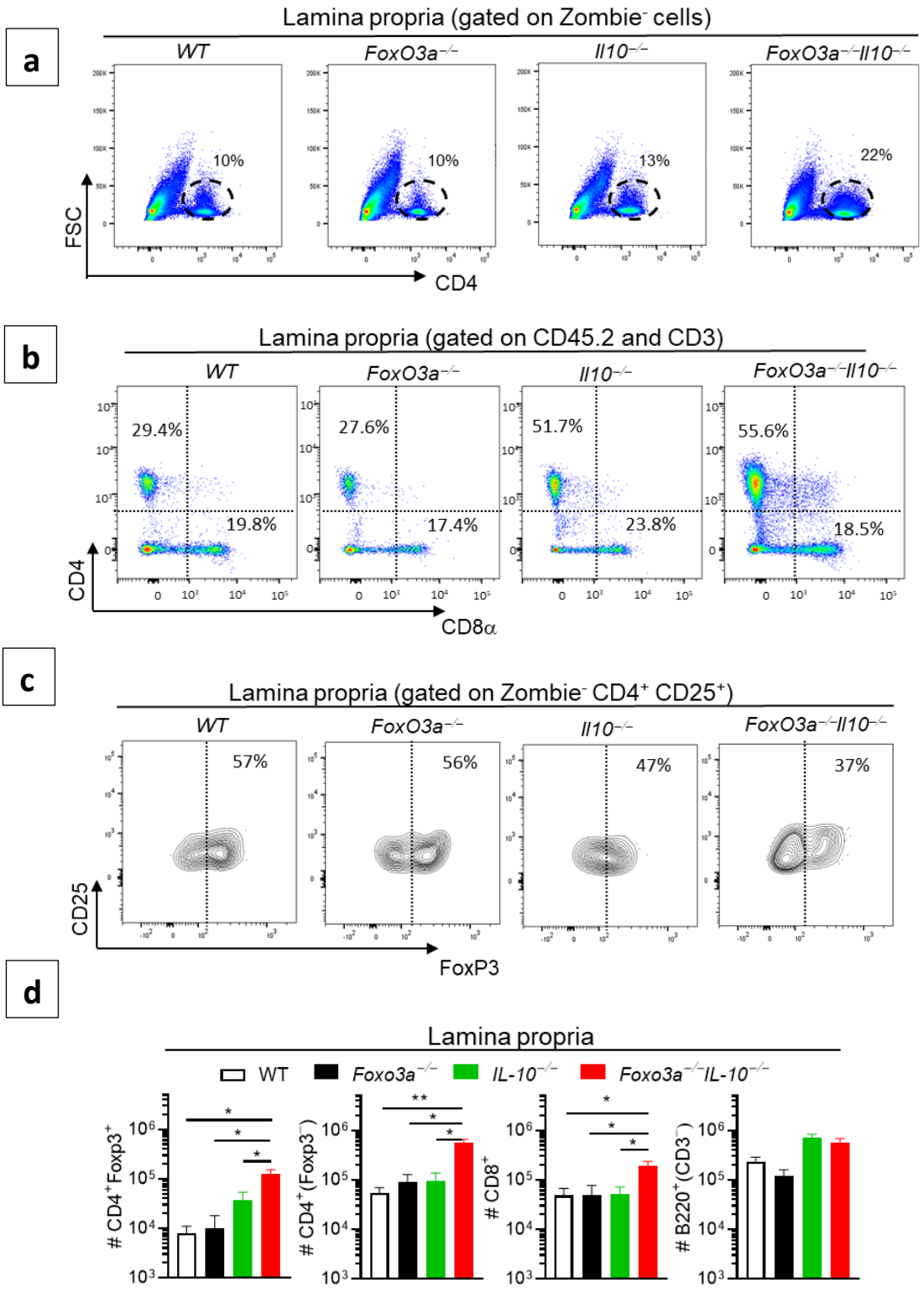
a
Lamina propria (gated on Zombie⁻ cells)
WT
FoxO3a−/−
Il10−/−
FoxO3a−/−Il10−/−
10%
10%
13%
22%
FSC
CD4
b
Lamina propria (gated on CD45.2 and CD3)
WT
FoxO3a−/−
Il10−/−
FoxO3a−/−Il10−/−
29.4%
19.8%
27.6%
17.4%
51.7%
23.8%
55.6%
18.5%
CD4
CD8α
c
Lamina propria (gated on Zombie⁻ CD4⁺ CD25⁺)
WT
FoxO3a−/−
Il10−/−
FoxO3a−/−Il10−/−
57%
56%
47%
37%
CD25
FoxP3
d
Lamina propria
WT
Foxo3a−/−
IL-10−/−
Foxo3a−/−IL-10−/−
CD4⁺Foxp3⁺
CD4⁺(Foxp3⁻)
CD8⁺
B220⁺(CD3⁻)

Figure 12. FoxO3a modulates the numbers of T cells in IL-10-deficient hosts.

(a-c) Representative FACS plots showing the gating strategies for lymphoid T cell subsets in the colonic LP of the four groups of mice. (d) Total numbers of lymphoid cell subsets in the colonic LP of the four groups of mice. Data are based on a minimum of three mice per group (8-12 weeks old). The experimental repeats were performed independently. All graphs depict mean ± SEM. Statistics were done using One-way ANOVA (*$P < 0.05$, ***$P < 0.001$, and ****$P < 0.0001$).

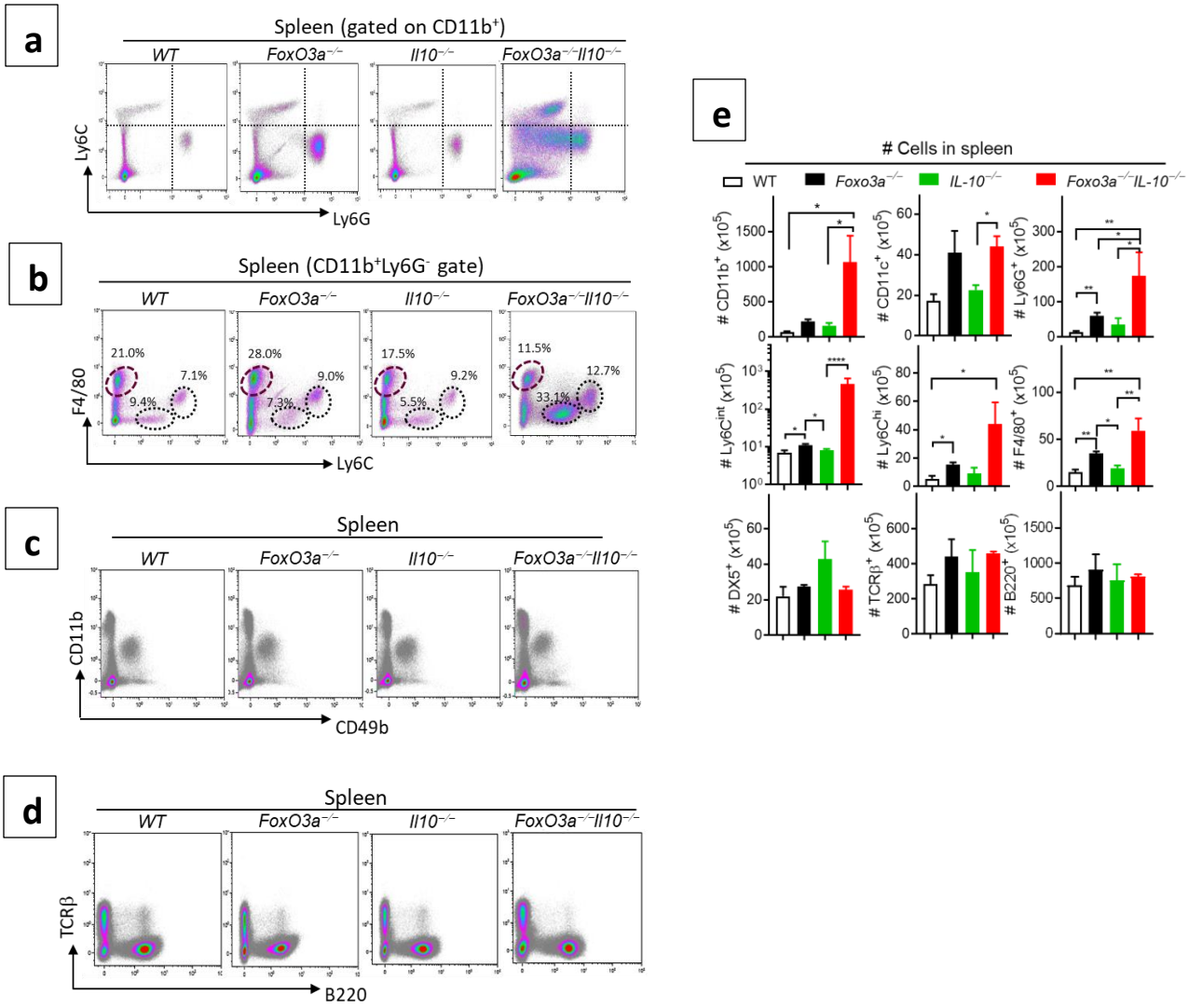

Figure 13. Increased hematopoiesis in the spleens of *FoxO3a*$^{-/-}$*Il10*$^{-/-}$ mice.

(a-b) Representative FACS plots showing the gating strategies of myeloid cells in the spleens of the four groups of mice. (c-d) Representative FACS plots showing the lymphoid cell subsets: NK cell population (CD49b^{+}) (c); T cell (TCRβ^{+}) and B cell (B220^{+}) populations (d). (e) Total numbers of myeloid and lymphoid cell subsets in the spleens of the four groups of mice. Data are based on a minimum of three mice per group (8-12 weeks old). The experimental repeats were performed independently. All graphs depict mean ± SEM. Statistics were done using One-way ANOVA (*$P < 0.05$, ***$P < 0.001$, and ****$P < 0.0001$).

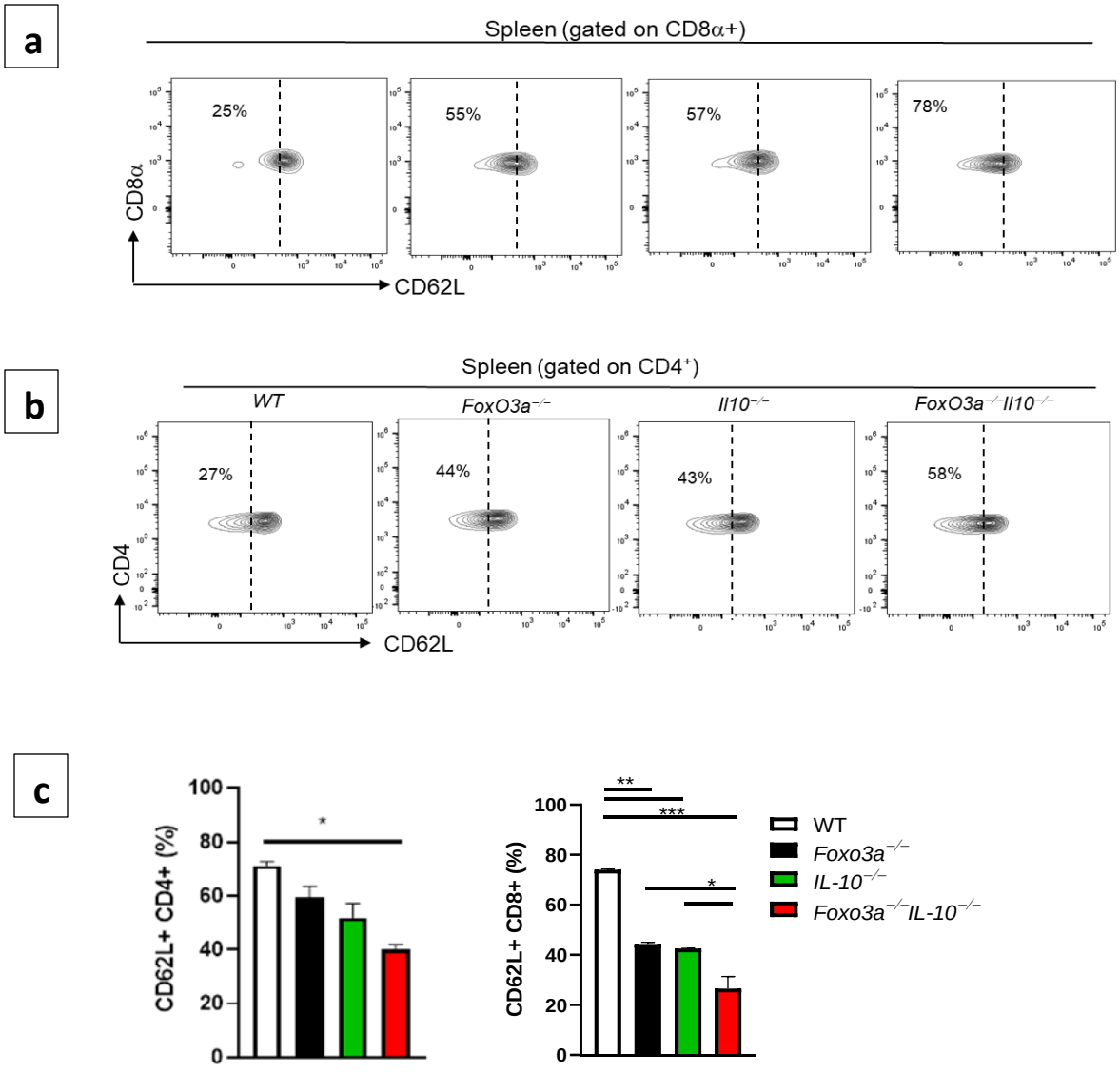

Figure 14. Downregulation of CD62L in splenic T cells of *FoxO3a*$^{-/-}$*Il10*$^{-/-}$ mice.

(a, b) Representative FACS plots showing CD62L expression in splenic CD4^{+} and CD8α^{+} T cells of the four groups of mice. (c) Quantification of total percentages of CD62L-expressing T cells in the four groups of mice. Data are based on a minimum of three mice per group (8-12 weeks old). The experimental repeats were performed independently. Statistics were done using One-way ANOVA (*$P < 0.05$, ***$P < 0.001$, and ****$P < 0.0001$).

By the same token, we wanted to examine how the inflammatory cells are regulated at their site of production, the bone marrow. Looking at the mature cells, we observed an increase in the myeloid $CD11b^+$ cells, most notably Ly6C ^{high} and Ly6C ^{int} monocytes. The proportions of other cell types seemed comparable among the four groups of mice, and the $B220^+$ population appeared to be reduced in the absence of FoxO3a (**Fig. 15**).

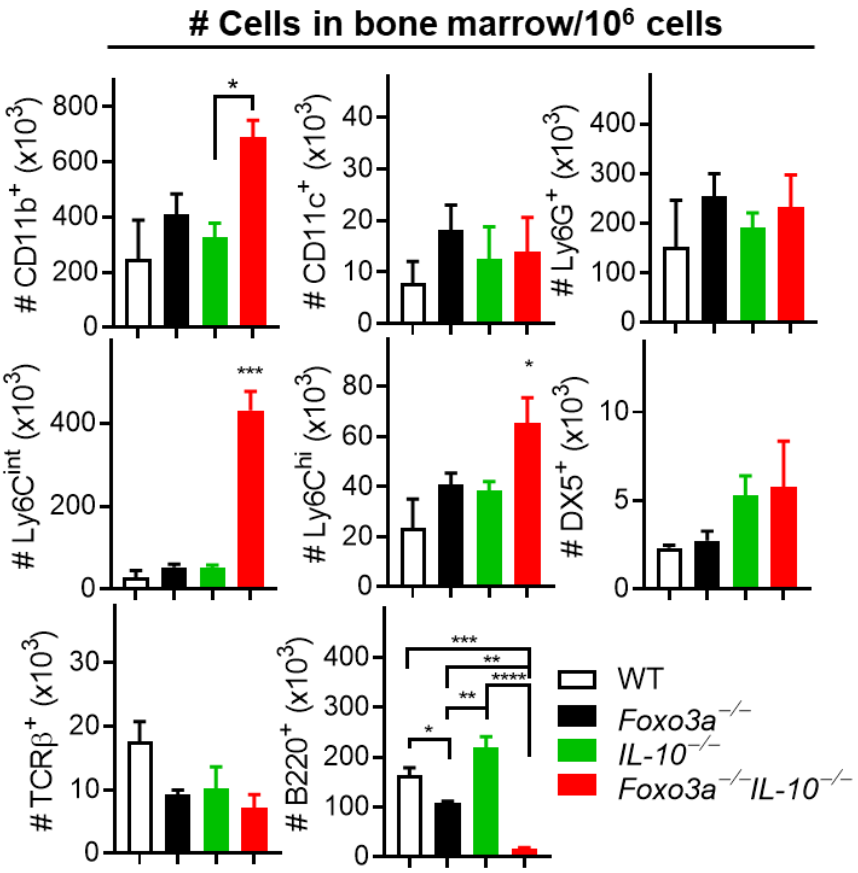

Figure15. Loss of FoxO3a results in the modulation of immune cell numbers in the bone marrow of IL-10-deficient hosts.

Numbers of myeloid and lymphoid cell subsets are presented per 10^6 bone marrow cells in the four groups of mice. The gating strategy applied is similar to the one in Figure 13 (a-d). Data are based on a minimum of three mice per group (8-12 weeks old). The experimental repeats were performed independently. All graphs depict mean ± SEM. Statistics were done using One-way ANOVA (*$P < 0.05$, ***$P < 0.001$, and ****$P < 0.0001$).

The persistent and long-standing accumulation of myeloid cells in the LP places substantial pressure on myelopoiesis in the bone marrow. Indeed, innate immune cells, particularly neutrophils, have a shorter lifespan compared to T cells and B cells; therefore, a tight regulation between the bone marrow supply and peripheral demand is critical. Since we observed substantial qualitative changes in the mature cell composition (Lin^+) in the bone marrow (**Fig. 16 a, e**), we were interested in checking whether the upstream stem/progenitor compartment was affected by the intestinal inflammation. The classic model of hematopoiesis postulates a pyramidal model, where HSCs are at the apex followed by the MPPs and immediate divergence of lymphoid and myeloid lineages through CLPs and CMPs. HSCs are rare (~0.01% of total BM cells) but are highly enriched among $Lin^-Sca1^+c\text{-}Kit^{hi}$ cells, designated as LSKs (Kondo, et al., 2003). The inflammatory environment in the colons of *FoxO3a*$^{-/-}$*Il10*$^{-/-}$ mice led to an increase in the percentage of LSKs among Lin^- cells in the bone marrow compared to the other three groups (**Fig. 16 b, e**). Also, the percentage of the myeloid progenitor population (MP; $Lin^-Sca\text{-}1^-c\text{-}Kit^{hi}$) was considerably increased in *FoxO3a*$^{-/-}$*Il10*$^{-/-}$ mice, and its cellular composition was dramatically altered with a skew towards GMP differentiation (**Fig. 16 c**). The percentages of MEPs and CMPs were not significantly altered but appeared to have a reducing trend in *FoxO3a*$^{-/-}$ *Il10*$^{-/-}$ mice (**Fig. 16 c, d, e**). In addition, no significant differences were seen in the numbers of IL-$7R^+$ CLPs (**Fig. 16 d**). We also found that, in the presence of inflammation, the spleen constitutes a reservoir of HSCs and GMPs that might have also contributed to the increase in the production of splenic myeloid cells and their potential migration to the colon in *FoxO3a*$^{-/-}$ *Il10*$^{-/-}$ mice (**Fig. 17a, b, c**). This finding complements the increase in the extra-medullary hematopoietic activity previously described.

Upon assessing the degree of cell death using Zombie Yellow and Annexin V stains, we observed that there was less cell death overall in all the cell types particularly in the LSK population. Despite this, we observed that there was enhanced viability in the LSKs, CMPs and GMPs populations of the *FoxO3a*$^{-/-}$ *Il10*$^{-/-}$ mice (**Fig. 18 a-e**). Low to none of necrotic cells were detected in the various subsets, which may be explained by their immediate phagocytic clearance (**Fig. 18 a-c**).

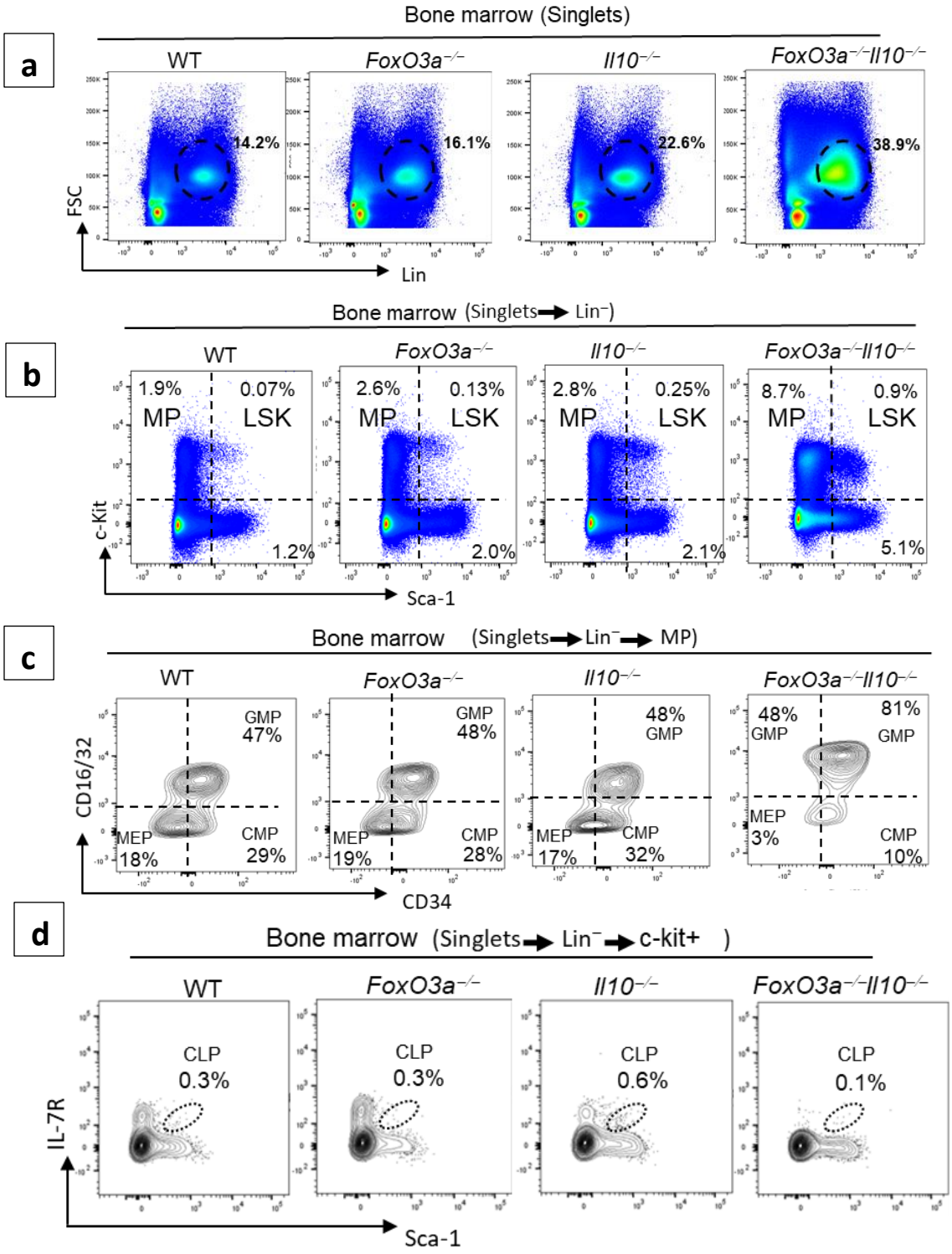
a
Bone marrow (Singlets)
WT
FoxO3a−/−
Il10−/−
FoxO3a−/−Il10−/−
14.2%
16.1%
22.6%
38.9%
FSC
Lin
b
Bone marrow (Singlets➡ Lin−)
WT
FoxO3a−/−
Il10−/−
FoxO3a−/−Il10−/−
1.9%
0.07%
MP
LSK
1.2%
2.6%
0.13%
MP
LSK
2.0%
2.8%
0.25%
MP
LSK
2.1%
8.7%
0.9%
MP
LSK
5.1%
c-Kit
Sca-1
c
Bone marrow (Singlets➡ Lin−➡ MP)
WT
FoxO3a−/−
Il10−/−
FoxO3a−/−Il10−/−
GMP
47%
MEP
18%
CMP
29%
GMP
48%
MEP
19%
CMP
28%
48%
GMP
MEP
17%
CMP
32%
48%
GMP
81%
GMP
MEP
3%
CMP
10%
CD16/32
CD34
d
Bone marrow (Singlets➡ Lin−➡ c-kit+)
WT
FoxO3a−/−
Il10−/−
FoxO3a−/−Il10−/−
CLP
0.3%
CLP
0.3%
CLP
0.6%
CLP
0.1%
IL-7R
Sca-1

e

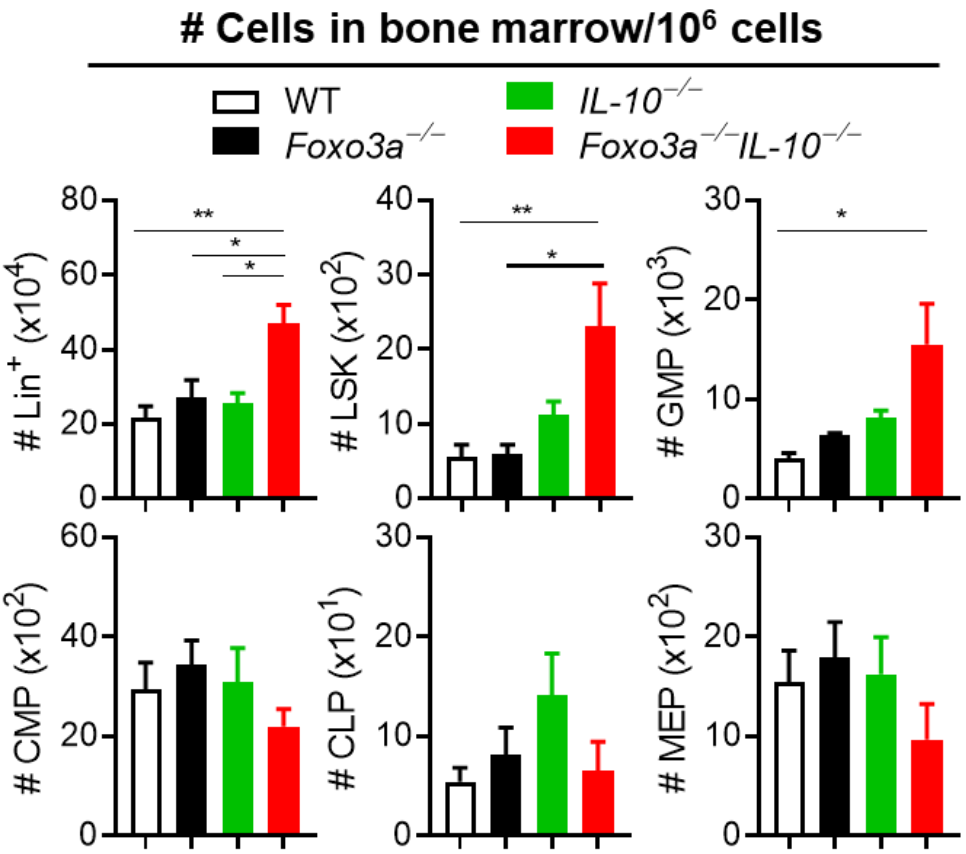

Figure 16. Differential regulation of hematopoietic lineages in *FoxO3a*$^{-/-}$*Il10*$^{-/-}$ mice.

(a-d) Representative FACS plots showing the gating strategy for hematopoietic stem/progenitor subsets (LSK: Lin^- $Sca\text{-}1^+$ $c\text{-}Kit^+$; CLP: Lin^- $Sca\text{-}1^+$ $c\text{-}Kit^+$ $IL\text{-}7R^+$; MP: Lin^- $Sca\text{-}1^-$ $c\text{-}Kit^+$; based on MP gate: CMP: $CD16/32^{lo}$ $CD34^+$, GMP: $CD16/32^+CD34^+$, MEP: $CD16/32^-CD34^-$). (e) Quantification of HSC and progenitor cell subsets per 10^6 bone marrow cells in the four groups of mice. Data are based on a minimum of three mice per group (8-12 weeks old). The experimental repeats were performed independently. All graphs depict mean ± SEM. Statistics were done using One-way ANOVA (*$P < 0.05$, ***$P < 0.001$, and ****$P < 0.0001$).

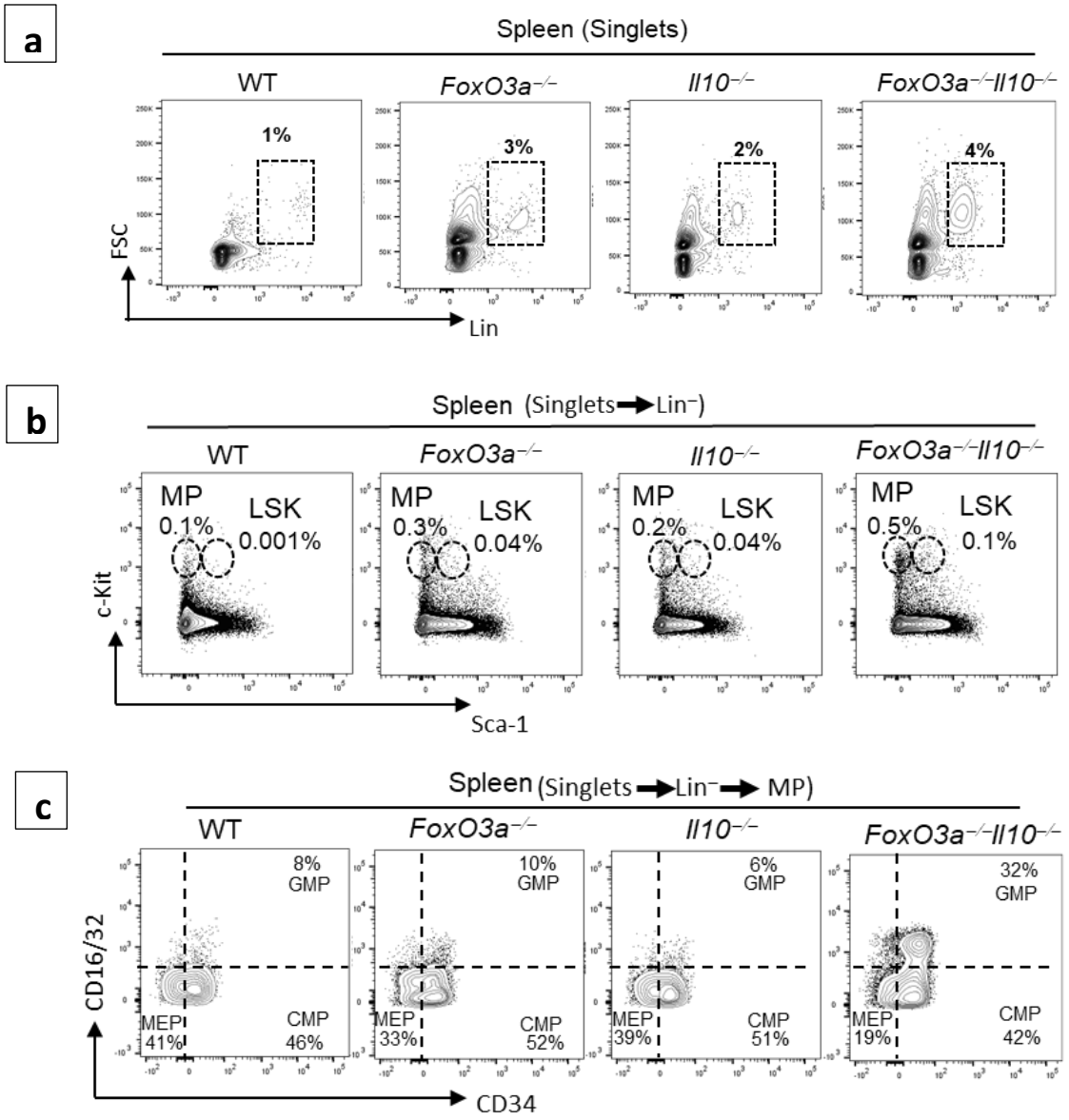

Figure 17. Accumulation of HSCs and GMPs in the spleen of *FoxO3a*$^{-/-}$*Il10*$^{-/-}$ mice.

(a-d) Representative FACS plots showing the gating strategy for hematopoietic stem/progenitor subsets (LSK: Lin$^-$ Sca-1$^+$ c-Kit$^+$; CLP: Lin$^-$ Sca-1$^+$ c-Kit$^+$ IL-7R$^+$; MP: Lin$^-$ Sca-1$^-$ c-Kit$^+$; based on MP gate: CMP: CD16/32^{lo} CD34$^+$, GMP: CD16/32$^+$CD34$^+$, MEP: CD16/32$^-$CD34$^-$). Data are based on a minimum of three mice per group (8-12 weeks old). The experimental repeats were performed independently.

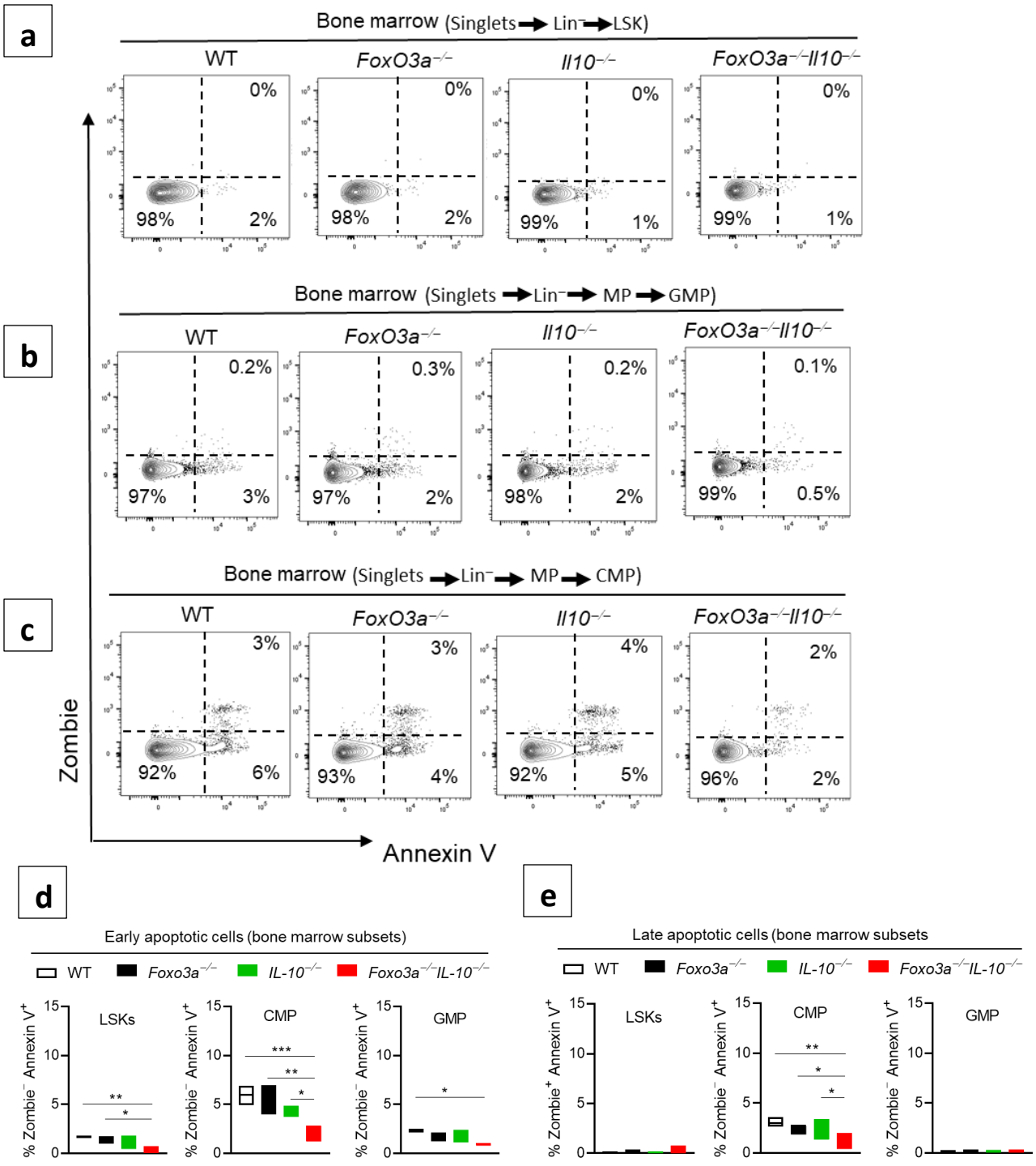
a
Bone marrow (Singlets → Lin⁻ → LSK)
WT
FoxO3a⁻/⁻
Il10⁻/⁻
FoxO3a⁻/⁻Il10⁻/⁻
0%
98%
2%
0%
98%
2%
0%
99%
1%
0%
99%
1%
b
Bone marrow (Singlets → Lin⁻ → MP → GMP)
WT
FoxO3a⁻/⁻
Il10⁻/⁻
FoxO3a⁻/⁻Il10⁻/⁻
0.2%
97%
3%
0.3%
97%
2%
0.2%
98%
2%
0.1%
99%
0.5%
c
Bone marrow (Singlets → Lin⁻ → MP → CMP)
WT
FoxO3a⁻/⁻
Il10⁻/⁻
FoxO3a⁻/⁻Il10⁻/⁻
3%
92%
6%
3%
93%
4%
4%
92%
5%
2%
96%
2%
Zombie
Annexin V
d
Early apoptotic cells (bone marrow subsets)
WT
Foxo3a⁻/⁻
IL-10⁻/⁻
Foxo3a⁻/⁻IL-10⁻/⁻
% Zombie⁻ Annexin V⁺
LSKs
CMP
GMP
e
Late apoptotic cells (bone marrow subsets
WT
Foxo3a⁻/⁻
IL-10⁻/⁻
Foxo3a⁻/⁻IL-10⁻/⁻
% Zombie⁺ Annexin V⁺
% Zombie⁻ Annexin V⁺
LSKs
CMP
GMP

Figure 18. Increased viability of HSCs and progenitor subsets in *FoxO3a*$^{-/-}$*Il10*$^{-/-}$ mice.

(a-c) Representative FACS plots showing Zombie Yellow vs. Annexin V staining in bone-marrow-derived LSK and MP subsets in the four groups of mice. (d) Quantitation of the percentages of early apoptotic cells in LSK and MP subsets of the bone marrow of the four groups of mice. (e) Quantitation of the percentages of late apoptotic cells in LSK and MP subsets of the bone marrow of the four groups of mice. Data are based on a minimum of three mice per group (8-12 weeks old). The experimental repeats were performed independently. All graphs depict mean ± SEM. Statistics were done using One-way ANOVA (*$P < 0.05$, ***$P < 0.001$, and ****$P < 0.0001$).

Conclusively, to determine whether the immune compartment is playing a role in propagating the disease in FoxO3a-IL-10 double-deficient mice, we performed biweekly antibody-mediated depletion of myeloid cells (using anti-Ly6C+Ly6G antibodies) or of T cells (using anti-CD4+CD8α antibodies) (**Fig. 19**). We observed a potent rescue of the phenotype in *FoxO3a*$^{-/-}$ *Il10*$^{-/-}$ mice upon depletion of T cells (**Fig. 19**). In comparison to this, deletion of myeloid cells resulted in a partial rescue of the phenotype. These results indicate that the T cell and myeloid compartments contribute to perpetuating gut inflammation in *FoxO3a*$^{-/-}$ *Il10*$^{-/-}$ mice.

Having obtained these results we therefore explored in the next aim the intracellular mechanism through which the double deficiency of FoxO3a and IL-10 results in an exacerbation of inflammatory response.

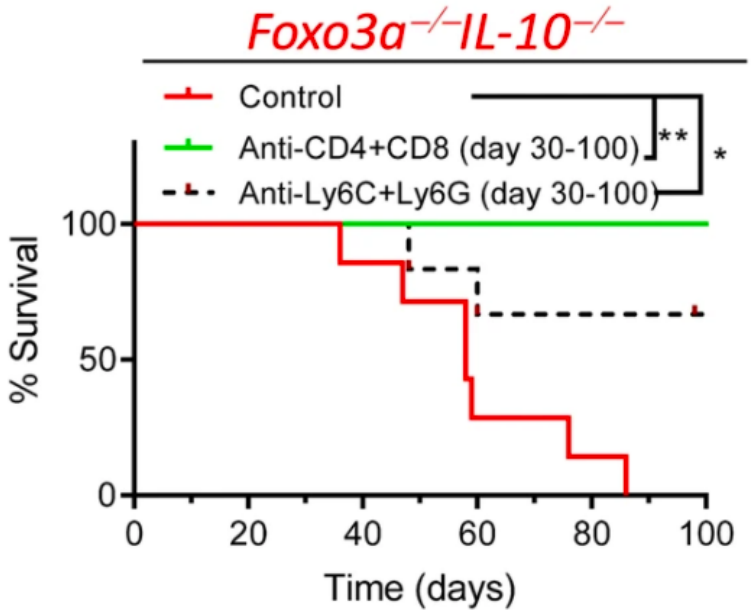

Figure 19. Depletion of myeloid cells or T cells prolongs the survival of *FoxO3a*$^{-/-}$*Il10*$^{-/-}$ mice.

Survival of *FoxO3a*$^{-/-}$*Il10*$^{-/-}$ mice (minimum n=5) depleted of myeloid cells or T cells using appropriate antibodies (mentioned in the methods section) given twice a week (200 µg/injection) from day 30 till day 100 of birth. The Mantel–Cox test was used for survival analysis.

Aim 3: Decipher the mechanistic pathways through which FoxO3a and IL-10 regulate the inflammatory response.

3. FoxO3a prevents the development of a hyperinflammatory response in the colons of IL-10-deficient mice.

Increased production of pro-inflammatory cytokines and chemokines is characteristic of both animal models of experimental colitis and human inflammatory bowel disease. To evaluate the inflammatory response in the four groups of mice, we profiled 84 different genes by RT2 Profiler PCR-array in the colons and spleens of naive mice. The mRNA levels of critical pro-inflammatory cytokines (members of TNF superfamily, IL-6, IFN-γ, IL-1α and IL-1β) and chemokines (CCL and CXCL families) were elevated in the colons of the *FoxO3a*$^{-/-}$*Il10*$^{-/-}$ mice compared to the FoxO3a- or IL-10- deficient mice (**Fig.20 a-c**). These changes were not observed in the spleens (**Fig. 21 a-c**). We also measured the mRNA expression (by qRT-PCR) of various pro-inflammatory genes and observed that the expression of *iNOS*, *Light* and *Nlrp3*, was significantly enhanced in the colons of *FoxO3a*$^{-/-}$*Il10*$^{-/-}$ mice (**Fig. 20 d**). Interestingly, the expression of the anti-inflammatory genes *XIAP*, *Pydc3* and *COX1* was reduced.

We have reported that during infection of mice with *Salmonella typhimurium*, the expression of ROS in immune cells is regulated by FoxO3a through transcription of ROS-detoxifying genes, *SOD1*, *SOD2* and *Catalase* (Joseph, et al. 2016). While a basal ROS level may play a protective role in the host, the oxidative stress derived from the imbalance between ROS production and the antioxidant system is harmful (Xu et al., 2012).

To evaluate the extent to which FoxO3a and IL-10 play a role in maintaining this balance, we injected mice with L-012 chemiluminescent probe intraperitoneally. Due to the limitation in the numbers of *FoxO3a*$^{-/-}$*Il10*$^{-/-}$ mice, these experiments were performed with *FoxO3a*$^{+/-}$*Il10*$^{-/-}$ mice. By measuring the average radiance, we observed significantly high levels of luminescence in the IL-10-deficient mice that were heterozygous for *FoxO3a* (**Fig. 22 a, b**). In contrast, *FoxO3a*$^{+/-}$ *or Il10*$^{-/-}$ mice did not show elevated ROS levels suggesting a protective role of FoxO3a in regulating ROS levels in the IL-10-deficient hosts (**Fig. 22 a, b**). Based on these results, we suspected that *FoxO3*$^{-/-}$*Il10*$^{-/-}$ mice produced high levels of ROS. Therefore, we

inhibited ROS production *in vivo* by feeding *FoxO3a*$^{-/-}$*Il10*$^{-/-}$ mice with N-acetyl cysteine (NAC), a precursor of intracellular cysteine and GSH, in drinking water and monitored their survival to determine if this reduces gut inflammation. Interestingly, promoting glutathione synthesis through NAC supplementation did not improve the survival of *FoxO3a*$^{-/-}$*Il10*$^{-/-}$ mice implicating other underlying mechanisms at play (**Fig. 22. c**).

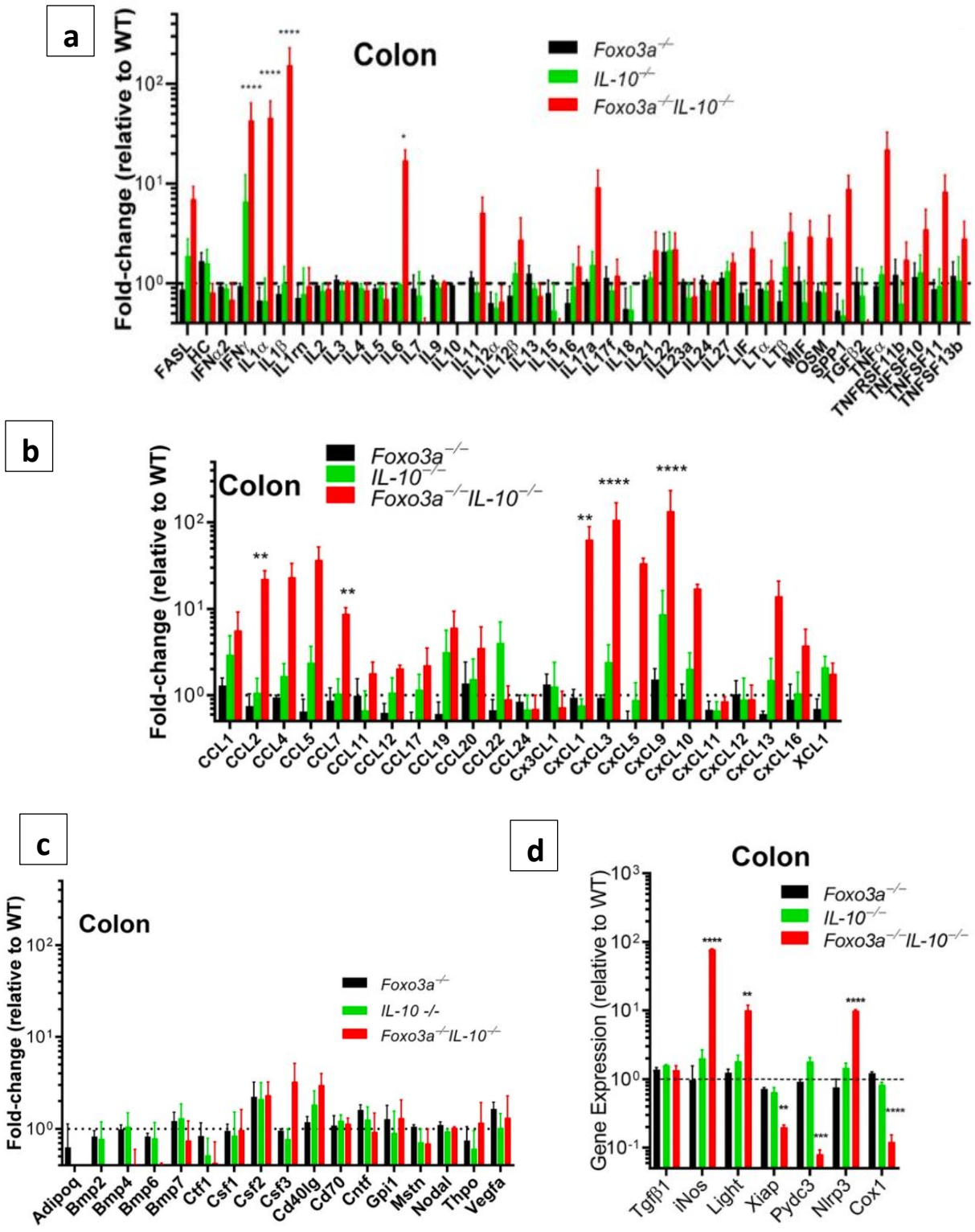
a
Colon
Foxo3a−/−
IL-10−/−
Foxo3a−/−IL-10−/−
Fold-change (relative to WT)
FASL HC IFNα2 IFNγ IL1α IL1β IL1rn IL2 IL3 IL4 IL5 IL6 IL7 IL9 IL10 IL11 IL12α IL12β IL13 IL15 IL16 IL17a IL17f IL18 IL21 IL22 IL23a IL24 IL27 LIF LTα LTβ MIF OSM SPP1 TGFβ2 TNFα TNFRSF11b TNFSF10 TNFSF11 TNFSF13b
b
Colon
Foxo3a−/−
IL-10−/−
Foxo3a−/−IL-10−/−
Fold-change (relative to WT)
CCL1 CCL2 CCL4 CCL5 CCL7 CCL11 CCL12 CCL17 CCL19 CCL20 CCL22 CCL24 Cx3CL1 CxCL1 CxCL3 CxCL5 CxCL9 CxCL10 CxCL11 CxCL12 CxCL13 CxCL16 XCL1
c
Colon
Foxo3a−/−
IL-10 -/-
Foxo3a−/−IL-10−/−
Fold-change (relative to WT)
Adipoq Bmp2 Bmp4 Bmp6 Bmp7 Ctf1 Csf1 Csf2 Csf3 Cd40lg Cd70 Cntf Gpi1 Mstn Nodal Thpo Vegfa
d
Colon
Foxo3a−/−
IL-10−/−
Foxo3a−/−IL-10−/−
Gene Expression (relative to WT)
Tgfβ1 iNos Light Xiap Pydc3 Nlrp3 Cox1

Figure 20. Loss of FoxO3a results in a hyper-inflammatory response in the colons of naïve IL-10-deficient mice.

(a-c) Expression of inflammatory cytokines and chemokines in the colons of the four groups of naïve 6-12 weeks old mice measured by qRT-PCR (RT^2 profiler array). Values are presented as fold-change relative to WT. (d) Expression of pro- and anti-inflammatory mediators in the colons of the four groups of naïve mice measured by qRT-PCR. Values are presented as fold-change relative to WT. Data are representative of a minimum of n=3 mice per group (6-12 weeks old), each being an average of 2 technical replicates. The experimental repeats were performed independently. Statistics were done using One-way ANOVA ($*P < 0.05$, $***P < 0.001$, and $****P < 0.0001$).

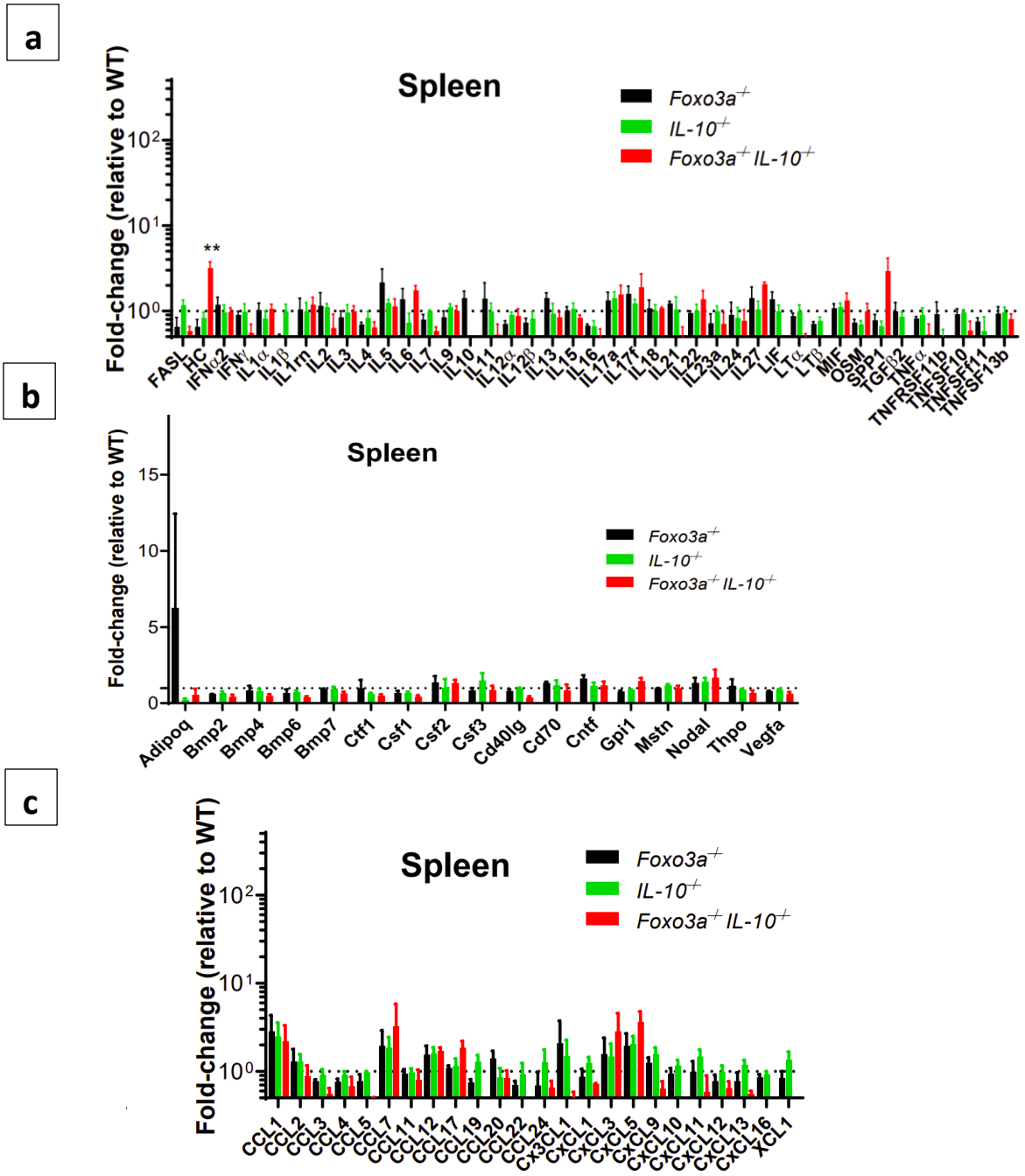

Figure 21. FoxO3a deficiency does not impact the inflammatory profile of cells in the spleens of naïve IL-10 -deficient mice.

(a-c) Expression of inflammatory cytokines and chemokines in the spleens of the four groups of naïve 6-12 weeks old mice measured by q-RT PCR (RT^2 profiler array). Values are fold-change relative to WT colons. Data are representative of a minimum of n=3 mice per group, each being an average of 2 technical replicates. The experimental repeats were performed independently. Statistics were done using One-way ANOVA (*$P < 0.05$, ***$P < 0.001$, and ****$P < 0.0001$).

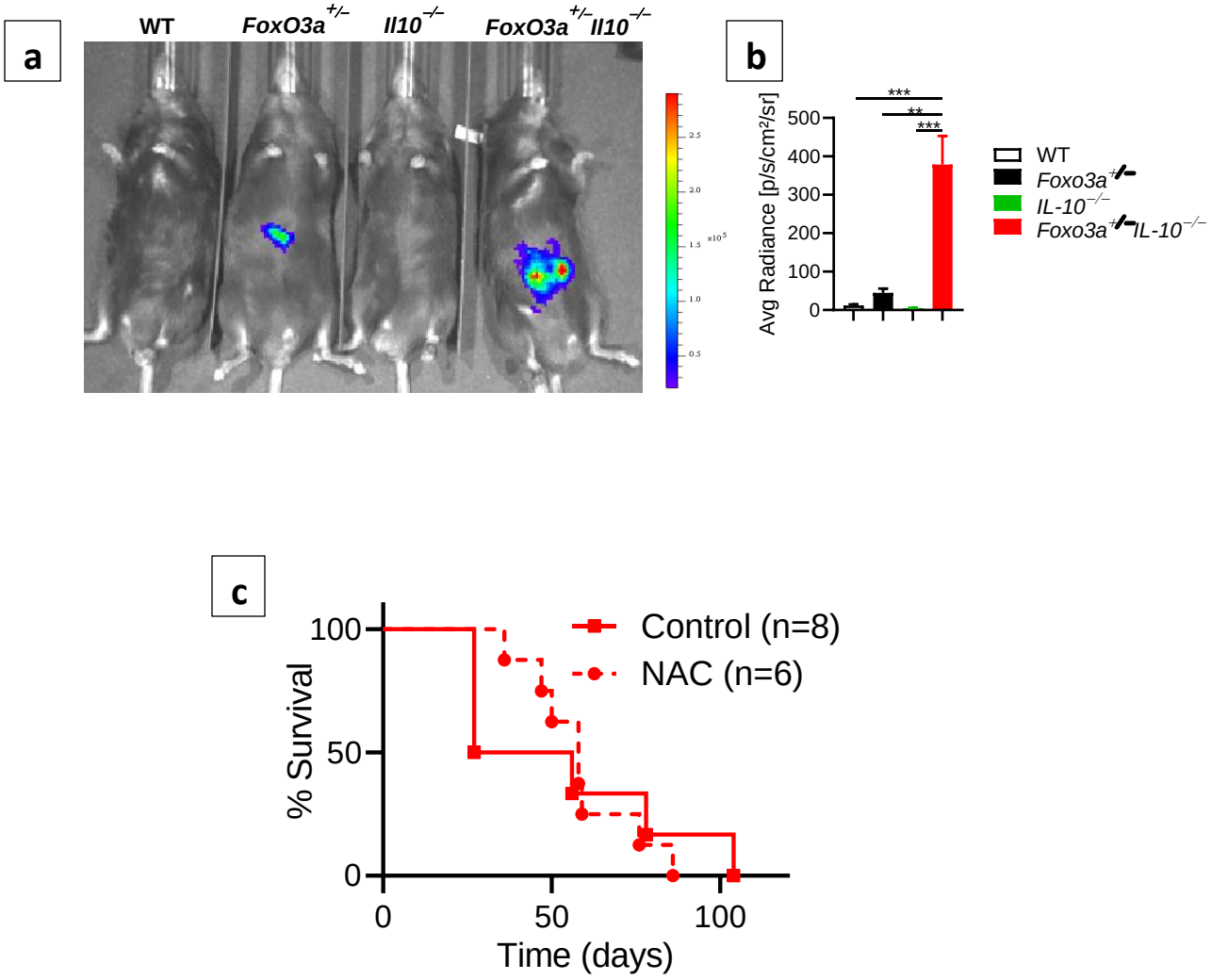

Figure 22. FoxO3a confers protection against excessive ROS production, but NAC treatment does not improve survival.

(a) *WT, FoxO3a*$^{+/-}$*, Il10*$^{-/-}$*and FoxO3a*$^{+/-}$*Il10*$^{-/-}$mice were injected with L-012 to measure ROS levels *in vivo* by bioluminescence imaging. (b) Bar graph represents quantification of ROS levels in the four groups of 6-8 weeks old mice (n=3 per group). (c) Survival graph for *FoxO3a*$^{-/-}$*Il10*$^{-/-}$ mice randomized to ad lib drinking water supplemented with 40 mM NAC or regular drinking water starting at 4 weeks old and proceeding throughout the duration of the study. The Mantel–Cox test was used for survival analysis. The graph in panel (b) depicts mean ± SEM. Statistics were done using One-way ANOVA.

Since we observed a hyperinflammatory response in the colons of naïve *FoxO3a*$^{-/-}$*Il10*$^{-/-}$ mice, we wanted to measure the cytokine levels in the sera of the four groups of mice. *FoxO3*$^{-/-}$*Il10*$^{-/-}$ mice expressed high systemic levels of IL-17A and IL-6 compared to the other groups of mice. No significant changes were observed in the expression of TNF-α, IL-12, IL-1β and IFN-γ (**Fig. 23**). Nevertheless, we did observe increased production of all pro-inflammatory cytokines upon stimulation of *FoxO3*$^{-/-}$*Il10*$^{-/-}$ cells *in vitro*. Specifically, we tested cytokine production by splenocytes in response to infection with ST (10 MOI). Our *in vitro* results revealed a significant exacerbation in the secretion of various pro-inflammatory cytokines (IL-12 p70, TNF-α, IL-1β, and IL-6) as well as the anti-inflammatory IL-10 in the absence of FoxO3a. When IL-10 is inactivated, the cytokine expression of IL-12 p70, TNF-α, and IL-1β is also upregulated. When both FoxO3a and IL-10 are inactivated, cytokine expression is greatly amplified after 6 hours surpassing the levels observed with either *FoxO3a*$^{-/-}$or *Il10*$^{-/-}$ cells (**Fig. 24 a**). A similar trend was observed when splenocytes were stimulated with LPS (**Fig. 24 b**). Measurement of intracellular TNF-α expression by flow cytometry indicated that both neutrophils and monocytes expressed TNF-α (**Fig. 24 c-e**).

We purified monocytes from the bone marrow of WT and *FoxO3a*$^{-/-}$ mice to see whether the trend of cytokine production is similar to that of splenocytes *in vitro*. Upon stimulation with LPS, purified *FoxO3a*$^{-/-}$ monocytes secreted higher levels of TNFα in comparison to WT monocytes, and the secretion was increased further when cells were co-treated with an anti-IL-10 antibody *in vitro* (**Fig. 25 a**).

LPS-stimulated *FoxO3a*$^{-/-}$*Il10*$^{-/-}$ bone marrow-derived macrophages also produced increased levels of pro-inflammatory cytokines (IL-12 p70, TNF-α, and IL-6) compared to the other three groups (**Fig. 25 b**). Moreover, splenic DCs exhibited a similar trend of cytokine production upon stimulation with LPS (**Fig. 25 c**) and ST (**Fig. 25 d**). Confirming previous findings, *FoxO3a*$^{-/-}$ cells produced very high levels of the anti-inflammatory cytokine IL-10 in comparison to WT cells.

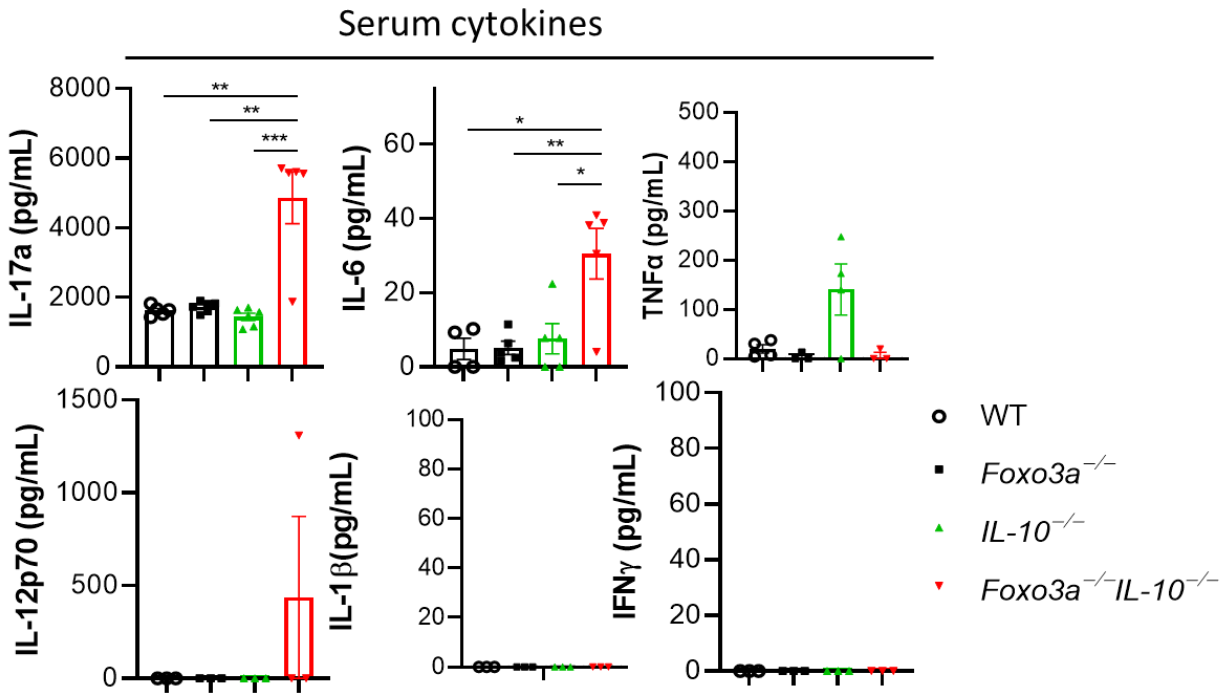

Figure 23. *FoxO3a*$^{-/-}$*Il10*$^{-/-}$ mice exhibit increased systemic pro-inflammatory cytokine production.

Quantification of cytokine expression in serum samples of the four groups of 10-12 weeks old mice. A minimum of 3 biological replicates per group have been used. All graphs depict mean ± SEM. Statistics were done using One-way ANOVA (*P < 0.05, ***P < 0.001 and ****P < 0.0001).

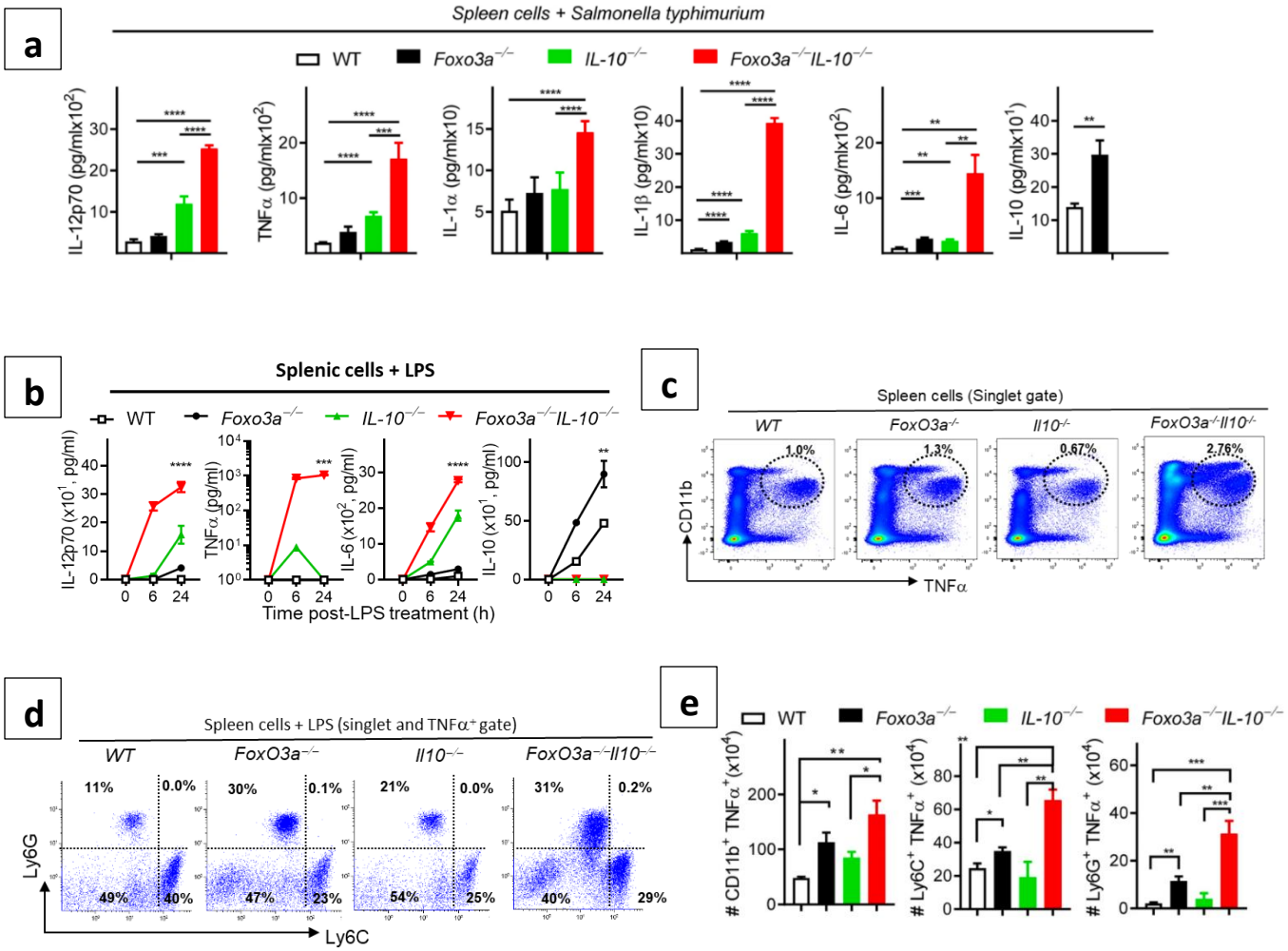

Figure 24. FoxO3a suppresses overt cytokine expression by IL-10 cells.

Cytokine levels were measured in the supernatants of spleen cells (10^7cells/300 µl) infected with *Salmonella typhimurium* (ST) (a) or treated with LPS 100 ng/mL (b) for 6 h. (c) Representative FACS plots showing TNF-α-producing myeloid cells ($CD11b^+$) in the spleens of the four groups of 6-8 weeks old mice at 6 h post-LPS stimulation. (d) Representative FACS plots showing intracellular TNFα-producing myeloid cell subsets (gated on TNF-α^+) following LPS treatment of spleen cells of the four groups of 6-8 weeks old mice. (e) Total numbers of TNFα-producing myeloid cell subsets following LPS treatment of spleen cells of the four groups of mice. Data are representative of a minimum of n=3 mice per group. The experimental repeats were performed independently. All graphs depict mean ± SEM. Statistics were done using One-way ANOVA (*$P < 0.05$, ***$P < 0.001$, and ****$P < 0.0001$).

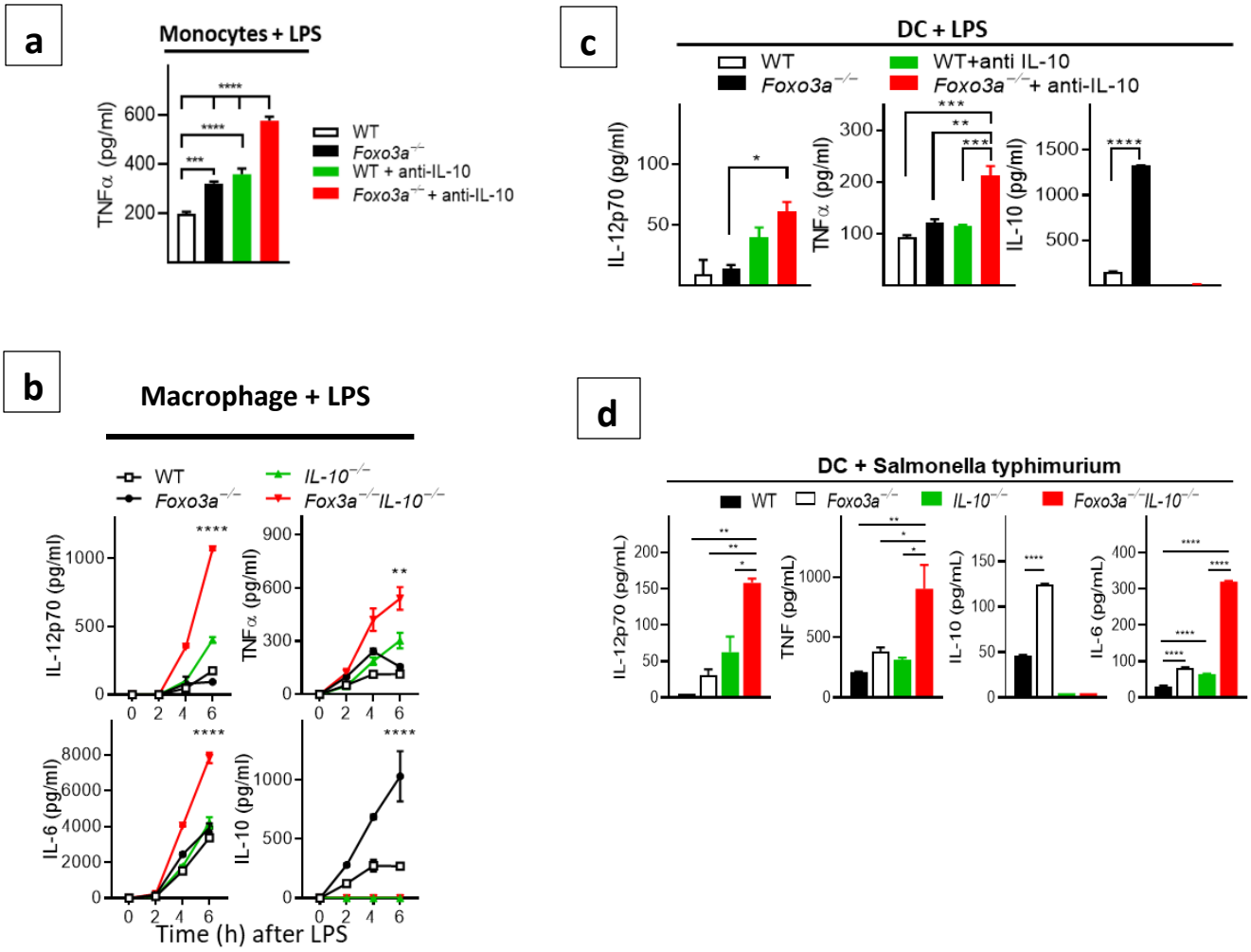

Figure 25. FoxO3a regulates the production of pro-inflammatory cytokines in IL10-deficient innate immune cells.

(a) TNF-α levels measured in the supernatants of bone marrow-purified monocytes from WT and *FoxO3a*$^{-/-}$ mice after treatment with LPS (1 ng/ml) in the presence or absence of an anti-IL-10 antibody (10 μg/ml) for 6 hours. (b) Cytokine levels measured in the supernatants of bone marrow-derived macrophages of the four groups of mice at various time intervals post-treatment with LPS (1 ng/mL). (c) Cytokine production in the supernatants of purified splenic DCs from WT and *FoxO3a*$^{-/-}$ mice after treatment with LPS (1 ng/ml) in the presence or absence of anti-IL-10 antibody (10 μg/ml) for 6 hours. (d) Cytokine levels measured in the supernatants of purified splenic DCs after stimulation with ST (10 MOI) for 6 hours. Data are representative of a minimum of n=3 mice (6-8 weeks old) per group. Experimental repeats were performed independently. All graphs depict mean ± SEM. Statistics were done using One-way ANOVA (*$P < 0.05$, ***$P < 0.001$, and ****$P < 0.0001$).

4. Regulation of cellular bioenergetics by FoxO3a and IL-10

MTT uptake (**Fig. 26 a**), which measures mitochondrial activity, and the total protein amount (**Fig. 26 b**) were highest in the *FoxO3a* $^{-/-}$ *Il10* $^{-/-}$ cells. Previous data has shown that FoxO3a regulates several genes in the glycolysis pathway (Joseph et al., 2016), and IL-10 controls the metabolic activity in cells (Ip et al., 2017). Since it was previously reported that FoxO3a inhibits IL-10 expression, and there was no detectable impact on L-lactate production in *FoxO3a*$^{-/-}$ cells, we suspected that this may be due to the compensatory increase in IL-10 expression in cells (Joseph et al., 2016). Hence, we evaluated the levels of L-Lactate, a by-product of glycolysis, in all the four groups of mice. In the non-stimulated spleen cells, L-lactate was detectable only in the *FoxO3a* $^{-/-}$*Il10* $^{-/-}$ cells, and it was increased substantially following LPS stimulation. In the other three experimental groups, the increase in L-lactate was not as potent (**Fig. 26 c**). Pyruvate, the key intermediate in glucose metabolism, is normally shuttled to the TCA cycle for oxidative phosphorylation and generation of ATP. However, pyruvate can also be converted to L-lactate during anaerobic glycolysis. Since we did not use hypoxic conditions, the increased production of L-lactate is indicative of enhanced "aerobic glycolysis".

We then measured the oxygen consumption rate (OCR) and extracellular acidification rate (ECAR) in spleen cells using the Seahorse analyzer. The functional profile of mitochondria was evaluated by determining real-time changes in OCR during sequential treatment of cells with Oligomycin (Inhibitor of ATP synthase; prevents electron transport through complex I-IV), Trifluoromethoxy carbonyl cyanide phenylhydrazone (FCCP; H^+ ionophore) and Antimycin/Rotenone (inhibitors of complexes I and III in the electron transport chain). In the absence of inhibitors, the basal respiration rate was the highest in *FoxO3a*$^{-/-}$*Il10*$^{-/-}$ spleen cells, and it was enhanced in response to FCCP (**Fig. 26 d, f; Fig. 27 a, b**) After the addition of Oligomycin, OCR decreased in the cells of the four groups; however, the residual OCR, which is representative of respiration due to proton-leakage, was still highest in *FoxO3a*$^{-/-}$*Il10*$^{-/-}$ cells (**Fig. 26 d, f; Fig. 27 a, b**). ATP-linked respiration, which represents the difference between basal and leak respiration after injection of Oligomycin, was highest in *FoxO3a*$^{-/-}$ and *FoxO3a*$^{-/-}$*Il10*$^{-/-}$ cells. This is reflective of an increased ATP demand in the absence of FoxO3a. *FoxO3a*$^{-/-}$ *Il10*$^{-/-}$ spleen cells displayed maximal respiration following addition of FCCP, which depolarizes the mitochondrial membrane potential and allows electron transport chain to function at the maximal

rate (**Fig. 26 d, f; Fig. 27 a, b**). Overall, *FoxO3a*$^{-/-}$*Il10*$^{-/-}$ cells were more metabolically energetic compared to the other three groups of cells (**Fig. 26 h**). ECAR was measured before and after the addition of glucose, Oligomycin and 2- Deoxy glucose. Our results showed that *FoxO3a*$^{-/-}$*Il10*$^{-/-}$ cells exhibited maximal ECAR in non-stimulated and LPS-stimulated cells (**Fig. 26 e, g; Fig. 27 c, d**). Furthermore, the spare respiratory capacity was significantly increased in the absence of FoxO3a (**Fig. 27 e**).

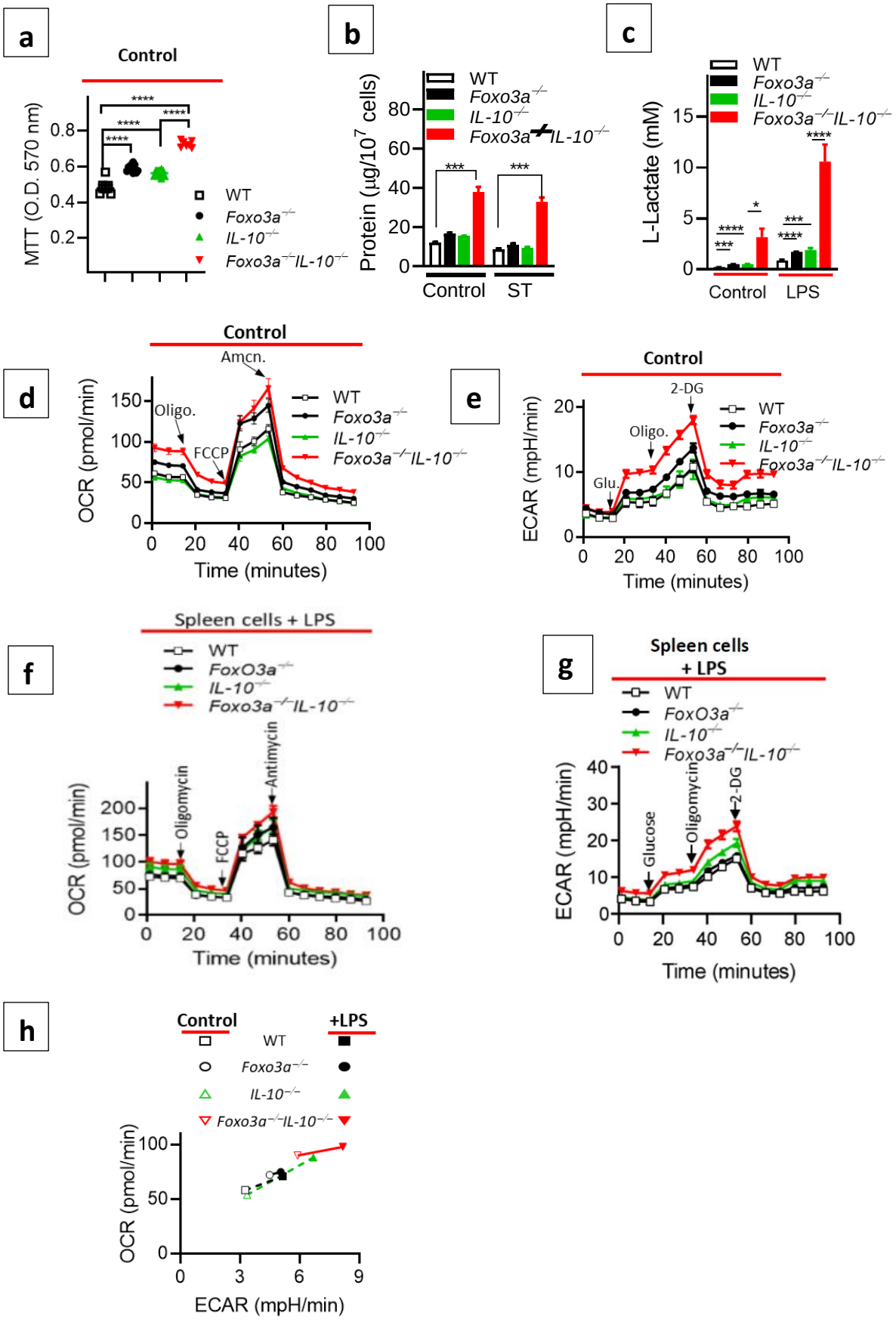
a
Control
MTT (O.D. 570 nm)
WT
Foxo3a−/−
IL-10−/−
Foxo3a−/−IL-10−/−
b
Protein (µg/10^7 cells)
Control
ST
c
L-Lactate (mM)
Control
LPS
d
Control
OCR (pmol/min)
Oligo.
FCCP
Amcn.
Time (minutes)
e
Control
ECAR (mpH/min)
Glu.
Oligo.
2-DG
Time (minutes)
f
Spleen cells + LPS
FoxO3a−/−
OCR (pmol/min)
Oligomycin
FCCP
Antimycin
Time (minutes)
g
Spleen cells + LPS
ECAR (mpH/min)
Glucose
Oligomycin
2-DG
Time (minutes)
h
Control
+LPS
OCR (pmol/min)
ECAR (mpH/min)

Figure 26. **FoxO3a controls cellular bioenergetics in IL-10-deficient spleen cells.**

(a) MTT uptake was evaluated in non-stimulated spleen cells of the four groups of 6-8 weeks old mice at 5 h post-culture in media. (b) Protein amount (μg) measured by BCA per 10^7 spleen cells before and after infection with ST in the four groups of mice. (c) L-lactate levels (mM) measured in control and LPS (100 ng/mL)-treated spleen cells of mice at 6 h post-treatment. Oxygen consumption rate (OCR) and extracellular acidification rate (ECAR) were measured in the spleen cells using a Seahorse XF 96 flux analyzer without stimulation (d, e) or with LPS stimulation (100 ng/mL) (f, g). (h) Metabolic phenotype profile of spleen cells. Data are representative of a minimum of n=3 mice per group. Experimental repeats were performed independently. All graphs depict mean ± SEM. Statistics were done using One-way ANOVA (*$P < 0.05$, ***$P < 0.001$ and ****$P < 0.0001$).

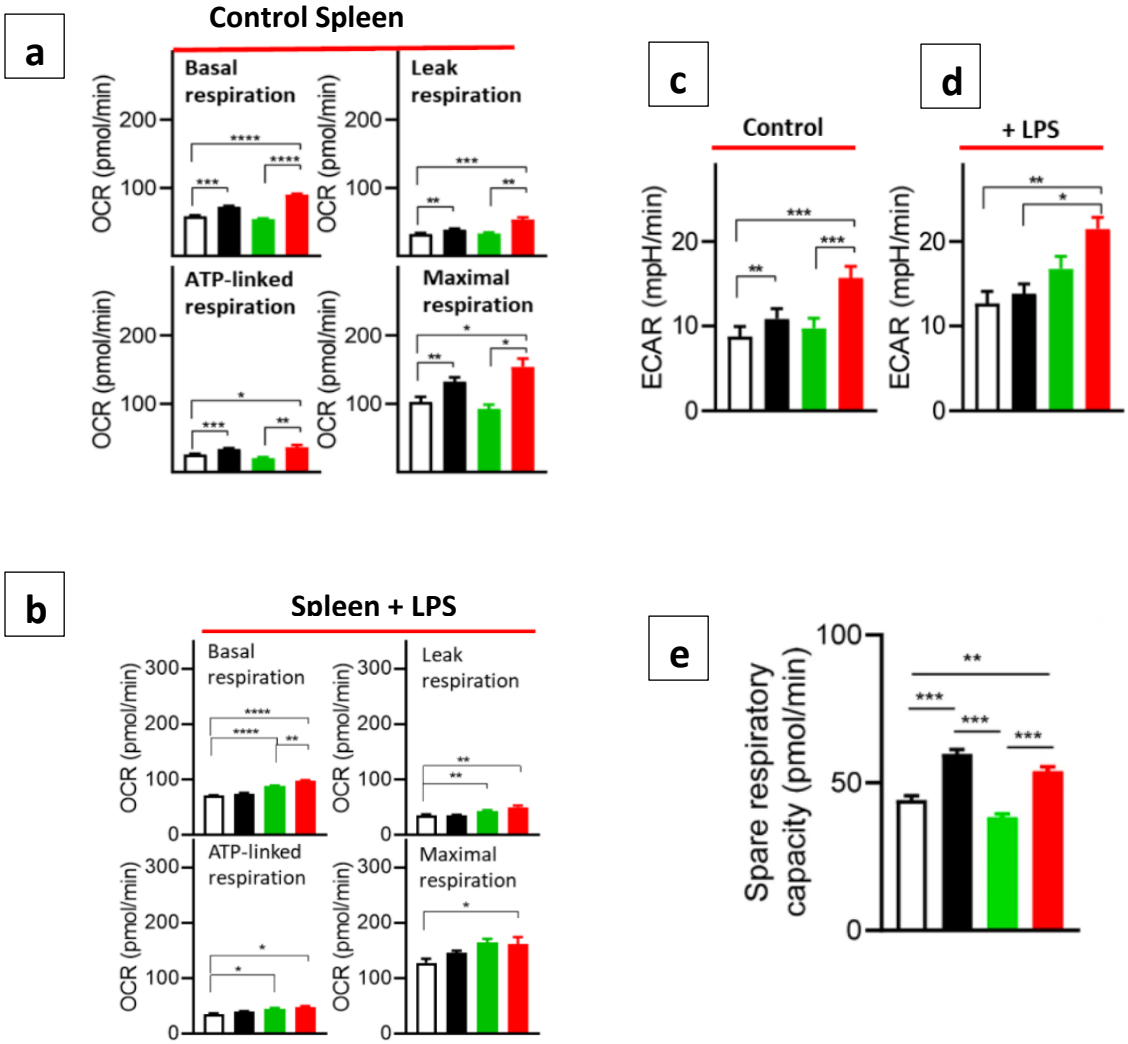

Figure 27. FoxO3a regulates various metabolic parameters in the absence of IL-10.

Basal respiration, leak respiration, ATP-linked and maximal respiration were measured in spleen cells of the four groups of 6-8 weeks old mice in the absence (a) and presence (b) of stimulation with LPS (100 ng/mL). ECAR in spleens cells in absence (c) or presence (d) of LPS (100 ng/mL). (e) Spare respiratory capacity of cells (pmol/min) was evaluated in the four groups of non-stimulated splenocytes by evaluating the difference between basal ATP production and the maximal activity of the mitochondria. Data are representative of a minimum of n=3 mice per group. Experimental repeats were performed independently. All graphs depict mean ± SEM. Statistics were done using One-way ANOVA (*$P < 0.05$, ***$P < 0.001$ and ****$P < 0.0001$).

5. FoxO3a regulates inflammatory and metabolic signaling in IL-10-deficient cells.

Considering the major metabolic alterations revealed by the Seahorse analyzer, we evaluated the impact of FoxO3a on mTORC1 signaling, since this complex plays a key role in metabolism. Phosphorylation of the mTORC1 downstream targets, namely ribosomal protein S6 kinase (S6K1) and eukaryotic initiation factor 4E-binding protein (4E-BP1), was highest in *FoxO3a*$^{-/-}$*Il10*$^{-/-}$ spleen cells and CD11b^{+} cells compared to the other three groups (**Fig. 28 a**). This suggests that FoxO3a and IL-10 restrain mTORC1 signaling. Interestingly, we observed that the basal expression of FoxO3a was barely detectable in WT cells, possibly due to suppression by IL-10, as inactivation of IL-10 enhanced the expression of FoxO3a (**Fig. 28 b, d**). We also observed enhanced expression and/or activation of major inflammatory mediators, notably MK2 downstream of P38^{MAPK} signaling, STAT3, and ERK in *FoxO3a*$^{-/-}$*Il10*$^{-/-}$ cells (**Fig. 28 b, c, d**).

Protein synthesis can be modulated in a cell-type specific manner, and the differences in translation regulate cellular development, differentiation, and responses to stress (Buszczak, Signer & Morrison, 2014). Hence, proteostasis is maintained partly through balanced protein synthesis and degradation. We wanted to evaluate the translational rate in various cell types. Administration of O-propargyl-puromycin (OP-Puro), an analog of puromycin that contains a terminal alkyne group, has facilitated the quantification of protein synthesis within individual cells in vivo. OP-Puro enters the acceptor site of ribosomes and is covalently incorporated into nascent polypeptide chains (San Jose & Signer, 2019). Here we report that neutrophils and monocytes exhibit a massive increase in the rate of protein synthesis in the absence of both FoxO3a and IL-10 as reflected by the enhanced Op-Puro incorporation into the cells (**Fig. 29 a-c**). This was also observed in the *FoxO3a*$^{-/-}$ *and FoxO3a*$^{-/-}$*Il10*$^{-/-}$ hematopoietic GMP population of the MP subset (**Fig. 29 d, e**). This highlights the role of FoxO3a in controlling the rate of protein synthesis in myeloid progenitors.

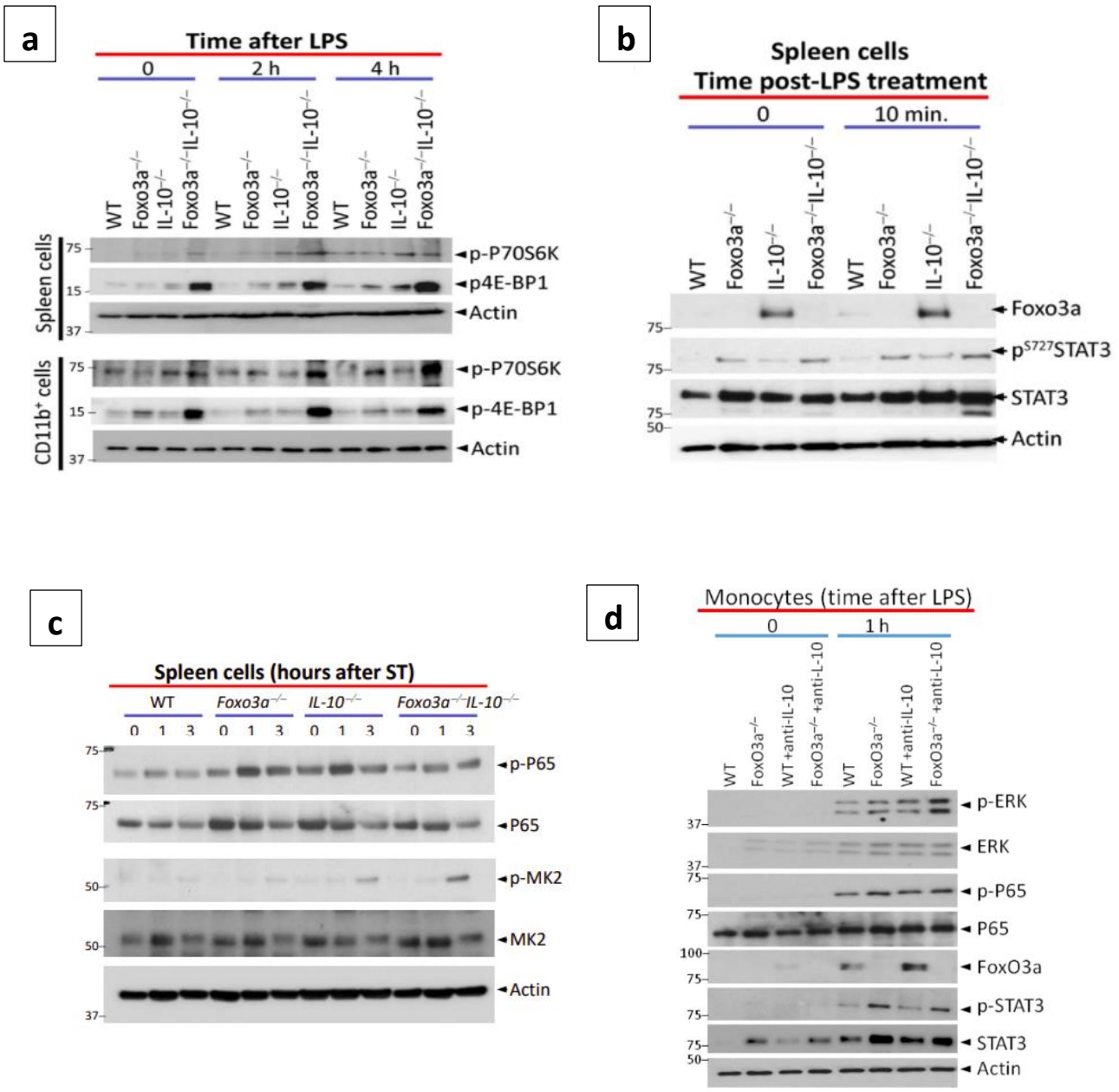

Figure 28. FoxO3a controls the synthesis of inflammatory and metabolic proteins in IL-10-deficient cells.

(a, b) Western blots of spleen cells and purified splenic CD11b^{+} cells at various time intervals post-treatment with LPS (100 ng/ml). (c) Western blots of spleen cells at various time intervals post-infection with ST (10 MOI). (d) Western blots of bone marrow-purified monocytes at 0H and 1H post-LPS treatment (1ng/mL) with or without anti-IL10 antibody (10 µg/ml). Data is representative of n=3 mice (8-12 weeks old) per group. Experimental repeats were performed independently.

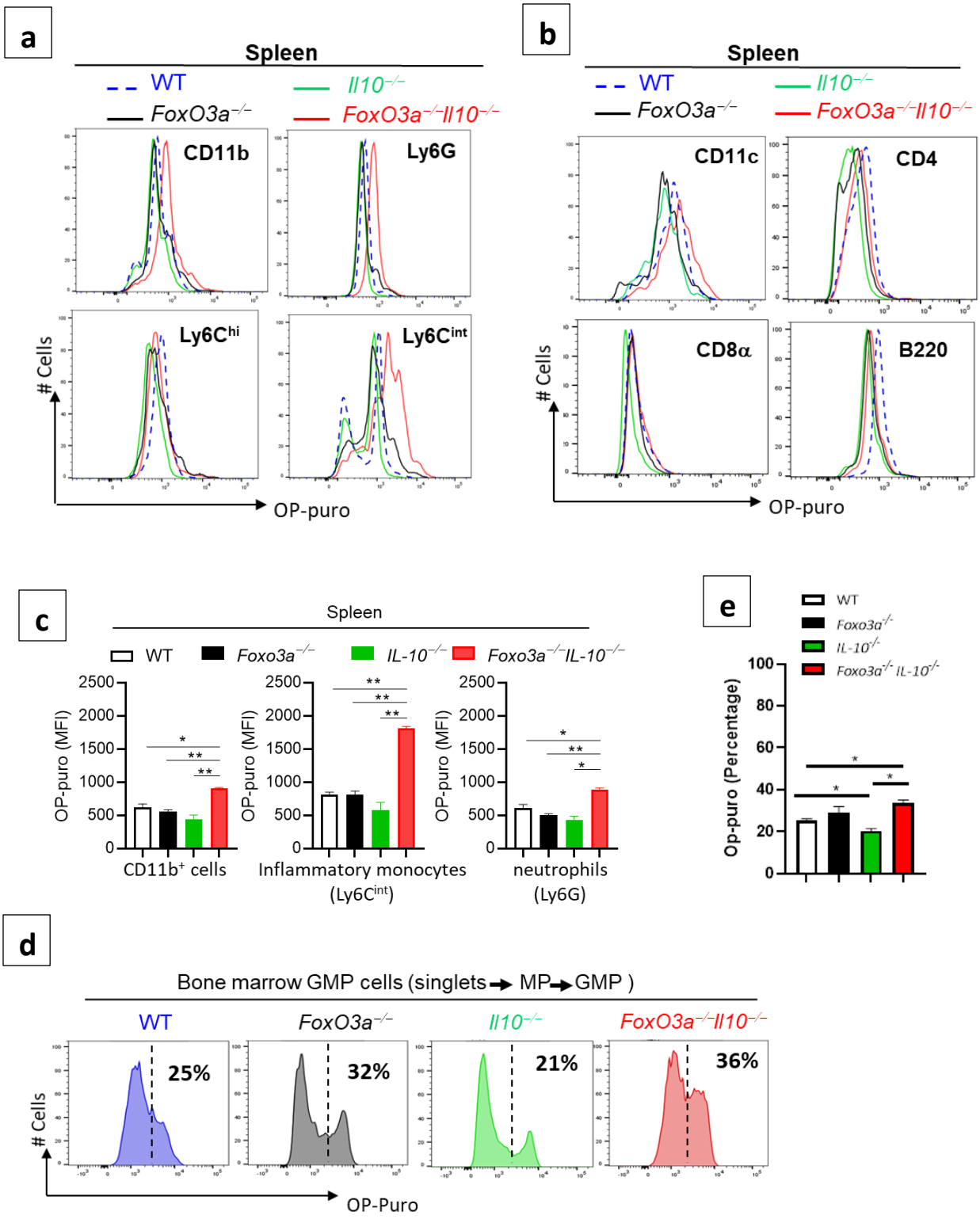
a
Spleen
WT
Il10−/−
FoxO3a−/−
FoxO3a−/−Il10−/−
CD11b
Ly6G
Ly6Chi
Ly6Cint
Cells
OP-puro
b
Spleen
WT
Il10−/−
FoxO3a−/−
FoxO3a−/−Il10−/−
CD11c
CD4
CD8α
B220
Cells
OP-puro
c
Spleen
WT
Foxo3a−/−
IL-10−/−
Foxo3a−/−IL-10−/−
OP-puro (MFI)
CD11b+ cells
Inflammatory monocytes (Ly6Cint)
neutrophils (Ly6G)
e
WT
Foxo3a-/-
IL-10-/-
Foxo3a-/- IL-10-/-
Op-puro (Percentage)
d
Bone marrow GMP cells (singlets → MP → GMP)
WT
FoxO3a−/−
Il10−/−
FoxO3a−/−Il10−/−
25%
32%
21%
36%
Cells
OP-Puro

Figure 29. FoxO3a regulates global protein synthesis in IL-10-deficient myeloid cells.

(a-b) Representative histograms showing OP-Puro uptake in various cell types in the spleens of the four groups of 10-12 weeks old naïve mice. (c) MFI quantitation for OP-Puro uptake in various cell types in the four groups of naive mice. (d) Representative histograms showing in *vivo* OP-Puro uptake in the GMP population in the bone marrow of the four groups of naïve mice. (e) Percentage quantitation for OP-Puro signals in panel (d). Two experimental repeats were performed independently, in which one mouse per group were used. All graphs depict mean ± SEM. Statistics were done using One-way ANOVA (*$P < 0.05$, ***$P < 0.001$ and ****$P < 0.0001$).

6. FoxO3a regulates the intrinsic activation of T cells and the suppressive function of Tregs

Considering the essential role of T cells in IBD, we checked whether there was excessive activation of effector T cells and/or alteration of T cell-mediated tolerance mechanisms. Our findings revealed that purified naïve splenic $CD4^+$ T cells, deficient in both FoxO3a and IL-10, produced high levels of IL-6 and IFN-γ at 24 h post-stimulation *in vitro* in comparison to the other three groups (**Fig. 30 a**). *FoxO3a*$^{-/-}$*Il10*$^{-/-}$ $CD25^+CD4^+$ T cells produced high levels of IFN-γ, IL17A and IL-6 at 72 H post-stimulation compared to the other groups (**Fig. 30 b**). These cells also displayed the highest metabolic activity, as measured by MTT (**Fig. 30 c**). Moreover, phosphorylation of mTORC1 downstream targets and activation of STAT3 and MK2 were also up-regulated in the absence of FoxO3a and IL-10 (**Fig. 30 d**). We also observed that the $CD25^+CD4^+$ T cells from *FoxO3a*$^{-/-}$*Il10*$^{-/-}$ mice exhibited better survival upon activation (**Fig. 31a, b**), and this correlates with increased cytokine production.

Despite the increase in the proportion of activated non-Treg $CD4^+$ T cells ($CD25^+$), the proportion of $FoxP3^+$ Tregs in the LP and spleens of *FoxO3a*$^{-/-}$*Il10*$^{-/-}$ mice was slightly decreased (**Fig. 32 a, c-e**). It was previously demonstrated that *ex vivo* expanded Tregs, high on forward scatter, display potent suppressive activities. We therefore evaluated the FSC^{hi} Treg population and found it to be reduced in the LP of *FoxO3a*$^{-/-}$*Il10*$^{-/-}$ mice (**Fig. 32 b, c**).

Besides looking at FoxP3 expression, we were interested in evaluating the expression of other markers relevant to Treg development and function. Analysis of mRNA expression (by qRT-PCR) of various genes in splenic $CD4^+CD25^+$ T cells activated *in vitro* revealed a significant increase in the expression of *Il-1r1* and *Bcl-3* in *FoxO3a*$^{-/-}$*Il10*$^{-/-}$ cells (**Fig. 33 a**). Expression of Bcl-3 and IL-1R1 on Tregs has been reported to impair their inhibitory function. The mRNA expression of *FoxP3* and *FoxO1*, which have been shown to impact Treg function, was not reduced in *FoxO3a*$^{-/-}$*Il10*$^{-/-}$ cells (**Fig. 33 a**).

Finally, the Tregs in the LP of *FoxO3a*$^{-/-}$*Il10*$^{-/-}$ mice expressed increased levels of IL-1R1 (**Fig. 33 b**). This is indicative of exposure to inflammatory cytokines and instability of their inhibitory function (Alvarez et al., 2019). Interestingly, splenic Tregs of *FoxO3a*$^{-/-}$*Il10*$^{-/-}$ mice did not display an upregulation of IL-1R1 (**Fig.33 c**). This observation complements the absence of an

upregulation of inflammatory cytokines in the spleen (**Fig. 21**). No changes in the expression of ST2 or PD-1 were observed in both the LP and spleen (**Fig. 33 a, b**).

To evaluate whether the increased activation of *FoxO3a*$^{-/-}$*Il10*$^{-/-}$ T cells stemmed from intrinsic mechanisms or was related to the increased activation of APCs (i.e., dendritic cells), we performed a series of T cell/DC co-culture experiments, in which we assessed the proliferative capacity and viability of T cells 72 hours post-activation with anti-CD3.

In the absence of DCs, *FoxO3a*$^{-/-}$*Il10*$^{-/-}$ CD4^{+} T cells displayed the highest proliferative capacity shown through the dilution of CFSE compared to the other groups (**Fig. 34 a, c**). The highly proliferating cells also exhibited better viability compared to the other three groups (**Fig. 34 b, c**). Upon co-culture with LPS-stimulated WT DCs, the viability and proliferation increased significantly in CD4^{+} T cells of all groups of mice implicating a general role for APCs in activating T cells (**Fig. 35 a, b**). The results also indicate that the proliferation and survival of the *FoxO3a*$^{-/-}$*Il10*$^{-/-}$ CD4^{+} T cells are further enhanced upon co-culture with LPS-activated WT DCs.

To assess of the role of FoxO3a and IL-10 in antigen presentation and co-stimulation, we co-cultured WT CD4^{+} T cells with DCs isolated from the four groups of mice. FoxO3a- deficient DCs slightly improved the proliferation of WT CD4^{+} T cells in the absence and presence of LPS (**Fig. 36 a, b**). *FoxO3a*$^{-/-}$*Il10*$^{-/-}$ DCs also improved the viability of CD4^{+} T cells (**Fig. 36 c, d**).

When purified CD4^{+} T cells were stimulated with anti-CD3 antibody in the absence of APC, activated *FoxO3a*$^{-/-}$*Il10*$^{-/-}$ CD4^{+} T cells produced high levels of IFN-γ and IL-6. In fact, no IL-6 production was observed by activated T cells pertaining to the other groups. Additionally, the level of IL-17A was comparable across the four groups (**Fig. 37 a**). Addition of WT DCs boosted and normalized the levels of IFN-γ and IL-6 along with an enhanced release of IL-17A in *Il-10*$^{-/-}$ and *FoxO3a*$^{-/-}$*Il10*$^{-/-}$ T cells compared to WT and *FoxO3a*$^{-/-}$ CD4^{+} T cells (**Fig. 37 b).**

In contrast to other groups of DCs, *FoxO3a*$^{-/-}$*Il10*$^{-/-}$ DCs promoted increased IL-17A production by activated WT CD4^{+} T cells. *FoxO3a*$^{-/-}$ and *FoxO3a*$^{-/-}$*Il10*$^{-/-}$ DCs promoted IL-6 production by activated WT CD4^{+} T cells. IFN-γ levels were normalized in all groups of cells (**Fig. 37 c**). Overall, the presence of DCs was required to promote IL-6 production by T cells (**Fig. 37 c**). Finally, loss of FoxO3a and IL-10 in both DCs and T cells resulted in potent T cell activation, as reflected by the boosted production of cytokines compared to the other groups (**Fig. 37 d**). These

results indicate that the loss of FoxO3a and IL-10 in both DCs and T cells results in potent augmentation of cytokine expression by T cells.

Despite the reduced proportion of FoxP3-expressing cells, the absolute Treg numbers were increased in the colons of *FoxO3a*$^{-/-}$*Il10*$^{-/-}$ mice compared to the other groups (**Fig. 12 & 32**). This is suggestive of a possible dysfunction through diminished suppressive capacity. To assess the impact of FoxO3a and IL-10 deficiency on the functional capacity of Tregs, we measured the proliferation of WT CD45.1^{+} CD4^{+} T cells upon co-culture with CD45.2^{+} Tregs purified from the four groups of mice. Interestingly, *FoxO3a*$^{-/-}$*Il10*$^{-/-}$ Tregs exhibited a dysfunction in their suppressive capacity as shown through the heightened proliferation of CD4^{+} T cells **(Fig. 38 a**) and the elevated IFN-γ levels (**Fig. 38 b**) without impacting their viability (**Fig. 38 c**). Tregs of the other three groups did not show impairment in their capacity to suppress T cell proliferation and activation. Overall, these results implicate an intrinsic impairment of the suppressive capacity of Tregs in the absence of both FoxO3a and IL-10.

Taken together, these results indicate that the absence of FoxO3a and IL-10 intrinsically impacts the function of T cells, DCs and Treg cells, and when FoxO3a and IL-10 are inactivated in all the three cell types, this results in a potent response that leads to pathology.

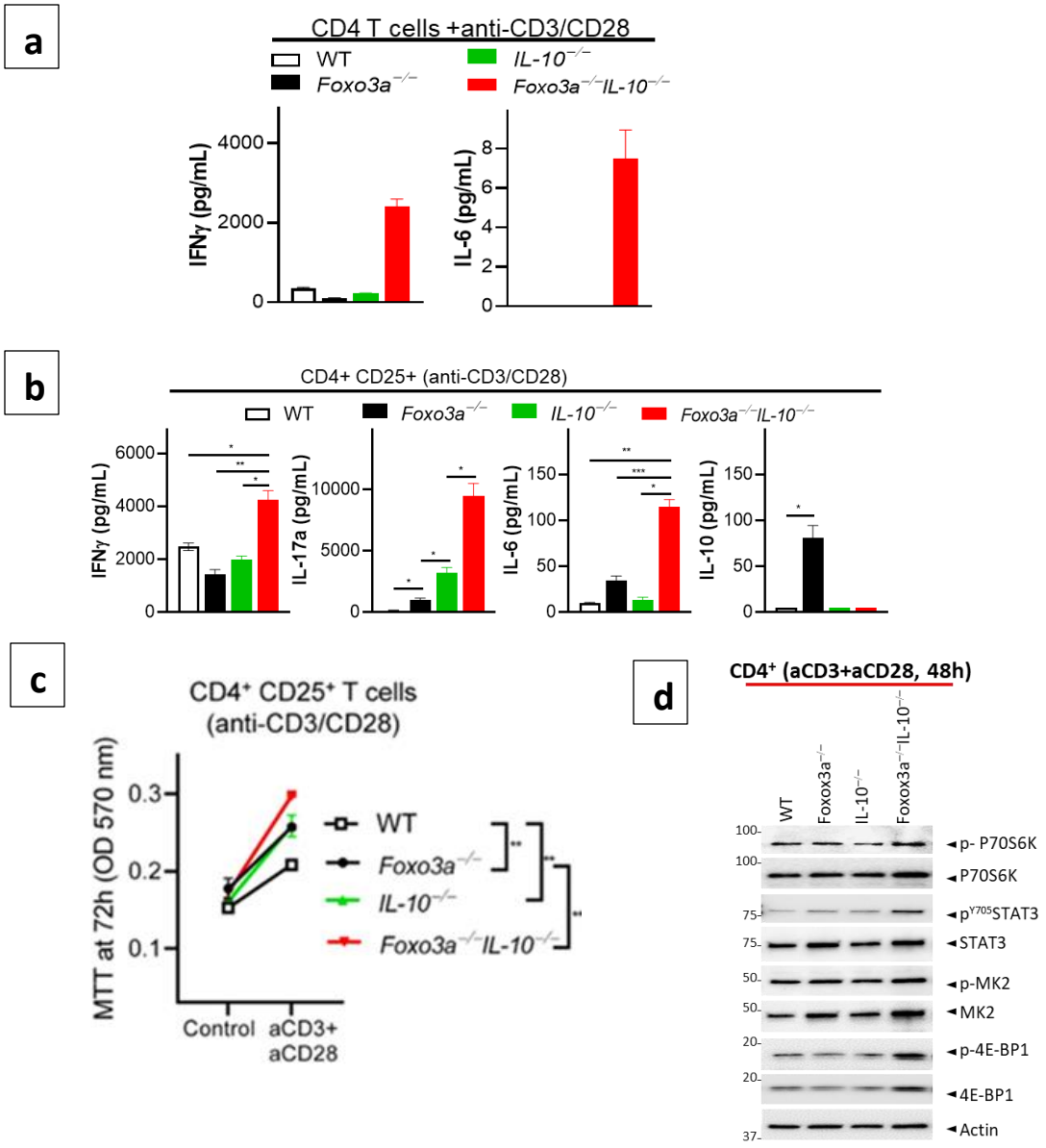

Figure 30. FoxO3a is required to suppress the hyperactivation of IL-10- deficient T cells.

(a) Cytokine levels measured in the supernatants of purified splenic $CD4^+$ T cells 24 h post-activation with anti-CD3/CD28. (b) Cytokine levels measured in the supernatants of purified splenic $CD25^+$ $CD4^+$ T cells 72 h post-activation with anti-CD3/CD28 in the presence of rIL-2/rTGF-β (2.5 ng/mL). (c) MTT uptake was evaluated in purified splenic $CD25^+CD4^+$ T cells 72h post-activation with anti-CD3/CD28. (d) Western blots of purified splenic $CD4^+$ T cells at 48 h post-activation with anti-CD3/CD28. A minimum of n=3 mice (6-12 weeks old) per group were used. Experimental repeats were performed independently. All graphs depict mean ± SEM. Statistics were done using One-way ANOVA (*$P < 0.05$, ***$P < 0.001$ and ****$P < 0.0001$).

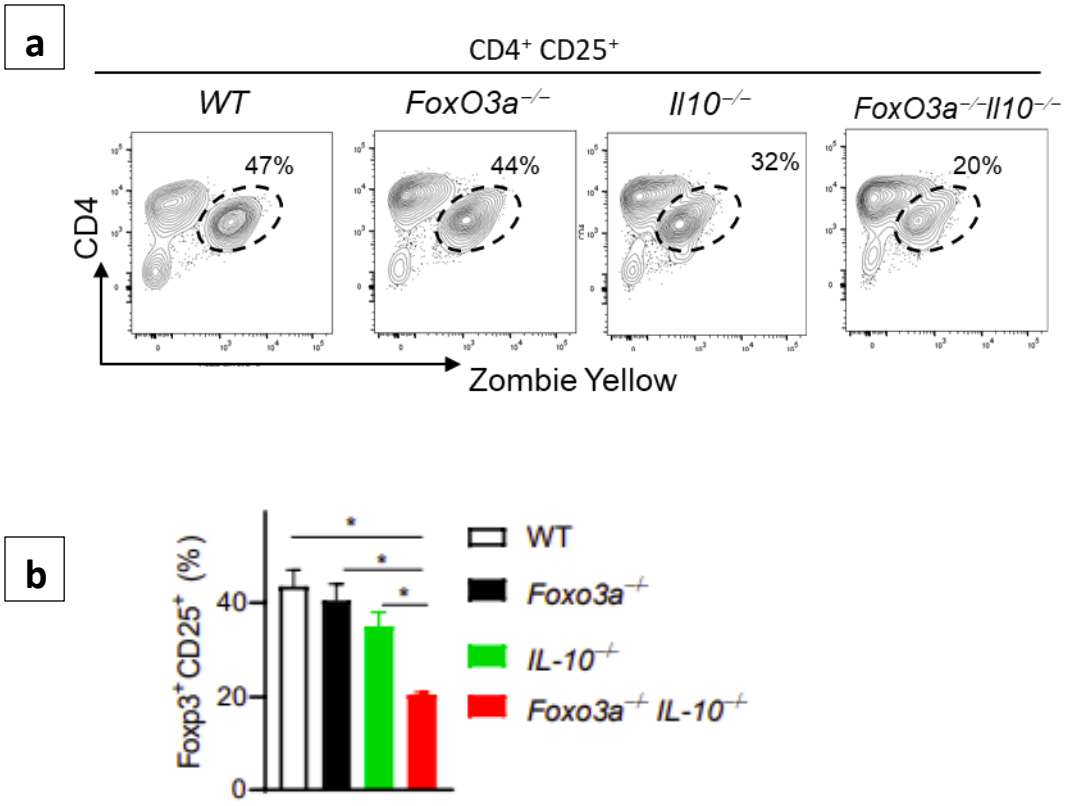

Figure 31. ***FoxO3a*$^{-/-}$*Il10*$^{-/-}$ CD4^{+}CD25^{+} T cells exhibit improved viability *in vitro*.**

(a) Representative FACS plots showing CD4 vs. Zombie yellow staining of purified splenic CD25^{+} CD4^{+} T cells 72h post-activation with anti-CD3/CD28. (b) Quantitation of data in panel (a). A minimum of n=3 mice were used per group. Experimental repeats are performed independently. All graphs depict mean ± SEM. Statistics were done using One-way ANOVA (*$P < 0.05$, ***$P < 0.001$ and ****$P < 0.0001$).

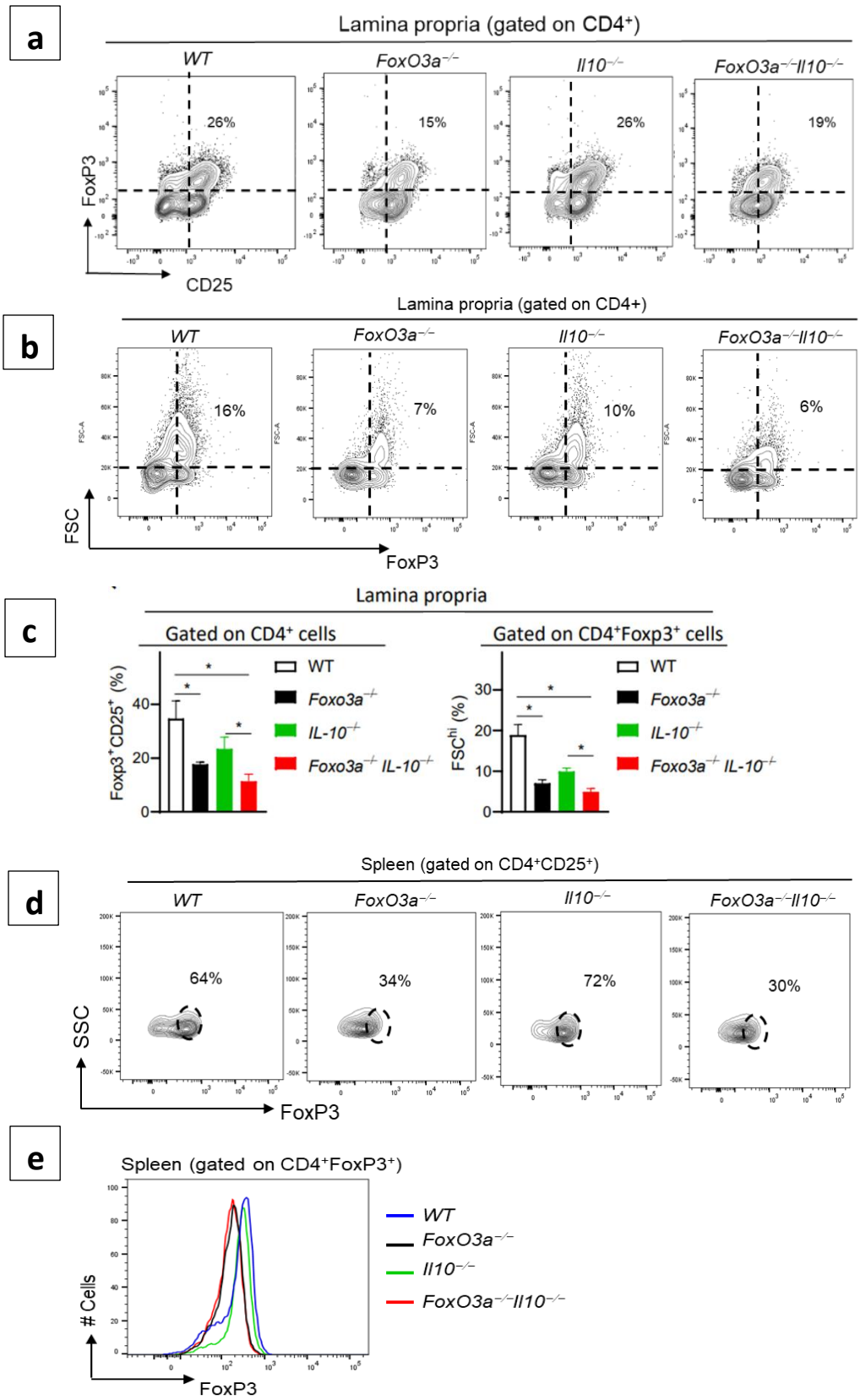
a
Lamina propria (gated on CD4+)
WT
FoxO3a−/−
Il10−/−
FoxO3a−/−Il10−/−
26%
15%
26%
19%
FoxP3
CD25
b
Lamina propria (gated on CD4+)
WT
FoxO3a−/−
Il10−/−
FoxO3a−/−Il10−/−
16%
7%
10%
6%
FSC
FoxP3
c
Lamina propria
Gated on CD4+ cells
Gated on CD4+Foxp3+ cells
Foxp3+CD25+ (%)
FSChi (%)
WT
Foxo3a−/−
IL-10−/−
Foxo3a−/− IL-10−/−
d
Spleen (gated on CD4+CD25+)
WT
FoxO3a−/−
Il10−/−
FoxO3a−/−Il10−/−
64%
34%
72%
30%
SSC
FoxP3
e
Spleen (gated on CD4+FoxP3+)
Cells
FoxP3
WT
FoxO3a−/−
Il10−/−
FoxO3a−/−Il10−/−

Figure 32. FoxO3a promotes FoxP3 expression in Tregs.

(a, b) Representative FACS plots showing the expressions of FoxP3 and CD25 in $CD4^+$ cells in the LP of the four groups of 6-12 weeks old mice. (c) Quantitation of data shown in (a) and (b) respectively. (d) Representative FACS plots showing SSC vs. FoxP3 expression in $CD4^+CD25^+$ cells in the spleens of the four groups of mice. (e) Representative histograms showing FoxP3 expression in splenic $CD4^+$ cells in the four groups of mice. Data are representative of a minimum of n=3 mice per group. Experimental repeats were performed independently. All graphs depict mean ± SEM. Statistics were done using One-way ANOVA (*$P < 0.05$, ***$P < 0.001$, and ****$P < 0.0001$).

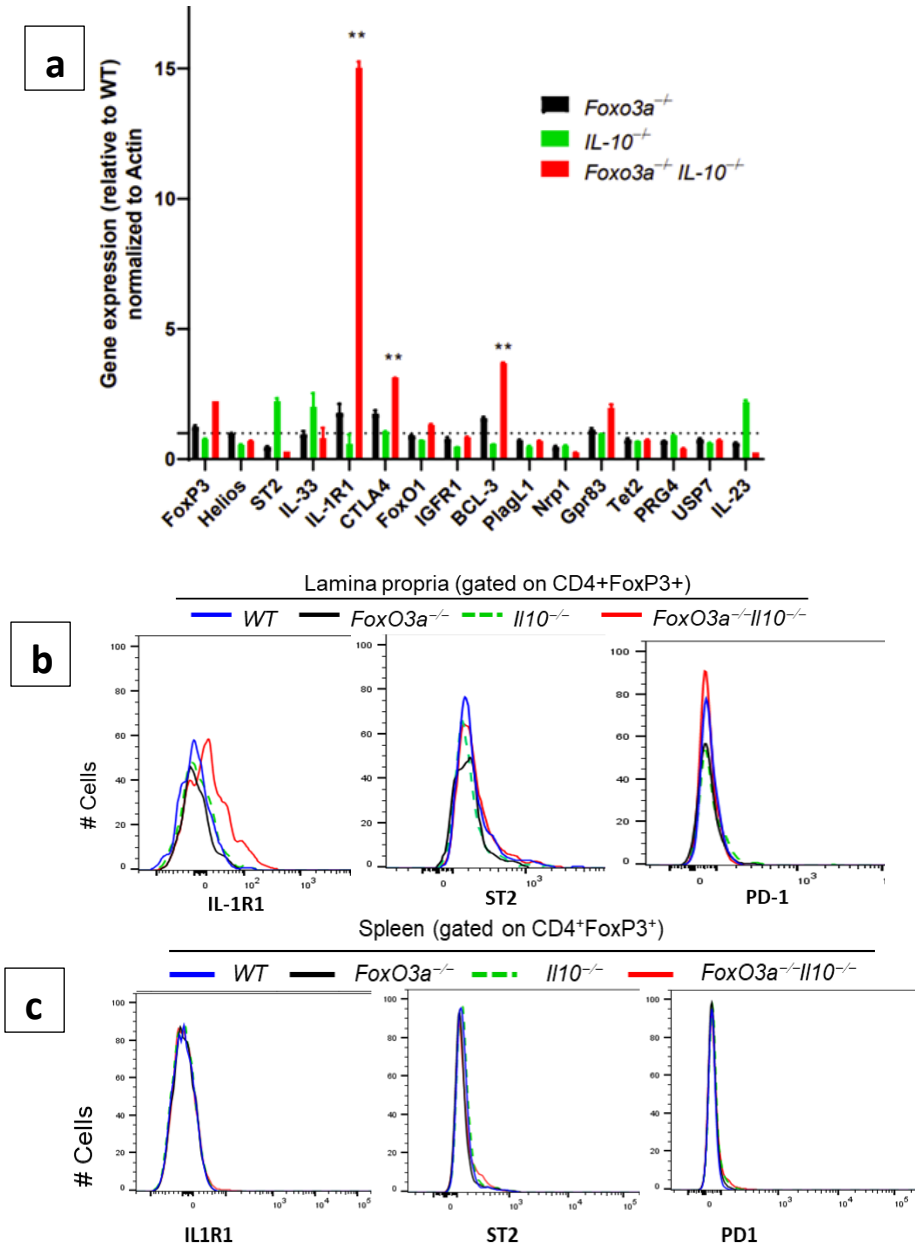

Figure 33. FoxO3a modulates the expression of Treg markers in the absence of IL-10.

(a) Expression of various transcripts involved in Treg function measured (by qRT-PCR) in purified splenic $CD25^{+}CD4^{+}$ T cells, activated with anti- CD3/CD28 in the presence of rIL-2/rTGF-β (2.5 ng/mL) for 72 h. Values are represented as fold-change relative to WT. Representative histograms showing the expressions of IL-1R1, PD-1 and ST2 in $CD4^{+}$ $FoxP3^{+}$ T cells in lamina propria (b) and spleen (c). Data are representative of a minimum of n=3 mice per group. Experimental repeats were performed independently. All graphs depict mean ± SEM. Statistics were done using One-way ANOVA (*$P < 0.05$, ***$P < 0.001$, and ****$P < 0.0001$).

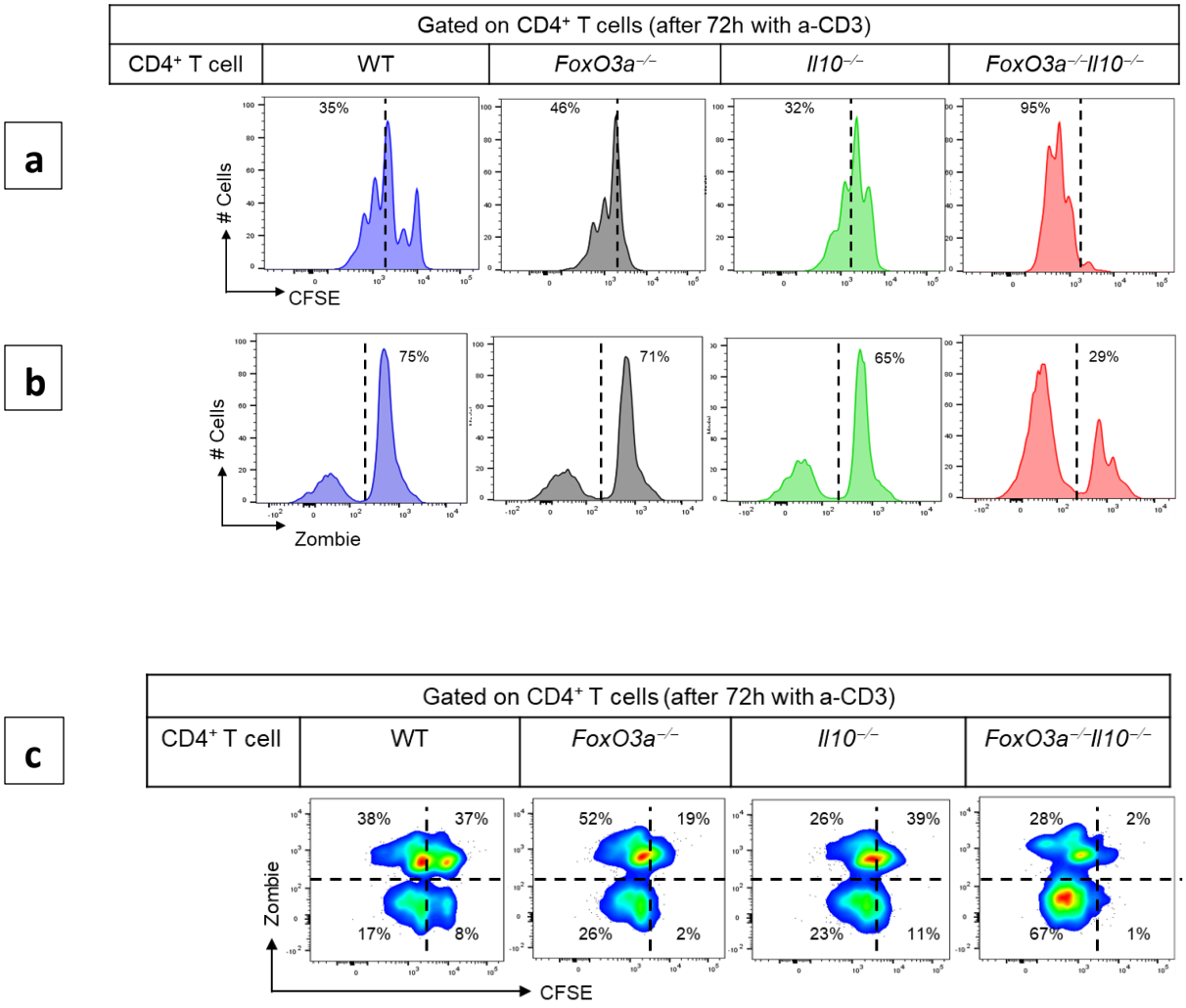

Figure 34. *FoxO3a*$^{-/-}$*Il10*$^{-/-}$ T cells exhibit an intrinsic increase in survival and proliferation.

(a) Representative FACS plots showing the dilution of CFSE in splenic CD4^{+}T cells, isolated from the four groups of 10-12 weeks old mice, upon activation with anti-CD3 for 72H. (b) Representative FACS plots showing Zombie Yellow staining in CD4^{+} T cells isolated from the four groups of mice upon activation with anti-CD3 for 72H. (c) Representative FACS plots showing Zombie Yellow staining vs CFSE dilution in CD4^{+} T cells isolated from the four groups of mice upon activation with a-CD3 for 72H. A minimum of n=3 mice were used, and experimental repeats were performed independently.

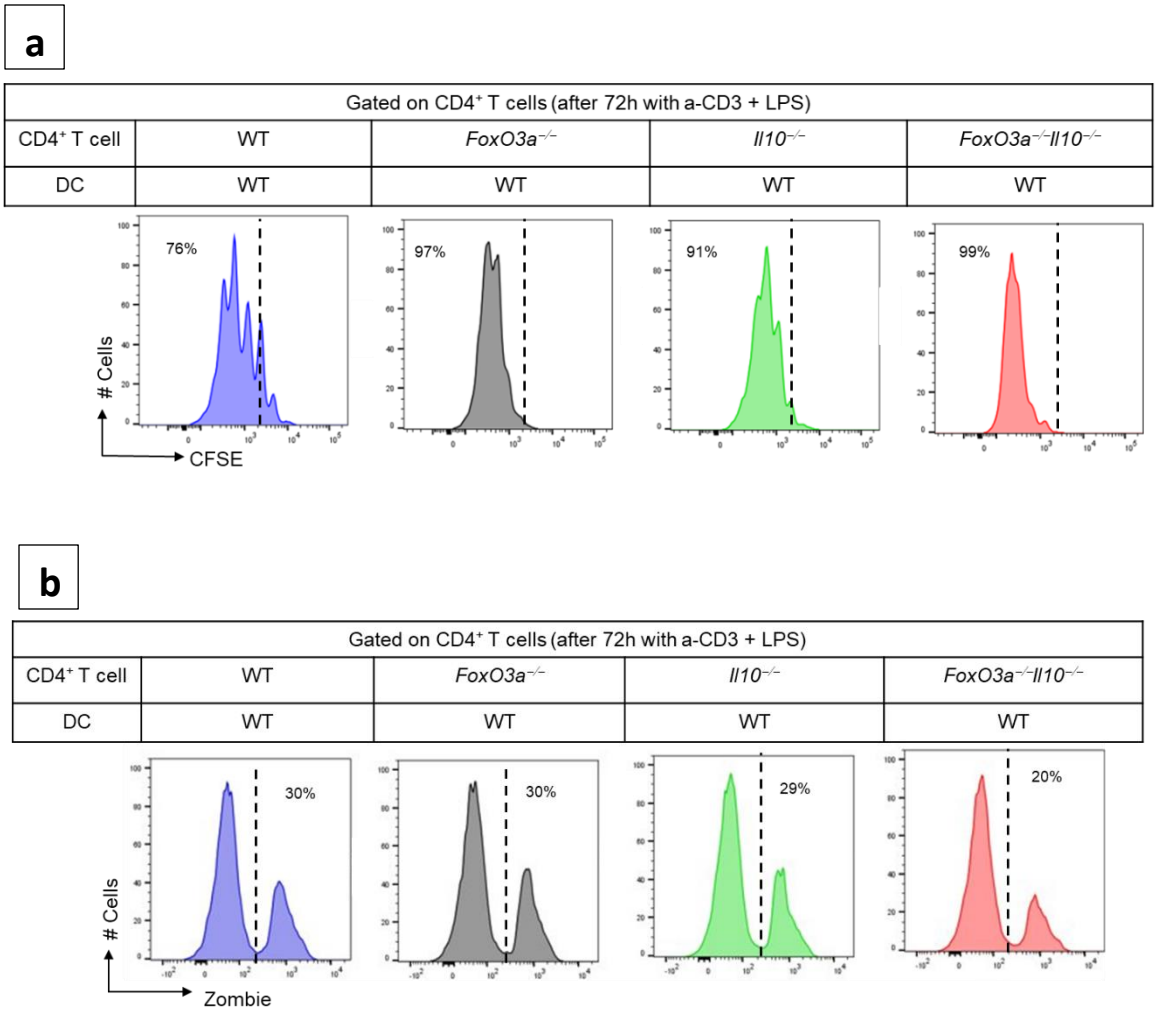

Figure 35. WT DCs improve the proliferation and survival of CD4$^+$ T cells in all groups of mice.

(a) Representative FACS plots showing the uptake of CFSE in splenic CD4$^+$ T cells, isolated from the four groups of mice, 72H post-activation with anti-CD3 and co-cultured with LPS-stimulated DCs at 1:1 ratio (100,000 cells each). (b) Representative FACS plots showing Zombie Yellow staining in CD4$^+$ T cells isolated from the four groups of mice 72H post- activation with anti-CD3 and co-cultured with LPS-stimulated DCs at 1:1 ratio (100,000 cells each). A minimum of n=3 mice were used, and experimental repeats were performed independently.

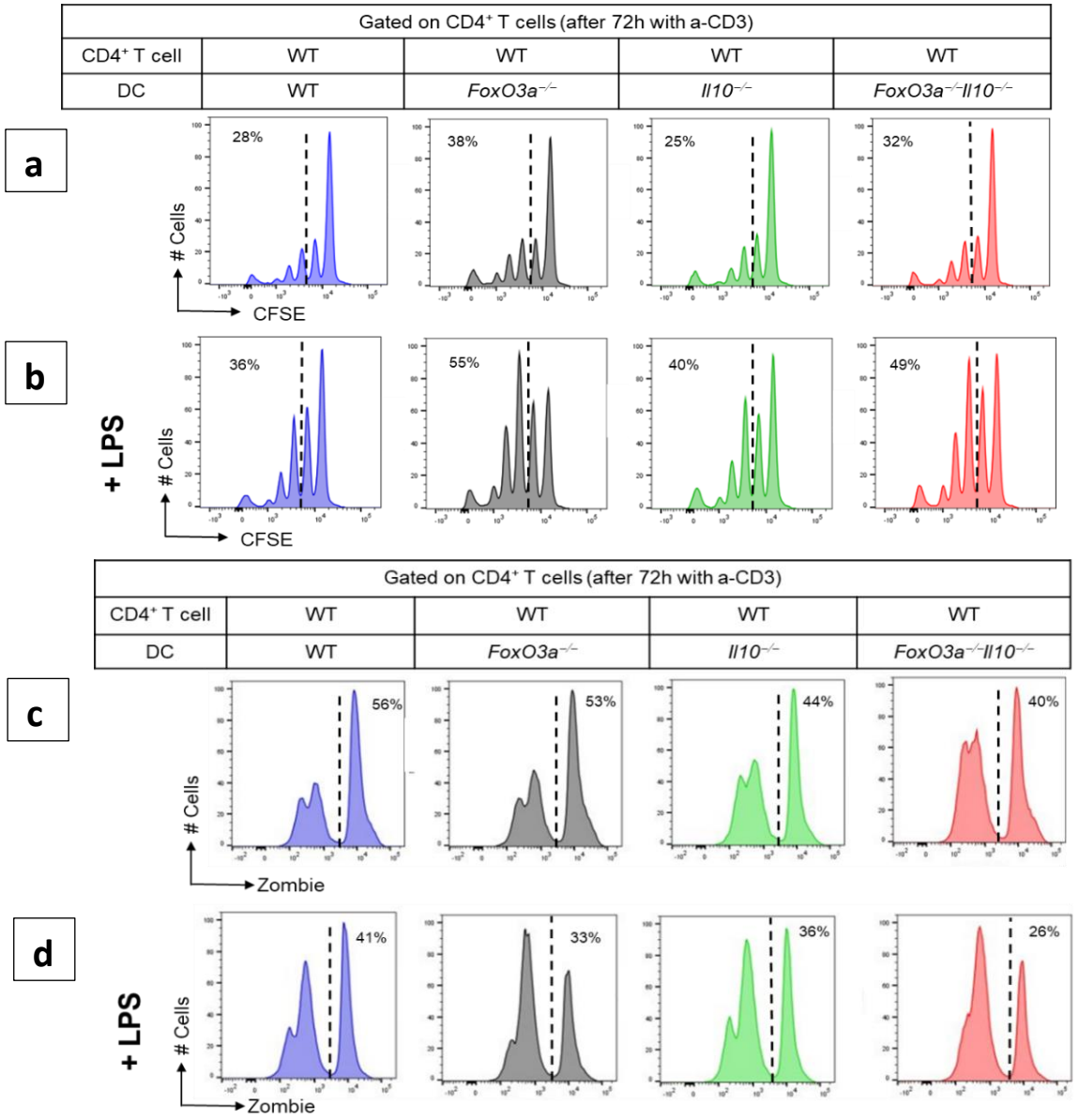

Figure 36. Deficiency of FoxO3a in DCs enhances their capacity to activate WT T cells.

Representative FACS plots showing the uptake of CFSE in purified splenic WT CD4$^+$ T cells at 72H post-activation with anti-CD3 and co-cultured with DCs isolated from the four groups of 10-12 weeks old mice in the absence (a) or presence of LPS (100 ng/mL) (b) at 1:1 ratio (100,000 cells each). Representative FACS plots showing Zombie Yellow staining in CD4$^+$T cells at 72 H post- activation with anti-CD3 and co-cultured with DCs isolated from the four groups of mice in the absence (c) or presence of LPS (100 ng/mL) (d) at 1:1 ratio (100,000 cells each). A minimum of n=3 mice were used, and experimental repeats were performed independently.

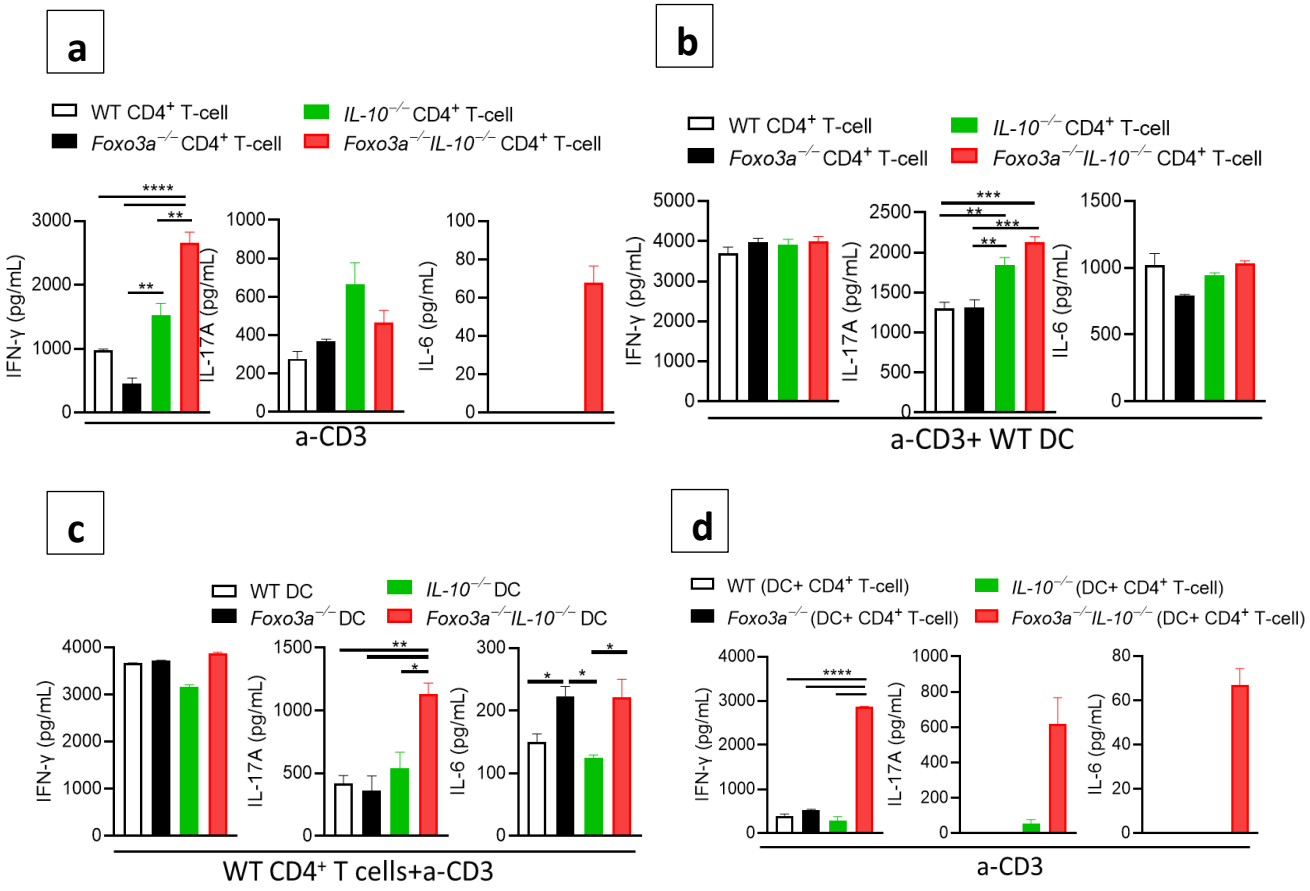

Figure 37. *FoxO3a*$^{-/-}$*Il10*$^{-/-}$ DCs intrinsically promote IL-17A production by activated T cells and *FoxO3a*$^{-/-}$*Il10*$^{-/-}$ T cells intrinsically secrete IFN-γ and IL-6.

Cytokine levels measured in the supernatants of splenic CD4^{+} T cells, isolated from the four groups of 10-12 weeks old mice and activated with anti-CD3 for 72H, without (a) and with (b) co-culture with WT DCs at 1:1 ratio (100,000 cells each). (c) Cytokine levels measured in the supernatants of splenic WT CD4^{+} T cells, activated with anti-CD3 for 72H and co-cultured with splenic DCs isolated from the four groups of mice at a ratio of 1:1 (100,000 cells each). (d) Cytokine levels measured in the supernatants of co-cultured splenic CD4^{+} T cells (5%) and splenic DCs isolated from the four groups of mice in the presence of anti-CD3 for 72H. A minimum of n=3 mice were used, and experimental repeats were performed independently. All graphs depict mean ± SEM. Statistics were done using One-way ANOVA (*$P < 0.05$, ***$P < 0.001$, and ****$P < 0.0001$).

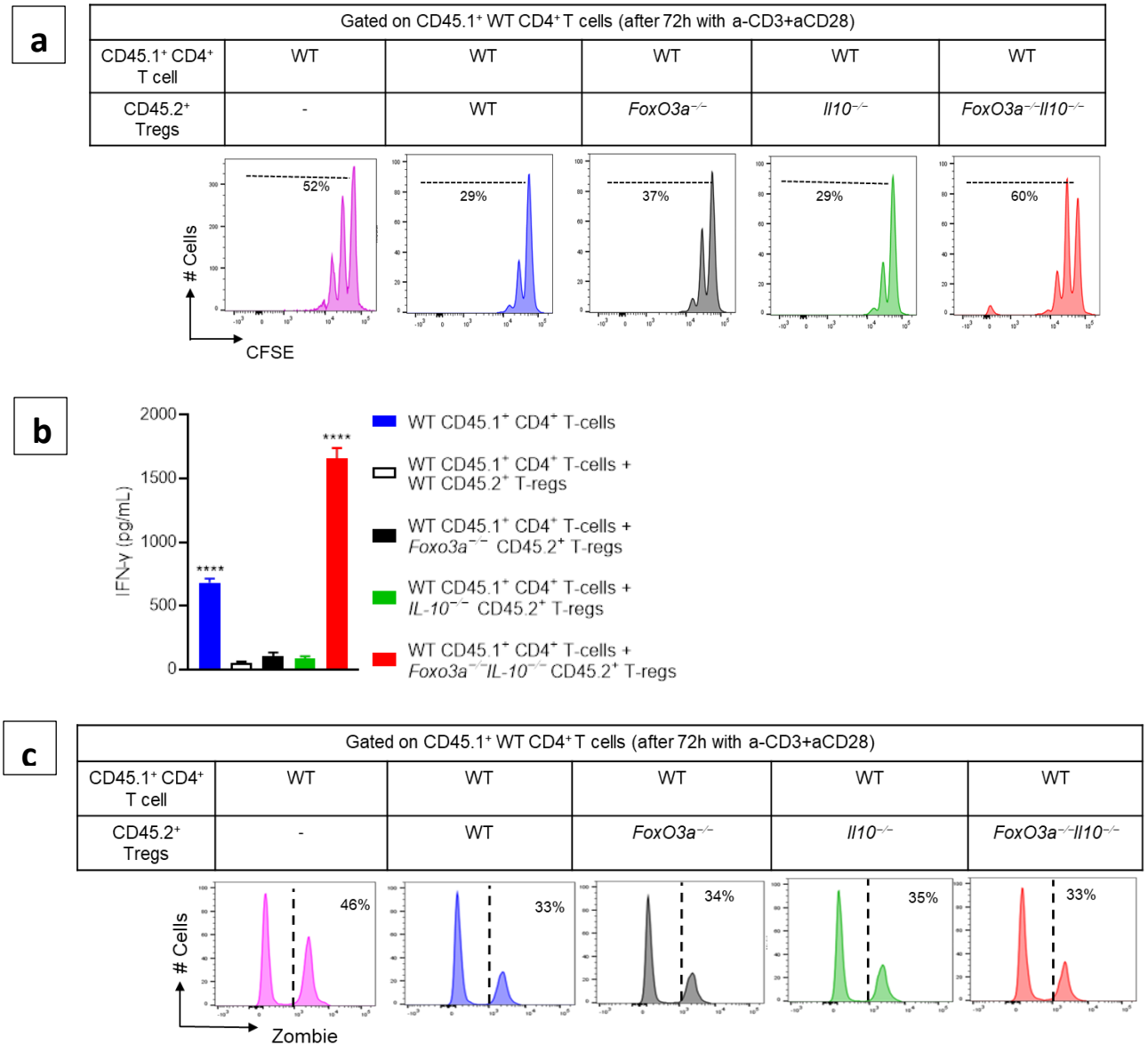

Figure 38. ***FoxO3a*$^{-/-}$*Il10*$^{-/-}$ Tregs are intrinsically impaired in their ability to suppress the activation of WT T cells.**

(a) Representative histograms showing the dilution of CFSE in CD45.1^{+} WT T cells co-cultured with CD45.2^{+} Tregs, isolated from the four groups of 10-12 weeks old mice, upon activation with anti-CD3/CD28 for 72H. (b) IFN-γ levels measured in the supernatants of WT CD45.1^{+} T cells without and with co-culture with CD45.2^{+} Tregs isolated from the four groups of mice upon activation with anti-CD3/CD28 for 72H. (c) Representative histograms showing the Zombie Yellow staining in CD45.1^{+} WT T cells co-cultured with CD45.2^{+} Tregs, isolated from the four groups of mice, upon activation with anti-CD3/CD28 for 72H. The graph in panel (b) depicts mean ±SEM. A minimum of n=3 mice were used, and experimental repeats were performed independently. Statistics were done using One-way ANOVA (*P< 0.05, ***P<0.001 and ****P<0.0001).

7. FoxO3a favors glutamine synthesis by repressing the expression of glutaminase and glutamine transporters.

Besides glucose oxidation, T cell activation induces a large increase in glutamine import, and glutamine metabolism has been shown to differentially regulate the development of T cells into Th17 or Th1 subsets as mentioned in the introduction section. Therefore, we measured cytokine production by $CD4^+$ T cells upon supplementing the glucose/glutamine free media with either 2 mM glutamine, 10 mM glucose or both. Dialyzed FBS was used for cell culture. Addition of glutamine was sufficient to induce cytokine production by *FoxO3a*$^{-/-}$*Il10*$^{-/-}$ $CD4^+$ T cells, and this was increased further by the addition of glucose (**Fig. 39 a**). Expression of cytokines was suppressed by treatment of cells with the inhibitors of glutamine metabolism, DON or GAH (**Fig. 39 b**). Inhibiting glutamine metabolism also normalized mitochondrial activity in *FoxO3a*$^{-/-}$ and *FoxO3a*$^{-/-}$*Il10*$^{-/-}$ cells to WT levels, while there was no impact on *Il-10*$^{-/-}$ $CD4^+$ T cells (**Fig. 39 c**).

We performed qRT-PCR to quantitate the expression of enzymes involved in the conversion of glutamine to glutamate and vice versa. We observed that the expression of *Gls/Gls2* (glutaminase), which convert glutamine to glutamate, was markedly enhanced in activated *FoxO3a*$^{-/-}$*Il10*$^{-/-}$ T cells with FoxO3a playing a dominant role (**Fig. 40 a**). On the other hand, the expression of *Glul* (glutamine synthetase), which converts glutamate back to glutamine, was not modulated by FoxO3a or IL-10 (**Fig. 40 a**). We also measured the expression of key transporters involved in glutamine metabolism. We observed that both FoxO3a and IL-10 seemed to modulate the transcription of major glutamine importers (SNAT 1,2, 5 and ASCT2) and exporters (LAT1/CD98 heterocomplex) in naïve and activated $CD4^+$ T cells (**Fig. 40 b-d**). Overall, naïve $CD4^+$ T cells isolated from the spleens of *FoxO3a*$^{-/-}$*Il10*$^{-/-}$ mice showed higher transcript levels for most of the transporters, and this possibly reflects enhanced glutamine metabolism in these cells *in vivo* (**Fig. 40 b**). At 48 h post-activation of $CD4^+$ T cells, the expression of some of the transporters was still elevated in *FoxO3a*$^{-/-}$*Il10*$^{-/-}$ cells in comparison to other groups (**Fig. 40 c**). Interestingly, the expression of SNAT2 was significantly increased in *FoxO3a*$^{-/-}$ and *Il10*$^{-/-}$ $CD4^+CD25^+$ T cells at 72 h post- activation, and it was elevated even further in *FoxO3a*$^{-/-}$*Il10*$^{-/-}$ cells (**Fig. 40 d**).

Based on this data, we hypothesized that activated *FoxO3a*$^{-/-}$*Il10*$^{-/-}$ T cells increased their glutamine consumption leading to increased mitochondrial activity. To this end, we evaluated the

levels of glutamine and glutamate in the serum of mice to determine the impact of FoxO3a, IL-10 and various cell depletions on global glutamine concentrations. The levels of glutamine were significantly reduced in the serum of *FoxO3a*$^{-/-}$mice in comparison to *Il10*$^{-/-}$ mice (**Fig. 41 a**). Interestingly, glutamine levels in the serum of *FoxO3a*$^{-/-}$*Il-10*$^{-/-}$ mice were abolished, and they were significantly restored in mice that were depleted of myeloid cells and T- cells (**Fig. 41 a**). This highlights the possibility that removing T cells or preventing their activation by myeloid APCs helps restore glutamine levels. We can also speculate that like T cells, *FoxO3a*$^{-/-}$*Il-10*$^{-/-}$ myeloid cells exhibit overconsumption of glutamine.

We also measured serum levels of glutamate and observed an inverse correlation with glutamine levels. *FoxO3a*$^{-/-}$ and *FoxO3a*$^{-/-}$*Il10*$^{-/-}$ mice had the highest level of serum glutamate compared to the other two groups, and that was normalized by depletion of myeloid and T cells (**Fig. 41 b, c**). These results suggest that FoxO3a plays a critical role in regulating glutamine consumption by immune cells. In addition to glutamine, the levels of serum glucose were modestly but significantly reduced in *FoxO3a*$^{-/-}$*Il10*$^{-/-}$ mice (**Fig. 41 d**). Overall, the impact of FoxO3a on glutamine levels was profound, and the double deficiency of FoxO3a and IL-10 leads to a massive decline in glutamine pools bordering on glutaminemia. These results indicate that FoxO3a represses glutaminolysis in T cells, which reaches a toxic state by an additional deficiency of IL-10.

Since FoxO3a was shown to modulate mTORC1 activity in IL-10-deficient myeloid and T cells, we treated *FoxO3a*$^{-/-}$*Il10*$^{-/-}$ mice with Rapamycin (5 mg/kg body weight; i.p. route) and monitored their survival. This resulted in a substantial rescue in their survival (**Fig. 42 a**) and an increase in the proportion of FoxP3^{+} CD25^{+} Tregs (**Fig. 42 b**). Additionally, *in vitro* treatment of activated CD25^{+} T cells with Rapamycin reduced IL-17A production in all four groups (**Fig. 42 c**). This suggests a possible suppression of a pathogenic Th17 polarizing milieu. We also observed that the expression of ST2, known to maintain the stable regulatory function of Tregs (Alvarez et al., 2019), was highly reduced in FoxO3a- as well as in IL-10- deficient cells, and this was restored by Rapamycin treatment (**Fig. 42 d**).

All in all, we have shown that FoxO3a plays a critical role in modulating the metabolic activity of activated T cells, and both FoxO3a and IL-10 appear to restrain mTORC1 signaling to prevent hyperactivation of immune cells.

The next aim is dedicated to evaluating the profiles of the gut microbiome in the four groups of mice. We explored the impact of FoxO3a and IL-10 deficiencies on the alterations in the abundance of commensal gut microbiota and their contribution to disease pathogenesis.

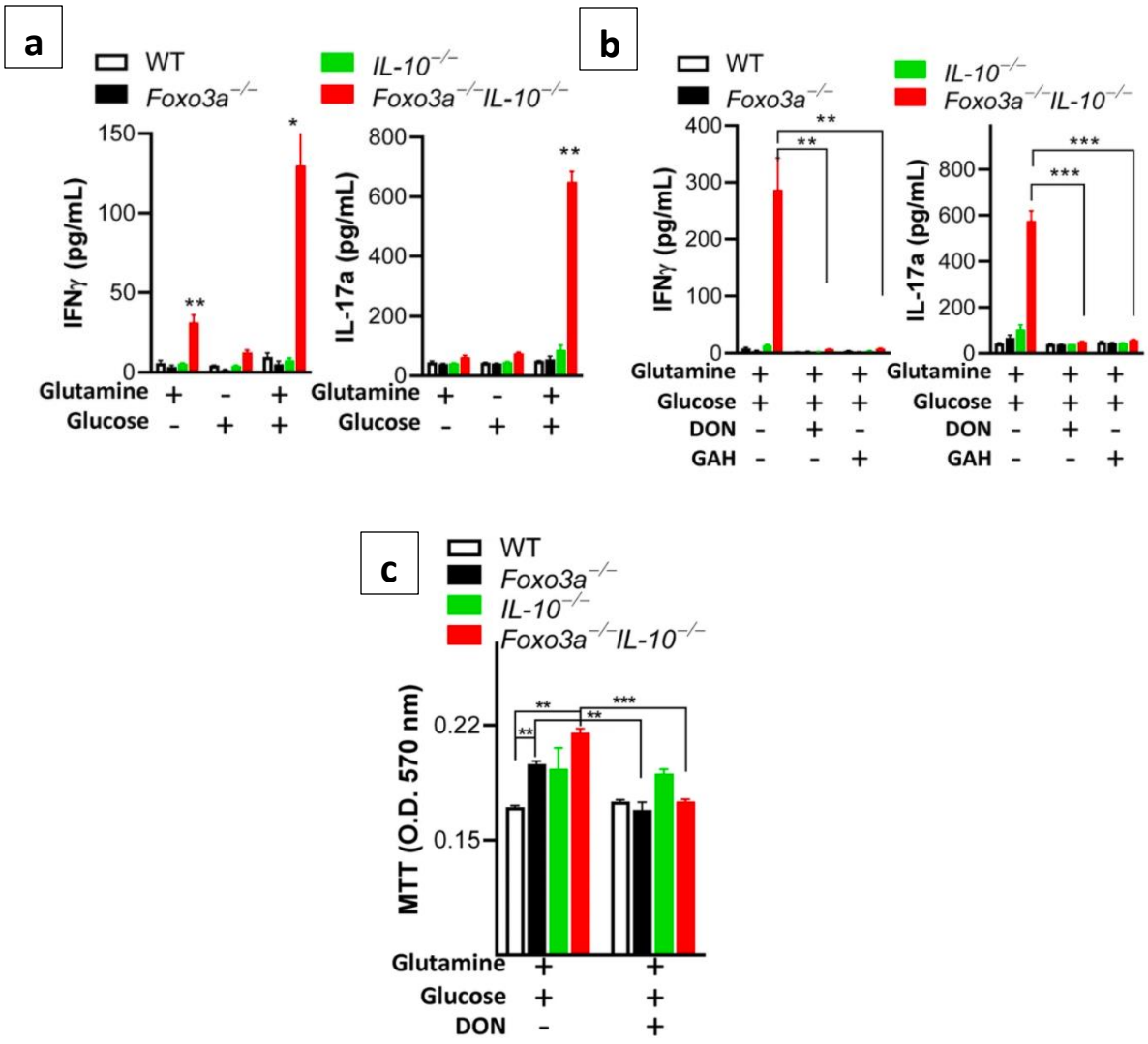

Figure 39. **Glutamine is required alongside glucose oxidation for optimal cytokine production and metabolic activity in *FoxO3a*$^{-/-}$*Il10*$^{-/-}$ T cells.**

IFN-γ and IL-17A levels were measured (at 72 h) in the supernatants of anti-CD3/CD28 activated $CD4^+$ T cells supplemented with either 10 mM glucose or 2 mM glutamine or both in the absence (a) or presence (b) of the glutamine antagonist DON (50 μM) and inhibitor of glutamine transport GAH (1 mM). (c) MTT uptake was evaluated in activated $CD4^+$ T cells in glucose/glutamine free media supplemented with either 10 mM glucose or 2 mM glutamine or both in the absence or presence of the inhibitors DON (50 μM) and GAH (1 mM) at 72H post activation. A minimum of n=3 mice were used, and experimental repeats were performed independently. All graphs depict mean ±SEM. Statistics were done using One-way ANOVA (*P< 0.05, ***P<0.001 and ****P<0.0001).

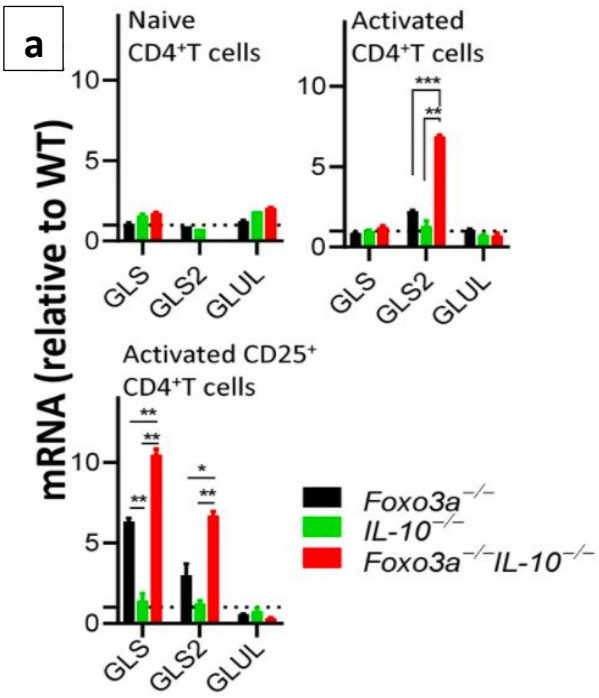
a
Naive CD4+T cells
Activated CD4+T cells
Activated CD25+ CD4+T cells
mRNA (relative to WT)
GLS
GLS2
GLUL
Foxo3a−/−
IL-10−/−
Foxo3a−/−IL-10−/−

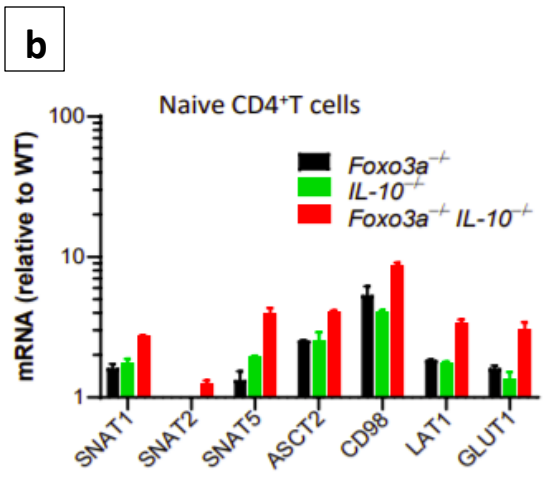
b
Naive CD4+T cells
mRNA (relative to WT)
Foxo3a−/+
IL-10−/+
Foxo3a−/+ IL-10−/+
SNAT1
SNAT2
SNAT5
ASCT2
CD98
LAT1
GLUT1

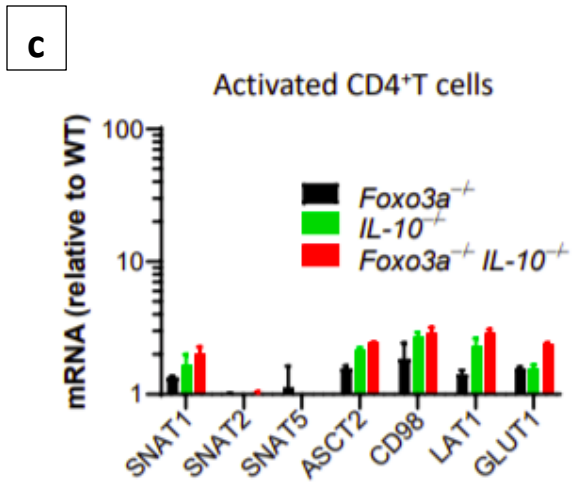
c
Activated CD4+T cells
mRNA (relative to WT)
Foxo3a−/+
IL-10−/+
Foxo3a−/+ IL-10−/+
SNAT1
SNAT2
SNAT5
ASCT2
CD98
LAT1
GLUT1

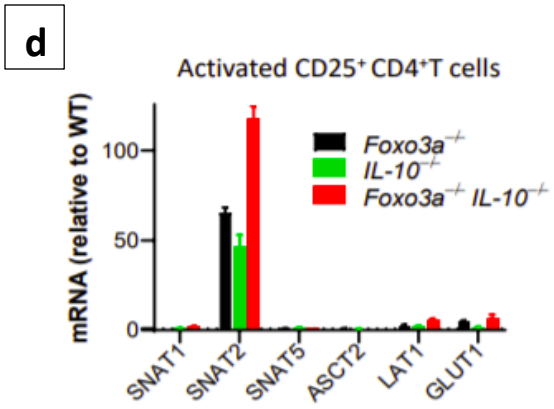
d
Activated CD25+ CD4+T cells
mRNA (relative to WT)
Foxo3a−/+
IL-10−/+
Foxo3a−/+ IL-10−/+
SNAT1
SNAT2
SNAT5
ASCT2
LAT1
GLUT1

Figure 40. FoxO3a favors glutamine synthesis by repressing the expression of glutaminase and glutamine transporters.

(a) mRNA expression of glutamine metabolism-associated enzymes was evaluated in $CD4^+$ T cells by qRT-PCR and normalized to actin. Values are fold-change relative to WT cells. mRNA expression of various glutamine and glucose transporters in non-activated splenic $CD4^+$ T cells (b), splenic $CD4^+$ T cells at 48h post-activation with anti-CD3/CD28 (c) and splenic $CD25^+CD4^+$ T cells at 72H post- activation anti-CD3/CD28 normalized to actin (d). All graphs depict mean ± SEM. A minimum of n=3 mice were used, and experimental repeats were performed independently. Statistics were done using One-way ANOVA (*$P < 0.05$, ***$P < 0.001$ and ****$P < 0.0001$).

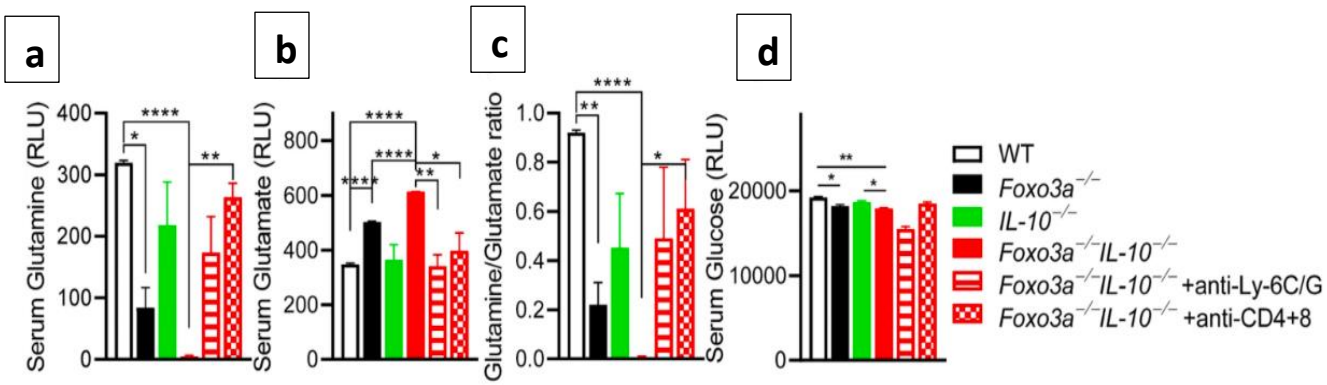

Figure 41. Double deficiency of FoxO3a and IL-10 leads to a massive decline in glutamine pools bordering on glutaminemia, which is restored by immune cell depletion.

Glutamine, glutamate, glutamine/glutamate ratio, and glucose levels were measured (as relative light units; RLU) in the sera of 10-15 weeks old mice. A minimum of 3 mice were used. All graphs depict mean ± SEM. Statistics were done using One-way ANOVA (*$P < 0.05$, ***$P < 0.001$ and ****$P < 0.0001$).

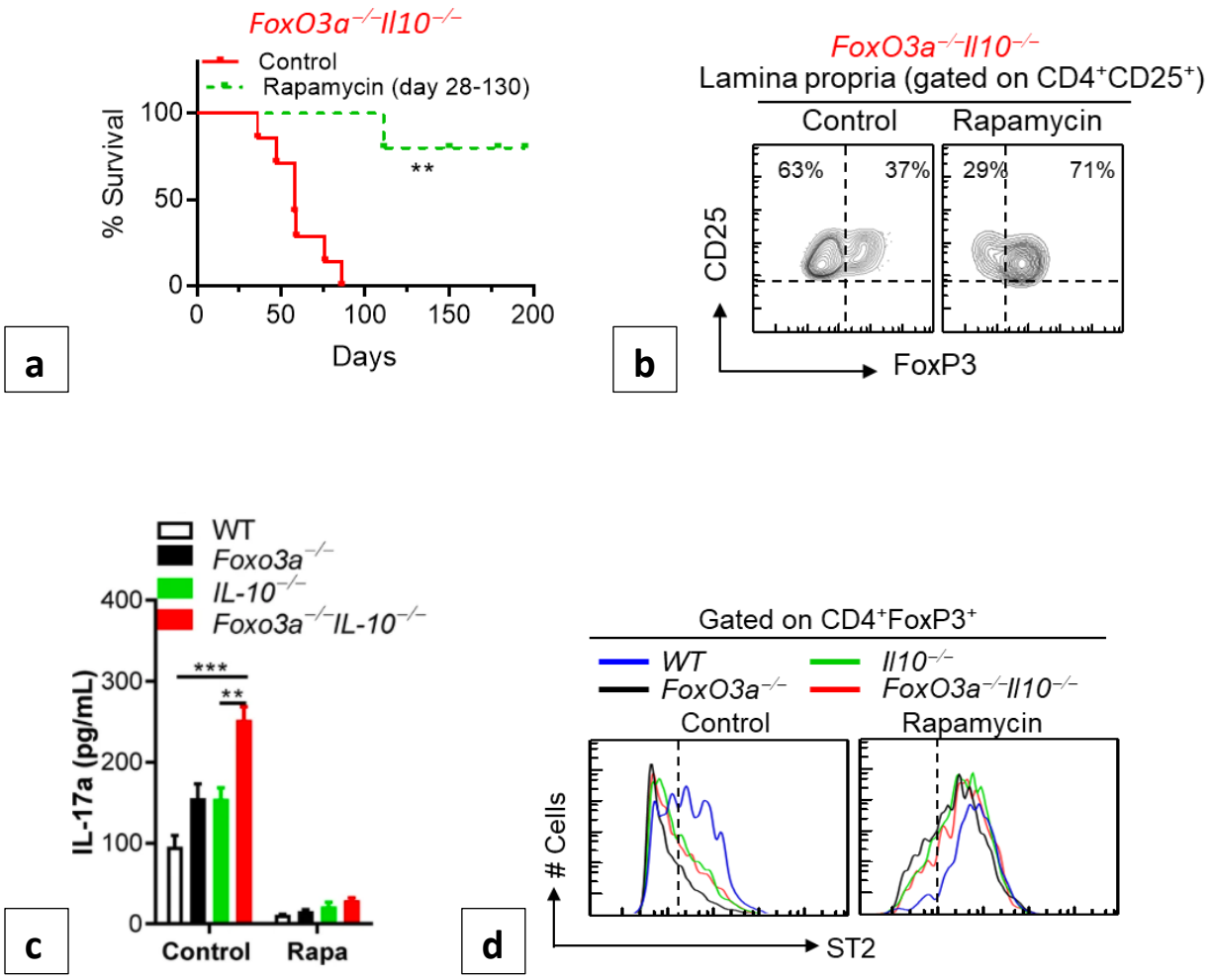

Figure 42. Rapamycin treatment improves the survival of *FoxO3a*$^{-/-}$*Il10*$^{-/-}$ mice, attenuates IL-17A production and boosts Treg differentiation.

(a) Survival of control-fed and rapamycin-fed *FoxO3a*$^{-/-}$ *Il10*$^{-/-}$ mice (a minimum of 5 mice per group). (b) Representative FACS plot showing CD25 vs. FoxP3 expression in colonic lamina propria-purified CD4^{+} CD25^{+} cells in control-fed and rapamycin-fed *FoxO3a*$^{-/-}$ *Il-10*$^{-/-}$ mice. (c) IL-17A secretion was measured in the supernatants of anti-CD3/CD28-activated CD25^{+}CD4^{+} T cells at 48 h post-stimulation with and without treatment with Rapamycin (100 nM). (d) Representative histograms in gated CD4^{+}FoxP3^{+} cells showing ST2 expression in cells described in panel (c) without and with Rapamycin treatment. The Mantel–Cox test was used for survival analysis. The graph in panel (c) depicts mean ± SEM. Statistics were done using One-way ANOVA (*$P < 0.05$, ***$P < 0.001$ and ****$P < 0.0001$).

Aim 4: Identify the gut microbiome signature that is created by the deficiency in FoxO3a and IL-10.

8. FoxO3a deficiency promotes the abundance of colitogenic microbiota in *Il10*$^{-/-}$ mice

Multiple studies have emphasized the role of intestinal bacteria in the pathogenesis of IBD (Kau et al., 2011; Elinav et al., 2011; Chen et al., 2017; Henao-Kejia et al., 2012; Assa et al., 2016). GWAS in CrD patient cohorts has implicated the involvement of FoxO3a in mediating the pathogenesis of the aggressive disease (Lee et al., 2017). Thus, it is likely that FoxO3a signaling helps maintain a balanced gut microbiome and understanding how FoxO3a impacts the gut microbial diversity and abundance will help delineate its role in regulating gut inflammation in our *FoxO3a*$^{-/-}$*Il10*$^{-/-}$ mouse model.

Shortly after weaning, *Il10*$^{-/-}$ mice predominantly develop cecal inflammation when susceptible strains (129 SvEv or mixed 129/C57Bl/6 background) are colonized with specific pathogen-free bacteria (Berg et al., 1996; Sellon et al., 1998). The development of inflammation progresses in the ascending and transverse colon and finally in the remainder of the colon and rectum. This does not occur under "germ free" conditions emphasizing the role of commensal intestinal organisms in the pathogenesis of chronic intestinal inflammation (Sellon et al., 1998). It has been reported that antibiotics, which selectively act on aerobic or anaerobic bacteria, have different therapeutic effects in the colons of IL-10-deficient mice (Hoentjen et al., 2003). Antibiotics, such as Ciprofloxacin and Metronidazole, demonstrated greater efficacy in preventing the induction of colitis rather than reversing established colitis. This may be explained by the different roles of various endogenous bacterial species in the different phases of the inflammatory process. Some bacterial species may initiate the inflammation, while others may perpetuate the disease (Rath et al., 2010).

We observed that the administration of both Metronidazole and Ciprofloxacin in the drinking water resulted in a significant improvement in the survival of *FoxO3a*$^{-/-}$*Il10*$^{-/-}$ mice implying the involvement of the gut microbiome in the disease progression (**Fig. 43**). Interestingly, treatment with antibiotics was not a permanent cure for these mice. These results indicate that FoxO3a might influence the gut microbiota of mice. Therefore, we assessed the diversity of gut microbiota in fecal samples of the four groups of mice that were collected when *FoxO3a*$^{-/-}$*Il10*$^{-/-}$ mice demonstrated signs of illness. Microbiota diversity was unchanged between WT, *Il10*$^{-/-}$ and

FoxO3a$^{-/-}$ mice. However, the microbiota of *FoxO3a*$^{-/-}$*Il10*$^{-/-}$ mice exhibited slightly lower diversity compared to WT mice (**Fig. 44 a, b**). While the overall richness seemed comparable across the four groups, as indicated by the Chao1 index, there appeared to be a decreasing trend in the absence of FoxO3a and IL-10 (**Fig. 44 a**). In fact, the Shannon index indicated a slightly lower evenness of species in *FoxO3a*$^{-/-}$*Il10*$^{-/-}$ samples (**Fig. 44 b**). Beta diversity analysis showed that the microbiota of different samples was partially clustered based on the mice phenotype, and adonis analysis showed that the tested mice phenotypes contributed to 21.039% of the microbiota variability among samples (R^2=0.21039; P =0.001; **Fig. 44 c**). We also characterized the composition of the gut microbiota in the various groups of mice. 8 bacterial phyla were generally identified with 76 - 90% of reads assigned to *Firmicutes* and *Bacteroidetes* (**Fig. 45 a**).

Deficiency of FoxO3a resulted in an expansion of the phylum *Verrucomicrobia*, and more specifically its genus *Akkermensia*, anaerobic Gram-negative mucin-degrading bacteria. *Akkermensia* supplies SCFA through mucin degradation to mucin-secreting goblet cells, thereby contributing to intestinal health (Shin et al., 2019). Moreover, the genus secretes several extracellular proteins, among which Amuc_1100 was found to induce IL-10 production via TLR2 signaling activation hence improving epithelial barrier integrity (**Fig. 45 b**) (Ottman et al., 2017). This may suggest that, in the absence of FoxO3a, *Akkermensia* may be contributing to the increased production of IL-10, which in turn protects mice from developing colitis. In contrast to *FoxO3a*$^{-/-}$ mice, *Il10*$^{-/-}$ mice displayed a slight increase in the abundance of the colitogenic *Proteobacteria* and a significant abundance of butyrate-producing *Coprococcus* species (**Fig. 45 b**).

In contrast to the single gene deficiencies, the deficiency in both FoxO3a and IL-10 has drastic consequences on the composition of the gut microbiome characterized by the dominance of certain colitogenic strains. Perhaps, such strains are creating a pro-inflammatory configuration that drives a spontaneous CrD-like phenotype. A reduction in microbial diversity is a biomarker for numerous human metabolic and inflammatory disorders including IBD, which was shown to be associated with a decrease in the level of resident *Firmicutes* and/or *Bacteroides* and an overabundance of *Proteobacteria* (**Fig. 45 b**) (Manichanh et al., 2006; Le Chatelier et al., 2013).

When looking at the phylum level, we observed a higher abundance of *Actinobacteria* and *Proteobacteria*, with an increased abundance level of *Enterobacteriaceae*, in *FoxO3a*$^{-/-}$*Il10*$^{-/-}$

mice. *Proteobacteria* are colitogenic strains found to be significantly more abundant in patients with aggressive CrD (Vester-Andersen et al., 2019). At the genus level, we observed that *Sutterella* was significantly enriched in *FoxO3a*$^{-/-}$*Il10*$^{-/-}$ mice. *Sutterella* has been shown to be increased in patients with IBD compared to healthy controls (Lavelle et al., 2016; Santoru et al., 2017). We also observed that the abundance of *Lactobacilli*, which suppress the production of pro-inflammatory cytokines (Chen et al., 2015), was particularly reduced in *FoxO3a*$^{-/-}$*Il10*$^{-/-}$ mice. Furthermore, we observed that *Roseburia*, a Gram-positive aerobic species of the *Firmicutes* phylum, was depleted in *FoxO3a*$^{-/-}$*Il10*$^{-/-}$ mice. *Roseburia* produces butyrate, which is the main energy source of anti-inflammatory SCFA for colonocytes; hence, its depletion negatively influences intestinal inflammation (Parada Venegas et al., 2019; Smith et al., 2013). A complete list of identified differential taxa are presented in **Fig. 46 a-d**. Overall, these results showed the abundance of colitogenic microbiota in *FoxO3a*$^{-/-}$*Il10*$^{-/-}$ mice.

The presence of commensal microbiota, confined to the intestinal lumen, is critical for shaping the gut health, and the biological homeostasis is maintained so long as the internal and external milieu are segregated (Kinashi & Hase, 2021). To this end, the intestinal epithelial barrier contributes to this segregation through the formation of tight junctions, which are protein complexes tightly connected to reduce paracellular permeability. The mucosal barrier also includes mucin, antimicrobial peptides, and dimeric (or more polymeric) IgA secreted by goblet cells, Paneth cells, and plasma cells, respectively (Kinashi & Hase, 2021). Dysbiosis, or altered microbial composition in the gut, has been shown to pre-dispose animals to IBD, due to the dysfunction in the maintenance the mucosal barrier, thus leading to potential leakage of microbes across the lumen and into the systemic circulation. Research has shown that pro-inflammatory cytokines, such as TNF-α and IFN-γ, impair the barrier integrity, while anti-inflammatory cytokines, such as IL-10, reinforce it. Given that the gut commensal microbiota can regulate the cytokine-induced barrier changes, we attempted to orally administer fluorescein isothiocyanate dextran (FITC-Dextran) into *FoxO3a*$^{-/-}$*Il10*$^{-/-}$ mice, since its passage into the blood is used as a marker for tight junction permeability. Mice were fasted for a total of 8 hours. Following the first four hours, the mice were injected with FITC-D, and after another period of four hours, they were sacrificed, and their sera were collected. Fluorescence signals were evaluated in the control group (i.e., receiving PBS) and the experimental group (receiving FITC-D). The results indicated that there was no apparent enteric leakiness observed in 13-15 weeks old *FoxO3a*$^{-/-}$*Il10*$^{-/-}$ mice (**Fig. 47**).

Despite the alterations observed in the gut microbial composition, there doesn't seem to be major microbial translocations into the systemic circulation of naïve *FoxO3a*$^{-/-}$*Il10*$^{-/-}$ mice. This complements the absence of a hyperinflammatory response in their spleens and further emphasizes the enhanced epithelial regenerative and healing capacity.

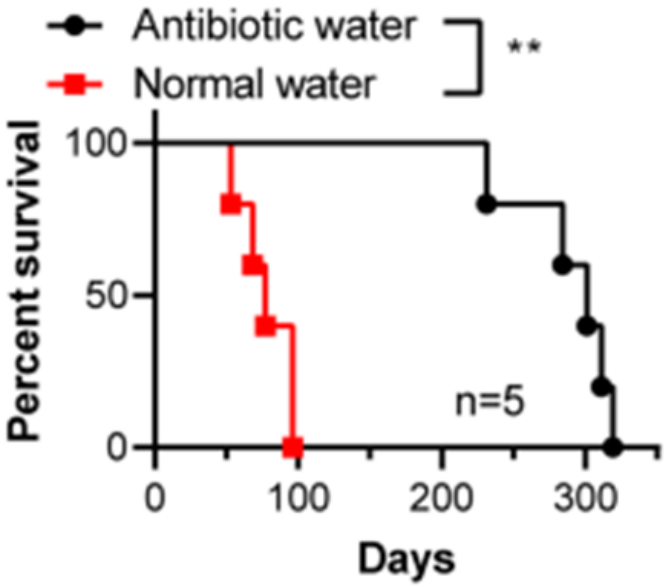

Figure 43. Improved survival of *FoxO3a*$^{-/-}$*Il10*$^{-/-}$ mice with antibiotic treatment.

FoxO3a$^{-/-}$*Il-10*$^{-/-}$ mice ($n = 5$; 5–8 weeks old) received a 2 month-course of antibiotic treatment consisting of Ciprofloxacin (0.225 mg/mL) and Metronidazole (0.45 mg/mL) in their drinking water. Then, they were maintained on antibiotic-free water for the remainder of the study. As a control group, 5 mice received antibiotic-free drinking water. The numbers of spontaneous deaths were recorded over the course of time. Data was analyzed using Mantel–Cox test.

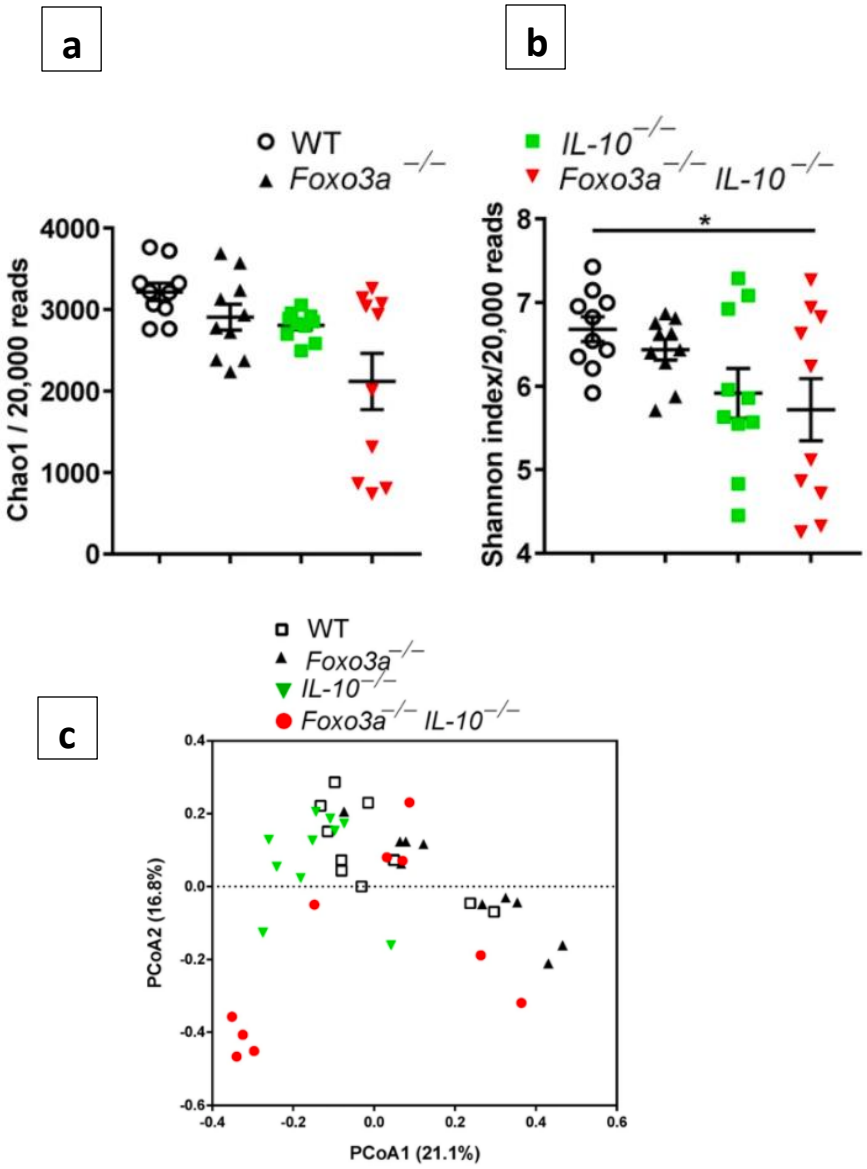

Figure 44. Deficiency in FoxO3a and IL-10 slightly modulates the diversity of the intestinal microbiota in mice.

(a, b) Diversity of intestinal microbiota in WT, *Il10*$^{-/-}$, *FoxO3a*$^{-/-}$, and *FoxO3a*$^{-/-}$*Il10*$^{-/-}$mice ($n = 10$ each; 10-15 weeks old). Chao1 estimates and Shannon indices were calculated from rarefied 20,000 reads per sample. Lines represent mean ± SEM. Data was analyzed using Kruskal-Wallis test and Two-stage Benjamini, Krieger, and Yekutieli FDR procedure (*$P < 0.05$). (c) Principal Coordinate Analyses (PCoA) based on Bray-Curtis distances were conducted using QIIME 1.9.0 on 20,000 randomly selected reads per sample. The samples were colored by mice phenotypes. PCoA1and PCoA2 represent the top two coordinates that captured the highest variability between samples, and the percentages shown indicate the fraction of variation represented by each coordinate. Adonis analysis was used to test for the statistical significance of sample grouping by the mice phenotypes ($R^2 = 0.21039$; $P = 0.001$).

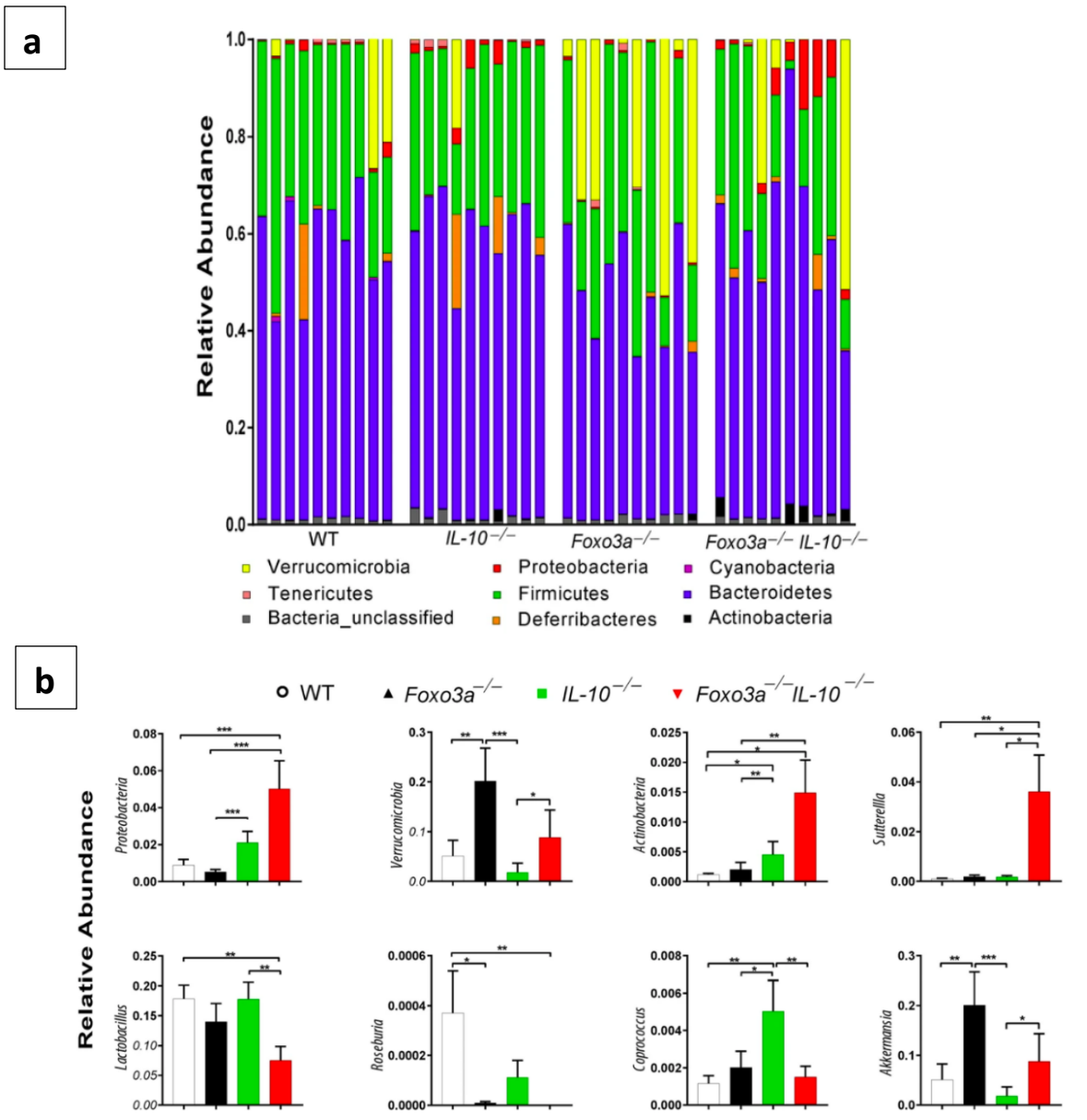

Figure 45. FoxO3a and IL-10 modulate the relative abundance of gut microbial species.

(a) Relative abundance of the identified phyla in each sample. Samples are grouped by mice phenotype ($n = 10$/group). **(b)** Relative abundance of differentially abundant taxa among the microbiota of WT, *Il10*$^{-/-}$, *FoxO3a*$^{-/-}$, and *FoxO3a*$^{-/-}$ *Il10*$^{-/-}$ mice. Lines represent mean ± SEM. Data was analyzed using Kruskal-Wallis test and Two-stage Benjamini, Krieger, and Yekutieli FDR procedure (*$P < 0.05$, **$P < 0.01$, and ***$P < 0.001$).

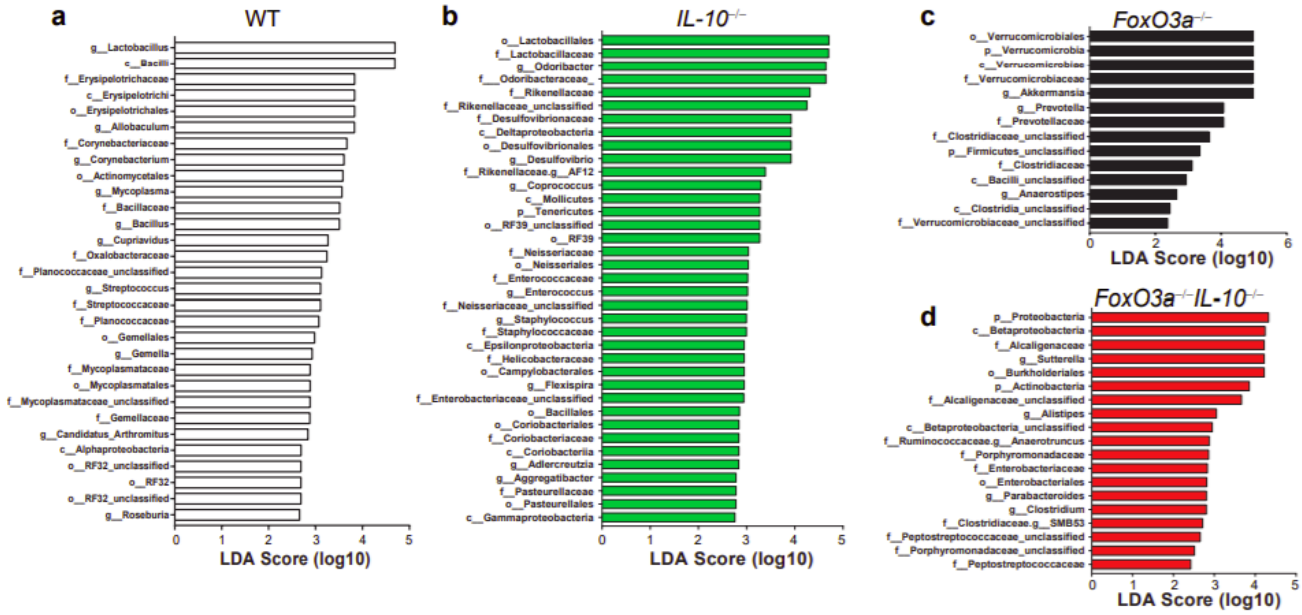

Figure 46. Deficiency in FoxO3a and IL-10 alters the enrichment of various bacterial taxa in the gut microbiome of mice.

Histogram of linear discriminant analysis effect size score of bacterial taxa uniquely and significantly enriched in the gut microbiota of (a) WT, (b) *Il10*$^{-/-}$, (c) *FoxO3a*$^{-/-}$ and (d) *FoxO3a* $^{-/-}$ *Il10* $^{-/-}$ mice (n=10 each).

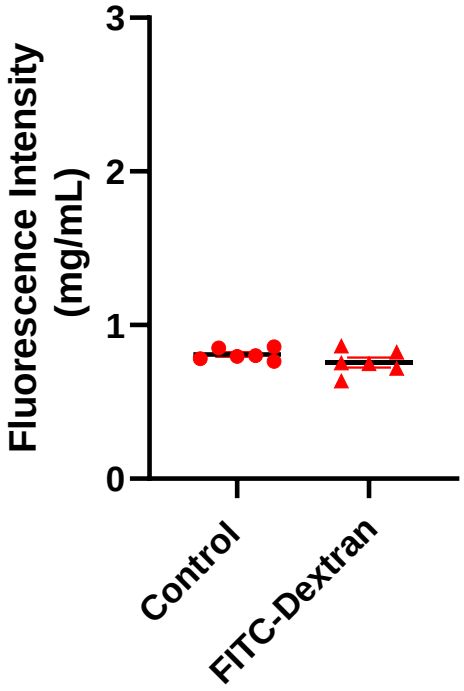

Figure 47. No apparent enteric leakiness is observed in 13-15 weeks old *FoxO3a*$^{-/-}$ *Il10*$^{-/-}$ mice.

Evaluation of enteric leakage by measuring the fluorescence intensity levels in the sera of 13-15 weeks old *FoxO3a*$^{-/-}$ *Il10*$^{-/-}$ mice (n=3 per group) upon oral-gavage with PBS (Control) or FITC-Dextran. Results are based on a single experiment. Data was analyzed using One Way ANOVA (*$P < 0.05$, ***$P < 0.001$, and ****$P < 0.0001$).

DISCUSSION

This thesis presents new frontiers in IBD research, studying how the transcription factor FoxO3a and the anti-inflammatory IL-10 cooperatively regulate intestinal homeostasis in a murine model.

We report that *FoxO3a*$^{-/-}$*Il10*$^{-/-}$ mice develop a spontaneous and aggressive inflammatory response in the gut that is reminiscent of CrD in humans. We reveal a novel antagonistic relationship between FoxO3a and IL-10, which regulates inflammation, immuno-metabolism and gut dysbiosis to prevent the development of a pathological inflammatory response in the gut. We provide novel clues regarding how FoxO3a signaling limits the severity of intestinal inflammation in *Il10*$^{-/-}$ mice without any deliberate manipulations (e.g., stressing mice by oral administration of DSS). Ultimately, the *FoxO3a*$^{-/-}$*Il10*$^{-/-}$ mouse may serve as a potential physiological model representing an aggressive form of CD, and this in turn may lead to the identification of novel avenues for therapy or provide insight for better management of chronic illness.

1. Prelude

The transcription factor FoxO3 (also called FoxO3a) is a key member of the FoxO family that is expressed in various tissues including the lymphoid organs, and it has been shown to promote healthy ageing and tumor suppression (Lin et al., 2004). At the cellular level, it regulates the transcription of genes involved in a variety of vital cellular processes that encompass proliferation, metabolism, stress resistance and cell death. FoxO3a has been shown to mediate apoptosis in HIV-1- infected human monocyte-derived macrophages (Cui et al., 2008) and in primed $CD8^+$ T cells in response to *Listeria monocytogenes* infection (Tzelepis et al., 2013). In models of acute infections, FoxO3a signaling was shown to impact the T cell response without affecting host survival (Tzelepis et al., 2013; Hedrick et al., 2012; Dejean et al., 2009; Sullivan et al., 2012). Its functions were found to be more pertinent during conditions of chronic cellular stress suggesting that FoxO3a may play a key role in regulating homeostasis (Joseph et al., 2016; Eijkelenboom and Burgering, 2013).

Generally, FoxO proteins are rendered inactive by phosphorylation, and this requires negative regulation by insulin and growth factor signaling. Several kinases, such as AKT, IKKβ, CK1, DYRK1A and SGK, induce the phosphorylation of FoxO3a (Eijkelenboom and Burgering, 2013). In fact, FoxO proteins are regulated through several PTMs that control their translocation into and

out of the nucleus (Eijkelenboom and Burgering, 2013). When excluded from the nucleus, FoxO3a becomes transcriptionally inactive.

Single nucleotide polymorphisms of the *FoxO3a* gene have shown a strong correlation with human longevity in Japanese, American, Jewish, and German centenarians (Willcox et al., 2008; Greer & Brunet, 2005; Flachsbart F, et al. 2009). Also, variations in *FoxO3a* were discovered to correlate with the prognosis of various diseases, such as malaria, rheumatoid arthritis and IBD (Lee et al., 2013; Lee et al., 2017). In the current thesis, we corroborate the GWAS findings by showing that the absence of FoxO3a exacerbates the development of CrD-like disease in *Il-10*$^{-/-}$ mice, and we comprehensively elucidate the immunomodulatory roles of both genes.

2. FoxO3a and IL-10: Key determinants in the development of IBD

IBD is a chronic inflammatory disease of the GI tract that has been traditionally classified into Crohn's disease and ulcerative colitis. Differentiated by their clinical manifestations, UC is relapsing and non-transmural and affects the colon solely, while CrD is segmental and granulomatous and affects any part of the GI tract (Podolsky, 2002; Xavier & Podolsky, 2007). Unlike other chronic inflammatory diseases that are caused by an inflammatory response to a known antigen (e.g., Celiac disease can be avoided with a gluten-free diet), the instigative antigen in IBD is generally presumed to be the commensal flora of the gut (Sartor, 1990; Chadwick & Anderson, 1992). As a matter of fact, the etiology of IBD is not clearly determined but has been implicated in several researched cross-talks among genetics, immunology, environmental factors, and microbiota dysregulation. Genome wide genetic-linkage and association studies have provided insights into the genetic complexity underlying these inflammatory conditions.

Recently, the field of human genetics has encompassed an enormous gain of knowledge due to the development of high-throughput techniques, growing cohorts, and new methods of analysis. Over the years, GWAS has ascertained more than 200 genetic risk loci to be associated with IBD, making it one of the complex traits that has been extensively studied (Liu et al., 2015; Jostins et al., 2012). Genome wide genetic-linkage and association studies have paved the way into deciphering the genetic complexity underlying the inflammatory conditions (Cho, 2008). Based on these studies, several "susceptibility" genes have been implicated in the pathogenesis of IBD through disrupting the immune system, the process of autophagy, the epithelial barrier and

activation of the ER stress response (Hugot et al., 2001; Hampe et al., 2007; Parkes et al., 2007; Franke et al., 2008; Kaser et el., 2008). Nevertheless, attempts to correlate the functional relevance of such genes in determining the progression or severity of the inflammatory diseases have resulted in limited success (Liu et al., 2015; Lee et al., 2017). Collectively, it has been established that the main genetic contribution to prognosis comes from loci that are distinct from those that drive disease susceptibility and demonstrate that disease initiation is not only temporally distinct from active symptomatic disease but also appears to be governed by separate genetics (Lee et al., 2017). This may explain why the clinical course and eventual outcome of the disease vary enormously among susceptible individuals.

In 2013, a GWAS provided insight into how a non-coding SNP in *FoxO3a* can determine the prognosis of CrD in patients despite not being a disease- associated variant (Lee et al., 2013). More specifically, minor (G) allele carriage in patients with indolent CrD course was shown to promote earlier recovery of nuclear FoxO3a accumulation. This initiated a TGF-β1-dependent pathway in monocytes that reduced the production of pro-inflammatory cytokines and enhanced IL-10 expression. In 2017, a GWAS conducted in a cohort of mild vs. progressive CrD patients correlated four different genetic loci (XACT, MHC, FoxO3, IGFBP1-3) with disease progression with none of them showing association with disease susceptibility (Lee et al., 2017). It was also shown that such mutations operate independently of the ones responsible for determining disease susceptibility (e.g., IL-10/IL-10R, NOD2, IL23A, ATG16L1). The role of FoxO3a in intestinal inflammation was also evaluated in *vivo* (Snoeks et al., 2009). In a mouse model of DSS-induced colitis, FoxO3a was increasingly translocated to the cytosol of inflamed epithelial cells rendering it inactive. Also, DSS-treated FoxO3a-deficient mice developed a more severe inflammatory response compared to WT mice (Snoeks et al., 2009). Hence, the important role of FoxO3a in limiting inflammation emerges from its ability to effectively balance its subcellular localization and thus its control for homeostasis-inducing transcriptional programs.

The role of IL-10 in colitis has emerged in both humans and murine models. Polymorphisms in the *Il10* locus confer a risk for IBD (Franke et al., 2008; Amre et al., 2009). In fact, the IL-10-IL10R axis plays an essential role in regulating intestinal tissue homeostasis and preventing IBD. IL-10 restricts excessive Th1 immune responses, and it limits the secretion of pro-inflammatory cytokines (Fiorentino et al., 1991). Most hematopoietic cells sense IL-10 via the

expression of IL-10R. While IL10R1 is expressed on many innate and adaptive immune cells, IL10R2 is expressed on both the immune cells and a wide range of non-immune cells, such as epithelial cells and keratinocytes. In fact, IL10R2 is a component of the receptors for IL-10, -22, -26, -28A, -28B, and -29. When IL-10 binds to its receptor, it signals predominantly through STAT3 to mediate its anti-inflammatory effects (Williams et al., 2004). Being a pleiotropic cytokine, it acts on various immune cells including T cells, B cells, macrophages, monocytes, and others (Moore, 2001). The lack of an IL-10-mediated negative-feedback signaling perturbs homeostasis of the intestinal immune system. Particularly, loss-of-function mutations in the genes encoding either of the IL-10R subunits, IL-10R1 and IL-10R2, can be found in children with very-early onset enterocolitis and in adults with severe IBD phenotype (Glocker et al., 2009). These findings were consistent with those regarding severe colitis in mice lacking either *Il10* or *Il10rb* (Kuhn et al., 1993; Spencer et al., 1998). However, some IL10R2-related functions may be independent of IL-10, since expression of the murine *Il22* gene in the appropriate cell types provided protection against colitis in two distinct models (Sugimoto et al., 2008; Zenewicz et al., 2008).

One of the best-characterized and commonly used genetic models is the IL-10-deficient mouse. *Il10*$^{-/-}$ mice were reported to spontaneously develop colitis (Kuhn, 1993). In this model, the disease is very much reliant on T cells and more specifically poor functioning of Tregs (Davidson, Leach et al. 1996; Chaudhry, 2011). This, however, was dependent on the genetic background of the mouse with the 129SvEv strain being susceptible and C57BL/6 J and C57BL/10 strains being resistant (Buchler, 2012; Kuhn, 1993). Moreover, administration of neutralizing antibodies against IFN-γ in young *Il10*$^{-/-}$ mice, as well as administration of recombinant IL-10, abrogated intestinal inflammation (Berg et al. 1996; Rennick et al. 1997). In adult *Il10*$^{-/-}$ mice, colitis onset can be prevented by anti-IL-12 antibody administration (Davidson, Hudak et al. 1998). With regards to human disease, *Il10*$^{-/-}$ mice develop colon cancer similarly to CrD and UC patients (Sturlan et al., 2001).

3. FoxO3a and IL-10 negatively regulate each other

In addition to previous work done in our lab by Joseph *et al.* (2016), we also show here that the protein expression of IL-10 was substantially increased in stimulated *FoxO3a*$^{-/-}$ cells. Our results are congruent with another study showing how FoxO3a represses IL-10 expression by mycobacteria-infected macrophages via direct binding to the *Il10* promoter (Bouzeyen et al., 2019). Meanwhile, we also show for the first time that *Il10*$^{-/-}$ cells exhibit a remarkable increase in total FoxO3a expression compared to WT cells. While IL-10 signaling through STAT3 has been shown to promote the nuclear localization and subsequent activation of FoxO3a (Oh et al., 2012), it is of great interest to evaluate how IL-10 deficiency alters the degree of FoxO3a activation and its subcellular localization in resting vs. activated cells. Further to the above, is FoxO3a overexpressed at the transcriptional level or is the protein expression stabilized? Moreover, the mechanisms underlying how FoxO3a and IL-10 suppress each other remain targets for investigation. Mainly, this thesis presents novel insight into how FoxO3a signaling may indirectly crosstalk with IL-10 signaling.

4. Loss of FoxO3a promotes the development of colitis in IL-10-deficient mice

To evaluate the role of IL-10 in the context of FoxO3a signaling, we generated mice with a double deficiency of both genes. WT, *Il10*$^{-/-}$ (C57BL/6) and *FoxO3a*$^{-/-}$ mice were used for this purpose. *FoxO3a*$^{-/-}$ mice were originally generated on a 129 background but were backcrossed more than 10 times to the C57BL/6 strain (Tzelepis et al., 2013).

Intriguingly, *FoxO3a*$^{-/-}$*Il10*$^{-/-}$ mice exhibited signs of severe illness (>20% loss in body weight, diarrhea, piloerection, hunching and occasional rectal bleeding) and reached humane endpoint within three months of birth. Loss of one copy of FoxO3a in IL-10-deficient mice was sufficient to induce 100% disease penetrance. FoxO3a-deficiency by itself had no impact, and only close to 13% of IL-10-deficient mice developed this phenotype.

To explore the observed phenotype, we evaluated the organs macroscopically. *FoxO3a*$^{-/-}$*Il10*$^{-/-}$ mice demonstrated a significant degree of visible intestinal inflammation, as their colons appeared significantly thicker, heavier, and inflamed compared to the other three groups. However, we did not observe colon shortening, which is a major hallmark in DSS-induced colitis models. Since we have observed macroscopic signs of colitis, we then investigated histological markers. For histological analysis, we sacrificed *FoxO3a*$^{-/-}$*Il10*$^{-/-}$ mice upon reaching the terminal stage of

illness. Blinded microscopic examination of the H&E-stained colon and small intestine sections by Dr. Sergey Pyatibrat revealed a patchy pattern of inflammation in *FoxO3a*$^{-/-}$*Il10*$^{-/-}$ mice that was reminiscent of CrD in humans. The histological changes were clearly characterized by reduced production of mucin, loss of crypts, crypt abscesses, granulomas, surface epithelial regeneration, epithelial hyperplasia, as well as moderate to severe infiltration of inflammatory cells to the LP and submucosa. The changes we observed in the intestines of *FoxO3a*$^{-/-}$*Il10*$^{-/-}$ mice represent typical histological changes in IBD mice models translatable to features that are characteristic of human IBD (Chassaing et al, 2014). The increase in mononuclear cell infiltration is accompanied by crypt architecture disarray and a substantial gap increase between the base of the crypts and muscularis mucosa (Chassaing et al, 2014). More importantly, granulomas and crypt abscesses are present in CrD only.

Seeing the major disruption in the epithelial barrier of the colons of *FoxO3a*$^{-/-}$*Il10*$^{-/-}$ mice, we sought to evaluate whether there was an increase in the crypt proliferative compartment. Intestinal inflammation seems to be invariably associated with increased epithelial proliferation, presumably in an effort to get rid of damaged/infected epithelial cells or to rapidly replace cells, which have been lost. It is noteworthy to keep in mind that the intestinal epithelial barrier varies anatomically and functionally between the small and the large intestines. Within the small intestine, epithelial structures form finger-like structures, called villi, which project into the intestinal lumen. Unlike the small intestine, the colon exhibits a smooth surface pocketed with crypts. Stem cells near the base of the intestinal crypts divide and differentiate into various cell types including goblet cells, enterocytes, enteroendocrine cells, and Paneth cells, the latter of which are unique to the small intestine, ultimately displacing the existing cells lining the epithelial monolayer (Gehart & Clevers, 2019). Essentially, epithelial cell proliferation can serve to repair and reseal large areas of damage to the barrier, and its regenerative ability has been shown to be influenced by peptides and growth factors (Laukoetter et al., 2008). Such damage to the intestinal epithelial barrier is followed by the crossing of luminal antigens and microbes into the mucosa (Bauer et al, 2010). Despite the disruption we observed in the intestinal epithelial barrier, the Ki67 staining in the colons of *FoxO3a*$^{-/-}$*Il10*$^{-/-}$ mice indicated increased proliferation of stem cells and enterocytes as they move away from the crypts. Ki67 staining was also detected in inflammatory cells infiltrating the LP of *FoxO3a*$^{-/-}$*Il10*$^{-/-}$ mice. The increased proliferation of the gut epithelium of *FoxO3a*$^{-/-}$*Il10*$^{-/-}$

mice may be the result of a compensatory mechanism in order to resist a complete breach in the barrier integrity.

5. Loss of FoxO3a perturbs myeloid and lymphoid lineages in IL-10-deficient mice

FoxO3a-deficient mice have been shown to display both lymphoproliferation (Lin et al., 2004) and myeloproliferation (Yalcin et al., 2010). Long-term FoxO deficiency (*FoxO1/3/4 triple conditional knockout)* resulted in the development of a nonfatal myeloproliferative phenotype characterized by increasing numbers of maturing myeloid elements in the spleen, with progressive involvement of the bone marrow, liver, and lungs. Complete rather than partial excision of all three FoxO alleles potentiated the disease (Tothova et al., 2007). Moreover, the mice exhibited aberrant differentiation in the lymphoid compartment. There was a significant reduction in the numbers of mature, pre- and pro- B cells along with an increase in the number of $CD3^+CD4^+$ T cells and a mild block in the T cell transition from DN1 to DN2 (Tothova et al., 2007). In fact, FoxO1 and FoxO3a have been shown to cooperatively regulate T cell homeostasis, since their deletion resulted in the significant expansion of $CD4^+$ T cells in the spleens and mesenteric lymph nodes of mice (Ouyang et al., 2010).

In accordance with the previous studies, our results show that FoxO3a controls the myeloid cell numbers in the spleens of naïve mice, as FoxO3a deficiency led to increased numbers of monocytes, neutrophils, and macrophages. Despite the high numbers in the spleen, there were no differences in the bone marrow and lamina propria myeloid cell counts in the absence of FoxO3a alone. While we did observe a mild increase in the numbers of immune cells in FoxO3a-deficient mice, this was far less in comparison to the situation in the *FoxO3a*$^{-/-}$*Il10*$^{-/-}$ mice. In the spleens of *FoxO3a*$^{-/-}$*Il10*$^{-/-}$ mice, we observed an expansion of the white pulp and increased extramedullary hematopoiesis (revealed by elevation in the numbers of megakaryocytes). We also observed a remarkable expansion of the myeloid cell compartment, especially macrophages, neutrophils, and monocytes.

Given the aggressive gut phenotype that we observed in the *FoxO3a*$^{-/-}$*Il10*$^{-/-}$ mice, we evaluated whether this correlated with increased numbers of various immune cell subsets in the colonic LP. The results showed an expansion in the numbers of innate myeloid cells (neutrophils, monocytes, and dendritic cells) as well as the adaptive lymphoid $CD4^+$ and $CD8^+$ T- cells in the colonic LP of *FoxO3a*$^{-/-}$*Il10*$^{-/-}$ mice.

Interestingly, we did not observe an increase in the neutrophilic population in the bone marrow of *FoxO3a*$^{-/-}$*Il10*$^{-/-}$ mice. This may be explained by their enhanced migration to the site of inflammation. The expansion of Ly6C^{int} and Ly6C^{hi} monocytic populations was also observed in the bone marrow of naive *FoxO3a*$^{-/-}$*Il10*$^{-/-}$ mice. In fact, Ly6C^{hi} monocytes in the blood account for 90% of the monocytes produced by the bone marrow. Receiving signals from the bone marrow microenvironment, Ly6C^{hi} monocytes activate a gene-expression program that equips them with the ability to migrate into tissues in response to homeostatic cues or danger signals. They act to homeostatically replenish the tissue macrophages and dendritic cells in any condition of infectious or sterile tissue injury and therein exert specific inflammatory functions (Ginhoux and Jung, 2014). For instance, macrophages in the intestines experience a high turnover rate, and in the presence of intestinal inflammation in *FoxO3a*$^{-/-}$*Il10*$^{-/-}$ mice, this may necessitate their accelerated supply through the increased production of "classical" inflammatory monocytes. Monocytes then activate a distinct transcriptional program resulting in the loss of Ly6C and enabling the cells to remain in the blood to exert endothelial patrolling activities and coordinate its repair by recruiting neutrophils as required (Auffrey et al., 2007; Carlin et al., 2013). Monocytes characterized by intermediate levels of Ly6C showed a high degree of heterogeneity including a vast number of intermediates caught at different stages of the transition.

As for the increase in T cell numbers, it is unlikely that it is attributed to defective FoxO1 expression, since we did not observe significant modulation in *FoxO1* mRNA levels in activated T cells *in vitro*. Unlike in the LP, the proportion of T cells was not modulated in the spleens of *FoxO3a*$^{-/-}$*Il10*$^{-/-}$ mice. However, the proportion of CD62L^{low} T cells among CD4^{+} and CD8^{+} T cells was highly upregulated.

While there were no differences in the numbers of T cells and NK cells, the number of B220^{+} cells was reduced in the bone marrow of both *FoxO3a*$^{-/-}$ and *FoxO3a*$^{-/-}$*Il10*$^{-/-}$ mice. The percentages of B220^{+} cells were comparable across the four groups of mice in the spleens and colonic LP. CD45R/B220 is a pan-B-lineage marker in mice, although it is not B-lineage specific. It is also expressed on non-B lineage cells, such as plasmacytoid DCs, minority of CD4^{+} T cells and NK cells (Nikolic et al., 2002). B220 is already present on the earliest identified pro-B cells, and its expression is continued in pre-B, immature B and mature B cells, and is only downregulated at the late plasma cell stage (Nikolic et al., 2002). It was previously reported that FoxO3a uniquely

regulates pre-B cell numbers while being dispensable for the normal sub-population distribution of splenic B cells (Hinman et al., 2009). FoxO3a may act in the bone marrow microenvironment to support the development or survival of pre-B cells. There was also a slight but not significant reduction in the numbers of pro-B cells (Hinman et al., 2009). FoxO3a deficiency also intrinsically resulted in a decreased frequency of recirculating B cells in the bone marrow and blood perhaps due to lower-than-normal expression of the receptor for sphingosine-1 phosphate, which mediates S1P-induced egress of B and T cells from lymphoid organs into the circulation (Hinman et al., 2009). Various studies have also pinpointed the important role of B cells in immunoregulation and protection from the development of intestinal inflammation (Gonnella et al., 2001; Mizoguchi et al., 2002). In fact, depletion of IL-10-producing "Bregs" has also been associated with exacerbation of intestinal inflammation regardless of the presence or absence of Tregs (Oka et al., 2014). Considering the heterogeneity of the $B220^{+}$ population and to undoubtedly explain the differences we see in B cell frequencies in the various organs of mice, we will need to perform further investigations using a combination of more lineage-restrictive markers (e.g., CD19, Cd1, CD22).

Based on these findings, it is conceivable that alterations in the numbers and inappropriate activation of innate immune cells and effector T cells contribute to a dysregulated mucosal immune response in *FoxO3a*$^{-/-}$*Il10*$^{-/-}$ mice. It is important to note that poor cell death of the various cell subsets may partly explain the increased immune cell numbers in these mice.

To determine which cellular compartment was contributing to the perpetuation of colitis, we performed antibody-mediated depletion experiments to exhaust the innate (monocyte/neutrophil) or adaptive ($CD4^{+}$/$CD8^{+}$ T cell) immune cell subsets in *FoxO3a*$^{-/-}$*Il10*$^{-/-}$ mice. Overall, we show that intestinal inflammation is immune-related, and the depletion of T cells has a more profound effect on the survival of mice compared to myeloid cell depletions. One shortcoming that may explain this difference is the short half-life of neutrophils that leads to their accelerated generation. We can also speculate the interference of DCs in promoting the inflammatory response in these mice, since myeloid cell depletions targeted only monocytes and neutrophils. In addition, despite not observing differences in NK cell numbers, we cannot rule out the possibility that intestinal mucosal NK cells may have altered activation and cytotoxic "disease-promoting" activities.

6. FoxO3a and IL-10 deficiencies promote the dominance of myeloid DCs

On the subject of the possible contribution of DCs to the propagation of intestinal inflammation, we were interested in evaluating the impact of FoxO3a and IL-10 deficiencies on the development of DC subtypes in our murine model of IBD.

Since studies have underscored the cardinal role of DCs in modulating the intestinal inflammation, it is therefore important to revisit the unique functional attributes of DCs as cells that are poised to maintain gut homeostasis and tolerance. DCs that associate with the barrier mediate immunosurveillance, sample luminal antigens and then deliver them to cells of the mucosal immune system (Laukoetter et al, 2008). DCs are present in the GALT, PPs and the LP of the intestines and lie in close proximity to the large and dynamic antigenic load in the gut lumen. DCs are considered as the most potent APCs due to their unique ability to stimulate resting naïve T cells efficiently (Hart, 1997). DCs can also control microbial-driven T cell polarization in part through the ligation of TLRs (Kaisho et al., 2003). The unique attribute of DCs lies in their ability to induce tolerance while responding to antigens in the gut (Viney et al., 1998; Williamson et al., 1999). To elaborate, DCs in murine PPs secrete more IL-10 compared to the ones residing in the spleen (Iwasaki & Kelsall, 1999). Due to their association with the external environment, an altered response to the microflora by DCs may lead to the development of an inflammatory response in CD. To corroborate, DCs from inflamed tissues of CrD patients expressed significantly higher levels of the maturation/activation marker CD40 and secreted more IL-12 and IL-6 (Hart et al., 2005). In IBD, DCs become hyperactivated through regulating their expression of PRRs, like TLR2 and TLR4, as well as their secretion of pathologically relevant cytokines. Hence, they participate in initiating or perpetuating the inflammatory response in the gut (Hart et al., 2005). In fact, DCs can be "educated" to preserve the gut homeostasis by mounting a non-inflammatory response through polarizing a Th2 response. Because DCs are near the intestinal epithelial cells (IECs), a reduction in the expression of IEC-derived mediators, such as thymic stromal lymphopoietin (TSLP), can impair their ability to mediate tolerance and polarize a Th1 response instead (Rimoldi et al., 2005).

By flow cytometry analysis, we demonstrated the predominance of $CD11b^{+}$ $SIRP\alpha^{+}$ cDC2 cells in the colonic LP of *FoxO3a*$^{-/-}$*Il10*$^{-/-}$ mice. We have also confirmed their pro-Th17 phenotype in

vitro, as *FoxO3a*$^{-/-}$*Il10*$^{-/-}$ DCs promoted increased IL-17A production by activated WT CD4^{+} T cells.

Our results are congruent with several studies that have elucidated the function of DC subsets isolated from the LP and MLNs using various combinations of markers. Studies showed that CD103^{+} DCs are tolerogenic and induce the generation of FoxP3^{+} Tregs in a TGF-β- and retinoic acid-dependent mechanism (Coombes and Powrie, 2008; Annacker et al., 2005). While we did not evaluate the expression of CD103 in DCs, it is plausible to hypothesize that a defect in their tolerogenic activity might contribute to the reduction in the percentages of FoxP3-expressing Tregs in the LP of *FoxO3a*$^{-/-}$*Il10*$^{-/-}$ mice. Denning *et al.* (2007) described a pro-inflammatory phenotype of CD11c^{hi} CX3CR1^{+} CD11b^{+} CD103^{-} LP DCs that promoted Th17 differentiation of naïve T cells at steady-state. In fact, it has been demonstrated that Th17-inducing DCs express high levels of Signal regulatory protein α (SIRPα). SIRPα or CD172 is an Ig superfamily protein that is highly expressed in macrophages, neutrophils and conventional DCs particularly cDC2. SIRPα comprises three extracellular Ig-like domains and an immunoreceptor tyrosine-based inhibition motif (ITIM) that binds the protein tyrosine phosphatases SHP1 and SHP2 in its intracellular region. Since SIRPα has been considered as a positive marker of the Th17-inducing DC subset, deficiency in SIRPα signaling led to a selective reduction in the CD11b^{+} subset of DCs together with a decrease in the generation of intestinal Th17 cells (Fortin et al., 2009; Saito et al., 2010; Scott et al., 2014; Washio et al., 2015). LP cDC2s were shown to display a pro-inflammatory mature-like gene signature along with an enhanced ability to migrate to lymph nodes (Fortin et al., 2009; Rivera et al., 2021). Moreover, the role of SIRPα signaling in DCs has been implicated in the generation of intestinal inflammation, such that *Il10*$^{-/-}$ mice backcrossed with *SIRPα*$^{-/-}$ mice were protected from spontaneous colitis (Kanazawa et al., 2010).

It remains unclear whether the deficiencies in FoxO3a and IL-10 drive the development of cDC2 cells at steady state or whether their dominance in the gut is a function of their exposure to inflammatory mediators in the intestines. In particular, the increasingly infiltrating monocytes in the inflamed intestines may be actively differentiating into CD103^{-}CD11b^{+} DCs. More in-depth insights into the intestinal DC subpopulations are required, especially in terms of uncovering the genetic programs impacted by FoxO3a and IL-10 deficiencies driving cDC2 development.

Whether DCs contribute to the initiation or progression of disease in our murine model of IBD also requires further investigation.

7. FoxO3a regulates the HSPC compartment and restricts myelopoiesis

To reiterate, poor cell death may account in part for the observed increase in the numbers of various immune cell subsets. More than this, this increase can also stem from their enhanced replenishment from precursors ultimately derived from the HSCs in the bone-marrow of adults during hematopoietic stress. It was therefore necessary to evaluate the impact of FoxO3a and IL-10 deficiencies on the differentiation of HSCs to the hematopoietic lineages.

Notably, FoxO proteins are among the very few transcription factors that are essential for the maintenance of pluripotency/multipotency in several types of stem cells including adult hematopoietic and neural, and embryonic pluripotent stem cells (Tothova et al., 2007; Miyamoto et al., 2007; Yalcin et al., 2008; Paik et al., 2009; Zhang et al., 2011; Renault et al., 2009).

In fact, FoxO transcription factors play a critical role in preserving hematopoietic homeostasis by regulating the HSC compartment and maintaining its self-renewal capacity. FoxOs cooperate to affect quiescence of HSCs by regulation of the cell cycle, inhibition of apoptosis, and mediation of resistance to physiologic oxidative stress (Tothova et al., 2007). It is of interest to associate the effects of *FoxO* deficiency in the HSC compartment with other contexts. For example, *FoxO3a* deficiency results in oocyte exhaustion and infertility due to global activation of the primordial ovarian follicle (Castrillon et al., 2003). FoxO proteins may play an important role in the maintenance and integrity of stem cell compartments in a broad spectrum of tissues.

HSCs are normally dormant but can undergo a swift metabolic switch from glycolysis to oxidative phosphorylation based on the demand to reconstitute the blood. Low levels of ROS are required to sustain HSC dormancy. Dormant HSCs are acutely sensitive to oxidative stress, and they contain relatively few and inactive mitochondria (Simsek et al., 2010; Norddahl et al., 2011).

The role of FoxO3a has been implicated specifically in the maintenance and quiescence of the HSC pool and in regulating their metabolic adaptation independent of ROS levels (Miyamoto et al., 2007; Yalcin et al., 2008; Bigarella et al., 2017; Rimmele et al., 2015). *FoxO3a*$^{-/-}$ HSCs and progenitor cells (HSPCs) were shown to accumulate defective mitochondria and high levels of ROS that cause oxidative DNA damage at the steady state. FoxO3a deficiency caused inefficiency

in key pathways implicated in the oxidative DNA damage repair, such as the Base Excision Repair (BER) and the Nucleotide Excision Repair (NER) pathways. This led to cell cycling impairment observed with the delay at the G2/M cell cycle checkpoint (Bigarella et al., 2017). It was also shown that *FoxO3a*$^{-/-}$ LSK cells might exhibit some resistance to oxidative stress-mediated apoptosis (Bigarella et al., 2017). The study by Tolotho et al. (2007) delineated how the deficiency in all three FoxO proteins, FoxO1, FoxO3 and FoxO4, profoundly impacted the HSC compartment without affecting the numbers or cell cycling capacity of myeloid progenitors. The triple genetic deletion reduced HSC numbers by jeopardizing their capacity to self-renew and impaired their long-term repopulating activity in competitive transplantation assays.

Loss of quiescence in *FoxO3a*$^{-/-}$ HSCs was associated with increased glycolysis and significant reduction of oxidative phosphorylation along with abnormalities in mitochondrial functions (Rimmele et al., 2015). As an interplay between mTORC1 and FoxO3a is implicated in the myeloid progenitor homeostasis, FoxO3a might inhibit mTOR signaling in primitive HSPCs. Interestingly, loss of FoxO3a increased the fraction of HSPCs expressing the phosphorylated form of the mTORC1 downstream target S6K (Yalcin et al., 2010; Zhang et al., 2014; Zoncu et al., 2011). Another study showed that in 8-12 weeks old mice, similar frequencies of LSK cells were present in the bone marrow of *FoxO3a*$^{+/+}$ and *FoxO3a* $^{-/-}$ mice, and no difference in the proliferation and differentiation was observed (Miyamoto et al., 2007). The frequencies however were reduced in aged mice (Miyamoto et al., 2007). The role of FoxO3a was also implicated in maintaining the repopulating capacity of HSCs in the long-term (Miyamoto et al., 2007; Rimmele et al., 2015).

In agreement with the previous findings, we did not detect a difference in the proportion of LSK cells in our *FoxO3a*$^{-/-}$ mice compared to the proportions in WT and *Il10*$^{-/-}$ mice. It is possible that this may change if the mice are aged. We observed a significant upregulation in the numbers of LSK cells only in the bone marrow of *FoxO3a*$^{-/-}$ *Il10*$^{-/-}$ mice. Our results provide evidence that HSC activity is dramatically modified during intestinal inflammation.

IBD is accompanied by extensive myelopoiesis and infiltration of myeloid cells into the colonic LP. Since neutrophils are among the first cells to infiltrate the gut mucosa, myelopoietic processes in the bone marrow were of particular interest. There was substantial skewing of HSC differentiation towards the myeloid GMP subset in the bone marrow and spleens of *FoxO3a*$^{-/-}$ *Il10*$^{-/-}$ mice indicating the profound effect of FoxO3a and IL-10 deficiencies on hematopoietic

homeostasis during the disease progression. Cells of the monocytic and granulocytic lineages increased significantly in the bone marrow and spleens of *FoxO3a*$^{-/-}$ *Il10*$^{-/-}$ mice with colitis, and this could promote or sustain inflammation and tissue damage in the gut. Multipotent progenitors (MPPs) differentiate to CMPs to a greater extent than to CLPs (Busch et al., 2015), which explains why the overall proportions of CLPs are relatively inappreciable in all the groups. Yet, we still do not see any significant differences in the IL-7R^{+} lymphoid progenitors.

A study by Yalcin et al. (2010) showed that FoxO3a-deficient mice (generated on on a different background (FVB/n)) exhibit an enlarged spleen, increased number of splenocytes and extramedullary hematopoiesis, which complement our observations. They also report the expansion of myeloid GMP colonies in the bone marrow, spleen, and peripheral blood of FoxO3a-deficient mice. Since we did not detect increased LSK or GMP numbers in the bone marrow of our *FoxO3a*$^{-/-}$ mice, we therefore suspect that possible causes for the increase in myeloid cell numbers in the spleens of *FoxO3a*$^{-/-}$ mice may comprise increased proliferation, reduced cell death, increased egress from bone marrow to the spleen, or enhanced extramedullary hematopoiesis.

8. FoxO3a prevents a hyperinflammatory response in the gut of IL-10-deficient mice

The transcriptome analysis revealed an elevation in the transcriptional expression of various inflammatory cytokines and chemokines in the colons but not in the spleens of *FoxO3a*$^{-/-}$*Il10*$^{-/-}$ mice compared to the other groups. Sample heterogeneity should be taken into consideration here. Since we are measuring gene expression levels within the heterogeneous colon and spleen tissues, cell type-specific signals may be cancelled out or differences in gene expression may be caused by variations in sample cell composition. Because we have previously shown the increased abundance of myeloid and lymphoid cells in the colonic LP of *FoxO3a*$^{-/-}$*Il10*$^{-/-}$ mice, it is fair to assume that the enhanced expression of pro-inflammatory mediators may be derived from the activated inflammatory immune cells. Yet, it remains elusive whether epithelial cells contribute to the production of the pro-inflammatory cytokines and chemokines and in turn regulate immune cell trafficking to the inflamed colon.

Despite the increased abundance of myeloid immune cells, the pattern of cytokine and chemokine expression was not observed in the spleens of the naïve *FoxO3a*$^{-/-}$*Il10*$^{-/-}$ mice. This may be explained by the fact that inflammatory cues need to be present to direct the activation of immune cells and subsequent production of pro-inflammatory mediators. In fact, along with the liver, lung

and peritoneum, the spleen is part of the reticuloendothelial system, which constitutes the next line of defense in case of microbial penetration through the initial epithelial and phagocytic barriers. The splenic red pulp has been shown to be efficient at removing debris and particulate matter in the blood, and the white pulp contains immune cells involved in antibody production, antigen presentation, and T cell activation. Large amounts of cytokines are produced by the phagocytic myeloid cells residing in the reticuloendothelial system upon bacterial sequestration. In the context of sepsis, peak TNF-α mRNA expression occurs around 3 h after septic surgery or LPS injection in mice, and the tissue TNF-α protein expression is easily detected within 90 min (Hadjiminas et al., 1994). In accordance with this, the lack of a massive systemic upregulation in the expression of the inflammatory mediators highlights the absence of the penetration of luminal content across the epithelial barrier of *FoxO3a*$^{-/-}$*Il10*$^{-/-}$ mice.

Transcripts encoding several CXC and CCL chemokines were increased in the colons of *FoxO3a*$^{-/-}$*Il10*$^{-/-}$ mice. The production of powerful neutrophil chemo-attractants, such as CXCL1 and CXCL5, indicates that neutrophil accumulation in the LP is an important aspect of this pathology, as it is generally thought to contribute to the promotion of intestinal inflammation.

Among the cytokines highly expressed in the colons of naïve *FoxO3a*$^{-/-}$*Il10*$^{-/-}$ mice are members of the TNF superfamily, IL-1β, IL-6, and IFN-γ.

Under physiological conditions, TNF-α activates effector cells generally leading to a pro-inflammatory response or apoptosis. This aids in the defense against infections and localized tissue injury. Elevated TNF-α levels have been detected in the mucosa and LP of IBD patients, and this was correlated with aberrant pro-inflammatory responses leading to dysregulation of mucosal immune cells and subsequent tissue damage (Atreya et al., 2011; MacDonald et al., 1990). In fact, TNF-α drives intestinal inflammation and has been reported to play an important role in the development and progression of the disease (Braegger et al., 1992). Its excessive production alters epithelial integrity and induces apoptotic death in IECs (Garrett et al., 2007; Pott et al., 2018). As a result, TNF-α neutralization has been an extensively explored therapeutic strategy in IBD. As a matter of fact, several anti-TNF antibodies have proven their efficacy in IBD, and one of the mechanisms through which this happens is based on indirect induction of apoptosis in mucosal $CD4^+$ T cells co-cultured with $CD14^+$ macrophages. Resistance to apoptosis in mucosal T cells is

alleviated indirectly by targeting the mTNF/TNFR2 pathway, thus abrogating NF-kB activation and IL-6 production that promotes survival (Atreya et al., 2011).

The pro-inflammatory nature of IL-6 has been implicated in the pathogenesis of IBD. In fact, it has been reproducibly shown that serum and intestinal IL-6 levels were substantially elevated in IBD patients, and that correlated with inflammatory activity (Holub et al., 1998; Hyams et al., 1993; Gross et al., 1992; Mahida et al., 1991; Reinisch et al., 1999). To elaborate, the role of a downstream IL-6 signaling pathway is demonstrated by evidence for augmented activation of IL-6-dependent STAT3 signaling in $CD4^+$ T cells in both CrD and UC. STAT3 signaling results in increased T- cell resistance to apoptosis through induction of the anti-apoptotic genes *Bcl-2* and *Bcl-xl* (Atreya et al., 2000; Boirivant et al., 1999; Ina et al., 1999). Hence, persistent T cell expansion can aggravate the chronicity of the inflammatory process in the gut. Upon challenge with inflammatory cytokines, IL-6 is produced by intestinal cells and in turn acts on mesenchymal and epithelial cells to recruit PMNs and macrophages for wound healing. At the same time, IL-6 promotes the survival of activated T cells. The blockade of IL-6 signaling prevents T cell expansion and attenuates Th1-cell-driven intestinal inflammation (Atreya et al., 2000; Yamamoto et al., 2000).

In IBD, the significant up-regulation of IL-1β expression is mainly attributed to the local mononuclear infiltration that exacerbates the severity of mucosal inflammation (Mahida et al., 1989). In fact, increased production of IL-1β and TNF-α in CD-associated inflamed mucosa induces the synthesis of the neutrophil chemoattractant IL-8 (Andus et al., 1993). One study showed that an increase in IL-1β induced chronic intestinal inflammation in mice and an increase in IL-17A-secreting innate lymphoid cells which express high levels of IL-1R1 (Coccia et al., 2012).

The pro-inflammatory nature of IFN-γ has been documented by an overwhelming body of literature. IFN-γ has been considered as a signature pro-inflammatory cytokine that mediates the pathogenesis of various chronic inflammatory and autoimmune diseases (i.e., EAE, CIA, IBD). In fact, it is one of the most highly upregulated cytokines in IBD (Neurath, 2014; Verma et al., 2013; Ito et al., 2006). In a DSS-induced model of murine colitis, a robust IFN-γ production was observed in the gut (Nava et al., 2010; Haep et al., 2015). More to the point, *IFN-γ*$^{-/-}$ mice showed decreased DSS-induced inflammation, indicating an important role of this cytokine in the pathogenesis of

gut inflammation. Paradoxically, although highly counterintuitive, IFN-γ was also shown to exert immunoregulatory effects. For instance, it was unexpectedly discovered that IFN-γ was required for the expression of FoxP3 and the peripheral conversion of $CD4^+$ Tregs in a murine model of EAE (Wang et al., 2006). Moreover, IFN-γ appears to induce the overexpression of negative costimulatory molecules (i.e., PD-1) in synovial inflammatory T cells and antagonize the function of IL-17 (Harrington et al., 2005; Sawitzki et al., 2005; Wan et al., 2006).

The production of the pro-inflammatory cytokines has also been detected at high levels in *vitro* upon stimulation of myeloid cells and T cells. In addition, the high IL-17A and IL-6 serum levels in *FoxO3a*$^{-/-}$*Il10*$^{-/-}$ mice emphasize the existence of a pro-inflammatory milieu in the intestines housing activated immune cells.

With the administration of specific antibodies targeting cytokines/receptors, such as TNF-α, IL-1β, and IL-6, anti-cytokine-based therapies have found a place in the treatment of autoimmune and inflammatory diseases "canonizing" their causative role in inflammation. Neutralization of cytokines has also shown major improvement in the treatment of various diseases compared to the metabolic consequences of long-term glucocorticoids (Dinarello, 2010). Nevertheless, immunogenicity against the antibodies, parenteral administration, and development of immunosuppression predisposing patients to opportunistic infections remain major drawbacks of anti-cytokine therapy (Fiorino et al., 2012).

To decipher which signaling pathways are responsible for the up regulation in pro-inflammatory cytokine expression, we evaluated the expression of several key proteins by western blotting. We observed increased activation of $p38^{MAPK}$/MK2 and STAT3 signaling, which may correlate with increased production of inflammatory cytokines. Transient activation of STAT3 is seen in healthy immune cells, but constitutive activation is associated with immune- activation in IBD patients and development of Th17 phenotype (Carey et al., 2008; Chaudhry et al., 2009). $p38^{MAPK}$, through MK2, can also upregulate the expression of some genes participating in intestinal inflammation, such as genes coding for TNF-α, IL-1, IL-6, and IL-8. TNF-α and IL-1 can in turn activate $p38^{MAPK}$, forming a vicious cycle in the perpetuation of an inflammatory response (Saklatvala et al., 2003; Winston et al., 1997). Both STAT3 and p38α were shown to phosphorylate FoxO3a and promote its nuclear localization (Ho et al., 2012; Oh et al., 2012). In turn, it appears that FoxO3a

restrains the activation of these signaling mediators, which is exacerbated in the absence of IL-10.

9. FoxO3a and IL-10 regulate cellular bioenergetics and mTOR signaling

Based on the flaming cytokine production by *FoxO3a*$^{-/-}$*Il10*$^{-/-}$ cells, we hypothesized that the activated immune cells undergo a profound reprogramming of their cellular metabolism, a key event in the inflammatory response.

Previous studies have demonstrated the role of IL-10 in controlling essential metabolic pathways, especially mTOR signaling (Ip et al., 2017). It was shown that IL-10 inhibits LPS-induced glucose uptake and glycolysis and promotes oxidative phosphorylation in BMDMs. IL-10 also promoted the induction of mitophagy to maintain mitochondrial fitness in a STAT3-DDIT4 dependent manner that inhibited mTORC1 signaling (Ip et al., 2017). Ip et al. observed sustained mTORC1 signaling and consequently impaired autophagy in *Il10*$^{-/-}$ macrophages, which was rescued with the addition of exogenous IL-10.

Alterations in mitochondrial functions were also observed based on FoxO3a activation status. Several studies have demonstrated the role of FoxO3a in regulating mitochondrial gene expression. One study showed that inducing FoxO3a activation in a non-malignant immortalized epithelial cell line resulted in a substantial downregulation of mitochondrial genes (e.g., *Tomm20*, a mitochondrial transporter, and *cytochrome c oxidase 1* (*COX1*), a mitochondria-encoded gene). This downregulation was mediated through c-MYC inhibition and was accompanied by a reduction in mtDNA copy number and lowered levels of respiratory complexes (Ferber et al., 2011). Another study showed that knockdown of *FoxOs* (1,3,4) alleviated energy stress-induced mTORC1 repression in both the murine and human systems. Knockdown of *FoxO1* or *FoxO3* was sufficient to alleviate mTORC1 inactivation under energy stress, but knockdown of both *FoxO1* and *FoxO3* had a more potent effect (Lin et al., 2013). FoxO3a-deficiency might promote a higher basal metabolism in cells, which could be a consequence of increased basal mTOR activity in FoxO3a-deficient cells (Yalcin et al., 2010).

Considering the firmly established independent roles of FoxO3a and IL-10 in hampering the over-activation of mTORC1 signaling, we sought to explore the impact of their simultaneous absence on the oxidative and glycolytic metabolic activities in spleen cells. We found that FoxO3a

deficiency was the main driver in boosting the metabolic activity of cells as shown through the enhanced basal respiration and glycolytic rate, especially in the absence of LPS stimulation. We then probed the metabolic flexibility of the splenocytes through the combined analyses of OCRs and ECARs. Our results clearly demonstrated enhanced metabolic activity in *FoxO3a*$^{-/-}$*Il10*$^{-/-}$ cells that was translated in the overall increased protein synthesis measured by BCA assay as well as by OP-Puro incorporation. Notably, the augmented translational rate was reflected by the OP-Puro incorporation in *FoxO3a*$^{-/-}$*Il10*$^{-/-}$ myeloid cells (neutrophils and monocytes) compared to the other groups. Of note, it appears that the increase in protein synthesis is restricted to the myeloid lineage as evidenced by the modest increase in OP-Puro uptake by *FoxO3a*$^{-/-}$ and *FoxO3a*$^{-/-}$*Il10*$^{-/-}$ GMPs. Protein synthesis is regulated by mTORC1 signaling, which also regulates ribosome biogenesis, lipid synthesis, mitochondrial metabolism, and nutrient uptake (Mayer et al. 2004; Porstmann et al. 2009; Cunningham et al. 2007; Shimobayashi and Hall 2014). In agreement with the enhanced protein synthesis, spleen cells and myeloid (CD11b^{+}) cells demonstrated increased phosphorylation of mTORC1 downstream targets, including P70S6K and 4E-BP1, which are major regulators of protein synthesis.

Rapamycin treatment in *vivo* reverted the phenotype suggesting that the impact of FoxO3a and IL-10 deficiencies on mTORC1 signaling is a major contributing factor. Inhibiting mTORC1 signaling could dampen the hypermetabolic activity of immune cells and hence suppress their cytokine production. It is observed that mTOR inhibition extends the life span and delays the onset of age-associated diseases in mammals. Specifically, mTORC1 inhibition can promote autophagy to clear damaged proteins and organelles, and it also boosts the self-renewal capacity of both hematopoietic and intestinal stem cells in mice (Chen et al., 2009; Yilmaz et al., 2012).

We should also bear in mind that the basis for the rapamycin effect could also be due to off-target effects or differential effects on the mTORC1 versus mTORC2 complexes that influence AKT activity (Sarbassov et al., 2006). Prolonged rapamycin treatment can abrogate mTORC2 signaling most likely due to the inability of rapamycin-bound mTOR to incorporate into new mTORC2 complexes (Lamming et al., 2012). The major drawback of prolonged rapamycin treatment, however, is the potential for side effects such as immunosuppression and glucose intolerance.

Knowing that mitochondrial glutathione redox balance is important to support the exceptionally high rates of oxidative reactions while minimizing oxidative stress, we examined the effects of

mouse in *vivo* supplementation of the glutathione precursor, NAC. Due to the fact that FoxO3a transcriptionally induces the antioxidant response and that *FoxO3*$^{+/-}$*Il10*$^{-/-}$ mice exhibited increase ROS production, we hypothesized that NAC would increase glutathione redox and thereby mitigate, at least in part, the disease progression in *FoxO3a*$^{-/-}$*Il10*$^{-/-}$ mice. Results showed that NAC treatment did not improve their survival. It is therefore conceivable that the supplementation with NAC is not sufficient to deplete the ROS levels or the intestinal inflammation in these mice is related to ROS-independent mechanisms.

10. FoxO3a regulates glutamine metabolism in IL-10-deficient T cells

Metabolic reprogramming is also imperative for appropriate T cell responses. To support the metabolic demands of cells during an immune response, the PI3K/Akt/mTORC1 signaling pathway is activated by signaling through the antigen-receptor signal and costimulatory molecules. In turn, the mTORC1 signaling pathway induces the metabolic flux through glycolysis and mitochondrial oxidative phosphorylation (Ho et al., 2015; Sena et al., 2013). Amino acids, such as glutamine, can be potent activators of mTOR signaling, and this is critical for T cell activation (Nakaya et al., 2014). Being the most abundant amino acid in the serum, glutamine is a readily available resource that is involved in numerous processes important for lymphocyte activation. While glutamine is adequately synthesized to meet metabolic needs, it can become conditionally essential during catabolic states. Systemic glutamine levels decline as glutamine utilization exceeds endogenous glutamine production. The process of glutaminolysis involves the conversion of glutamine to glutamate by the enzyme glutaminase that exists as two isozymes: kidney-type GLS and liver-type GLS2, which have been shown to play opposing roles in cancer (Xiang et al., 2019; Zhang et al., 2016).

T cell activation is a highly energetic event that requires a substantial increase in nutrient metabolism to promote the increase in cell size, rapid proliferation, and differentiation. It was previously reported that T cells have an absolute requirement for a large external supply of glutamine, and that even moderate reductions within the normal physiological range impair T cell function (Carr et al., 2010). Glutamine import outweighs that of glutamate and is CD28-dependent. Glutamine could not be substituted with other amino acids, including direct biosynthetic precursors, and depletion of glutamine blocks T cell proliferation and cytokine production. Indeed, besides glucose oxidation, T cell activation induces a large increase in glutamine import by

actively coordinating the up-regulation in the expression of glutamine transporters and activities of enzymes required to allow the use of glutamine as a Krebs cycle substrate in T cells (Carr et al., 2010).

To investigate the regulation of glutamine utilization by T cells in our murine model, we characterized the impact of removing/adding exogenous glutamine on T cell activation and cytokine production *in vitro*. Our findings indicated the absolute requirement of glutamine besides glucose in boosting cytokine production by activated *FoxO3a*$^{-/-}$*Il10*$^{-/-}$ CD4^{+} T cells. Additionally, glutamine inhibition, mediated by DON or GAH, completely suppressed the production of cytokines and normalized the metabolic activity of *FoxO3a*$^{-/-}$*Il10*$^{-/-}$ cells. It is important to note here that we are not dismissing the imperative role of glucose oxidation. In fact, T cells deficient for the glucose transporter Glut1 failed to proliferate well and produce cytokines (Macintyre et al., 2014). However, this prevented effector T cell responses while sparing Treg suppression. Indeed, the specification of T cells into various subsets is contingent upon their critical metabolic differences. For instance, glutamine deprivation or inactivation of the glutamine transporter ASCT2 did not impair T cell proliferation but impaired both Th1 and Th17 cell specification while promoting the expression of Treg marker FoxP3 (Nakaya et al., 2014). Inflammatory T cells such as Th17 cells have been shown to favor glutaminolysis through up regulating glutaminase expression (Johnson et al., 2018). These studies strengthen our proposition that FoxO3a and IL-10 are required to restrain the skewing of activated T cells towards a Th1/Th17-like phenotype, as observed with the enhanced IL-17A and IFN-γ production *in vitro*. Admittedly, excessive glutamine consumption seems to be driving this differentiation.

But how is FoxO3a or IL-10 altering glutamine metabolism in T cells?

To answer the question, we showed that FoxO3a suppressed glutaminolysis by repressing the transcriptional expression of glutaminase (*gls/gls2*) in activated T cells. Of note, *gls2* expression seems to be inducible, as it was only detected 48 h post-activation. There was also no impact on the expression of glutamine synthetase (*glul*), which converts glutamate back to glutamine. This suggests that the increase in the levels of glutamate that we observed in *FoxO3a*$^{-/-}$ and *FoxO3a*$^{-/-}$*Il10*$^{-/-}$ mice cannot be due to poor conversion to glutamine but most likely due to the excessive shuttling of glutamate out of the cells. We also demonstrated that both FoxO3a and IL-10 are critical for restraining the expression of various glutamine transporters. Glutamine

consumption was markedly increased in *FoxO3a*$^{-/-}$*Il10*$^{-/-}$ mice, such that their systemic glutamine levels were profoundly depleted. As a result, we speculate that activated T cells constitute a major source of glutamine utilization, such that depleting them or abrogating their activation via disrupting their interactions with myeloid APCs results in the restoration of glutamine levels. We should also entertain the possibility that glutamine consumption is increased in myeloid cells.

11. FoxO3a regulates Treg cell development in IL-10-deficient mice

Although we noticed a marked reduction in the percentage of FoxP3- expressing CD25^{+}CD4^{+} T cells in the absence of FoxO3a, the absolute cell numbers of Tregs were remarkably increased in the colons of *FoxO3a*$^{-/-}$ *Il10*$^{-/-}$ mice compared to the other groups. This is suggestive of a dysfunction through diminished suppressive capacity. This is ascertained by the compromised ability of Tregs to suppress T cell activation, only by concomitant deletion of FoxO3a and IL-10, as revealed by the enhanced cytokine expression.

We know that impairment in Tregs (whether in numbers or in suppressive function) contributes to the development of autoimmune or inflammatory diseases including colitis in both mice and humans (Mottet et al., 2003; Miyara et al., 2005; Pop et al., 2005). In a cutting-edge study, a single transfer of CD4^{+}CD25^{+} Tregs, and not CD4^{+}CD25^{-} cells, into colitic mice gradually improved their clinical status, survival rate and intestinal pathology. This is partly justified by the better homing tendencies of Tregs to colons and mesenteric lymph nodes along with their ability to remain in the vicinity of APCs and effector T- cells (Mottet et al., 2003).

FoxO1 and FoxO3 have been shown to cooperatively control the differentiation of Tregs, with FoxO1 playing a more dominant role (Kerdiles et al., 2010; Ouyang et al., 2010). Kerdiles et al. (2010) reported that the absence of FoxO1 in CD4^{+} T cells severely curtailed the development of thymic FoxP3^{+} Tregs, whereas FoxO1-deficient FoxP3^{+} Tregs expanded in the peripheral lymphoid organs but were non-functional *in vivo*. Ouyang et al. (2010) reported that the combined deletion of FoxO1 and FoxO3 in T cells resulted in the impaired suppressive function of peripheral FoxP3^{+} Tregs. In our experiments, the CD4^{+}CD25^{+} T cells in all the experimental groups expressed similar transcript levels of *FoxO1*, and this may indicate the possibility that there wasn't any compensatory modulation of FoxO1 expression in Tregs in the absence of FoxO3a or IL-10. Knowing that both FoxO1 and FoxO3 bind to the *FoxP3* promoter (Ouyang et al., 2010), the

modest reduction we saw in FoxP3 protein expression in FoxO3a-deficient T cells hints at the fact that FoxO1 is not fully compensating for the loss of FoxO3a.

The use of CD25 to define Tregs can be problematic because it is also expressed by activated effector T cells. FoxP3 was adopted as a better marker; nevertheless, $FoxP3^+$ Tregs are phenotypically and functionally heterogeneous. This prompted the search for specific markers crucial for delineating Treg functionality. Tregs express a panel of co-stimulatory/co-inhibitory molecules (CD28, CTLA-4, ICOS and PD-1 etc.).

Tregs are characterized by their expression for the fork-head transcription factor FoxP3, whose sustained expression is essential for their development and suppressive function (Gavin et al., 2007). Moreover, IL-10 production and signaling endow Tregs with the ability to suppress the pathogenic Th17 cells in a STAT3-dependent manner (Chaudhry et al., 2011). Activated STAT3 and FoxP3 co-operatively regulate a subset of genes that endow Tregs with their ability to suppress Th17 cell-driven colitis (Chaudhry et al., 2009). Innate immune cell production of IL-10 is required to maintain FoxP3 expression. However, loss of FoxP3 was not shown to be the sole explanation for the observed inability of IL-10R-deficient Treg cells to suppress intestinal inflammation (Chaudhry et al., 2011). Also, the inhibition of Th17 differentiation in *Il-6*$^{-/-}$ mice correlated with an increase in Treg numbers (Korn et al., 2007).

To depict the impact of FoxO3a and IL-10 on the suppressive function of Tregs, we evaluated the expression of various genetic markers pertaining to Treg function/development. We found a significant increase in the mRNA expression of *Il-1r1* and *Bcl-3* in *FoxO3a*$^{-/-}$*Il10*$^{-/-}$ $CD4^+$ $CD25^+$ T cells compared to the other groups. Only in the *FoxO3a*$^{-/-}$ *Il10*$^{-/-}$ colons, Tregs in the LP displayed an upregulation of IL-1R1, which has been previously reported to destabilize Tregs towards a Th17 phenotype (Alvarez et al., 2019). This was not detected in the splenic Tregs indicating the potential confinement of the inflammatory response to the gut. Under physiologic conditions, Th17 cells are found predominantly in the small and large intestines and the associated lymphoid tissues, where they facilitate the production of antimicrobial peptides, reinforce the integrity of the epithelial barrier, and recruit and activate granulocytes and macrophages to restrain pathogens (Weaver et al., 2007). Bcl-3 was also defined as a potential prognostic marker for colitis as its overexpression in mice was shown to alter NF-κB activity in Tregs causing an impairment in their function and leading to spontaneous development of severe intestinal inflammation (Reibig

et al., 2017). Additionally, massive infiltration of Bcl-3^{+} cells was observed in the LP of CrD and UC patients (Reibig et al., 2017).

Surprisingly, the mRNA expression of *Ctla-4*, a target of FoxP3, was also increased in *FoxO3a*$^{-/-}$*Il10*$^{-/-}$ CD4^{+} CD25^{+} T cells. CTLA-4 expression is induced within 24 hours and peaks within 2 to 3 days post-activation of naïve T cells. Although closely related to CD28, which acts as a positive co-stimulator, CTLA-4 antagonizes T cell activating signals and maintains peripheral T cell tolerance, thus reducing inflammation (Chambers et al., 2001). Its function is akin to putting the brake on the proliferative influence of TCR-CD28 interaction. Since FoxO1 also binds to the promoter of *ctla-4*, this strengthens our hypothesis that there is no FoxO1-mediated compensatory role in restoring Treg function in our murine model.

In addition, we did not observe changes in the protein expression of PD-1 in LP Tregs of the groups relative to WT. PD-1 is also defined as a negative costimulatory receptor that inhibits TCR-mediated T cell activation. Furthermore, ST2 mRNA and protein levels were reduced in *vitro* cultured *FoxO3a*$^{-/-}$*Il10*$^{-/-}$ CD4^{+} CD25^{+} T cells. As previously discussed, the IL-33/ST2 axis plays an important role in maintaining the stability and function of Tregs. In fact, the release of IL-33 promotes increased expression of ST2 by colonic Tregs, and this results in the amplification of ST2-signaling. ST2 deficiency impairs the ability of Tregs to adapt to the inflammatory tissue environment and restrain gut inflammation. IL-33 signaling is important to preserve the Treg function in *vivo* (Schiering et al., 2014). The cell surface expression of the IL-33R (ST2, IL1RL1) identifies a subset of functionally stable Helios^{+}FoxP3^{+} Tregs that are resistant to plasticity and loss of suppressive function. IL1R1 expression identifies RORγT^{+} Helios^{-} Tregs that acquire a Th17 cell phenotype and fail to suppress (Alvarez et al., 2019.). IL-1R1 deficiency favors Treg responses, which highlights the inhibitory role of IL-1 in the stability and function of Tregs (Alvarez et al., 2019).

Taken together, since FoxO3a and IL-10 deficiencies modulated the expression of various Treg markers, we speculated that the existence of a pro-inflammatory milieu, created by the inflammatory cytokines in *FoxO3a*$^{-/-}$*Il10*$^{-/-}$ mice, drive the plasticity of Tregs towards highly inflammatory T cells thus compromising their suppressive function.

12. FoxO3a and IL-10 regulate the crosstalk between T cells and APCs and maintain Treg suppressive function.

While FoxO3a was shown to induce the activation-induced cell death of T- cells in a cell intrinsic manner (Tzelepis et al., 2013; Riou et al., 2007; Sullivan et al., 2012), it was also shown to restrict the exaggerated expansion of activated T cells during a viral infection in a T cell extrinsic manner by inhibiting IL-6 production by DCs (Dejean et al., 2009). These results differ substantially from the study by Lin et al. (2014) that utilized a mutant allele generated by 'gene-trap' technology (*FoxO3*^{Trap}) on the 129 strain to reveal spontaneous T cell activation, lymphoproliferative disease, and organ infiltration. In fact, differences in autoimmunity between mixed C57BL/6 and 129 mouse strains are not uncommon.

Productive DC-T cell interactions require DCs to take up the antigen in the periphery then migrate into secondary lymphoid organs and to undergo maturation through up-regulation of costimulatory molecules and cytokine release. Such interactions have the potential to enhance or suppress T cell activation, viability, and/or function. To explore the effect of FoxO3a and IL-10 deficiencies on such interactions, we performed a series of DC/T cell co-culture experiments. Following stimulation, *FoxO3a*$^{-/-}$*Il10*$^{-/-}$ CD4^{+} T cells intrinsically displayed greater viability and proliferative capacity compared to the other groups. Moreover, *FoxO3a*$^{-/-}$*Il-10*$^{-/-}$ CD4^{+}T cells produced significantly higher amounts of IFN-γ and IL-6 without the presence of DCs suggesting that the expression of these cytokines is regulated by FoxO3a and IL-10 in a T cell intrinsic manner. In contrast, IL-17A producing CD4^{+} T cells required the presence of *FoxO3a*$^{-/-}$*Il-10*$^{-/-}$ DCs. This may be explained by the documented capacity of murine DCs to activate Th17 cells, which are the major producers of IL-17A (Leibundgut-Landmann et al., 2007; Bailey et al., 2007).

Taking into account the increased IL-6 production and the reduced viability in *FoxO3a*$^{-/-}$*Il10*$^{-/-}$ T cells, we postulated that IL-6 may be rescuing T cells from apoptosis. This is supported by different studies showing how IL-6 inhibits the downregulation of Bcl-2 in a dose-dependent manner to enhance the survival of antigen-stimulated T cells (Teague et al., 1997; Rochman et al., 2005). Also, since *FoxO3a*$^{-/-}$*Il10*$^{-/-}$ DCs were shown to express high levels of pro-inflammatory cytokines in *vitro* and seemed to improve the survival and proliferation of co-cultured WT T cells, we concluded that they are intrinsically hyperactivated. In fact, unlike IL-10, FoxO3a deficiency in DCs had the greatest impact on the proliferation of WT T cells.

Following the previous findings of the alterations in the expression of Treg markers, we further tested the Treg suppressive function in an in *vitro* co-culture suppression assay with CD45.1^{+} WT T cells. Unlike WT or single gene-deficient Tregs, *FoxO3a*$^{-/-}$*Il10*$^{-/-}$ Tregs exhibited an impairment in their ability to suppress WT T cell proliferation and IFN-γ production without impacting cell viability.

Since the depletion of both the neutrophils/monocytes and T cells ameliorated the disease, it is likely that the myeloid cells are responsible for compromising the function of regulatory T cells leading to increased T cell activation. It is likely that the disease outcome is the result of modulation in the communication between these three cell types.

13. FoxO3a regulates gut microbial homeostasis in *Il10*$^{-/-}$ mice.

The interaction between a balanced and stable microbiota and the mucosal immune system promotes the maintenance of intestinal homeostasis. However, alterations in the microbial community (dysbiosis) can lead to pro-inflammatory immune responses.

In our *FoxO3a*$^{-/-}$*Il10*$^{-/-}$ murine model, it is also conceivable that the crosstalk between the immune cells, gut epithelial cells and the gut microbiome collectively results in fulminant CrD-like disease, and neutralization of one cell type or modulation of gut microbiota can offset this crosstalk in favor of host survival. In *FoxO3a*$^{-/-}$ *Il10*$^{-/-}$ mice, the diversity and richness appeared to have a decreasing trend compared to WT mice. Depletion of the gut flora with a cocktail of Ciprofloxacin and Metronidazole significantly improved the survival of *FoxO3a*$^{-/-}$ *Il10*$^{-/-}$ mice, suggesting the involvement of the microbiome in driving the pathogenesis of the inflammation. However, treatment with antibiotics did not cure the illness indicating other underlying mechanisms at play. In humans, suppurative complications of CD, including abscesses and fistulas, require drainage and antibiotic therapy, most often ciprofloxacin, metronidazole, or a combination of both. Antibiotics might also play a role in the maintenance of remission and prevention of post operative recurrence of CrD (Nitzan et al., 2016). Some of the downsides to antibiotic treatment, however, include significant side effects that often cause intolerance to treatment, *Clostridium difficile* infection, and increasing antibiotic resistance (Nitzan et al., 2016).

The microbiome of IBD patients is associated with decreased levels of resident *Firmicutes* and/or *Bacteroides* and an overabundance of *Proteobacteria* (Le Chatelier et al., 2013; Manichanh et al.,

2006). At the phylum level, we observed a higher abundance of *Actinobacteria* and *Proteobacteria*, with increased *Enterobacteriaceae*, in *FoxO3a*$^{-/-}$*Il10*$^{-/-}$ mice. *Proteobacteria* are colitogenic strains that are significantly abundant in patients with aggressive CrD courses (Vester-Andersen et al., 2019). In a healthy GI tract, the relative abundance of *Proteobacteria* varies between 2 and 5% and increases up to 15% in metabolic disorders and intestinal inflammation (Lavelle et al., 2015; Shin et al., 2015). At the genus level, we observed that *Sutterella* was significantly enriched in *FoxO3a*$^{-/-}$ *Il10*$^{-/-}$ mice. Although *Sutterella* has been suspected to play a part in the pathogenesis of IBD, other studies indicated no difference in its prevalence between IBD patients and the healthy subjects (Santoru et al., 2017; Lavelle et al., 2015; Mukhopadhya et al., 2011; Hansen et al., 2013).

The abundance of *Lactobacilli*, which suppresses the production of pro-inflammatory cytokines, was particularly reduced in *FoxO3a*$^{-/-}$ *Il10*$^{-/-}$ mice. In a DSS model of colitis, administration of *L. acidophilus* suppressed Th17 cell-mediated secretion of proinflammatory cytokine IL-17 through downregulation of IL-23 and TGF-β1 expression and downstream phosphorylation of p-STAT3 (Chen et al., 2015). Commensal *Lactobacillus* species are common inhabitants of the natural microbiota in the human gut. The *Lactobacillus* species can rebalance homeostasis and thus have a protective role against IBD.

Furthermore, we observed that *Roseburia*, a Gram-positive aerobic species of the *Firmicutes* phylum, was depleted in *FoxO3a*$^{-/-}$*Il10*$^{-/-}$ mice. *Roseburia* produces the short chain fatty acid butyrate, which is a key energy source for colonocytes that also signals through the G-protein coupled receptors to regulate immune responses. Butyrate is produced in collaboration by many commensal bacteria in the colon. Butyrate has been shown to suppress pro-inflammatory responses by acting on Tregs and favoring the M2 macrophage polarization. Moreover, butyrate reinforces the mucous layer, upregulates epithelial tight junction proteins, and stimulates the production of antimicrobial peptides (Smith et al., 2013). Thus, depletion of butyrate negatively influences intestinal inflammation (Smith et al., 2013; Parada et al., 2019). However, the effect of butyrate on the intestinal barrier function may be concentration-dependent, as high butyrate concentrations (5-8 mM) may disrupt the intestinal barrier by promoting apoptosis (Peng et al., 2009; Huang et al., 2013). A study has shown that levels of butyrate and substrates involved in its synthesis were significantly associated with clinical remission following anti-TNF therapy in IBD

patients. These metabolites were less frequently exchanged among bacterial communities from patients who did not show therapeutic efficacy in response to anti-TNF therapy (Aden et al., 2019). It is therefore posited that butyrate supplementation could improve treatment efficacy with other anti-cytokine therapies.

All in all, it appears that FoxO3a modulates the bacterial composition of the gut microbiome, such that its deficiency may cause intestinal dysbiosis in IL-10-deficient mice. Due to the fact that a metabolically complex cohort of bacterial interactions predominate in the gut, intestinal luminal dysbiosis remains a difficult outcome to correct.

CONCLUSION

In this research project, I have pursued several avenues of discovery regarding how FoxO3a and IL-10 modulate the immune system to prevent the development of a spontaneous and aggressive form of CrD-like disease in mice. I have provided evidence that FoxO3a is required to protect IL-10-deficient mice from developing severe intestinal illness that leads to death within three months of birth. This occurs by limiting the extensive infiltration of inflammatory immune cells into their colons. I have shown that FoxO3a deficiency triggers "emergency myelopoiesis" in IL-10-deficient hosts. I have demonstrated that FoxO3a limits the over-activation of immune cells, alleviates their resistance to death and restrains their hypermetabolic activity in the IL-10-deficient host by hampering excessive STAT3, $p38^{MAPK}$ and mTORC1signaling. I have shown that FoxO3a and IL-10 cooperate in modulating glutamine metabolism in T cells to prevent their pathological specification towards an inflammatory phenotype. I have revealed how the deficiency of FoxO3a and IL-10 impacts the functional crosstalk between DCs, effector T cells and Tregs, both intrinsically and extrinsically, such that eliminating either the innate or adaptive arms results in an improvement in survival (**Figure 48**). Finally, I have shed light on how FoxO3a restricts the dominance of potentially colitogenic bacteria in IL-10-deficient hosts to keep gut microbial homeostasis in check.

This *FoxO3a*$^{-/-}$*Il10*$^{-/-}$ murine model described herein highlights the prognostic value of FoxO3a in determining the progression and severity of IBD. Our study complements GWAS that have elucidated the specific functional effects of FoxO3a expression by integrating genetic, clinical, and functional data in both human and murine systems.

To date, IBD is an incurable disease, and there is no one-size-fits-all treatment approach. It is my hope that this study will provide a launching point to perform further investigations to uncover additional pathways where FoxO3a and IL-10 might crosstalk, both in immune cells and non-immune cells. With our lab currently undertaking new follow-up projects, I hope that I will be able to contribute to future discoveries of potential biomarkers that are prognostically informative and can drive personalized selection of therapy in IBD patients.

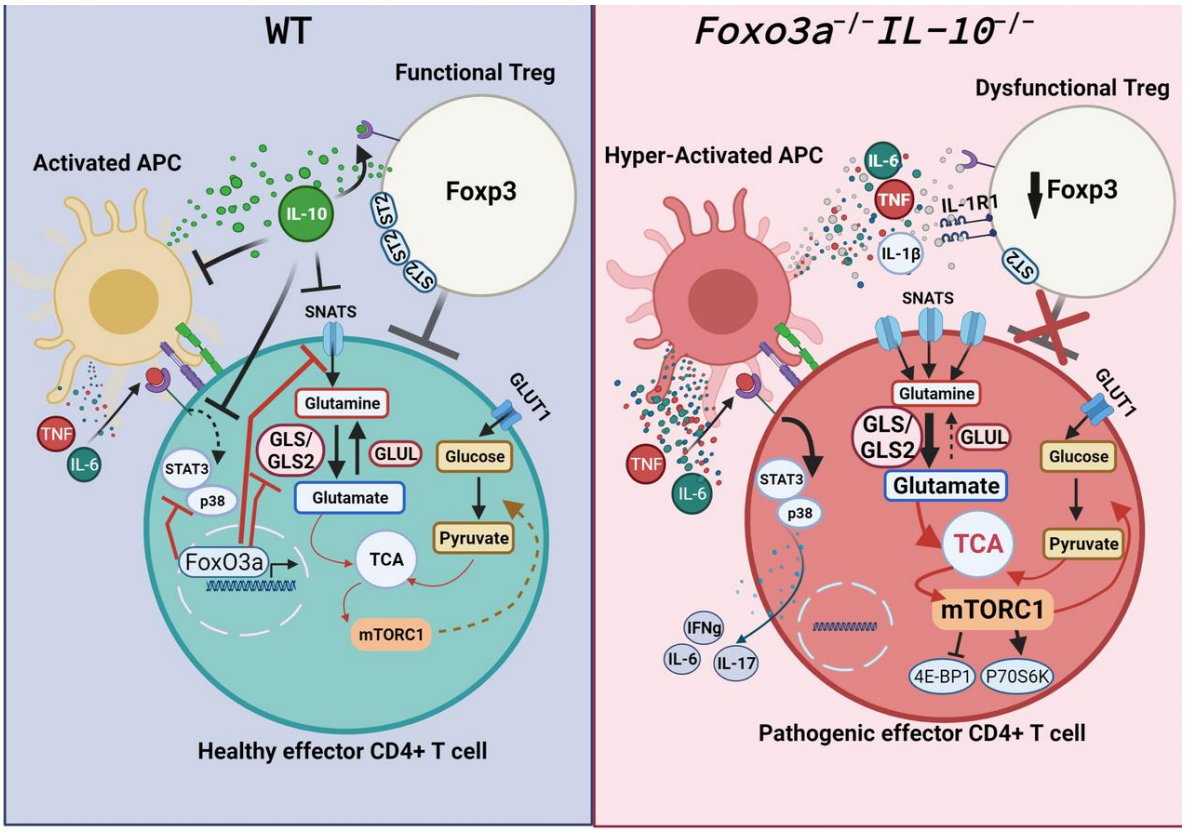

Figure 48. FoxO3a and IL-10 regulate the crosstalk between APCs, effector T cells and Tregs.

The diagram (left) shows homeostatic interactions between the three cell types in a WT host. Activated antigen presenting cells (APCs) trigger the activation of effector $CD4^+$ T cells by MHC: TCR signaling, co-stimulation and cytokine release. Pro-inflammatory cytokines, such as TNF-α and IL-6, activate downstream $p38^{MAPK}$ and STAT3 signaling pathways in effector T cells. FoxO3a restricts the persistent activation of inflammatory signaling pathways and represses the expression of glutaminase and glutamine transporters to prevent excessive glutamine consumption by T cells. IL-10, secreted by both APCs and T cells, limits the pro-inflammatory response, and enhances Treg suppressive function, which inhibits the over-activation of T cells. The diagram (right) depicts aberrant interactions between the three cell types in the absence of both FoxO3a and IL-10. APCs are hyperactivated and secrete a storm of pro-inflammatory cytokines, which activate $p38^{MAPK}$ and STAT3 in effector T cells promoting further release of IL-17A, IFN-γ and IL-6. The repression of glutamine uptake and metabolism is alleviated allowing increased glutamine conversion to glutamate, which potentially feeds into the TCA cycle and activates mTORC1 signaling. Activated mTORC1 phosphorylates its downstream targets P70S6K and 4E-BP1 ultimately leading to increased translation and protein synthesis. Dysfunctional Tregs lose their FoxP3 and ST2 expression and upregulate IL-1R1 expression in response to the pro-inflammatory milieu. Such Tregs are unable to suppress the differentiation of the effector T cell towards a pathologically inflammatory phenotype. *GLS/GLS2: isoforms of glutaminase; GLUL: glutamine synthase; GLUT1: Glucose Transporter 1; P70S6K: Ribosomal protein S6 kinase; 4E-BP1: Eukaryotic translation initiation factor 4E-binding protein 1; ST2: Suppression of Tumorigenicity 2 protein. This figure was created in Biorender.*

REFERENCES

1. Abreu, M.T. (2010). Toll-like receptor signalling in the intestinal epithelium: how bacterial recognition shapes intestinal function. Nat Rev Immunol. 10(2): 131-144
2. Aden, K., et al. (2019). Metabolic Functions of Gut Microbes Associate with Efficacy of Tumor Necrosis Factor Antagonists in Patients with Inflammatory Bowel Diseases. Gastroenterology, 157(5), 1279–1292.e11.
3. Aggarwal, B.B., Gupta, S.C., Kim, J.H. (2012). Historical perspectives on tumor necrosis factor and its superfamily: 25 years later, a golden journey. Blood. 119(3):651-665.
4. Aggarwal, S., Ghilardi, N., Xie, M. H., de Sauvage, F. J., & Gurney, A. L. (2003). Interleukin-23 promotes a distinct CD4 T cell activation state characterized by the production of interleukin-17. The Journal of biological chemistry, 278(3), 1910–1914.
5. Akira, S., Taga, T., & Kishimoto, T. (1993). Interleukin-6 in biology and medicine. Advances in Immunology, 54, 1–78.
6. Alliot, F., Godin, I. and Pessac B. (1999). Microglia derive from progenitors, originating from the yolk sac, and which proliferate in the brain. Brain Res Dev Brain Res. 117(2): p. 145-52.
7. Al-Sadi R, Ye D, Dokladny K, Ma TY. Mechanism of IL-1beta-induced increase in intestinal epithelial tight junction permeability. J Immunol. 2008; 180:5653–61. 10.4049/jimmunol.180.8.5653.
8. Alvarez, F., Istomine, R., Shourian, M. et al. (2019). The alarmins IL-1 and IL-33 differentially regulate the functional specialisation of Foxp3+ regulatory T cells during mucosal inflammation. Mucosal Immunol 12, 746–760.
9. Álvarez-Errico, D., Vento-Tormo, R., Sieweke, M. et al. (2015). Epigenetic control of myeloid cell differentiation, identity and function. Nat Rev Immunol 15, 7–17.
10. Alzoghaibi, M. A. (2013). Concepts of oxidative stress and antioxidant defense in Crohn's disease. 19 6540–6547. 10.3748/wjg.v19.i39.6540
11. Ananthakrishnan, A. N., Khalili, H., Higuchi, L. M., Bao, Y., Korzenik, J. R., Giovannucci, E. L., Richter, J. M., Fuchs, C. S., & Chan, A. T. (2012). Higher predicted vitamin D status is associated with reduced risk of Crohn's disease. Gastroenterology, 142(3), 482–489.
12. Ananthakrishnan, A. N., et al. (2013). A prospective study of long-term intake of dietary fiber and risk of Crohn's disease and ulcerative colitis. Gastroenterology, 145(5), 970–977.
13. Anderson, C.A., et al. (2011). Meta-analysis identifies 29 additional ulcerative colitis risk loci, increasing the number of confirmed associations to 47. Nat Genet. 43:246–252.
14. Anderson, M. J., Viars, C. S., Czekay, S., Cavenee, W. K., Arden, K. C. (1998). Cloning and characterization of three human forkhead genes that comprise an FKHR-like gene subfamily. Genomics 47(2):187-99.
15. Andus, T., Geiger, T., Hirano, T., Kishimoto, T., Tran-Thi, T.-A., Decker, K., & Heinrich, P. C. (n.d.). Regulation of synthesis and secretion of major rat acute-phase proteins by recombinant human interleukin-6 (BSF-2/1L-6) in hepatocyte primary cultures. European Journal of Biochemistry, 173(2), 287–293.
16. Andus, T., Targan, S.R., Deem, R., Toyoda, H. (1993). Measurement of tumor necrosis factor alpha mRNA in small numbers of cells by quantitative polymerase chain reaction. Reg Immunol. 5:11–17.

17. Annunziato, F., et al. (2007). Phenotypic and functional features of human Th17 cells. The Journal of experimental medicine, 204(8), 1849–1861.
18. Ardawi MS. (1988). Glutamine and glucose metabolism in human peripheral lymphocytes. Metabolism. 37:99–103
19. Ardawi, M,S., Newsholme, E.A. (1983). Glutamine metabolism in lymphocytes of the rat. Biochem J. 212:835–842.
20. Arden, K.C. (2006). Multiple roles of FOXO transcription factors in mammalian cells point to multiple roles in cancer. Exp Gerontol. 41(8):709-17.
21. Assa A, et al. (2016) Mucosa-Associated Ileal Microbiota in New-Onset Pediatric Crohn's Disease. Inflamm Bowel Dis 22(7):1533-1539.
22. Atreya, R., et al. (2011). Antibodies against tumor necrosis factor (TNF) induce T cell apoptosis in patients with inflammatory bowel diseases via TNF receptor 2 and intestinal $CD14^{+}$ macrophages. Gastroenterology, 141(6),2026–2038.
23. Atreya, R., et al. (2000). Blockade of interleukin 6 trans signaling suppresses T cell resistance against apoptosis in chronic intestinal inflammation: evidence in crohn disease and experimental colitis in vivo. Nature medicine, 6(5), 583–588.
24. Atuma, C., Strugala, V., Allen, A., Holm, L. (2001). The adherent gastrointestinal mucus gel layer: Thickness and physical state in vivo. Am J Physiol Gastrointest Liver Physiol. 280:G922–G929.
25. Auffray, C., Fogg, D., Garfa, M., Elain, G., Join-Lambert, O., Kayal, S., Sarnacki, S., Cumano, A., Lauvau, G., & Geissmann, F. (2007). Monitoring of blood vessels and tissues by a population of monocytes with patrolling behavior. Science (New York, N.Y.), 317(5838), 666–670.
26. Bachem, A., et al. (2019). Microbiota-Derived Short-Chain Fatty Acids Promote the Memory Potential of Antigen-Activated CD8+ T Cells. Immunity, 51(2), 285–297.e5.
27. Bailey, S.L., Schreiner, B., McMahon, E.J., Miller, S.D. (2007). CNS myeloid DCs presenting endogenous myelin peptides 'preferentially' polarize CD4+ T(H)-17 cells in relapsing EAE. Nat Immunol. 8:172–180.
28. Bain, C., Scott, C., Uronen-Hansson, H. et al. (2013). Resident and pro-inflammatory macrophages in the colon represent alternative context-dependent fates of the same Ly6Chi monocyte precursors. Mucosal Immunol 6, 498–510.
29. Baldauf, S. L. (1999). A search for the origins of animals and fungi: comparing and combining molecular data. Am Nat 154, S178– S188.
30. Balmer, M. L., et al., (2016). Memory CD8(+) T Cells Require Increased Concentrations of Acetate Induced by Stress for Optimal Function. Immunity, 44(6), 1312–1324. https://doi.org/10.1016/j.immuni.2016.03.016
31. Banchereau, J., R. M. Steinman. (1998). Dendritic cells and the control of immunity. Nature, 392: 245–252.
32. Bar-Peled, L., Schweitzer, L.D., Zoncu, R., Sabatini, D.M. (2012). Ragulator is a GEF for the rag GTPases that signal amino acid levels to mTORC1. Cell 150: 1196–1208.
33. Baumgart, D.C., & Sandborn, W.J. (2007). Inflammatory bowel disease: clinical aspects and established and evolving therapies. Lancet. 369(9573):1641–57
34. Beaugerie, L., Svrcek, M., Seksik, P., Bouvier, A.-M., Simon, T., Allez, M., Brixi, H., Gornet, J.-M., Altwegg, R., Beau, P., Duclos, B., Bourreille, A., Faivre, J., Peyrin-Biroulet, L., Fléjou, J.-F., Carrat, F., and CESAME Study Group. (2013). Risk of colorectal high-

grade dysplasia and cancer in a prospective observational cohort of patients with inflammatory bowel disease. Gastroenterology. 145, 166–175.e8
35. Bedoui, S., Whitney, P., Waithman, J. et al. Cross-presentation of viral and self-antigens by skin-derived CD103+ dendritic cells. Nat Immunol 10, 488–495 (2009).
36. Begitt, A., Droescher, M., Meyer, T., Schmid, C.D., Baker, M., Antunes, F., Knobeloch, K.-P., Owen, M.R., Naumann, R., Decker, T., et al. (2014). STAT1-cooperative DNA binding distinguishes type 1 from type 2 interferon signaling. Nat. Immunol. 15, 168– 176.
37. Ben-Sahra, I., Howell, J.J., Asara, J.M., and Manning, B.D. (2013). Stimulation of de Novo Pyrimidine Synthesis by Growth Signaling Through mTOR and S6K1. Science 339, 1323– 1328.
38. Ben-Sahra, I., Hoxhaj, G., Ricoult, S.J.H., Asara, J.M., and Manning, B.D. (2016). mTORC1 induces purine synthesis through control of the mitochondrial tetrahydrofolate cycle. Science 351, 728–733.
39. Berg, D.J., Davidson, N., Kuhn, R., Muller, W., Menon, S., Holland, G., Thompson-Snipes, L., Leach, M.W. and Rennick, D. (1996). Enterocolitis and colon cancer in interleukin-10-deficient mice are associated with aberrant cytokine production and CD4(+) TH1-like responses. The Journal of clinical investigation, 98(4), pp. 1010-1020.
40. Bergsbaken, T., Fink, S. L., & Cookson, B. T. (2009). Pyroptosis: host cell death and inflammation. Nature reviews. Microbiology, 7(2), 99-109. doi:10.1038/nrmicro2070
41. Bettelli, E., Carrier, Y., Gao, W., Korn, T., Strom, T. B., Oukka, M., Weiner, H. L., & Kuchroo, V. K. (2006). Reciprocal developmental pathways for the generation of pathogenic effector TH17 and regulatory T cells. Nature, 441(7090), 235–238.
42. Bevins, C.L. and Salzman, N.H. (2011). Paneth cells, antimicrobial peptides and maintenance of intestinal homeostasis. Nature reviews. Microbiology, 9(5), pp. 356-368
43. Bigarella, C. L., Li, J., Rimmelé, P., Liang, R., Sobol, R. W., & Ghaffari, S. (2017). FOXO3 Transcription Factor Is Essential for Protecting Hematopoietic Stem and Progenitor Cells from Oxidative DNA Damage. The Journal of biological chemistry, 292(7), 3005–3015.
44. Blasius, AL., Cella, M., Maldonado, J., Takai, T., Colonna, M. (2006). Siglec-H is an IPC-specific receptor that modulates type I IFN secretion through DAP12. Blood. 107:2474–2476.
45. Blommaart, E.F., Luiken, J.J., Blommaart, P.J., van Woerkom, G.M., Meijer, A.J. (1995). Phosphorylation of ribosomal protein S6 is inhibitory for autophagy in isolated rat hepatocytes. The Journal of biological chemistry 270: 2320–2326.
46. Boehm, U., Klamp, T., Groot, M. & Howard, J.C. (1997). Cellular responses to interferon-gamma. Annu Rev Immunol 15, 749-95.
47. Bogunovic, M., et al. (2009). Origin of the lamina propria dendritic cell network. Immunity. 31(3): p. 513-25.
48. Boirivant, M., Marini, M., Di Felice, G., et al. (1999). Lamina propria T cells in Crohn's disease and other gastrointestinal inflammation show defective CD2 pathway-induced apoptosis. Gastroenterology ;116:557-565.
49. Boisson, B., et al. (2013). A biallelic ACT1 mutation selectively abolishes interleukin-17 responses in humans with chronic mucocutaneous candidiasis. Immunity. 39:676–86.
50. Bonilla FA, Oettgen HC. (2010). Adaptive immunity. J. Allergy Clin. Immunol.125:S33–S40.

51. Bottomly, K. (1988). A functional dichotomy in CD4+ T lymphocytes. Immunol Today 9:268–274.
52. Bouzeyen, R., Haoues, M., Barbouche, M.R., Singh, R., Essafi, M. (2019). FOXO3 Transcription Factor Regulates IL-10 Expression in Mycobacteria-Infected Macrophages, Tuning Their Polarization and the Subsequent Adaptive Immune Response. Front Immunol. 10:2922.
53. Braegger, C. P., Nicholls, S., Murch, S. H., Stephens, S., & MacDonald, T. T. (1992). Tumour necrosis factor alpha in stool as a marker of intestinal inflammation. Lancet (London, England), 339(8785), 89–91.
54. Brand S. (2009). Crohn's disease: Th1, Th17 or both? The change of a paradigm: new immunological and genetic insights implicate Th17 cells in the pathogenesis of Crohn's disease. Gut. 58:1152–1167.
55. Brand, K., Williams, J.F., Weidemann, M.J. (1984). Glucose and glutamine metabolism in rat thymocytes. Biochem J.221:471–475.
56. Braun, A., et al. (2009). Alterations of phospholipid concentration and species composition of the intestinal mucus barrier in ulcerative colitis: A clue to pathogenesis. Inflamm Bowel Dis. 15:1705–20.
57. Bronte, V., & Pittet, M. J. (2013). The spleen in local and systemic regulation of immunity. Immunity, 39(5), 806–818.
58. Brown, C.C., et al. (2019). Transcriptional Basis of Mouse and Human Dendritic Cell Heterogeneity. Cell, 179(4):846-863.e24.
59. Broz, M.L., et al. (2014). Dissecting the tumor myeloid compartment reveals rare activating antigen-presenting cells critical for T cell immunity. Cancer Cell, 26, 638–652.
60. Brunkow, M.E., et al. (2001). Disruption of a new forkhead/winged-helix protein, scurfin, results in the fatal lymphoproliferative disorder of the scurfy mouse. Nat Genet. 27:68.
61. Buchler G, et al. (2012) Strain-specific colitis susceptibility in IL10-deficient mice depends on complex gut microbiota-host interactions. Inflamm Bowel Dis 18(5):943-954
62. Budarf, M. L., Labbé, C., David, G., & Rioux, J. D. (2009). GWA studies: rewriting the story of IBD. Trends in genetics : TIG, 25(3), 137–146.
63. Cadenas, E. (1997). Basic mechanisms of antioxidant activity. BioFactors Oxf. Engl. 6, 391– 397.
64. Cadwell, K., et al. (2008). A key role for autophagy and the autophagy gene Atg16l1 in mouse and human intestinal Paneth cells. Nature. 456(7219):259-63.
65. Calnan, D. R., Brunet, A. (2008). The FoxO code. Oncogene 27(16):2276-88.
66. Carey, R., et al. (2008). Activation of an IL-6: STAT3-dependent transcriptome in pediatric-onset inflammatory bowel disease. Inflamm Bowel Dis. 14:446–57.
67. Carlin, L. M. et al. (2013). Nr4a1-dependent Ly6Clow monocytes monitor endothelial cells and orchestrate their disposal. Cell 153, 362–375.
68. Carr, E.L. et al. (2010). Glutamine uptake and metabolism are coordinately regulated by ERK/MAPK during T lymphocyte activation. J Immunol. 185(2): 1037-1044.
69. Carswell, E.A., Old, L.J., Kassel, R.L., Green, S., Fiore, N., Williamson, B. (1975). An endotoxin-induced serum factor that causes necrosis of tumors. Proc Natl Acad Sci U S A. 72(9):3666-70.
70. Castrillon, D.H., Miao, L., Kollipara, R., Horner, J.W., and DePinho, R.A. (2003). Suppression of ovarian follicle activation in mice by the transcription factor Foxo3a. Science 301, 215–218.

71. Cavaillon, J.M. (2001). Pro- versus anti-inflammatory cytokines: myth or reality. Cell. Mol. Biol. (Noisy-Le-Grand). 47, 695–702.
72. Cella, M., Engering. A., Pinet, V., Pieters, J., and Lanzavecchia, A. (1997). Inflammatory stimuli induce accumulation of MHC class II complexes on dendritic cells. Nature. 388(6644):782-7.
73. Chadwick, V.S., and R.P. Anderson. (1992). Microorganisms and their products in inflammatory bowel disease. In Inflammatory Bowel Disease. R.P. McDermott and W.F. Stenson, editors. Elsevier Science Publishers, New York. 241-258.
74. Chambers, C.A., Kuhns, M.S., Egen, J.G., Allison, J.P. (2001). CTLA-4-mediated inhibition in regulation of T cell responses: mechanisms and manipulation in tumor immunotherapy. Annu Rev Immunol, 19, 565–594.
75. Chandramohan, V., Jeay, S., Pianetti, S., Sonenshein, G.E. (2004). Reciprocal control of Forkhead box O 3a and c-Myc via the phosphatidylinositol 3-kinase pathway coordinately regulates p27Kip1 levels. J Immunol. 172:5522-5527.
76. Chang, C. H., et al. (2013). Posttranscriptional control of T cell effector function by aerobic glycolysis. Cell, 153(6), 1239–1251.
77. Chang, S.H., and Dong, C. (2011). Signaling of interleukin-17 family cytokines in immunity and inflammation. Cell Signal. 23:1069–75.
78. Chassaing, B., Aitken, J.D., Malleshappa, M., Vijay-Kumar, M. (2014). Dextran sulfate sodium (DSS)-induced colitis in mice. Curr Protoc Immunol. 104: Unit 15.25
79. Chaudhry, A., et al. (2009). CD4+ regulatory T cells control TH17 responses in a Stat3-dependent manner. Science. 326:986–91.
80. Chaudhry, A. et al. (2011). Interleukin-10 signaling in regulatory T cells is required for suppression of Th17 cell-mediated inflammation. Immunity 34, 566-578.
81. Chen L, et al. (2017) NLRP12 attenuates colon inflammation by maintaining colonic microbial diversity and promoting protective commensal bacterial growth. Nat Immunol 18(5):541-551.
82. Chen L, Zou Y, Peng J, Lu F, Yin Y, Li F, et al. (2015). Lactobacillus acidophilus suppresses colitis-associated activation of the IL-23/Th17 axis. J Immunol Res. 2015:909514.
83. Chen Z, O'Shea JJ. (2008). Th17 cells: a new fate for differentiating helper T cells. Immunol Res. 41(2):87-102.
84. Chen, C., Liu, Y., Liu, Y., Zheng, P. (2009). mTOR regulation and therapeutic rejuvenation of aging hematopoietic stem cells. Science signaling. 2:ra75.
85. Chen, J., et al. (2010). Constitutively nuclear FOXO3a localization predicts poor survival and promotes Akt phosphorylation in breast cancer. PLoS One.5: e12293.
86. Chen, K.W., Demarco, B., Heilig, R., Shkarina, K., Boettcher, A., Farady, C.J., Pelczar, P., Broz, P. (2019), Extrinsic and intrinsic apoptosis activate pannexin-1 to drive NLRP3 inflammasome assembly. EMBO J 38: e101638
87. Chen, L., et al. (2017). NLRP12 attenuates colon inflammation by maintaining colonic microbial diversity and promoting protective commensal bacterial growth. Nat Immunol. 18:541–51.
88. Chen, L., Zou, Y., Peng, J., Lu, F., Yin, Y., Li, F., and Yang, J. (2015). Lactobacillus acidophilus suppresses colitis-associated activation of the IL-23/Th17 axis. J Immunol Res 2015, 909514.

89. Cheng, H., and Leblond, C.P. (1974b). Origin, differentiation, and renewal of the four main epithelial cell types in the mouse small intestine. V. Unitarian Theory of the origin of the four epithelial cell types. Am. J. Anat. 141, 537–561.
90. Cheshier, S. H., Morrison, S. J., Liao, X., & Weissman, I. L. (1999). In vivo proliferation and cell cycle kinetics of long-term self-renewing hematopoietic stem cells. Proceedings of the National Academy of Sciences of the United States of America, 96(6), 3120–3125.
91. Clark, K. L., Halay, E. D., Lai, E., Burley, S. K. (1993). Co-crystal structure of the HNF-3/fork head DNA-recognition motif resembles histone H5. Nature 364, 412-20.
92. Clevers H. (2013). The intestinal crypt, a prototype stem cell compartment. Cell, 154(2), 274–284.
93. Coccia, M., Harrison, O.J., Schiering, C., Asquith, M.J., Becher, B., Powrie, F., Maloy, K.J. (2012). IL-1β mediates chronic intestinal inflammation by promoting the accumulation of IL-17A secreting innate lymphoid cells and CD4(+) Th17 cells. J Exp Med. 209:1595–609. 10.1084/jem.20111453.
94. Corral, J., Forster, A., Thompson, S., Lampert, F., Kaneko, Y., Slater, R., Kroes, W.G., van der Schoot , C.E., Ludwig, W. D., Karpas,A. (1993). Acute leukemias of different lineages have similar MLL gene fusions encoding related chimeric proteins resulting from chromosomal translocation Proceedings of the National Academy of Sciences. 90 (18) 8538-8542.
95. Cosnes, J. (2004). Tobacco and IBD: relevance in the understanding of disease mechanisms and clinical practice. Best practice & research.Clinical gastroenterology, 18(3), pp. 481-496.
96. Courtois, G., Gilmore, T.D. (2006). Mutations in the NF-κB signaling pathway: Implications for human disease. Oncogene 25:6831–6843.
97. Coyle, A. J. et al. (1999). Crucial role of the interleukin 1 receptor family member T1/ST2 in T helper cell type 2-mediated lung mucosal immune responses. J. Exp. Med. 190, 895–902.
98. Cross, C.E., Halliwell, B., Borish, E.T., Pryor, W.A., Ames, B.N., Saul, R.L., McCord, J.M., Harman, D. (1987). Oxygen radicals and human disease. Ann Intern Med107.526545.
99. Cui, M., Huang, Y., Zhao, Y., & Zheng, J. (2008). Transcription factor FOXO3a mediates apoptosis in HIV-1-infected macrophages. *Journal of immunology (Baltimore, Md. : 1950), 180*(2), 898–906.
100. Cunningham, J. T., Rodgers, J. T., Arlow, D. H., Vazquez, F., Mootha, V. K., & Puigserver, P. (2007). mTOR controls mitochondrial oxidative function through a YY1-PGC-1alpha transcriptional complex. Nature, 450(7170), 736–740.
101. Cyktor, J.C., Turner, J. (2011). Interleukin-10 and immunity against prokaryotic and eukaryotic intracellular pathogens. Infect. Immun. 79:2964 – 2973.
102. Dai, W.J., Kohler, G., Brombacher, F. (1997). Both innate and acquired immunity to Listeria monocytogenes infection are increased in IL-10- deficient mice. J. Immunol. 158:2259 –2267.
103. Dansen, T. B., & Burgering, B. M. (2008). Unravelling the tumor-suppressive functions of FOXO proteins. Trends in Cell Biology, 18(9), 421–429.
104. Davidson, N.J., Leach, M.W., Fort, M.M., Thompson-Snipes, L., Kühn, R., Müller, W., Berg, D.J., Rennick, D.M. (1996). T helper cell 1-type CD4+ T cells, but not B cells, mediate colitis in interleukin 10-deficient mice. J Exp Med. 184(1):241-51.

105. De Carli, M., D'Elios, M.M., Zancuoghi, G., Romagnani, S., Del Prete, G. (1994). Human Th1 and Th2 cells: functional properties, regulation of development and role in autoimmunity. Autoimmunity.18(4):301-8.
106. De Filippo, K., & Rankin, S. M. (2018). CXCR4, the master regulator of neutrophil trafficking in homeostasis and disease. European journal of clinical investigation, 48 Suppl 2(Suppl Suppl 2), e12949.
107. De Souza, H.S., Fiocchi, C. (2016). Immunopathogenesis of IBD: current state of the art. Nat Rev Gastroenterol Hepatol.13:13–27.
108. De Waal Malefyt R, Haanen J, Spits H, Roncarolo MG, te Velde A, Figdor C, et al. (1991). Interleukin 10 (IL-10) and viral IL-10 strongly reduce antigen-specific human T cell proliferation by diminishing the antigen-presenting capacity of monocytes via downregulation of class II major histocompatibility complex expression. J Exp Med. 174(4):915-24. 259.
109. Delaleu, N., Bickel, M. (2004). Interleukin-1 beta and interleukin-18: regulation and activity in local inflammation. Periodontol 2000. 35:42-52.
110. Delves, P.J., and Roitt, I.M. (2000). The immune system. First of two parts. N. Engl. J. Med. 343, 37–49.
111. Den Haan, J. M., Lehar, S. M., & Bevan, M. J. (2000). CD8(+) but not CD8(-) dendritic cells cross-prime cytotoxic T cells in vivo. The Journal of experimental medicine, 192(12), 1685–1696.
112. DeVoss, J.& Diehl, L. (2014). Murine models of inflammatory bowel disease (IBD): challenges of modeling human disease. Toxicol Pathol. 42(1):99–110.
113. Dieleman, L. A., Palmen, M. J., Akol, H., Bloemena, E., Peña, A. S., Meuwissen, S. G., & Van Rees, E. P. (1998). Chronic experimental colitis induced by dextran sulphate sodium (DSS) is characterized by Th1 and Th2 cytokines. Clinical and experimental immunology, 114(3), 385–391.
114. Dinarello, C.A. (2000). Proinflammatory cytokines. Chest 118, 503–508
115. Dinarello, C.A. (2010). Anti-inflammatory agents: present and future. Cell. 140:935–50.
116. Duerr, R.H., Taylor, K.D., Brant, S.R., et al. (2006). A genome-wide association study identifies IL23R as an inflammatory bowel disease gene. Science.314(5804):1461-3.
117. Duque, G.A. and Descoteaux, A. (2014). Macrophage cytokines: Involvement in immunity and infectious diseases. Front. Immunol. 5.
118. Eaden, J.A., Abrams, K.R. and Mayberry, J.F. (2001). The risk of colorectal cancer in ulcerative colitis: a meta-analysis Gut, 48(4), pp. 526-535.
119. Eckelman, B. P., Salvesen, G. S., & Scott, F. L. (2006). Human inhibitor of apoptosis proteins: why XIAP is the black sheep of the family. *EMBO reports*, *7*(10), 988–994.
120. Egerton, M., David R. Fitzpatrick, Andrew D. Catling, and Anne Kelso. (1996). "Differential Activation of T Cell Cytokine Production by the Extracellular Signal-Regulated Kinase (ERK) Signaling Pathway." European Journal of Immunology.
121. Eijkelenboom, A., Burgering, B.M. (2013). FOXOs: signalling integrators for homeostasis maintenance. Nat Rev Mol Cell Biol. 14(2):83-97.
122. Elinav E, et al. (2011) NLRP6 inflammasome regulates colonic microbial ecology and risk for colitis. Cell 145(5):745-757.
123. Elmore, S. (2007). Apoptosis: a review of programmed cell death. Toxicologic pathology, 35(4), 495-516.

124. Elson, C. O., Sartor, R. B., Tennyson, G. S., & Riddell, R. H. (1995). Experimental models of inflammatory bowel disease. Gastroenterology, 109(4), 1344–1367.
125. Engelhardt, K.R., and Grimbacher, B. (2014). IL-10 in humans: lessons from the gut, IL-10/IL-10 receptor deficiencies, and IL-10 polymorphisms. Curr Top Microbiol Immunol. 380:1- 18.
126. Erdman, S., Fox, J.G., Dangler, C.A., Feldman, D. and Horwitz, B.H. (2001). Typhlocolitis in NF-kappa B-deficient mice. Journal of immunology (Baltimore, Md.: 1950), 166(3), pp. 1443-1447.
127. Feagan, B.G., Sy, R. (2003). Epidemiology of inflammatory bowel disease. The clinician's guide to inflammatory bowel disease. G. R. Lichtenstein. Thorofare, Slack incorporated: 1-8.
128. Feng, Y.J., and Li, Y.Y. (2011). The role of p38 mitogen-activated protein kinase in the pathogenesis of inflammatory bowel disease. J. Dig. Dis. 12, 327–332.
129. Ferber, E., Peck, B., Delpuech, O. et al. (2012). FOXO3a regulates reactive oxygen metabolism by inhibiting mitochondrial gene expression. Cell Death Differ 19, 968–979.
130. Fernandez-Checa, J.C., and Kaplowitz, N. (2005). Hepatic mitochondrial glutathione: transport and role in disease and toxicity. Toxicol. Appl. Pharmacol. 204, 263–273.
131. Fink, S.L., and Cookson, B.T. (2005). Apoptosis, Pyroptosis , and Necrosis : Mechanistic Description of Dead and Dying Eukaryotic Cells. Infect. Immun. 73, 1907–1916.
132. Fiore, M., Forli, S., Manetti, F. (2016). Targeting Mitogen-Activated Protein Kinase-Activated Protein Kinase 2 (MAPKAPK2, MK2): Medicinal Chemistry Efforts to Lead Small Molecule Inhibitors to Clinical Trials. J Med Chem.59(8):3609-34.
133. Fiorino, G., Peyrin-Biroulet, L., Naccarato, P., Szabò, H., Sociale, O. R., Vetrano, S., Fries, W., Montanelli, A., Repici, A., Malesci, A., & Danese, S. (2012). Effects of immunosuppression on immune response to pneumococcal vaccine in inflammatory bowel disease: a prospective study. Inflammatory bowel diseases, 18(6), 1042–1047.
134. Flachsbart, F., Caliebe, A., Kleindorp, R., Blanché, H., von Eller-Eberstein, H., Nikolaus, S., Schreiber, S., Nebel, A. (2009). Association of FOXO3A variation with human longevity confirmed in German centenarians. Proc Natl Acad Sci U S A.106(8):2700-5.
135. Fox, C. J., Hammerman, P. S., & Thompson, C. B. (2005). Fuel feeds function: energy metabolism and the T cell response. Nature reviews. Immunology, 5(11), 844–852.
136. Fortin, G., Raymond, M., Van, V.Q., Rubio, M., Gautier, P., Sarfati, M., Franchimont, D. (2009). A role for CD47 in the development of experimental colitis mediated by SIRPα^{+}CD103^{-} dendritic cells. J. Exp. Med. 206:1995–2011.
137. Franke, A., et al. (2008). Sequence variants in IL10, ARPC2 and multiple other loci contribute to ulcerative colitis susceptibility. *Nature genetics*, *40*(11), 1319–1323.
138. Frank, D.N., et al. (2011). Disease phenotype and genotype are associated with shifts in intestinal-associated microbiota in inflammatory bowel diseases. Inflamm Bowel Dis. 17(1):179–184.
139. Frauwirth, K. A., Riley, J. L., Harris, M. H., Parry, R. V., Rathmell, J. C., Plas, D. R., Elstrom, R. L., June, C. H., & Thompson, C. B. (2002). The CD28 signaling pathway regulates glucose metabolism. Immunity, 16(6), 769–777.
140. Fuchs, Y., & Steller, H. (2011). Programmed cell death in animal development and disease. Cell, 147(4), 742-758.

141. Fujino, S., Andoh, A., Bamba, S., Ogawa, A., Hata, K., Araki, Y., Bamba, T., & Fujiyama, Y. (2003). Increased expression of interleukin 17 in inflammatory bowel disease. Gut. 52(1), 65–70.
142. Furuyama, T., Nakazawa, T., Nakano, I., and Mori, N. (2000). Identification of the differential distribution patterns of mRNAs and consensus binding sequences for mouse DAF-16 homologues. Biochem. J. 349, 629–634.
143. Galili, N., Davis, R.J., Fredericks, W.J., Mukhopadhyay, S., Rauscher, F.J 3rd, Emanuel, B.S., Rovera, G., Barr, F.G. (1993). Fusion of a fork head domain gene to PAX3 in the solid tumour alveolar rhabdomyosarcoma. Nat Genet. 5(3):230-5.
144. Galloway, J.L., Zon, LI. (2003). Ontogeny of hematopoiesis: examining the emergence of hematopoietic cells in the vertebrate embryo. Curr Top Dev Biol; 53: 139–158.
145. Galluzzi, L., Vitale, I., Aaronson, S. A., Abrams, J. M., Adam, D., Agostinis, P., Kroemer, G. (2018). Molecular mechanisms of cell death: recommendations of the Nomenclature Committee on Cell Death 2018. Cell Death & Differentiation, 25(3), 486-541.
146. Gao, Y., Nish, S.A., Jiang, R., Hou, L., Licona-Limo´ n, P., Weinstein, J.S., Zhao, H., and Medzhitov, R. (2013). Control of T helper 2 responses by transcription factor IRF4-dependent dendritic cells. Immunity 39, 722–732.
147. Garcia Rodriguez, L.A., Ruigomez, A. and Panes, J., 2006. Acute gastroenteritis is followed by an increased risk of inflammatory bowel disease Gastroenterology, 130(6), pp. 1588-1594.
148. Garrett, W. S., Lord, G. M., Punit, S., Lugo-Villarino, G., Mazmanian, S. K., Ito, S., Glickman, J. N., & Glimcher, L. H. (2007). Communicable ulcerative colitis induced by T-bet deficiency in the innate immune system. Cell, 131(1), 33–45.
149. Gaubitz, C.,etal. (2015). Molecular Basis of the Rapamycin Insensitivity of Target Of Rapa mycin Complex 2. Mol. Cell 58, 977–988.
150. Gehart, H. & Clevers, H. (2019). Tales from the crypt: new insights into intestinal stem cells. Nat. Rev. Gastroenterol. Hepatol. 16, 19–34.
151. Giannakou, M.E., Goss, M., Jünger, M.A., Hafen, E., Leevers, S.J., Partridge, L. (2004). Long-lived Drosophila with overexpressed dFOXO in adult fat body. Science.305(5682):361.
152. Gilchrist, J.J., MaClennan, C.A., and Hill, A.V.S. (2015). Genetic susceptibility to invasive Salmonella disease. Nat. Rev. Immunol. 15, 452–463.
153. Ginhoux, F., et al. (2010). Fate mapping analysis reveals that adult microglia derive from primitive macrophages. Science. 330(6005): p. 841-5.
154. Ginhoux, F., Jung, S. (2014). Monocytes and macrophages: developmental pathways and tissue homeostasis. Nat Rev Immunol 14, 392–404. https://doi.org/10.1038/nri3671
155. Girardin SE, Travassos LH, Hervé M, Blanot D, Boneca IG, Philpott DJ, Sansonetti PJ, Mengin-Lecreulx D. (2003). Peptidoglycan molecular requirements allowing detection by Nod1 and Nod2. J Biol Chem. 278(43):41702-8.
156. Glocker EO, et al. (2009) Inflammatory bowel disease and mutations affecting the interleukin-10 receptor. The New England journal of medicine 361(21):2033-2045.
157. Godfrey, D., MacDonald, H., Kronenberg, M. et al. (2004). NKT cells: what's in a name?. Nat Rev Immunol 4, 231–237.
158. Godin, I., Garcia-Porrero, J.A., Dieterlen-Lievre, F., Cumano, A. (1999). Stem cell emergence and hemopoietic activity are incompatible in mouse intraembryonic sites. J Exp Med. 190: 43–52.

159. Gonnella, P.C., Waldner, H.P., and Weiner, H.L. (2001). B cell-deficient (mMT) mice have alterations in the cytokine microenvironment of the gut-associated lymphoid tissue (GALT) and a defect in the low dose mechanism of oral tolerance. J. Immunol. 166, 4456–4464.
160. Greenberger, M.J., Strieter, R.M., Kunkel, S.L., Danforth, J.M., Goodman, R.E., Standiford, T.J. (1995). Neutralization of IL-10 increases survival in a murine model of Klebsiella pneumonia. J. Immunol. 155:722–729.
161. Greer, E. L., Oskoui, P. R., Banko, M. R., Maniar, J. M., Gygi, M. P., Gygi, S. P., Brunet, A. (2007). The energy sensor AMP-activated protein kinase directly regulates the mammalian FOXO3 transcription factor. J Biol Chem. 282(41):30107-19.
162. Greer, E.L., and Brunet, A. (2005). FOXO transcription factors at the interface between longevity and tumor suppression. Oncogene. 24, 7410–7425
163. Groom, J. R., Richmond, J., Murooka, T. T., Sorensen, E. W., Sung, J. H., Bankert, K., von Andrian, U. H., Moon, J. J., Mempel, T. R., & Luster, A. D. (2012). CXCR3 chemokine receptor-ligand interactions in the lymph node optimize CD4+ T helper 1 cell differentiation. Immunity, 37(6), 1091–1103.
164. Gross, V., Andus, T., Caesar, I., Roth, M., & Schölmerich, J. (1992). Evidence for continuous stimulation of interleukin-6 production in Crohn's disease. Gastroenterology, 102(2), 514–519.
165. Groux, H., O'Garra, A., Bigler, M., Rouleau, M., Antonenko, S., de Vries, J. E., & Roncarolo, M. G. (1997). A CD4+ T cell subset inhibits antigen-specific T cell responses and prevents colitis. Nature, 389(6652), 737–742.
166. Gu, C., Wu, L., Li, X. (2013). IL-17 family: cytokines, receptors and signaling. Cytokine. 64:477–85.
167. Guermonprez, P., Valladeau, J., Zitvogel, L., Théry, C., and Amigorena S. (2002). Antigen presentation and T cell stimulation by dendritic cells. Annu Rev Immunol. 20:621-67.
168. Gwinn, D. M. et al. (2008). AMPK phosphorylation of raptor mediates a metabolic checkpoint. Mol. Cell 30, 214–226.
169. Hadjiminas, D. J., McMasters, K. M., Peyton, J. C., & Cheadle, W. G. (1994). Tissue tumor necrosis factor mRNA expression following cecal ligation and puncture or intraperitoneal injection of endotoxin. The Journal of surgical research, 56(6), 549–555.
170. Haep L, et al. (2015). Interferon gamma counteracts the angiogenic switch and induces vascular permeability in dextran sulfate sodium colitis in mice. Inflamm Bowel Dis. 21(10):2360–2371.
171. Hagar, J.A., Powell, D.A., Aachoui, Y., Ernst, R.K., and Miao, E.A. (2013). Cytoplasmic LPS activates caspase-11: Implications in TLR4-independent endotoxic shock. Science (80). 341, 1250–1253.
172. Hagenbuchner, J., et al. (2012) FOXO3-induced reactive oxygen species are regulated by BCL2L11 (Bim) and SESN3. J Cell Sci 125(Pt 5):1191-1203.
173. Hampe, J., et al. (2007). A genome-wide association scan of nonsynonymous SNPs identifies a susceptibility variant for Crohn disease in ATG16L1. *Nature genetics*, *39*(2), 207–211.
174. Hannenhalli, S., Kaestner, K. H. (2009). The evolution of Fox genes and their role in development and disease. Nat Rev Genet 10(4):233-40.

175. Hansen, R., et al. (2013). The microaerophilic microbiota of de-novo paediatric inflammatory bowel disease: the BISCUIT study. PLoS ONE 8:e58825 10.1371/journal.pone.0058825
176. Hansen, T.S., Jess, T., Vind, I., Elkjaer, M., Nielsen, M.F., Gamborg, M. and Munkholm, P. (2011). Environmental factors in inflammatory bowel disease: a case control study based on a Danish inception cohort Journal of Crohn's & colitis, 5(6), pp. 577- 584.
177. Harrington L.E., et al. (2005). Interleukin 17-producing CD4+ effector T cells develop via a lineage distinct from the T helper type 1 and 2 lineages. Nat. Immunol. 6:1123–1132.
178. Harrington, L.E., Hatton, R.D., Mangan, P.R., Turner, H., Murphy, T.L., Murphy, K.M., Weaver, C.T. (2005). Interleukin 17-producing CD4+ effector T cells develop via a lineage distinct from the T helper type 1 and 2 lineages. Nat Immunol. 6(11):1123-32.
179. Hart, A.L., Al-Hassi, H.O., Rigby, R.J., et al. (2005). Characteristics of intestinal dendritic cells in inflammatory bowel diseases. Gastroenterology. 129:50–65.
180. Hart, D.N. (1997). Dendritic cells: unique leukocyte populations which control the primary immune response. Blood. 90, 3245-3287.
181. Hauck, L., Harms, C., Grothe, D., An, J., Gertz, K., Kronenberg, G., Dietz, R., Endres, M., and von Harsdorf, R. (2007). Critical role for FoxO3a-dependent regulation of p21CIP1/WAF1 in response to statin signaling in cardiac myocytes. Circ Res. 100:50
182. He, W.T., Wan, H., Hu, L., Chen, P., Wang, X., Huang, Z., Yang, Z.H., Zhong, C.Q., and Han, J. (2015). Gasdermin D is an executor of pyroptosis and required for interleukin-1β secretion. Cell Res. 25, 1285–1298
183. Heckmann, B. L., Tummers, B., & Green, D. R. (2019). Crashing the computer: apoptosis vs. necroptosis in neuroinflammation. Cell Death Differ, 26(1), 41-52.
184. Hedrick, S. M., Hess Michelini, R., Doedens, A. L., Goldrath, A. W., & Stone, E. L. (2012). FOXO transcription factors throughout T cell biology. *Nature reviews. Immunology*, *12*(9), 649–661.
185. Henao-Mejia J, et al. (2012) Inflammasome-mediated dysbiosis regulates progression of NAFLD and obesity. Nature 482(7384):179-185.
186. Herzig, S. & Shaw, R. J. (2018). AMPK: guardian of metabolism and mitochondrial homeostasis. Nat. Rev. Mol. Cell Biol. 19, 121–135.
187. Hickey W. F. (2001). Basic principles of immunological surveillance of the normal central nervous system. Glia, 36(2), 118–124.
188. Hillion, J., Le Coniat, M., Jonveaux, P., Berger, R. & Bernard, O.A. (1997). AF6q21, a novel partner of the MLL gene in t(6;11)(q21;q23), defines a forkhead transcriptional factor subfamily. Blood 90 3714–3719.
189. Hinman, R. M., Nichols, W. A., Diaz, T. M., Gallardo, T. D., Castrillon, D. H., & Satterthwaite, A. B. (2009). Foxo3-/- mice demonstrate reduced numbers of pre-B and recirculating B cells but normal splenic B cell sub-population distribution. International immunology, 21(7), 831–842. https://doi.org/10.1093/intimm/dxp049
190. Hirsch, R.L., Panitch, H.S., Johnson, K.P. (1985). Lymphocytes from multiple sclerosis patients produce elevated levels of gamma interferon in vitro. J Clin Immunol. 5(6):386–9.
191. Hitti, E., Iakovleva, T., Brook, M., Deppenmeier, S., Gruber, A.D., Radzioch, D., Clark, A.R., Blackshear, P.J., Kotlyarov, A., & Gaestel, M. (2006). Mitogen-activated protein kinase-activated protein kinase 2 regulates tumor necrosis factor mRNA stability and

translation mainly by altering tristetraprolin expression, stability, and binding to adenine/uridine-rich element. Mol Cell Biol.26(6):2399-407.
192. Hoentjen F, et al. (2003) Antibiotics with a selective aerobic or anaerobic spectrum have different therapeutic activities in various regions of the colon in interleukin 10 gene deficient mice. Gut 52(12):1721-1727.
193. Hoffmann, J.C., Pawlowski, N.N., Kuhl, A.A., Hohne, W. and Zeitz, M. (2002). Animal models of inflammatory bowel disease: an overview. Pathobiology: journal of immunopathology, molecular and cellular biology, 70(3), pp. 121-130.
194. Holczer, M., Hajdú, B., Lőrincz, T., Szarka, A., Bánhegyi, G., & Kapuy, O. (2019). A Double Negative Feedback Loop between mTORC1 and AMPK Kinases Guarantees Precise Autophagy Induction upon Cellular Stress. International journal of molecular sciences, 20(22), 5543.
195. Holtmeier, W., Kabelitz, D. (2005). gammadelta T cells link innate and adaptive immune responses. Chem Immunol Allergy. 86:151-183.
196. Holub, M. C., Makó, E., Dévay, T., Dank, M., Szalai, C., Fenyvesi, A., & Falus, A. (1998). Increased interleukin-6 levels, interleukin-6 receptor and gp130 expression in peripheral lymphocytes of patients with inflammatory bowel disease. Scandinavian journal of gastroenterology. Supplement, 228, 47–50.
197. Horig, H., Spagnoli, G.C., Filgueira, L., Babst, R., Gallati, H., Harder, F., Juretic, A., Heberer, M. (1993). Exogenous glutamine requirement is confined to late events of T cell activation. J Cell Biochem.53:343–351.
198. Huang X, Li Z, Zhu L, Huang H, Hou L, Lin J. (2014). Inhibition of p38 mitogen-activated protein kinase attenuates butyrate-induced intestinal barrier impairment in a Caco-2 cell monolayer model. J Pediatr Gastroenterol Nutr.59:264–9
199. Huehn, J., Polansky, J.K., Hamann, A. (2009). Epigenetic control of FOXP3 expression: the key to a stable regulatory T cell lineage? Nat Rev Immunol 9: 83–89.
200. Hugot, JP., Chamaillard, M., Zouali, H. et al. (2001). Association of NOD2 leucine-rich repeat variants with susceptibility to Crohn's disease. Nature 411, 599–603.
201. Hwangbo D.S., Gershman B., Tu M.P., Palmer M., Tatar M. (2004). Drosophila dFOXO controls lifespan and regulates insulin signalling in brain and fat body. Nature. 429:562–566.
202. Hyams, J. S., Fitzgerald, J. E., Treem, W. R., Wyzga, N., & Kreutzer, D. L. (1993). Relationship of functional and antigenic interleukin 6 to disease activity in inflammatory bowel disease. Gastroenterology, 104(5), 1285–1292.
203. Igietseme, J.U., et al. (2000). Suppression of endogenous IL-10 gene expression in dendritic cells enhances antigen presentation for specific Th1 induction: potential for cellular vaccine development. J. Immunol. 164:4212–4219.
204. Ina, K., et al. (1999). Resistance of Crohn's disease T cells to multiple apoptotic signals is associated with a Bcl-2/Bax mucosal imbalance. J Immunol. 163:1081-1090.
205. Inohara N, Ogura Y, Fontalba A, Gutierrez O, Pons F, Crespo J, Fukase K, Inamura S, Kusumoto S, Hashimoto M, Foster SJ, Moran AP, Fernandez-Luna JL, Nuñez G. (2003). Host recognition of bacterial muramyl dipeptide mediated through NOD2. Implications for Crohn's disease. J Biol Chem. 278(8):5509-12.
206. Inoki, K., Li, Y., Zhu, T., Wu, J., Guan, K.L. (2002). TSC2 is phosphorylated and inhibited by Akt and suppresses mTOR signalling. Nature cell biology 4: 648–657.

207. Inoki, K., Zhu, T. & Guan, K. L. (2003). TSC2 mediates cellular energy response to control cell growth and survival. Cell 115, 577–590.
208. Ip, W.K.E, Hoshi, N., Shouval, D.S., Snapper, S., Medzhitov, R. (2017). Anti-inflammatory effect of IL-10 mediated by metabolic reprogramming of macrophages. Science. 356:513–9.
209. Iqbal, N., Oliver, J.R., Wagner, F.H., Lazenby, A.S., Elson, C.O. and Weaver, C.T. (2002). T helper 1 and T helper 2 cells are pathogenic in an antigen-specific model of colitis. The Journal of experimental medicine, 195(1), pp. 71-84.
210. Ito R, et al. (2006). Interferon-gamma is causatively involved in experimental inflammatory bowel disease in mice. Clin Exp Immunol. 2006;146(2):330–338.
211. Ivanov, I. I., McKenzie, B. S., Zhou, L., Tadokoro, C. E., Lepelley, A., Lafaille, J. J., Cua, D. J., & Littman, D. R. (2006). The orphan nuclear receptor RORgammat directs the differentiation program of proinflammatory IL-17+ T helper cells. Cell, 126(6), 1121–1133.
212. Iyer, S.S., and Cheng, G. (2012). Role of interleukin 10 transcriptional regulation in inflammation and autoimmune disease. Crit Rev Immunol. 32(1):23-63.
213. Jakobsen, C., Paerregaard, A., Munkholm, P. and Wewer, V. (2013). Environmental factors and risk of developing paediatric inflammatory bowel disease -- a population-based study 2007-2009 Journal of Crohn's & colitis, 7(1), pp. 79-88.
214. Jastroch, M., Divakaruni, A.S., Mookerjee, S., Treberg, J.R., and Brand, M.D. (2010). Mitochondrial proton and electron leaks. Essays Biochem. 47, 53–67.
215. Jenkins, M.K. (1994). "The Ups and Downs of T Cell Costimulation." Immunity.
216. Johansson, M. E., et al. (2011). Composition and functional role of the mucus layers in the intestine. Cellular and molecular life sciences: CMLS, 68(22), 3635–3641.
217. Johansson, M.E.V., et al. (2008). The inner of the two Muc2 mucin-dependent mucus layers in colon is devoid of bacteria. Proc Natl Acad Sci USA. 105:15064–15069.
218. Johnson, M.O., Wolf, M.M., Madden, M.Z., Andrejeva, G., Sugiura, A., Contreras, D.C., et al. (2018). Distinct regulation of Th17 and Th1 cell differentiation by glutaminase-dependent metabolism. Cell. 175:1780–95. e1719
219. Jorgensen, I., and Miao, E.A. (2015). Pyroptotic cell death defends against intracellular pathogens. Immunol. Rev. 265, 130–142.
220. Jostins, L., et al. (2012). Host-microbe interactions have shaped the genetic architecture of inflammatory bowel disease. Nature. 491(7422):119-24.
221. Karrasch, T. & Jobin, C. (2008). NF-kappaB and the intestine: friend or foe? Inflamm Bowel Dis 14(1):114-124.
222. Karsunky, H., Merad, M., Cozzio, A., Weissman, IL., Manz, MG. (2003). Flt3 ligand regulates dendritic cell development from Flt3+ lymphoid and myeloid-committed progenitors to Flt3+ dendritic cells in vivo. J Exp Med; 198: 305–313.
223. Kaser, A., Lee, A. H., Franke, A., Glickman, J. N., Zeissig, S., Tilg, H., Nieuwenhuis, E. E., Higgins, D. E., Schreiber, S., Glimcher, L. H., & Blumberg, R. S. (2008). XBP1 links ER stress to intestinal inflammation and confers genetic risk for human inflammatory bowel disease. *Cell*, *134*(5), 743–756.
224. Kau, A.L., Ahern, P.P., Griffin, N.W., Goodman, A.L., & Gordon, J.I. (2011). Human nutrition, the gut microbiome and the immune system. Nature 474(7351):327-336.
225. Kayagaki, N., et al. (2011). Non-canonical inflammasome activation targets caspase-11. Nature 479, 117–121.

226. Kayagaki, N., et al. (2013). Noncanonical inflammasome activation by intracellular LPS independent of TLR4. Science (80-.). 341, 1246–1249.
227. Kenyon, C., Chang, J., Gensch, E., Rudner, A., & Tabtiang, R. (1993). A C. elegans mutant that lives twice as long as wild type. Nature, 366(6454), 461–464.
228. Keshet, Y., and Seger, R. (2010). The MAP kinase signaling cascades: a system of hundreds of components regulates a diverse array of physiological functions. Methods 143 Mol. Biol. 661, 3–38.
229. Khan, N., et al. (2020). M. tuberculosis Reprograms Hematopoietic Stem Cells to Limit Myelopoiesis and Impair Trained Immunity. Cell, 183(3), 752–770.e22.
230. Kidd, P. (2003). Th1/Th2 balance: the hypothesis, its limitations, and implications for health and disease. Altern Med Rev. 8(3):223-46.
231. Kiel, M. J., He, S., Ashkenazi, R., Gentry, S. N., Teta, M., Kushner, J. A., Jackson, T. L., & Morrison, S. J. (2007). Hematopoietic stem cells do not asymmetrically segregate chromosomes or retain BrdU. Nature, 449(7159), 238–242.
232. Kiesler, P., Fuss, I. J., & Strober, W. (2015). Experimental Models of Inflammatory Bowel Diseases. Cellular and molecular gastroenterology and hepatology, 1(2), 154–170.
233. Kinashi, Y., & Hase, K. (2021). Partners in Leaky Gut Syndrome: Intestinal Dysbiosis and Autoimmunity. Front Immunol. 12:673708.
234. Kindt, T.J., Goldsby, R.A., Osborne, B.A., and Kuby, J. (2012). Kuby immunology, 6th edition (New York: W.H. Freeman).
235. Kirsner, J.B. (1961). Experimental "colitis" with particular reference to hypersensitivity reactions in the colon. Gastroenterology, 40, pp. 307-312
236. Klein Geltink, R. I., et al.(2017). Mitochondrial Priming by CD28. Cell, 171(2), 385–397.e11. https://doi.org/10.1016/j.cell.2017.08.018
237. Kobayashi, K.S., Chamaillard, M., Ogura, Y., Henegariu, O., Inohara, N., Nuñez, G., Flavell, R.A. (2005). Nod2-dependent regulation of innate and adaptive immunity in the intestinal tract. Science.;307(5710):731-4.
238. Korn, T., Bettelli, E., Gao, W., Awasthi, A., Jäger, A., Strom, T. B., Oukka, M., & Kuchroo, V. K. (2007). IL-21 initiates an alternative pathway to induce proinflammatory T(H)17 cells. Nature, 448(7152), 484–487.
239. Kornblau, S.M., Singh, N., Qiu, Y., Chen, W., Zhang, N., and Coombes, K.R. (2010). Highly phosphorylated FOXO3A is an adverse prognostic factor in acute myeloid leukemia. Clin. Cancer Res. 16, 1865–1874.
240. Kotlyarov, A., Neininger, A., Schubert, C., Eckert, R., Birchmeier, C., Volk, H.D., and Gaestel, M. (1999). MAPKAP kinase 2 is essential for LPS-induced TNF-α biosynthesis. Nat. Cell Biol. 1, 94–97.
241. Kuhn, R., Lohler, J., Rennick, D., Rajewsky, K., & Muller, W. (1993) Interleukin-10-deficient mice develop chronic enterocolitis. Cell 75(2):263-274.
242. Kurebayashi, Y., et al. (2012). PI3K-Akt-mTORC1-S6K1/2 axis controls Th17 differentiation by regulating Gfi1 expression and nuclear translocation of RORγ. Cell reports, 1(4), 360–373.
243. Lamkanfi, M., and Dixit, V.M. (2014). Mechanisms and functions of inflammasomes. Cell 157, 1013–1022.
244. Lamming, D.W., et al. (2012). Rapamycin-induced insulin resistance is mediated by mTORC2 loss and uncoupled from longevity. Science. 335:1638–1643.

245. Langrish, C. L., et al. (2005). IL-23 drives a pathogenic T cell population that induces autoimmune inflammation. The Journal of experimental medicine, 201(2), 233–240.
246. Laukoetter, M. G., Nava, P., & Nusrat, A. (2008). Role of the intestinal barrier in inflammatory bowel disease. *World journal of gastroenterology*, *14*(3), 401–407.
247. Lanzavecchia, A, and F Sallusto. 2001. "The Instructive Role of Dendritic Cells on T Cell Responses: Lineages, Plasticity and Kinetics." Curr Opin Immunol 13 (3): 291–98.
248. Lapid, K., Glait-Santar, C., Gur-Cohen, S., et al. (2012). Egress and Mobilization of Hematopoietic Stem and Progenitor Cells: A Dynamic Multi-facet Process. Cambridge (MA): Harvard Stem Cell Institute.
249. Laplante, M., Sabatini, D.M. (2012). mTOR signaling in growth control and disease. Cell 149: 274–293.
250. Laurence, A., et al. (2007). Interleukin-2 signaling via STAT5 constrains T helper 17 cell generation. Immunity. 26(3):371-81.
251. Lavelle, A., et al. (2015). Spatial variation of the colonic microbiota in patients with ulcerative colitis and control volunteers. Gut. 64:1553–61.
252. Le Chatelier, E., et al. (2013). Richness of human gut microbiome correlates with metabolic markers. Nature. 500:541–6.
253. Leach, M. W., Bean, A. G., Mauze, S., Coffman, R. L., & Powrie, F. (1996). Inflammatory bowel disease in C.B-17 scid mice reconstituted with the CD45RBhigh subset of CD4+ T cells. The American journal of pathology, 148(5), 1503–1515.
254. Lebeis, S.L., Bommarius, B., Parkos, C.A., Sherman, M.A., & Kalman, D. (2007). TLR signaling mediated by MyD88 is required for a protective innate immune response by neutrophils to Citrobacter rodentium. J Immunol 179(1):566-577.
255. Lebwohl, M. & Lebwohl, O. (1998). Cutaneous manifestations of inflammatory bowel disease Inflammatory bowel diseases, 4(2), pp. 142-148
256. Lee, J.C., et al. (2013). Human SNP links differential outcomes in inflammatory and infectious disease to a FOXO3-regulated pathway. Cell.155:57–69.
257. Lee JC, et al. (2017). Genome-wide association study identifies distinct genetic contributions to prognosis and susceptibility in Crohn's disease. Nat Genet 49(2):262-268.
258. Leibundgut-Landmann, S., et al. (2007). Syk- and CARD9-dependent coupling of innate immunity to the induction of T helper cells that produce interleukin 17. Nat Immunol. 8:630–638.
259. Lewis KL., et al. (2011). Notch2 receptor signaling controls functional differentiation of dendritic cells in the spleen and intestine. Immunity. 35(5):780-91..
260. Li, E., et al. (2012). Inflammatory bowel diseases phenotype, C. difficile and NOD2 genotype are associated with shifts in human ileum associated microbial composition. PLoS One. 7(6):e26284.
261. Li, J., Butcher, J., Mack, D. & Stintzi, A. (2015). Functional impacts of the intestinal microbiome in the pathogenesis of inflammatory bowel disease. Inflamm. Bowel Dis. 21, 139–153.
262. Li, L., and Clevers, H. (2010). Coexistence of quiescent and active adult stem cells in mammals. Science 327, 542–545.
263. Li, Y., et al. (2009). Genetic association of FOXO1A and FOXO3A with longevity trait in Han Chinese populations. Hum Mol Genet.18(24):4897-904.
264. Li, Z., Zhang, H., Chen, Y., Fan, L., & Fang, J. (2012). Forkhead transcription factor FOXO3a protein activates nuclear factor kappaB through B cell lymphoma/leukemia 10

(BCL10) protein and promotes tumor cell survival in serum deprivation. The Journal of biological chemistry 287(21):17737-17745.
265. Liew, F. Y., Girard, J. P. & Turnquist, H. R. (2016). Interleukin-33 in health and disease. Nat. Rev. Immunol. 16, 676–689.
266. Lin, A., Yao, J., Zhuang, L. et al. (2014). The FoxO–BNIP3 axis exerts a unique regulation of mTORC1 and cell survival under energy stress. Oncogene 33, 3183–3194.
267. Lin, L., Hron, J.D., & Peng, S.L. (2004). Regulation of NF-kappaB, Th activation, and autoinflammation by the forkhead transcription factor Foxo3a. Immunity. 21(2):203-213.
268. Linkermann, A., & Green, D.R. (2014). Necroptosis. N Engl J Med. 370(5):455-65.
269. Littman, D.R., Rudensky, A.Y.(2010). Th17 and regulatory T cells in mediating and restraining inflammation. Cell.140(6):845-58.
270. Liu, X. et al. (2013). Structural insights into the interaction of IL-33 with its receptors. Proc. Natl Acad. Sci. USA 110, 14918–14923.
271. Liu, X., et al. (2016). Tanshinone IIA Protects against Dextran Sulfate Sodium (DSS) Induced Colitis in Mice by Modulation of Neutrophil Infiltration and Activation. Oxid Med Cell Longev. 7916763.
272. Loftus, R.M., Finlay, D.K. (2016). Immunometabolism: Cellular Metabolism Turns Immune Regulator. J Biol Chem. 291(1):1-10.
273. Ludowyk, P. A., Willenborg, D. O., & Parish, C. R. (1992). Selective localisation of neuro-specific T lymphocytes in the central nervous system. Journal of neuroimmunology, 37(3), 237–250.
274. Luo, J., Liang, A., Liang, M., Xia, R., Rizvi, Y., Wang, Y., Cheng, J. (2016). Serum glucocorticoid-regulated kinase 1 blocks CKD-induced muscle wasting via inactivation of FoxO3a and SMAD2/3. J Am Soc Nephrol. 27(9):2797–808.
275. Luther, S., Cyster, J. (2001). Chemokines as regulators of T cell differentiation. Nat Immunol 2, 102–107.
276. MacDonald, T. T., Hutchings, P., Choy, M. Y., Murch, S., & Cooke, A. (1990). Tumour necrosis factor-alpha and interferon-gamma production measured at the single cell level in normal and inflamed human intestine. Clinical and experimental immunology, 81(2), 301–305.
277. Macpherson, A. J., & Uhr, T. (2004). Induction of protective IgA by intestinal dendritic cells carrying commensal bacteria. Science (New York, N.Y.), 303(5664), 1662–1665.
278. Mahida, Y. R., Kurlac, L., Gallagher, A., & Hawkey, C. J. (1991). High circulating concentrations of interleukin-6 in active Crohn's disease but not ulcerative colitis. Gut, 32(12), 1531–1534.
279. Mahida, Y.R., Wu, K., Jewell, D.P. (1989). Enhanced production of interleukin 1-beta by mononuclear cells isolated from mucosa with active ulcerative colitis of Crohn’s disease. Gut. 30:835–38. 10.1136/gut.30.6.835.
280. Mailloux, R.J., McBride, S.L., and Harper, M.-E. (2013a). Unearthing the secrets of mitochondrial ROS and glutathione in bioenergetics. Trends Biochem. Sci. 38, 592–602.
281. Mailloux, R.J., Seifert, E.L., Bouillaud, F., Aguer, C., Collins, S., and Harper, M.-E. (2011). Glutathionylation acts as a control switch for uncoupling proteins UCP2 and UCP3. J. Biol. Chem. 286, 21865–21875.
282. Makinoshima, H., et al. (2015). Signaling through the Phosphatidylinositol 3-Kinase (PI3K)/Mammalian Target of Rapamycin (mTOR) Axis Is Responsible for Aerobic

Glycolysis mediated by Glucose Transporter in Epidermal Growth Factor Receptor (EGFR)-mutated Lung Adenocarcinoma. The Journal of biological chemistry, 290(28), 17495–17504.
283. Malmberg, E.K., et al. (2006). Increased levels of mucins in the cystic fibrosis mouse small intestine, and modulator effects of the Muc1 mucin expression. Am J Physiol Gastrointest Liver Physiol. 291:G203–G210.
284. Manichanh, C., et al. (2006). Reduced diversity of faecal microbiota in Crohn's disease revealed by a metagenomic approach. Gut. 55:205–11.
285. Manichanh, C., et al. (2006). Reduced diversity of faecal microbiota in Crohn's disease revealed by a metagenomic approach. Gut. 55:205–11.
286. Marguerat, S., Macdonald, H.R., Kraehenbuhl, J.P. and Van Meerwijk, J.P.(1999). Protection from radiation-induced colitis requires MHC class II antigen expression by 201 cells of hemopoietic origin. Journal of immunology (Baltimore, Md.: 1950), 163(7), pp. 4033-4040
287. Marinkovic, D., Zhang, X., Yalcin, S., Luciano, J.P., Brugnara, C., Huber, T., and Ghaffari, S. (2007). Foxo3 is required for the regulation of oxidative stress in erythropoiesis. J. Clin. Invest. 117, 2133–2144.
288. Marshman, E., Booth, C., and Potten, C.S. (2002). The intestinal epithelial stem cell. Bioessays 24, 91–98.
289. Martin, S. J., & Henry, C. M. (2013). Distinguishing between apoptosis, necrosis, necroptosis and other cell death modalities. Methods, 61(2), 87-89.
290. Martinon, F., Burns, K., Tschopp, J. (2002). The inflammasome: a molecular platform triggering activation of inflammatory caspases and processing of proIL-beta. Mol Cell. 10(2):417-26.
291. Martinvalet, D., Zhu, P., & Lieberman, J. (2005). Granzyme A induces caspase-independent mitochondrial damage, a required first step for apoptosis. Immunity, 22(3), 355–370.
292. Mashayekhi, M., et al. (2011). CD8α(+) dendritic cells are the critical source of interleukin-12 that controls acute infection by Toxoplasma gondii tachyzoites. Immunity. 35(2):249-59.
293. Mason, K. L., Huffnagle, G. B., Noverr, M. C., & Kao, J. Y. (2008). Overview of gut immunology. Advances in Experimental Medicine and Biology, 635, 1–14.
294. Matsumoto, S., Okabe, Y., Setoyama, H., Takayama, K., Ohtsuka, J., Funahashi, H., Imaoka, A., Okada, Y., & Umesaki, Y. (1998). Inflammatory bowel disease-like enteritis and caecitis in a senescence accelerated mouse P1/Yit strain. Gut, 43(1), 71–78.
295. Mayer, C., Zhao, J., Yuan, X., & Grummt, I. (2004). mTOR-dependent activation of the transcription factor TIF-IA links rRNA synthesis to nutrient availability. Genes & development, 18(4), 423–434.
296. McGeachy, M. J., & Cua, D. J. (2008). Th17 cell differentiation: the long and winding road. Immunity, 28(4), 445–453.
297. McGeachy, M. J., Cua, D. J., & Gaffen, S. L. (2019). The IL-17 Family of Cytokines in Health and Disease. Immunity, 50(4), 892–906.
298. McGrath, K.E., Palis, J. (2005). Hematopoiesis in the yolk sac: more than meets the eye. Exp Hematol; 33: 1021–1028.
299. McNab, F., Mayer-Barber, K., Sher, A., Wack, A., and O'Garra, A. (2015). Type I interferons in infectious disease. Nat. Rev. Immunol. 15, 87–103.

300. Medzhitov, R. (2008). Origin and physiological roles of inflammation. Nature 454, 428–435. 168.
301. Medzhitov, R., and Janeway, C.A. (1997). Innate immunity: The virtues of a nonclonal system of recognition. Cell 91, 295–298
302. Medzhitov, R., and Janeway, C.A. (2000). How does the immune system distinguish self from nonself? Semin. Immunol. 12, 185–188.
303. Metlay, JP., Witmer-Pack, MD., Agger, R., Crowley, MT., Lawless, D., Steinman, RM. (1990). The distinct leukocyte integrins of mouse spleen dendritic cells as identified with new hamster monoclonal antibodies. J Exp Med.171(5):1753-71.
304. Michalek, R.D. and Rathmell, J.C. (2010), The metabolic life and times of a T cell. Immunological Reviews, 236: 190-202.
305. Mikkola, HK., Orkin, SH. (2006). The journey of developing hematopoietic stem cells. Development; 133: 3733–3744.
306. Mildner, A., and Jung, S. (2014). Development and Function of Dendritic Cell Subsets. Immunity 40, 642-656.
307. Mintz, R., Feller, E.R., Bahr, R.L. and Shah, S.A. (2004). Ocular manifestations of inflammatory bowel disease Inflammatory bowel diseases, 10(2), pp. 135-139
308. Mitroulis, I., et al. (2018). Modulation of Myelopoiesis Progenitors Is an Integral Component of Trained Immunity. Cell, 172(1-2), 147–161.e12.
309. Mittal, S.K. and Roche, P.A. (2015). Suppression of antigen presentation by IL-10. Curr Opin Immunol. 34:22-7.
310. Miyamoto, K., et al. (2007) Foxo3a is essential for maintenance of the hematopoietic stem cell pool. Cell Stem Cell 1, 101–112
311. Miyara, M., et al. (2005). Global natural regulatory T cell depletion in active systemic lupus erythematosus. J Immunol. 175:8392–8400.
312. Mizoguchi, A., Mizoguchi, E., Takedatsu, H., Blumberg, R. S., & Bhan, A. K. (2002). Chronic intestinal inflammatory condition generates IL-10-producing regulatory B cell subset characterized by CD1d upregulation. Immunity, 16(2), 219–230.
313. Mondal, K. & Kugathasan, S. (2017). IBD: Genetic differences in Crohn's disease susceptibility and outcome. Nat Rev Gastroenterol Hepatol 14(5):266-268.
314. Moore, K.W., de Waal Malefyt , R., Coffman, R.L., and O'Garra, A. (2001).Interleukin-10 and the interleukin-10 receptor. Annu Rev Immunol. 19:683-765.
315. Moore, K.W., O'Garra, A., de-Waal, M.R., Vieira, P., and Mosmann, T.R. (1993). Interleukin-10. AnnuRevImmunol, 11: 165-190.
316. Morrison, D.K. (2012). MAP kinase pathways. Cold Spring Harb. Perspect. Biol. 4.
317. Morrissey, P. J., Charrier, K., Braddy, S., Liggitt, D., & Watson, J. D. (1993). CD4+ T cells that express high levels of CD45RB induce wasting disease when transferred into congenic severe combined immunodeficient mice. Disease development is prevented by cotransfer of purified CD4+ T cells. The Journal of experimental medicine, 178(1), 237–244.
318. Mosmann, T.R., Cherwinski, H., Bond, M.W., Giedlin, M.A., Coffman, R.L. (1986). Two types of murine helper T cell clone. I. Definition according to profiles of lymphokine activities and secreted proteins. J Immunol.136(7):2348-57.
319. Mosmann, T.R., Coffman, R.L. (1989). TH1 and TH2 cells: different patterns of lymphokine secretion lead to different functional properties. Annu Rev Immunol. 7:145-73.

320. Mottawea, W., et al. (2016). Altered intestinal microbiota-host mitochondria crosstalk in new onset Crohn's disease. Nature communications, 7, 13419.
321. Mottet, C., Uhlig, H.H., Powrie, F. (2003). Cutting edge: cure of colitis by CD4+CD25+ regulatory T cells. J Immunol.170:3939–43.
322. Moussion, C., Ortega, N. & Girard, J. P. (2008). The IL-1-like cytokine IL-33 is constitutively expressed in the nucleus of endothelial cells and epithelial cells in vivo: a novel 'alarmin'? PLoS ONE 3, e3331.
323. Mukhopadhya, I., Hansen, R., Nicholl, C. E., Alhaidan, Y. A., Thomson, J. M., Berry, S. H., et al. (2011). A comprehensive evaluation of colonic mucosal isolates of Sutterella wadsworthensis from inflammatory bowel disease. PLoS ONE 6:e27076 10.1371/journal.pone.0027076
324. Murphy, P.M., Baggiolini, M., Charo, I.F., Hébert, C.A., Horuk, R., Matsushima, K., Miller, L.H., Oppenheim, J.J. & Power, C.A. (2000). International union of pharmacology. XXII. Nomenclature for chemokine receptors. Pharmacol Rev 52, 145–176.
325. Nakaya, M. et al. (2014). Inflammatory T cell responses rely on amino acid transporter ASCT2 facilitation of glutamine uptake and mTORC1 kinase activation. Immunity 40, 692–705.
326. Nava P, et al. (2010). Interferon-gamma regulates intestinal epithelial homeostasis through converging beta-catenin signaling pathways. Immunity, 32(3):392–402. doi: 10.1016/j.immuni.2010.03.001.
327. Nemoto, S., Takeda, K., Yu, Z.X., Ferrans, V.J., and Finkel, T. (2000). Role for mitochondrial oxidants as regulators of cellular metabolism. Mol. Cell. Biol. 20, 7311–7318.
328. Neurath MF. (2014). Cytokines in inflammatory bowel disease. Nat Rev Immunol. 14(5):329–342.
329. Nicholls, D.G., and Ferguson, S.J. (2002). Bioenergetics (Gulf Professional Publishing).
330. Nikolic, T., Dingjan, G.M., Leenen, P.J.M. and Hendriks, R.W. (2002), A subfraction of B220+ cells in murine bone marrow and spleen does not belong to the B cell lineage but has dendritic cell characteristics. Eur. J. Immunol., 32: 686-692.
331. Nitzan, O., Elias, M., Peretz, A., & Saliba, W. (2016). Role of antibiotics for treatment of inflammatory bowel disease. World journal of gastroenterology, 22(3), 1078–1087.
332. Norddahl, G.L., Pronk, C.J., Wahlestedt, M., Sten, G., Nygren, J.M., Ugale, A., Sigvardsson, M., Bryder, D. (2011). Accumulating mitochondrial DNA mutations drive premature hematopoietic aging phenotypes distinct from physiological stem cell aging. Cell Stem Cell 8: 499 – 510
333. Nowak, K., Killmer, K., Gessner, C., & Lutz, W. (2007). E2F-1 regulates expression of FOXO1 and FOXO3a. Biochimica et biophysica acta, 1769(4), 244–252.
334. Oeckinghaus, A., and Ghosh, S. (2009). The NF-kappaB family of transcription factors and its regulation. Cold Spring Harb. Perspect. Biol. 1.
335. Oka, A., et al. (2014). Role of regulatory B cells in chronic intestinal inflammation: association with pathogenesis of Crohn's disease. Inflammatory bowel diseases, 20(2), 315–328.
336. O'Neill, L. A., Kishton, R. J., & Rathmell, J. (2016). A guide to immunometabolism for immunologists. Nature reviews. Immunology, 16(9), 553–565.

337. Ono, S. J., Nakamura, T., Miyazaki, D., Ohbayashi, M., Dawson, M., & Toda, M. (2003). Chemokines: roles in leukocyte development, trafficking, and effector function. The Journal of allergy and clinical immunology, 111(6), 1185–1200.
338. Oochard, T.R., Wordsworth, B.P. and Jewell, D.P., (1998). Peripheral arthropathies in inflammatory bowel disease: their articular distribution and natural history Gut, 42(3), pp. 387-391.
339. Open Questions. Front Immunol. 6: p. 423.
340. Orning, P., Weng, D., Starheim, K., Ratner, D., Best, Z., Lee, B., Brooks, A., Xia, S., Wu, H., Kelliher, M.A. et al. (2018). Pathogen blockade of TAK1 triggers caspase-8-dependent cleavage of gasdermin D and cell death. Science 362: 1064–1069
341. Ottman, N., Reunanen, J., Meijerink, M., Pietila, T.E., Kainulainen, V., Klievink, J., et al. (2017). Pili-like proteins of Akkermansia muciniphila modulate host immune responses and gut barrier function. PLoS One. 12: e0173004.
342. Paik, J. H., Kollipara, R., Chu, G., Ji, H., Xiao, Y., Ding, Z., et al. (2007). FoxOs are lineage-restricted redundant tumor suppressors and regulate endothelial cell homeostasis. Cell, 128(2), 309 323.
343. Paik, J.H., et al. (2009) FoxOs cooperatively regulate diverse pathways governing neural stem cell homeostasis. Cell Stem Cell 5: 540 – 553.
344. Papayannopoulos, V. (2018). Neutrophil extracellular traps in immunity and disease. Nat Rev Immunol 18, 134–147.
345. Parada Venegas, D., et al. (2019). Short Chain Fatty Acids (SCFAs)-Mediated Gut Epithelial and Immune Regulation and Its Relevance for Inflammatory Bowel Diseases. Frontiers in immunology 10, 277. pa
346. Parameswaran, N., Patial, S. (2010). Tumor necrosis factor-alpha signaling in macrophages. Crit Rev Eukaryot Gene Expr.20(2):87-103.
347. Park, H., et al. (2005). A distinct lineage of CD4 T cells regulates tissue inflammation by producing interleukin 17. Nat Immunol. 6(11):1133-41.
348. Parkes, M., et al. (2007). Sequence variants in the autophagy gene IRGM and multiple other replicating loci contribute to Crohn's disease susceptibility. *Nature genetics, 39*(7), 830–832.
349. Parkin, J., and Cohen, B. (2001). An overview of the immune system. Lancet 357, 1777–1789.
350. Pasparakis, M., and Vandenabeele, P. (2015). Necroptosis and its role in inflammation. Nature 517, 311–320.
351. Pastille, E., et al. (2019). The IL-33/ST2 pathway shapes the regulatory T cell phenotype to promote intestinal cancer. Mucosal Immunol 12, 990–1003.
352. Patsoukis, N., Bardhan, K., Weaver, J., Herbel, C., Seth, P., Li, L., & Boussiotis, V. A. (2016). The role of metabolic reprogramming in T cell fate and function. Current trends in immunology, 17, 1–12.
353. Pauleau, A.L., & Murray, P.J. (2003). Role of NOD2 in the response of macrophages to toll-like receptor agonists. Mol Cell Biol.23(21):7531-9.
354. Pawlikowska, L., et al. (2009). Study of Osteoporotic Fractures. Association of common genetic variation in the insulin/IGF1 signaling pathway with human longevity. Aging Cell. 8(4):460-72.
355. Pearce, E. L., et al. (2009). Enhancing CD8 T cell memory by modulating fatty acid metabolism. Nature, 460(7251), 103–107.

356. Peck, B., Ferber, E. C., & Schulze, A. (2013). Antagonism between FOXO and MYC Regulates Cellular Powerhouse. Frontiers in oncology, 3, 96.
357. Penrose, H.M., et al. (2019). Loss of Forkhead Box O3 Facilitates Inflammatory Colon Cancer: Transcriptome Profiling of the Immune Landscape and Novel Targets. Cell Mol Gastroenterol Hepatol. 7(2):391-408.
358. Petvises, S. and O'Neill, H.C. (2012), Hematopoiesis leading to a diversity of dendritic antigen-presenting cell types. Immunol Cell Biol, 90: 372-378.
359. Pfeiffer, T., Schuster, S., & Bonhoeffer, S. (2001). Cooperation and competition in the evolution of ATP-producing pathways. Science (New York, N.Y.), 292(5516), 504–507.
360. Piccirillo, C.A. (2020). Transcriptional and translational control of Foxp3+ regulatory T cell functional adaptation to inflammation. Curr Opin Immunol. 67:27-35.
361. Pieper, K.., Grimbacher, B., Eibel, H. (2013). B-cell biology and development. J. Allergy Clin. Immunol. 131 (4), pp. 959-971.
362. Platanias, L.C. (2005). Mechanisms of type-I- and type-II-interferon-mediated signalling. Nat. Rev. Immunol. 5, 375–386.
363. Podolsky, D.K. (2002). Inflammatory bowel disease. N Engl J Med. 347:417–29.
364. Pop, S.M., Wong, C.P., Culton, D.A., Clarke, S.H., Tisch, R. (2005). Single cell analysis shows decreasing FoxP3 and TGF-β 1 coexpressing CD4+CD25+ regulatory T cells during autoimmune diabetes. J Exp Med. 201:1333–46.
365. Porstmann, T., Santos, C. R., Lewis, C., Griffiths, B., & Schulze, A. (2009). A new player in the orchestra of cell growth: SREBP activity is regulated by mTORC1 and contributes to the regulation of cell and organ size. Biochemical Society transactions, 37(Pt 1), 278–283.
366. Porter, C. K., Tribble, D. R., Aliaga, P. A., Halvorson, H. A., & Riddle, M. S. (2008). Infectious gastroenteritis and risk of developing inflammatory bowel disease. Gastroenterology, 135(3), 781–786.
367. Pott, J., Kabat, A. M., & Maloy, K. J. (2018). Intestinal Epithelial Cell Autophagy Is Required to Protect against TNF-Induced Apoptosis during Chronic Colitis in Mice. Cell host & microbe, 23(2), 191–202.e4.
368. Potten, C.S. (1977). Extreme sensitivity of some intestinal crypt cells to X and gamma irradiation. Nature 269, 518–521.
369. Powrie, F., Leach, M.W., Mauze, S., Caddle, L.B. and Coffman, R.L., (1993). Phenotypically distinct subsets of CD4+ T cells induce or protect from chronic intestinal inflammation in C. B-17 scid mice. International immunology, 5(11), pp. 1461-1471.
370. Powrie, F., Leach, M.W., Mauze, S., Menon, S., Caddle, L.B. and Coffman, R.L., (1994). Inhibition of Th1 responses prevents inflammatory bowel disease in scid mice reconstituted with CD45RBhi CD4+ T cells. Immunity, 1(7), pp. 553-562.
371. Proudfoot A. E. (2002). Chemokine receptors: multifaceted therapeutic targets. Nature reviews. Immunology, 2(2), 106–115.
372. Puel, A., Cypowyj, S., Bustamante, J., Wright, J.F., Liu, L., Kim, H.K., et al. (2011). Chronic mucocutaneous candidiasis in humans with inborn errors of interleukin-17 immunity. Science. 332:65–68.
373. Qiu, J., et al. (2019). Acetate Promotes T Cell Effector Function during Glucose Restriction. Cell reports, 27(7), 2063–2074.e5.
374. Raj, V. and Lichtenstein, D.R. (1999). Hepatobiliary manifestations of inflammatory bowel disease Gastroenterology clinics of North America, 28(2), pp. 491-513.

375. Rath HC, et al. (2001). Different subsets of enteric bacteria induce and perpetuate experimental colitis in rats and mice. Infect Immun. 69:2277–85.
376. Redza-Dutordoir, M., Averill-Bates, D.A. (2016). Activation of apoptosis signalling pathways by reactive oxygen species. Biochim Biophys Acta. 1863(12):2977-2992.
377. Reinisch, W., et al. (1999). Clinical relevance of serum interleukin-6 in Crohn's disease: single point measurements, therapy monitoring, and prediction of clinical relapse. The American journal of gastroenterology, 94(8), 2156–2164.
378. Reißig, S., Tang, Y., Nikolaev, A. et al. (2017). Elevated levels of Bcl-3 inhibits Treg development and function resulting in spontaneous colitis. Nat Commun 8, 15069.
379. Rena, G., Woods, Y. L., Prescott, A. R., Peggie, M., Unterman, T. G., Williams, M. R., Cohen, P. (2002). Two novel phosphorylation sites on FKHR that are critical for its nuclear exclusion. EMBO J 21(9):2263-71.
380. Renault, V.M., et al. (2009). FoxO3 regulates neural stem cell homeostasis. Cell Stem Cell 5: 527 – 539
381. Rennick, D.M., Fort, M.M. and Davidson, N.J. (1997). Studies with IL-10-/- mice: an overview. Journal of leukocyte biology, 61(4), pp. 389-396.
382. Rimoldi, M., et al. (2005). Intestinal immune homeostasis is regulated by the crosstalk between epithelial cells and dendritic cells. Nat Immunol. 6:507–514.
383. Riou, C., Yassine-Diab, B., Van grevenynghe, J., Somogyi, R., Greller, L. D., Gagnon, D., Gimmig, S., Wilkinson, P., Shi, Y., Cameron, M. J., Campos-Gonzalez, R., Balderas, R. S., Kelvin, D., Sekaly, R. P., & Haddad, E. K. (2007). Convergence of TCR and cytokine signaling leads to FOXO3a phosphorylation and drives the survival of CD4+ central memory T cells. *The Journal of experimental medicine*, *204*(1), 79–91.
384. Rivera, C.A., et al. (2021). Epithelial colonization by gut dendritic cells promotes their functional diversification. Immunity. 55(1):129-144.e8.
385. Rochman, I., Paul, W.E., Ben-Sasson, S.Z. (2005). IL-6 increases primed cell expansion and survival. J Immunol. 174:4761–4767.
386. Romagnani, S. (1996). Understanding the role of Th1/Th2 cells in infection. Trends Microbiol. 4(12):470-3..
387. Rosenbauer, F., and Tenen, D.G. (2007). Transcription factors in myeloid development: balancing differentiation with transformation. Nat. Rev. Immunol. 7, 105–117.
388. Rubtsov, Y.P., et al. (2008). Regulatory T cell-derived interleukin-10 limits inflammation at environmental interfaces. Immunity.28(4):546-58.
389. Rutter, M.D., et al. (2006). Thirty-year analysis of a colonoscopic surveillance program for neoplasia in ulcerative colitis Gastroenterology, 130(4), pp. 1030-1038.
390. Sabat, R., Grutz, G., Warszawska, K., Kirsch, S., Witte, E., Wolk, K., Geginat, J. (2010). Biology of interleukin-10. Cytokine Growth Factor Rev. 21:331–344. 10.1016/j.cytogfr.2010.09.002
391. Sagiv, J. Y., et al. (2015). Phenotypic diversity and plasticity in circulating neutrophil subpopulations in cancer. Cell reports, 10(4), 562–573.
392. Sagiv, J. Y., Voels, S., & Granot, Z. (2016). Isolation and Characterization of Low- vs. High-Density Neutrophils in Cancer. Methods in molecular biology (Clifton, N.J.), 1458, 179–193.
393. Saito, Y., et al. (2010) Regulation by SIRPα of dendritic cell homeostasis in lymphoid tissues. Blood 116:3517–3525.

394. Sakamaki, J., Daitoku, H., Yoshimochi, K., Miwa, M., Fukamizu, A. (2009). Regulation of FOXO1-mediated transcription and cell proliferation by PARP-1. Biochem Biophys Res Commun 382(3):497-502.
395. Saklatvala, J., Dean, J., Clark, A. (2003). Control of the expression of inflammatory response genes. Biochem Soc Symp. 70: 95–106
396. Salih, D. A., et al. (2012). FoxO6 regulates memory consolidation and synaptic function. Genes & development, 26(24), 2780–2801.
397. Sancak, Y., et al. (2007) PRAS40 is an insulin-regulated inhibitor of the mTORC1 protein kinase. Molecular cell, 25: 903–915.
398. Santoru ML, et al. (2017). Cross sectional evaluation of the gut-microbiome metabolome axis in an Italian cohort of IBD patients. Sci Rep. 7:9523.
399. Saraiva, M., and O'Garra, A. (2010). The regulation of IL-10 production by immune cells. Nat Rev Immunol.10(3):170-81.
400. Sarbassov, D.D., Ali, S.M., Sengupta, S., Sheen, J.H., Hsu, P.P., Bagley, A.F., Markhard, A.L.,and Sabatini, D.M. (2006). Prolonged Rapamycin Treatment Inhibits mTORC2 Asse mbly and 101 Akt/PKB. Mol. Cell 22, 159–168
401. Sarhan, J., et al. (2018). Caspase-8 induces cleavage of gasdermin D to elicit pyroptosis during Yersinia infection. Proceedings of the National Academy of Sciences of the United States of America, 115(46), E10888–E10897.
402. Sartor, R.B. (1990). Role of intestinal microflora in initiation and perturbation of inflammatory bowel disease. Can. J. Gastroenterol. 4:271-277.
403. Saruta, M., Yu, Q. T., Fleshner, P. R., Mantel, P. Y., Schmidt-Weber, C. B., Banham, A. H., & Papadakis, K. A. (2007). Characterization of FOXP3+CD4+ regulatory T cells in Crohn's disease. Clinical immunology (Orlando, Fla.), 125(3), 281–290.
404. Sarvetnick, N., et al. (1990). Loss of pancreatic islet tolerance induced by beta-cell expression of interferon-gamma. Nature. 346:844–7.
405. Satpathy AT, et, al. (2013). Notch2-dependent classical dendritic cells orchestrate intestinal immunity to attaching-and-effacing bacterial pathogens. Nat Immunol. 14(9):937-48.
406. Sawitzki B., et al. (2005). IFN-gamma production by alloantigen-reactive regulatory T cells is important for their regulatory function in vivo. J. Exp. Med. 2011925–1935.
407. Saxton, R. A. & Sabatini, D. M. (2017). mTOR signaling in growth, metabolism, and disease. Cell, 168, 960–976.
408. Scheller, J., Chalaris. A., Schmidt-Arras, D., and Rose-John, S. (2011). The pro- and anti-inflammatory properties of the cytokine interleukin-6. Biochim Biophys Acta. 1813(5):878-88.
409. Schiering, C. et al. (2014). The alarmin IL-33 promotes regulatory T cell function in the intestine. Nature 513, 564–568.
410. Schmitt, N., & Ueno, H. (2015). Regulation of human helper T cell subset differentiation by cytokines. Current opinion in immunology, 34, 130–136.
411. Schopf LR, Hoffmann KF, Cheever AW, Urban JF, Jr, Wynn TA. (2002). IL-10 is critical for host resistance and survival during gastrointestinal helminth infection. J. Immunol. 168:2383–2392
412. Schreiber, S., Nikolaus, S., & Hampe, J. (1998). Activation of nuclear factor kappa B inflammatory bowel disease. Gut 42(4):477-484.
413. Schroder, K., and Tschopp, J. (2010). The inflammasomes. Cell. 19;140(6):821-32.

414. Schultze, J. L., & Beyer, M. (2016). Myelopoiesis Reloaded: Single-Cell Transcriptomics Leads the Way. Immunity, 44(1), 18–20.
415. Scott, C. L., Tfp, Z. M., Beckham, K. S., Douce, G., & Mowat, A. M. (2014). Signal regulatory protein alpha (SIRPα) regulates the homeostasis of CD103(+) CD11b(+) DCs in the intestinal lamina propria. *European journal of immunology, 44*(12), 3658–3668.
416. Sellon RK, et al. (1998). Normal enteric bacteria are necessary for the development of spontaneous colitis and immune system activation in IL-10 deficient mice. Infect Immun. 66:5224–31.
417. Shats, I., Gatza, M. L., Liu, B., Angus, S. P., You, L., & Nevins, J. R. (2013). FOXO transcription factors control E2F1 transcriptional specificity and apoptotic function. Cancer research, 73(19), 6056–6067.
418. Shi, C., Pamer E. G. (2011). Monocyte recruitment during infection and inflammation. Nat. Rev. Immunol. 11: 762–774.
419. Shi, J., Zhao, Y., Wang, Y., Gao, W., Ding, J., Li, P., Hu, L., and Shao, F. (2014). Inflammatory caspases are innate immune receptors for intracellular LPS. Nature 514, 187–192.
420. Shimobayashi, M., Hall, M. (2014). Making new contacts: the mTOR network in metabolism and signaling crosstalk. Nat Rev Mol Cell Biol 15, 155–162.
421. Shin, J., et al. (2019). Elucidation of Akkermansia muciniphila probiotic traits driven by Mucin depletion. Front Microbiol. 10:1137.
422. Shin, N. R., Whon, T. W., Bae, J. W. (2015). Proteobacteria: microbial signature of dysbiosis in gut microbiota. Trends Biotechnol. 33 496–503. 10.1016/j.tibtech.2015.06.011
423. Shortman, K., and Liu, Y.J. (2002). Mouse and human dendritic cell subtypes. Nat Rev Immunol 2, 151-161.
424. Shtrichman, R., and Samuel, C.E. (2001). The role of gamma interferon in antimicrobial immunity. Curr. Opin. Microbiol. 4, 251–259.
425. Simsek, T., et al. (2010) The distinct metabolic profile of hematopoietic stem cells reflects their location in a hypoxic niche. Cell Stem Cell 7: 380 – 390
426. Sinclair, L. V., Rolf, J., Emslie, E., Shi, Y. B., Taylor, P. M., & Cantrell, D. A. (2013). Control of amino-acid transport by antigen receptors coordinates the metabolic reprogramming essential for T cell differentiation. Nature immunology, 14(5), 500–508.
427. Singh, R.K., Najmi, A.K., Dastidar, S.G. (2017). Biological functions and role of mitogen-activated protein kinase activated protein kinase 2 (MK2) in inflammatory diseases. Pharmacol Rep. 69(4):746-756.
428. Singh, V.K., Mehrotra, S., Agarwal, S.S. (1999). The paradigm of Th1 and Th2 cytokines: its relevance to autoimmunity and allergy. Immunol Res. 20(2):147-61.
429. Siska, P. J., et al. (2016). Fluorescence-based measurement of cystine uptake through xCT shows requirement for ROS detoxification in activated lymphocytes. Journal of immunological methods, 438, 51–58.
430. Slack, E., et al. (2009). Innate and adaptive immunity cooperate flexibly to maintain host-microbiota mutualism. Science (New York, N.Y.), 325(5940), 617–620.
431. Smith, P. D., Smythies, L. E., Shen, R., Greenwell-Wild, T., Gliozzi, M., & Wahl, S. M. (2011). Intestinal macrophages and response to microbial encroachment. Mucosal immunology, 4(1), 31–42.

432. Smith, P.M., et al. (2013). The microbial metabolites, short-chain fatty acids, regulate colonic Treg cell homeostasis. Science 341, 569-573.
433. Snoeks, L., Weber, C. R., Wasland, K., Turner, J. R., Vainder, C., Qi, W., & Savkovic, S. D. (2009). Tumor suppressor FOXO3 participates in the regulation of intestinal inflammation. Laboratory investigation; a journal of technical methods and pathology, 89(9), 1053–1062.
434. Sonnenburg, J. L., Xu, J., Leip, D. D., Chen, C. H., Westover, B. P., Weatherford, J., Buhler, J. D., & Gordon, J. I. (2005). Glycan foraging in vivo by an intestine-adapted bacterial symbiont. Science (New York, N.Y.), 307(5717), 1955–1959.
435. Spencer, S. D., Di Marco, F., Hooley, J., Pitts-Meek, S., Bauer, M., Ryan, A. M., Sordat, B., Gibbs, V. C., & Aguet, M. (1998). The orphan receptor CRF2-4 is an essential subunit of the interleukin 10 receptor. *The Journal of experimental medicine*, *187*(4), 571–578.
436. Spits, H., & Cupedo, T. (2012). Innate lymphoid cells: emerging insights in development, lineage relationships, and function. Annual Review of Immunology, 30, 647–675.
437. Srinivasan, R., Chinyu, G., Lichtenstein, G.R. (2003). Medical therapy for Crohn's disease. The clinician's guide to inflammatory bowel disease. G. R. Lichtenstein. Thorofare, Slack Incorporated: 221-254.
438. Steinman, L. (2010). Mixed results with modulation of TH-17 cells in human autoimmune diseases. Nat Immunol. 11(1):41–44.
439. Steinman, RM., Kaplan, G., Witmer, MD., Cohn, ZA. (1979). Identification of a novel cell type in peripheral lymphoid organs of mice. V. Purification of spleen dendritic cells, new surface markers, and maintenance in vitro. J Exp Med.149(1):1-16.
440. Sturlan, S., Oberhuber, G., Beinhauer, B.G., Tichy, B., Kappel, S., Wang, J. and Rogy, M.A. (2001). Interleukin-10-deficient mice and inflammatory bowel disease associated cancer development. Carcinogenesis, 22(4), pp. 665-671.
441. Sugimoto, K., Ogawa, A., Mizoguchi, E., Shimomura, Y., Andoh, A., Bhan, A. K., Blumberg, R. S., Xavier, R. J., & Mizoguchi, A. (2008). IL-22 ameliorates intestinal inflammation in a mouse model of ulcerative colitis. *The Journal of clinical investigation*, *118*(2), 534–544.
442. Sullivan, J.A., Kim, E.H., Plisch, E.H., Peng, S.L., Suresh, M. (2012). FOXO3 regulates CD8 T cell memory by T cell-intrinsic mechanisms. PLoSPathog. 8:e1002533.
443. Summers, C., et al. (2010). Neutrophil kinetics in health and disease. Trends Immunol. 31(8): p. 318-24.
444. Sundberg, J. P., Elson, C. O., Bedigian, H., & Birkenmeier, E. H. (1994). Spontaneous, heritable colitis in a new substrain of C3H/HeJ mice. Gastroenterology, 107(6), 1726–1735.
445. Sunderkotter, C., et al. (2004). Subpopulations of mouse blood monocytes differ in maturation stage and inflammatory response. J Immunol. 172(7): p. 4410-7.
446. Sung, J. H., et al. (2012). Chemokine guidance of central memory T cells is critical for antiviral recall responses in lymph nodes. Cell, 150(6), 1249–1263.
447. Sutherland, L. R., Ramcharan, S., Bryant, H., & Fick, G. (1990). Effect of cigarette smoking on recurrence of Crohn's disease. Gastroenterology, 98(5Pt1),1123–1128.
448. Sutherland, L., et al. (1991). Double-blind, placebo-controlled trial of metronidazole in Crohn's disease. Gut; 32: 1071-1075.
449. Szondy, Z., Newsholme, E.A. (1989). The effect of glutamine concentration on the activity of carbamoyl-phosphate synthase II and on the incorporation of [3H]thymidine into DNA

in rat mesenteric lymphocytes stimulated by phytohaemagglutinin. Biochem J.261:979–983.
450. Tanaka, T., Narazaki, M., & Kishimoto, T. (2014). IL-6 in inflammation, immunity, and disease. 47 Cold Spring Harbor Perspectives in Biology, 6(10), a016295.
451. Taylor, C. T., and Colgan, S. P. (2007) Hypoxia and gastrointestinal disease. J. Mol. Med. (Berl.) 85, 1295–1300
452. Taylor, R.C., Cullen, S.P., Martin, S.J. (2008). Apoptosis: controlled demolition at the cellular level. Nat Rev Mol Cell Biol. 9(3):231-41.
453. Teague, T.K., Marrack, P., Kappler, J.W., Vella, A.T. (1997). IL-6 rescues resting mouse T cells from apoptosis. J Immunol. 158:5791–5796.
454. Thomas, G., et al. (2015). Nonclassical patrolling monocyte function in the vasculature. Arterioscler Thromb Vasc Biol. 35(6): p. 1306-16.
455. Tothova, Z., et al. (2007) FoxOs are critical mediators of hematopoietic stem cell resistance to physiologic oxidative stress. Cell 128: 325 – 339
456. Tran, H., Brunet, A., Grenier, J.M., Datta, S.R., Fornace, A.J., DiStefano, P.S., Chiang, L.W., and Greenberg, M.E. (2002). DNA Repair Pathway Stimulated by the Forkhead Transcription Factor FOXO3a Through the Gadd45 Protein. Science 296, 530–534.
457. Travassos, L.H., et al. (2010). Nod1 and Nod2 direct autophagy by recruiting ATG16L1 to the plasma membrane at the site of bacterial entry. Nat Immunol. 11(1):55-62.
458. Turner, D., Zlotkin, S. H., Shah, P. S., & Griffiths, A. M. (2009). Omega 3 fatty acids (fish oil) for maintenance of remission in Crohn's disease. The Cochrane database of systematic reviews, (1), CD006320.
459. Tussiwand,R., et al. (2015). Klf4 expression in conventional dendritic cells is required for T helper 2 cell responses. Immunity. 42 pp. 916-928, 10.1016/j.immuni.2015.04.017
460. Tuteja, G., Kaestner, K. H. (2007a). SnapShot: forkhead transcription factors I. Cell. 130(6):1160.
461. Tuteja, G., Kaestner, K. H. (2007b). SnapShot: forkhead transcription factors II. Cell 131(1):192.
462. Tzelepis, F., Joseph, J., Haddad, E. K., Maclean, S., Dudani, R., Agenes, F., Peng, S. L., Sekaly, R. P., & Sad, S. (2013). Intrinsic role of FoxO3a in the development of CD8+ T cell memory. *Journal of immunology (Baltimore, Md. : 1950)*, *190*(3), 1066–1075.
463. Valko, M., Leibfritz, D., Moncol, J., Cronin, M.T.D., Mazur, M., and Telser, J. (2007). Free radicals and antioxidants in normal physiological functions and human disease. Int. J. Biochem. Cell Biol. 39, 44–84.
464. Van der Flier, L. G., & Clevers, H. (2009). Stem cells, self-renewal, and differentiation in the intestinal epithelium. Annual review of physiology, 71, 241–260.
465. Van Eeden, S. F. & Sin, D. D. (2013). Oxidative stress in chronic obstructive pulmonary disease: a lung and systemic process. 20 27–29.
466. Vantourout, P., & Hayday, A. (2013). Six-of-the-best: unique contributions of γδ T cells to immunology. Nature reviews. Immunology, 13(2), 88–100.
467. Varol, C., Mildner, A., and Jung, S. (2015). Macrophages: development and tissue specialization. Annu Rev Immunol. 33: p. 643-75.
468. Verma, R., Verma, N., Paul, J. (2013). Expression of inflammatory genes in the colon of ulcerative colitis patients varies with activity both at the mRNA and protein level. Eur Cytokine Netw. 24(3):130–138.

469. Vester-Andersen, M.K., Mirsepasi-Lauridsen, H.C., Prosberg, M.V., Mortensen, C.O., Trager, C., Skovsen, K., Thorkilgaard, T., Nojgaard, C., Vind, I., Krogfelt, K.A., et al. (2019). Increased abundance of proteobacteria in aggressive Crohn's disease seven years after diagnosis. Sci Rep 9, 13473.
470. Vester-Andersen, M.K., et al. (2019). Increased abundance of proteobacteria in aggressive Crohn's disease seven years after diagnosis. Sci Rep. 9:13473.
471. Visekruna, A., et al. (2006) Proteasome-mediated degradation of IkappaBalpha and processing of p105 in Crohn disease and ulcerative colitis. The Journal of clinical investigation 116(12):3195-3203.
472. Von Freeden-Jeffry, U., Davidson, N., Wiler, R., Fort, M., Burdach, S. and Murray, R., 1998. IL-7 deficiency prevents development of a non-T cell non-B cell mediated colitis. Journal of immunology (Baltimore, Md.: 1950), 161(10), pp. 5673-5680
473. Wan B., et al. (2006). Aberrant regulation of synovial T cell activation by soluble co-stimulatory molecules in rheumatoid arthritis. J. Immunol. 177:8844–8850.
474. Wang Z., et al. (2006). Role of IFN-γ in induction of Foxp3 and conversion of CD4+ CD25– T cells to CD4+ Tregs. J. Clin. Invest. 116:2434–2441.
475. Wang, F., Nguyen, M., Qin, F.X., Tong, Q. (2007). SIRT2 deacetylates FOXO3a in response to oxidative stress and caloric restriction. Aging Cell. 6(4):505–14.
476. Wang, J. X., et al. (2012). Ly6G ligation blocks recruitment of neutrophils via a β2-integrin-dependent mechanism. Blood, 120(7), 1489–1498.
477. Wang, K., Lin, Z. Q., Long, B., Li, J. H., Zhou, J., Li, P. F. (2011). Cardiac hypertrophy is positively regulated by miR-23a. J Biol Chem PMID: 22084234.
478. Washio K, et al. (2015) Dendritic cell SIRPα regulates homeostasis of dendritic cells in lymphoid organs. Genes Cells 20:451–463
479. Weaver, C.T., Hatton, R.D., Mangan, P.R., Harrington, L.E. (2007). IL-17 family cytokines and the expanding diversity of effector T cell lineages. Annu Rev Immunol. 25:821–852.
480. Weigel, D., Jackle, H. (1990). The fork head domain: a novel DNA binding motif of eukaryotic transcription factors? Cell 63, 455–456.
481. Weigel, D., Jurgens, G., Kuttner, F., Seifert, E. and Jackle, H. (1989). The homeotic gene fork head encodes a nuclear protein and is expressed in the terminal regions of the Drosophila embryo. Cell 57, 645–658.
482. Weigmann, B., Tubbe, I., Seidel, D., Nicolaev, A., Becker, C., Neurath, MF. (2007). Isolation and subsequent analysis of murine lamina propria mononuclear cells from colonic tissue. Nat Protoc.2:2307–11.
483. Wheelock, E.F. (1965). Interferon-like virus-inhibitor induced in human leukocytes by phytohemagglutinin. Science 149, 310-1.
484. Willcox, B.J., et al. (2008). FOXO3A genotype is strongly associated with human longevity. Proc Natl Acad Sci U S A.105(37):13987-92.
485. Williams, L., Bradley, L., Smith, A., Foxwell, B. (2004). Signal transducer and activator of transcription 3 is the dominant mediator of the anti-inflammatory effects of IL-10 in human macrophages. J Immunol. 172:567–76.
486. Wilson, A., et al. (2008). Hematopoietic stem cells reversibly switch from dormancy to self-renewal during homeostasis and repair. Cell; 135: 1118–1129.

487. Wilson, M.K., McWhirter. S.M., Amin, R.H., Huang, D., and Schlissel, M.S. (2010). Abelson virus transformation prevents TRAIL expression by inhibiting FoxO3a and NF-kappaB. Mol Cells. 29:333-341.
488. Winston, B.W., Chan, E.D., Johnson, G.L., Riches, D.W. (1997). Activation of p38mapk, MKK3, and MKK4 by TNF-alpha in mouse bone marrow-derived macrophages. J Immunol. 159: 4491–7.
489. Wirtz, S., & Neurath, M. F. (2000). Animal models of intestinal inflammation: new insights into the molecular pathogenesis and immunotherapy of inflammatory bowel disease. International journal of colorectal disease, 15(3), 144–160.
490. Wirtz, S., & Neurath, M. F. (2007). Mouse models of inflammatory bowel disease. Advanced drug delivery reviews, 59(11), 1073–1083.
491. Wong, H.K., Veremeyko, T., Patel, N., Lemere, C.A., Walsh, D.M., Esau, C., Vanderburg, C., Krichevsky, A.M. (2013). De-repression of FOXO3a death axis by microRNA-132 and -212 causes neuronal apoptosis in Alzheimer's disease. Hum Mol Genet. 22(15):3077-92.
492. Wu, C., Yosef, N., Thalhamer, T., Zhu, C., Xiao, S., Kishi, Y., Regev, A., Kuchroo, V.K. (2013). Induction of pathogenic TH17 cells by inducible salt-sensing kinase SGK1. (2013). Nature. ;496(7446):513-7.
493. Wyllie, A. H., Kerr, J. F., & Currie, A. R. (1980). Cell death: the significance of apoptosis. Int Rev Cytol, 68, 251-306
494. Xavier, R.J., Podolsky, D.K. (2007). Unravelling the pathogenesis of inflammatory bowel disease. Nature. 448:427–34.
495. Xiang, L., Mou, J., Shao, B., Wei, Y., Liang, H., Takano, N., et al. (2019). Glutaminase 1 expression in colorectal cancer cells is induced by hypoxia and required for tumor growth, invasion, and metastatic colonization. Cell death Dis. 10:40.
496. Yalcin, S., Marinkovic, D., Mungamuri, S. K., Zhang, X., Tong, W., Sellers, R., & Ghaffari, S. (2010). ROS-mediated amplification of AKT/mTOR signalling pathway leads to myeloproliferative syndrome in Foxo3(-/-) mice. The EMBO journal, 29(24), 4118–4131.
497. Yalcin, S., Zhang, X., Luciano, J. P., Mungamuri, S. K., Marinkovic, D., Vercherat, C., Sarkar, A., Grisotto, M., Taneja, R., and Ghaffari, S. (2008) Foxo3 is essential for the regulation of ataxia telangiectasia mutated and oxidative stress-mediated homeostasis of hematopoietic stem cells. J. Biol.Chem. 283, 25692–25705
498. Yamamoto, M., Yoshizaki, K., Kishimoto, T., & Ito, H. (2000). IL-6 is required for the development of Th1 cell-mediated murine colitis. Journal of immunology (Baltimore, Md.: 1950), 164(9), 4878–4882.
499. Yang, H., Rudge, D.G., Koos, J.D., Vaidialingam, B., Yang, H.J., and Pavletich, N.P. (201 3). mTOR kinase structure, mechanism and regulation. Nature 497, 217–223.
500. Yang, J.Y., Zong, C.S., Xia, W., Yamaguchi, H., Ding, Q., Xie, X., Lang, J.Y., Lai, C.C., Chang, C.J., Huang, W.C., et al. (2008). ERK promotes tumorigenesis by inhibiting FOXO3a via MDM2-mediated degradation. Nat Cell Biol. 10(2):138–48.
501. Yang, Y., Jiang, G., Zhang, P., and Fan, J. (2015). Programmed cell death and its role in inflammation. Mil. Med. Res. 2, 1–12.
502. Yang, Y., Jiang, G., Zhang, P., and Fan, J. (2015b). Programmed cell death and its role in inflammation. Mil. Med. Res. 2.

503. Yaqoob P, Calder PC. (1997). Glutamine requirement of proliferating T lymphocytes. Nutrition. 13:646–651.
504. Yen, D., et al. (2006). IL-23 is essential for T cell-mediated colitis and promotes inflammation via IL-17 and IL-6. J Clin Invest. 116(5):1310–1316.
505. Yilmaz, O.H., et al. (2012). mTORC1 in the Paneth cell niche couples intestinal stem-cell function to calorie intake. Nature. 486:490–495.
506. Yokosuka, T., and Takashi S. (2010). "The Immunological Synapse, TCR Microclusters, and T Cell Activation." Current Topics in Microbiology and Immunology. 340:81-107.
507. Yoon, S.I., Logsdon, N.J., Sheikh, F., Donnelly, R.P., and Walter, MR. (2006). Conformational changes mediate interleukin-10 receptor 2 (IL-10R2) binding to IL-10 and assembly of the signaling complex. J Biol Chem. 281(46):35088-96.
508. Yurchenko, E. et al. (2012). Inflammation-driven reprogramming of CD4+ Foxp3+ regulatory T cells into pathogenic Th1/Th17 T effectors is abrogated by mTOR inhibition in vivo. PLoS ONE 7, e35572.
509. Zaiatz Bittencourt, V., Jones, F., Doherty, G., & Ryan, E. J. (2021). Targeting Immune Cell Metabolism in the Treatment of Inflammatory Bowel Disease. Inflammatory bowel diseases, 27(10), 1684–1693.
510. Zaph, C., et al. (2007) Epithelial-cell-intrinsic IKK-beta expression regulates intestinal immune homeostasis. Nature 446(7135):552-556.
511. Zarubin, T., and Han, J. (2005). Activation and signaling of the p38 MAP kinase pathway. Cell Res. 15, 11–18.
512. Zdanov, A., Schalk-Hihi, C., Gustchina, A., Tsang, M., Weatherbee, J., and Wlodawer, A. (1995). Crystal structure of interleukin-10 reveals the functional dimer with an unexpected topological similarity to interferon gamma. Structure.3(6):591-601.
513. Zenewicz, L. A., Yancopoulos, G. D., Valenzuela, D. M., Murphy, A. J., Stevens, S., & Flavell, R. A. (2008). Innate and adaptive interleukin-22 protects mice from inflammatory bowel disease. *Immunity*, *29*(6), 947–957.
514. Zeng, H., Yang, K., Cloer, C., Neale, G., Vogel, P., Chi, H. (2013). mTORC1 couples immune signals and metabolic programming to establish T(reg)-cell function. Nature.499:485–490.
515. Zhang, C. et al. (2016). Glutaminase 2 is a novel negative regulator of small GTPase Rac1 and mediates p53 function in suppressing metastasis. Elife.5: e10727.
516. Zhang, J. M., & An, J. (2007). Cytokines, inflammation, and pain. International anesthesiology clinics, 45(2), 27–37.
517. Zhang, J., et al. (2006). Characterization of Siglec-H as a novel endocytic receptor expressed on murine plasmacytoid dendritic cell precursors. Blood.107(9):3600-8.
518. Zhang, X., Camprecios, G., Rimmele, P., Liang, R., Yalcin, S., Mungamuri, SK., Barminko, J., D'Escamard, V., Baron, MH., Brugnara, C. et al. (2014). FOXO3- mTOR metabolic cooperation in the regulation of erythroid cell maturation and homeostasis. Am J Hematol 89: 954 – 963
519. Zhang, X., Goncalves, R., and Mosser, D.M. (2008). The isolation and characterization of murine macrophages. Curr Protoc Immunol. Chapter 14: Unit 14.1.
520. Zhang, X., Tang, N., Hadden, T.J., Rishi, A.K. (2011). Akt, FoxO and regulation of apoptosis. Biochimica et biophysica acta 1813: 1978–1986.
521. Zhang, X., et al. (2011). FOXO1 is an essential regulator of pluripotency in human embryonic stem cells. Nat Cell Biol 13: 1092 – 1099

522. Zhernakova, A., et al. (2008). Genetic analysis of innate immunity in Crohn's disease and ulcerative colitis identifies two susceptibility loci harboring CARD9 and IL18RAP. American journal of human genetics, 82(5), 1202–1210.
523. Zhu, J., & Emerson, S. G. (2002). Hematopoietic cytokines, transcription factors and lineage commitment. Oncogene, 21(21), 3295–3313.
524. Ziegler-Heitbrock, L. (2015). Blood Monocytes and Their Subsets: Established Features and
525. Zlotnik, A. & Yoshie, O. (2000) Chemokines: a new classification system and their role in immunity. Immunity 12, 121–127.
526. Zoncu R, Efeyan A, Sabatini DM (2011) mTOR: from growth signal integration to cancer, diabetes, and ageing. Nat Rev Mol Cell Biol 12: 21 – 35